University of Nottingham

UK | CHINA | MALAYSIA

PERFORMANCE OPTIMIZATION OF INDUSTRIAL SCALE IN-GROUND LAGOON ANAEROBIC DIGESTER FOR PALM OIL MILL EFFLUENT (POME) TREATMENT

MOHD AMRAN BIN MOHD YUSOF (ID: 20385147)

Thesis submitted to the University of Nottingham,

Malaysia Campus for the degree of Doctor of Philosophy

APRIL 2024

ACKNOWLEDGEMENT

This thesis stands as a testament to my twelve years of professional experience—an incredible journey indeed. Its purpose is to share my insights with the biogas community and anyone interested in learning about biogas. Becoming a biogas engineer has been a dream come true for me, but the opportunity to compile this thesis has been even more exhilarating. I aspire for this thesis to offer valuable insights to stakeholders in the global biogas industry, particularly those engaged in the treatment of palm oil mill effluent.

I am immensely grateful to Associate Professor Dr. Chan Yi Jing for her invaluable guidance and support throughout my entire Ph.D. journey. The continuous support and abundant advice she provided during the thesis-writing process go beyond what words can express. Despite my demanding work schedule, her significant role was instrumental in helping me successfully navigate the final stages of my Ph.D. She has consistently been there for me whenever I needed assistance.

Additionally, I wish to extend my appreciation to my former employer, Concord Renewable Energy Sdn Bhd, especially to Tan Sri Mohd Hussin, Datuk Khairuddin and Irma, for granting me the opportunity to pursue my aspirations and for permitting the collection of data from all four biogas plants under the Concord Group. The operational team played a crucial role in ensuring the success of the study. Over the course of our five-year collaboration, we successfully implemented a robust data collection system and recorded information that has been utilized in this thesis. I

want to express my thanks specifically to the Chief of Plant members (Mizi, Syahid, Adnan, Hadi, Asyraf, and Suhaimi) for their continuous support during the data collection period.

Very special thanks to my current employer, reNIKOLA Group for giving me the opportunity to carry out my doctoral research and for their financial support. It would have been impossible for me to complete this journey without them.

Finally, I would like to dedicate this thesis to my beloved wife, Farhana, my parents, Mohd Yusof and Sugerah Biby, all my family members (Baie, Didi, Ika, Mustafa, Phabi, Rezzaq, Umairah, Naqiyyah, Umar, Abu Bakar and Nursyaza), and my best friend (Andy, Raka, Tharma, Romdi and Khasanul) for their unwavering support and sacrifices. Their dedication played a pivotal role, and I acknowledge that I would not have successfully completed my Ph.D. journey without their constant encouragement.

ABSTRACT

Despite advancements in treating Palm Oil Mill Effluent (POME) using anaerobic methods, challenges persist in optimising biogas production and effluent treatment due to unpredictable characteristics influenced by palm oil extraction efficiency and mill processes. Recent changes in Malaysia's Feed-In Tariff (FiT) program, particularly the introduction of an e-bidding system have led to reduced average FiT rates, impacting biogas plant developers with high capital expenditure. Additionally, long-term operational challenges in biogas plants require an understanding of POME characteristics and factors influencing anaerobic digestion performance throughout the Renewable Power Purchase Agreement (REPPA) period of 21 years. Therefore, the main objective of this study is to maximise methane yield of the biogas plant through optimisation analysis and assess its feasibility via techno-economic analysis.

Initially, this study evaluates different operating systems based on two years of experimental data in four Palm Oil Mills (POMs) and in-ground lagoon anaerobic digesters (AD) to identify the most critical operating parameters. This step is crucial as it contributes valuable insights to optimize biogas plant operations and enhance their overall efficiency. As most biogas plants in Malaysia are built for power generation, the focus of this study is on evaluating four industrial-size biogas plants (BGPs) participating in Malaysia's FiT Program. The analysis shows that POM A was the only mill equipped with a three-phase decanter, which reduced the total solid (TS) concentration in POME and

recorded the lowest TS content (25,580 mg/L) compared to POM B, C, and D. However, the chemical oxygen demand (COD) of POM A was still high due to the continuous addition of effluent from the empty fruit bunch (EFB) press station. POM B and D had the highest COD (more than 80,000 mg/L) due to low water consumption, absence of decanter, and direct discharge of sterilizer condensate to the sludge pit. ANOVA analysis concluded that different equipment and processes in POM produced different qualities of POME characteristics.

Two years of biogas plants (BGPs) operation and process data show that all BGPs are still functioning well with satisfactory methane yield (0.135 - 0.364 Nm^3 $CH4/kgCOD_{removed}$) and COD removal efficiencies (67% - 85%). Sensitivity analysis concluded that moderate OLR (<1.6), moderate T (<44°C), and moderate RR (<2.3) are required to achieve optimum COD removal and biogas production for each biogas plant.

While temperature is identified as a crucial parameter through the performance evaluation analysis, the existing pretreatment facilities were not able to control, stabilize, and provide a consistent temperature of POME entering the AD. To address this, a twin packed crossflow induced draft cooling tower (CT) was installed at BGP A to control the inlet POME temperature below 40°C. This strategy was coupled with anaerobic co-digestion (ACoD) of POME with decanter cake (DC), which is a waste product in the palm oil mill, to enhance methane yield. The integration of both the cooling tower and ACoD technology successfully improved the methane yield by more than 40%.

Performance evaluation, prediction and optimisation of the cooling tower and ACoD system was conducted using Artificial Neural Network (ANN) and response surface methodology (RSM) based on six months of operation data. After the implementation of the cooling tower, the average outlet temperature of POME in 2022 was 39.29°C±0.91, within the target range for the operating temperature of mesophilic bacteria. The methane (CH_4) content averaged 65.71%±0.97, with an average biogas production rate of 12,683 m^3/day and a methane yield of 0.3135 $Nm^3/kgCOD_{removed}$. In the ACoD process, the highest methane yield (0.379 Nm^3 CH_4/ $kgCOD_{removed}$) was found to be at an OLR of 2.5 kg COD/m^3.day and a Treated Effluent/DC ratio of 10. Economic analysis shows that both cooling tower and ACoD technologies has the potential to generate revenue of RM879,000/year with a payback period of less than one year, indicating its effectiveness in improving the economics aspect of the biogas plants, which can be replicated in existing and new biogas plants in the near future.

The findings from this research benefit all FiT Biogas Plant Developers in Malaysia. Future works could focus on evaluating different pretreatment methods for the DC in the ACoD system to further improve methane yield and stable biogas production throughout the 21-year REPPA period. Furthermore, investigating the potential utilization of byproducts from ACoD, such as the residual sludge, for value-added applications would be beneficial. This comprehensive approach could continuously improve the sustainability and profitability of anaerobic digestion processes in the palm oil industry.

LIST OF PUBLICATIONS

Published Papers:

1) **Mohd Yusof Mohd Amran Bin**, Yi Jing Chan, Chien Hwa Chong, and Chien Lye Chew, 2023, Effects of operational processes and equipment in palm oil mills on characteristics of raw Palm Oil Mill Effluent (POME): A comparative study of four mills, Cleaner Waste Systems 5, 100101.

2) **Mohd Yusof Mohd Amran Bin**, Yi Jing Chan and Chien Hwa Chong, 2023, Comparative analysis in the performances of four in-ground lagoon anaerobic digesters treating palm oil mill effluent (POME), Asia-Pacific Journal of Chemical Engineering 18(2)

3) **Mohd Yusof Mohd Amran Bin**, Yi Jing Chan, Daniel Jia Sheng Chong and Chien Hwa Chong, 2023, In-ground lagoon anaerobic digester in the treatment of palm oil mill effluent (POME): Effects of process parameters and optimisation analysis, Fuel, Volume 357 (129916)

Papers Under Review/In Progress for Publication:

1) Alvin V.G. Lim, **Mohd Amran Bin Mohd Yusof**, Yi Jing Chan, Abu Danish Aiman Bin Abu Sofian, Yoke Kin Wan, Chien Hwa Chong, Pau Loke Show, Boosting Biogas Returns from Palm Oil Mills: An Exploration of Cooling Tower, Process Simulations, and Neural Network Models with Techno-Economic Analysis.

   Status: Under consideration by editor of Biofuels Research Journal.

2) **Mohd Amran Bin Mohd Yusof** ,Yi Jing Chan, Abu Danish Aiman Bin Abu Sofian, Chien Hwa Chong, The use of palm oil mill Decanter Cake (DC) as a co-substrate of Palm Oil Mill Effluent (POME) in the In-Ground Lagoon Anaerobic Digester.

Status: Will submit to Biomass and Bioenergy Journal.

3) **Mohd Amran Bin Mohd Yusof**, Yi Jing Chan, Abu Danish Aiman Bin Abu Sofian, Ashok Pandey, Chien Hwa Chong, Wei-Hsin Chen and Pau-Loke Show, Enhancing Biogas Production from Palm Oil Mill Effluent: A Comprehensive Study on Cooling Tower Integration for Temperature Optimization and Biogas Quality Improvement

Status: Will submit to Applied Energy

LOCAL CONFERENCE AND PROCEEDING

No	Event	Description
1.	Speaker for Biogas workshop (5th January 2022)	Host: Concord Green Energy Sdn Bhd Topic: Biogas processes and operation
2.	Speaker at 19th Asian Pacific Confederation of Chemical Engineering (APCChE) Congress 2022 (9th to 12th August 2022)	Host: Institute of Engineers Malaysia Submitted two abstracts, and both were accepted: a) Comparative Analysis in the Performances of Four In-ground Lagoon Anaerobic Digesters treating Palm Oil Mill Effluent (POME) b) Effects of Operational Differences in Palm Oil Mills on Palm Oil Mill Effluent (POME) Characteristics
3.	Participant in Malaysia Oil & Gas Services Exhibition and Conference (MOGSEC) (13th to 15th Sept 2022)	Host: Malaysian Oil & Gas Services Council
4.	Speaker (sharing session) in Solving Industrial Wastewater Treatment Problems via Metagenomic Approach (29th September 2022)	Host: Collaboration between Universiti Malaya and Japan-ASEAN Science, Technology and Innovation Platform (JASTIP) Paper presented: Comparative Analysis in the Performances of Four In-ground Lagoon Anaerobic Digesters treating Palm Oil Mill Effluent (POME)
5.	Participant in International Greentech & Eco Products Exhibition & Conference Malaysia (IGEM) (12th to 14th Oct 2022)	Host: Ministry of Environment and Water Malaysia
6.	Speaker at International Conference on Pollution Control and Sustainable Environment 2022 (24th to 25th Nov 2022)	Host: World Research Forum Submitted abstract and accepted. Paper presented: A review of Palm Oil Milling Processes and Their Impacts on Palm Oil Mill Effluent (POME) Characteristics
7.	Speaker at International Conference on Biogas Engineering for Sustainable Applications 2022 (29th to 30th Nov 2022)	Host: International Research Conference Submitted abstract and accepted. Paper presented: Comparative Analysis in the Performances of Four In-ground Lagoon Anaerobic Digesters treating Palm Oil Mill Effluent (POME) Received Best Presentation Award
8.	Speaker at 1st International Conference on Water and Environment for Sustainability	Host: University of Nottingham, Malaysia Campus Submitted two extended abstracts, and both were accepted:

	2022 (7^{th} to 9^{th} Dec 2022)	a) Presented in Plenary Talks: Comparative Analysis in the Performances of Four In-ground Lagoon Anaerobic Digesters treating Palm Oil Mill Effluent (POME) b) Effects of Operational Differences in Palm Oil Mills on Palm Oil Mill Effluent (POME) Characteristics- From Biogas Plant Developer Perspective

TABLE OF CONTENTS

ACKNOWLEDGEMENT ii

ABSTRACT iv

LIST OF PUBLICATIONS vii

LOCAL CONFERENCE AND PROCEEDING ix

TABLE OF CONTENTS xi

LIST OF TABLES xx

LIST OF FIGURES xxiv

LIST OF ABBREVIATION xxix

CHAPTER ONE INTRODUCTION 1

1.1 Overview of Palm Oil Industry in Malaysia 1

1.2 Overview of Biogas Industry in Malaysia 4

1.3 Palm Oil Mill Effluent (POME) Characteristics 5

1.4 In-ground Lagoon Anaerobic Digester Processes and Technology 9

1.4.1 Temperature..... 11

1.4.2 pH 11

1.4.3 Solid & Hydraulic Retention Time..... 11

1.4.4 Organic Loading Rate (OLR)..... 12

1.5 Cooling Tower 12

1.6 Decanter Cake 14

1.7 Problem Statements 15

1.8 Research Objectives 18

1.9 Research Scope 20

1.10 Thesis Organisation 24

CHAPTER TWO LITERATURE REVIEW 29

2.1 Palm Oil Industry in Malaysia 29

2.2 Biogas Industry in Malaysia 32

2.3 POME Characteristics and POM Processes 33

2.4 In-ground Lagoon Anaerobic Digester Processes and Technology 38

2.4.1 Anaerobic Digestion 38

2.4.2 Anaerobic Digestion Stages 39

2.4.2.1 Hydrolysis..... 40

2.4.2.2 Acidogenisis 42

2.4.2.3 Acetogenesis..... 43

2.4.2.4 Methanogenesis 44

2.4.3 Parameters Affecting Anaerobic Digestion 46

2.4.3.1 Temperature..... 46

2.4.3.2 pH 49

2.4.3.3 Solid & Hydraulic Retention Time..... 52

2.4.3.4 Organic Loading Rate 54

2.4.4 Biogas 55

2.5 Cooling Tower 58

2.5.1 Importance of Pre-treatment in Anaerobic Digester..... 58

2.5.2 Sensitivity of Methanogenic Bacteria on Temperature 59

2.5.3 Optimum Growth Temperature Range 60

2.5.4 Design of CT 61

2.6 Decanter Cake 66

2.6.1 Decanter Centrifuge 67

2.6.2 Types of Decanter Centrifuge 68
2.6.3 Working Principle of POME 3-Phase Decanter Centrifuge 68
2.6.4 Characteristics of Palm Oil Decanter Cake 69
2.6.5 Anaerobic Digestion of Palm Oil Decanter Cake 73
2.6.5 Pre-treatment of Palm Oil Decanter Cake 79
CHAPTER THREE MATERIALS AND METHODS 85
3.1 POM Profiling and POME Characteristics Study 86
3.1.1 Site Locations 86
3.1.2 POMs Processing Information 87
3.1.3 Sampling Method of POME 87
3.1.4 Parameters for the Characteristic Study of POME and Analytical Methods 88
3.2 Biogas Plant Profiling and In-ground Lagoon AD Performance Study 89
3.2.1 Site Locations 89
3.2.2 Biogas Plant Profiling 90
3.2.3 Biogas Plant and AD Data Collection 90
3.2.4 AD Process Data Analysis Methods 93
3.2.4.1 Analysis of Variance (ANOVA) 95
3.2.4.2 Development of Mathematical Model and Statistical Analysis 96
3.2.4.3 Optimisation Model for each BGP 97
3.2.4.4 Application of Theoretical Models for Prediction of Methane Production 98

3.3 Methods and Parameters of Optimisation Study 1: Cooling Tower 99
3.3.1 Site Location 101
3.3.2 CT Unit Design Parameters 101
3.3.3 Methodology of Effluent and Sludge Data Collection for CT Study 104
3.3.4 CT Process Data Analysis Methods 105
3.3.4.1 Data Standardisation 105
3.3.4.2 Artificial Neural Network (ANN) 106
3.3.4.3 Performance Evaluation of ANN 107
3.3.4.4 Optimisation Analysis of Cooling Tower Study 109
3.3.4.5 Sensitivity Analysis of Cooling Tower Study 110
3.3.4.6 Techno-economic Analysis of Cooling Tower Study 110
3.4 Methods and Parameters of Optimisation Study 2: Decanter Cake 111
3.4.1 Characteristic Study 112
3.4.2 Operation of Biogas Plant for Co-digestion of POME with DC 113
3.4.3 Anaerobic co-digestion (ACoD) performance analysis methodology 115
3.4.3.1 Machine learning using Neural Networks 117
3.3.3.2 Parameter Selection of ACoD 117
3.4.4 Economic analysis of ACoD 118

CHAPTER FOUR RESULTS AND DISCUSSION 120

4.1 POMs Profiling and POME Characteristics Study 120

4.1.1 POMs Profile 120

4.1.2 POME Characteristics for all POMs 125

4.1.3 Factors affecting the quality of POME in different mills . 133

4.1.3.1 Selection of Clarifier System 134

4.1.3.2 Amount of Water Consumed 135

4.1.3.3 Installation of EFB Press Station 138

4.1.3.4 Selection of Steriliser Type 139

4.2 Inground Lagoon AD Profiling and Performance Study 140

4.2.1 In-ground Lagoon AD Profile 140

4.2.2 Analysis of Pre-treated POME at the Mixing Tank 146

4.2.3 Analysis of Treated Effluent at Anaerobic Digester 151

4.2.4 Operating Parameters and Performance Indicators of Anaerobic Digester 156

4.3 Statistical Analysis of AD Performance Study 172

4.3.1 Box Plot Analysis 175

4.3.2 Development of Mathematical Model 178

4.3.3 Effects of Process Parameters on the Studied Output Variables 180

4.3.3.1 Effect of OLR on COD Removal 180

4.3.3.2 Effect of Temperature on COD Removal 181

4.3.3.3 Effect of Recirculation Ratio and Location of the Plant on COD Removal 182

4.3.3.4 Effect of OLR on Biogas Production 183

4.3.3.5 Effect of Temperature on Biogas Production.... 183
4.3.3.6 Effect of Recirculation Ratio and Location on Biogas Production 184
4.3.4 Optimisation and Sensitivity Analysis of AD Performance Study 199
4.3.5 Theoretical Models for Prediction of Methane Production 203
4.3.6 Limitations and Further Improvements of AD Performance Study Analysis..... 204
4.4 Six Months Operation Data Analysis of Cooling Tower Application 206
4.4.1 Analysis of the Temperature and pH Change..... 206
4.4.1.1 Analysis of the Effect of Applying CT on the Temperature Inlet and Outlet..... 206
4.4.1.2 Analysis of the Effect of Applying CT on the pH Outlet 209
4.4.2 Analysis of Bottom Sludge..... 211
4.4.2.1 Temperature change of Bottom Sludge 211
4.4.3 Analysis on Treated Effluent..... 212
4.4.3.1 Temperature of Treated Effluent 212
4.4.4 Analysis on Raw Biogas Quality in Lepar Hilir 213
4.4.4.1 Analysis of Gas Quality from January 2022 until June 2022 213
4.4.4.2 Comparison of CH4 Quality (Pre and Post-CT Installation) 216

4.4.4.3 Comparison of CO2 Quality (Pre and Post-CT Application) 217
4.4.4.5 Comparison of Hydrogen Sulphide Quality (Pre and Post CT) 217
4.4.5 Optimisation of AD by Cooling Tower Application 218
4.4.5.1 Performance Evaluation of Biogas Plant Using Artificial Neural Network (ANN) 218
4.4.5.2 Sensitivity analysis of cooling tower study 225
4.4.5.3 Parameter Comparison between Process Simulation and BGP A Data 226
4.4.6 Techno-Economic Analysis of Cooling Tower Application 228
4.4.6.1 Capital and Operational Expenditure 229
4.4.6.2 Potential Revenue with CT application..... 229
4.4.6.3 Economic analysis indicator..... 230
4.5 Six Months Operation Data Analysis of Decanter Cake Application 231
4.5.1 Analysis of Decanter Cake Characteristics..... 231
4.5.1.1 pH 231
4.5.1.2 Chemical Oxygen Demand (COD) 232
4.5.1.3 Total Solids (TS) 233
4.5.1.4 Suspended Solids (SS) 233
4.5.1.5 Biological Oxygen Demand (BOD)..... 234
4.5.2 Analysis of Decanter Cake Dilutions..... 235

4.5.3 Performance of Anaerobic Co-digestion of POME with DC 235
4.5.3.1 Bottom Sludge Quality 236
4.5.3.2 Biogas Composition 236
4.5.3.3 Biogas Yield 237
4.5.4 Simulation Results 239
4.5.5 Optimisation of Anaerobic Co-digestion Process 242
4.5.6 Artificial Neural Network (ANN) of anaerobic co-digestion study 247
4.5.7 Economic analysis of anaerobic co-digestion of DC with POME 251
4.5.7.1 Capital and operational expenditure 251
4.5.7.2 Potential Revenue from anaerobic co-digestion of DC with POME 252
4.5.7.3 Economic Analysis Indicator 253
CHAPTER FIVE CONCLUSIONS AND RECOMMENDATIONS 255
5.1 Conclusions 255
5.2 Recommendations 261
REFERENCES 267
APPENDICES 297
Appendix 1: Questionnaire for POM Profiling Study 297
Appendix 2: Biogas Plant and AD Profiling Study Form 299
Appendix 3: Biogas Plant and AD Logsheet and Checklist 300
Appendix 4: Biogas Plant 2 Years Processes and Operational Datasheets 307

Appendix 5: Biogas Plant Process Monitoring Guideline 318

LIST OF TABLES

TABLE 1.1: COMPOSITION OF POME (IGWE & ONYEGBADO, 2007; LAM & LEE, 2011A; ZINATIZADEH ET AL., 2006) 7

TABLE 1.2: CHARACTERISTICS OF POME AND DISCHARGE LIMITS SET BY MALAYSIAN DEPARTMENT OF ENVIRONMENT 7

TABLE 1.3: NUTRIENTS & HEAVY METAL IN POME (A AZIZ ET AL., 2020A; ALHAJI ET AL., 2016B; IZZAH ET AL., 2017; LEE ET AL., 2019A; LOH ET AL.,2017; ZAINAL ET AL., 2017)..... 8

TABLE 2.1**:** COMPOSITION OF PRODUCTS/WASTES FROM THE PRODUCTION OF FFB (ABDULLAH & SULAIMAN, 2013)..... 29

TABLE 2.2: CHARACTERISTICS OF EACH SOURCE OF EFFLUENT OF POME IN PALM OIL MILLS (AHMED ET AL., 2015A) 34

TABLE 2.3: LITERATURE DATA OF RAW POME CHARACTERISTICS 37

TABLE 2.4: COMPARISON BETWEEN MESOPHILIC AND THERMOPHILIC CONDITION FOR ANAEROBIC DIGESTION 49

TABLE 2.5: THE INFLUENCE OF SRT ON THE BREAKDOWN EFFICIENCY (KHADAROO ET AL., 2019B) 54

TABLE 2.6: THE RANGE OF PERCENTAGE COMPOSITION OF BIOGAS (SRI ET AL., 2015) 57

TABLE 2.7: COMPARISON OF BIOGAS, METHANE YIELD AND METHANE CONTENT FROM DIFFERENT POTENTIAL FEEDSTOCKS 58

TABLE 2.8: ESTIMATED METHANE PRODUCTION FROM POME BASED ON THE CPO PRODUCTION OF MALAYSIA IN 2020..... 58

TABLE 2.9: OPERATING TEMPERATURE FOR MESOPHILES 61

TABLE 2.10: CHARACTERISTICS OF PALM OIL DECANTER CAKE73

TABLE 2.11: COMPARISON OF VARIOUS LITERATURE ON THE ANAEROBIC DIGESTION OF DECANTER CAKE 78

TABLE 2.12: PRE-TREATMENT METHODS OF LIGNOCELLULOSIC MATERIALS, THEIR EFFECTS, AND LIMITATIONS 82

TABLE 2.13: COMPARISON OF VARIOUS LITERATURE ON THE PRE-TREATMENT OF DECANTER CAKE..... 84

TABLE 3.1: METHODOLOGIES IMPLEMENTED IN ANALYSING POME CHARACTERISTICS PARAMETERS 88

TABLE 3.2: METHODS IMPLEMENTED IN ANALYSING EFFLUENT AND SLUDGE PARAMETERS..... 91

TABLE 3.3: PARAMETERS ANALYSED FOR THE AD PERFORMANCE STUDY 94

TABLE 3.4: OVERVIEW OF THE BMPTH MODELS 98

TABLE 3.5: COOLING TOWER DATABASE DESIGN..... 103

TABLE 3.6: STATISTICAL DATA VALUE USED IN ANN MODELLING 106

TABLE 3.7: EQUATION OF ERROR FUNCTIONS FOR PERFORMANCE EVALUATION OF ANN MODEL..... 118

TABLE 3.8: COST INDICATORS FOR ECONOMIC EVALUATION . 119

TABLE 4.1: SUMMARY OF THE PROCESSING UNITS OF MILLS . 122

TABLE 4.2: TWO YEARS OF POME CHARACTERISTICS DATA ... 126

TABLE 4.3: PROFILE FOR ALL IN-GROUND LAGOON AD 142

TABLE 4.4: SUMMARY OF TWO YEARS AD PROCESS PARAMETERS..... 144

TABLE 4.5: COMPOSITION OF BIOGAS COMPONENTS IN ALL BIOGAS PLANTS AND LITERATURE VALUES 168

TABLE 4.6: DESCRIPTIVE STATISTICS OF THE AD DATA UTILISED IN THE FOUR POME TREATMENT PLANTS 172

TABLE 4.7: ANOVA AND SIGNIFICANCE TEST OF EACH MODEL TERM FOR COD REMOVAL 172

TABLE 4.8: ANOVA AND SIGNIFICANCE TEST OF EACH MODEL TERM FOR BIOGAS PRODUCTION 173

TABLE 4.9: OPTIMISED VALUES FOR EACH BGP PLANT 199

TABLE 4.10: COMPARISON BETWEEN INLET TEMPERATURE AND OUTLET TEMPERATURE FROM 2019 UNTIL 2022..... 208

TABLE 4.11: TEMPERATURE OF BOTTOM SLUDGE FROM 2019 UNTIL 2022 212

TABLE 4.12: TEMPERATURE OF TREATED EFFLUENT FROM 2019 UNTIL 2022 213

TABLE 4.13: PERCENTAGE OF CH_4 IN RAW BIOGAS FROM 2019 UNTIL 2022 216

TABLE 4.15: PRESENCE OF HYDROGEN SULPHIDE IN BIOGAS FROM 2019 UNTIL 2022..... 218

TABLE 4.16: ATTRIBUTES OF NEURAL NETWORK UTILIZED 220

TABLE 4.17: SUMMARY OF PARAMETER PERFORMANCE BETWEEN SIMULATION AND BGP A 228

TABLE 4.18: INDICATIVE CAPEX AND OPEX FOR COOLING POND, MIXING TANK AND COOLING TOWER 229

TABLE 4.19: CAPEX AND OPEX OF COOLING TOWER APPLICATION 229

TABLE 4.20: POTENTIAL REVENUE CALCULATION WITH IMPLEMENTATION OF CT 230

TABLE 4.21: ECONOMIC ANALYSIS INDICATORS FOR CT APPLICATION..... 231

TABLE 4.22: CHARACTERISTICS OF POME AND DILUTED DC FROM KILANG SAWIT LEPAR HILIR 234

TABLE 4.23: CHARACTERISTICS OF DC DILUTIONS FROM KILANG SAWIT LEPAR HILIR 234

TABLE 4.24: BOTTOM SLUDGE QUALITY FROM MONO- AND CO-DIGESTION..... 236

TABLE 4.25: BIOGAS COMPOSITIONS FROM MONO- AND CO-DIGESTION..... 237

TABLE 4.26: EQUATION FOR MONOD KINETIC AND RATE OF SUBSTRATE UTILIZATION 240

TABLE 4.27: SUMMARY OF ACOD PERFORMANCE IN SIMULATION SCENARIO AND INDUSTRIAL CASE 240

TABLE 4.28: SUMMARY OF ACOD PERFORMANCE WITH DILUTION RATIO OF DC: TE OF 1:10 243

TABLE 4.29: SUMMARY OF CHARACTERISTICS OF NEURAL NETWORK 248

TABLE 4.30: CAPEX AND OPEX OF ANAEROBIC CO-DIGESTION 252

TABLE 4.31: POTENTIAL REVENUE CALCULATION WITH CO-DIGESTION OF DC 253

TABLE 4.32: POTENTIAL REVENUE CALCULATION 254

TABLE 5.1: DESIRABLE POME CHARACTERISTICS FOR MAXIMUM BIOGAS GENERATION 261

LIST OF FIGURES

FIGURE 1.1: WORLD PALM OIL PRODUCTION FROM 2016 TO 2023 (USDA, 2024) 1

FIGURE 1.2: WORLD PALM OIL PRODUCTION IN 2023 (USDA, 2024) 2

FIGURE 1.3: GENERAL REACTION OF ANAEROBIC DIGESTION ... 9

FIGURE 1.4: ANAEROBIC DIGESTION PROCESSES 10

FIGURE 1.5: SUMMARY OF THE ENTIRE RESEARCH OBJECTIVES AND PLAN 25

FIGURE 2.1: NUMBER OF PALM OIL MILLS OPERATING IN MALAYSIA FROM 2013 TO APRIL 2021 30

FIGURE 2.2: ESTIMATED POME GENERATION BASED ON THE CPO PRODUCTION IN MALAYSIA 30

FIGURE 2.3: PROCESS FLOW DIAGRAM OF THE PALM OIL MILL EFFLUENTS (POME) TREATMENT SYSTEM IN MILLS 31

FIGURE 2.4: GENERAL REACTION OF ANAEROBIC DIGESTION .. 39

FIGURE 2.5: ANAEROBIC DIGESTION PROCESSES 40

FIGURE 2.6: HYDROLYSIS PROCESS 41

FIGURE 2.7: HRT CALCULATION FORMULA 53

FIGURE 2.8: HORSEPOWER REQUIRED PER SQUARE FEET OF TOWER AREA 63

FIGURE 2.9: APPROXIMATE EFFICIENCIES OF ELECTRIC MOTORS 64

FIGURE 2.10: MOLLIER'S CHART 66

FIGURE 2.11: ILLUSTRATION OF A 3-PHASE DECANTER 69

FIGURE 2.12: COMPONENTS AND STRUCTURE OF LIGNOCELLULOSIC PLANT CELL WALLS (BRETHAUER ET AL., 2020) 79

FIGURE 3.1: SUMMARY OF OVERALL RESEARCH METHODOLOGIES 85

FIGURE 3.2: PALM OIL MILLS LOCATION 86

FIGURE 3.3: POME SAMPLING POINT 88

FIGURE 3.4: SCADA SYSTEM FOR BIOGAS PLANT 92

FIGURE 3.5: ONLINE AND PORTABLE BIOGAS ANALYSER 93

FIGURE 3.6: PROCESS FLOW DIAGRAM OF AD PROCESS DATA ANALYSIS 94

FIGURE 3.7: SUMMARY OF OVERALL CT STUDY 102

FIGURE 3.8: CONCEPT OF TWIN-PACKED CROSSFLOW INDUCED DRAFT CT 103

FIGURE 3.9: CT INSTALLED AT BGP A 103

FIGURE 3.10: SUMMARY OF POME TEMPERATURE AND PH DATA COLLECTION 104

FIGURE 3.11: SAMPLING POINT OF INLET CT TEMPERATURE AT INLET OF CP 105

FIGURE 3.12: DECANTER CAKE PRODUCED AT POM A 112

FIGURE 3.13: FLOWCHART OF THE DC CHARACTERISATION STUDY 113

FIGURE 3.14: COLLECTION OF DECANTER CAKE FROM PALM OIL MILL 114

FIGURE 3.15**:** DILUTION OF DECANTER CAKE IN TEMPORARY MIXING FACILITY 115

FIGURE 3.16: DC APPLICATION AND DATA COLLECTION PROCESSES 115

FIGURE 3.17: SUMMARY OF OVERALL ACOD STUDY 116

FIGURE 4.1: GENERAL FLOW CHART OF ALL POMS 121

FIGURE 4.2: AVERAGE COD, BOD LEVELS, AND TS CONTENT OF RAW POME 132

FIGURE 4.3: AVERAGE OG AND SS CONTENT IN RAW POME ... 133

FIGURE 4.4: AVERAGE PH CONTENT IN RAW POME 133

FIGURE 4.5: WATER USAGE IN THE MILLS. THE ERROR BARS ARE THE STANDARD DEVIATIONS 137

FIGURE 4.6: ANALYSIS OF MIXING TANK OUTLET (A)TEMPERATURE, (B)PH AND (C)RR OF BIOGAS PLANTS FROM JULY-19 TO JUN-21 149

FIGURE 4.7: A) TEMPERATURE AND B) PH OF THE TREATED EFFLUENT IN BIOGAS PLANTS FROM JULY-19 TO JUN-21 153

FIGURE 4.8: A) BOD, B) COD AND C) TS OF THE TREATED POME IN BIOGAS PLANTS FROM JULY-19 TO JUN-21 154

FIGURE 4.9: A) OLR, B) HRT AND C) TS OF BOTTOM SLUDGE IN BIOGAS PLANTS..... 157

FIGURE 4.10: A) TOTAL COD REMOVED B) COD REMOVAL (%) C) MAXIMUM COD REMOVAL FOR EACH BIOGAS PLANT 158

FIGURE 4.11: A) TOTAL BIOGAS PRODUCTION B) METHANE COMPOSITION C) H_2S CONCENTRATION OF BIOGAS D) MAXIMUM BIOGAS PRODUCTION RATE FOR EACH PLANT 160

FIGURE 4.12: BOX PLOTS OF THE STUDIED INPUT PARAMETERS FOR EACH BIOGAS PLANT (A) OLR (B) TEMPERATURE (C) RECIRCULATION RATIO. 176

FIGURE 4.13: BOX PLOTS OF THE STUDIED RESPONSE PARAMETERS FOR EACH BIOGAS PLANT (A) COD REMOVAL (B) BIOGAS PRODUCTION..... 178

FIGURE 4.14: (A) SURFACE AND CONTOUR PLOT FOR COD REMOVAL AS A FUNCTION OF OLR AND TEMPERATURE; (B) SURFACE AND CONTOUR PLOT FOR COD REMOVAL AS A FUNCTION OF OLR AND RECIRCULATION RATIO. 188

FIGURE 4.15: INTERACTION PLOT FOR COD REMOVAL AS A FUNCTION OF OLR AND LOCATION..... 189

FIGURE 4.16: (A) SURFACE AND CONTOUR PLOT FOR COD REMOVAL AS A FUNCTION OF TEMPERATURE AND RECIRCULATION RATIO; (B) INTERACTION PLOT FOR COD REMOVAL AS A FUNCTION OF TEMPERATURE AND LOCATION191

FIGURE 4.18: (A) SURFACE AND CONTOUR PLOT FOR BIOGAS PRODUCTION AS A FUNCTION OF TEMPERATURE AND OLR; (B) SURFACE AND CONTOUR PLOT FOR BIOGAS PRODUCTION AS A FUNCTION OF RECIRCULATION RATIO AND OLR; (C) INTERACTION PLOT FOR BIOGAS PRODUCTION AS A FUNCTION OF RECIRCULATION RATIO AND LOCATION. 195

FIGURE 4.19: (A) SURFACE AND CONTOUR PLOT FOR BIOGAS PRODUCTION AS A FUNCTION OF RECIRCULATION RATIO AND TEMPERATURE; (B) INTERACTION PLOT FOR BIOGAS

PRODUCTION AS A FUNCTION OF TEMPERATURE AND LOCATION. 197

FIGURE 4.20: INTERACTION PLOT FOR BIOGAS PRODUCTION AS A FUNCTION OF RECIRCULATION RATIO AND LOCATION..... 198

FIGURE 4.21: SENSITIVITY ANALYSIS OF OLR, TEMPERATURE AND RR ON A) BGP A, B) BGP B, C) BGP C, D) BGP D 201

FIGURE 4.22: AVERAGE METHANE PRODUCTIVITY OF EACH BIOGAS PLANT. 204

FIGURE 4.23: INLET AND OUTLET TEMPERATURE OF CT FROM JANUARY 2022 UNTIL JUNE 2022 207

FIGURE 4.24: OUTLET TEMPERATURE RECORDED FROM JULY 2019 TO JUNE 2022 208

FIGURE 4.25: PH INLET OF CT FROM JANUARY 2022 UNTIL JUNE 2022 210

FIGURE 4.26: PH OUTLET OF CT FROM JANUARY 2022 UNTIL JUNE 2022 210

FIGURE 4.27: TEMPERATURE OF BOTTOM SLUDGE RECORDED FROM JANUARY 2022 UNTIL JUNE 2022..... 211

FIGURE 4.28: TEMPERATURE OF TREATED EFFLUENT FROM JANUARY 2022 UNTIL JUNE 2022 213

FIGURE 4.29: PERCENTAGE OF CO_2 AND CH_4 IN BIOGAS FROM JANUARY 2022 UNTIL JUNE 2022 214

FIGURE 4.30: PERCENTAGE OF O_2 INSIDE BIOGAS COLLECTED FROM JANUARY 2022 UNTIL JUNE 2022..... 215

FIGURE 4.31: PRESENCE OF RAW H_2S INSIDE BIOGAS COLLECTED FROM JANUARY 2022 UNTIL JUNE 2022..... 215

FIGURE 4.32: REGRESSION PLOT FROM TRAINING, VALIDATION, TEST AND OVERALL PHASE IN NEURAL NETWORK 220

FIGURE 4.33: (A) PERFORMANCE PLOT WITH MSE FUNCTION; (B) ERROR HISTOGRAM PLOT WITH 20 BINS IN ANNMODEL 223

FIGURE 4.34: PLOT OF METHANE YIELD AGAINST BIOGAS PRODUCTION RATE..... 223

FIGURE 4.35: SENSITIVITY ANALYSIS ON INPUT PARAMETERS TO (A) BIOGAS PRODUCTION RATE (B) METHANEYIELD..... 226

FIGURE 4.36: SIMULATION FLOWSHEET FOR BIOGAS PRODUCTION FROM POME WITH COOLING TOWER..... 227

FIGURE 4.37: CHART OF CUMULATIVE BIOGAS YIELD OVER TIME 238

FIGURE 4.38: BIOGAS PRODUCTION INDICATOR..... 239

FIGURE 4.39: RESPONSE SURFACE CURVE OF METHANE YIELD WITH VARIABLE POME FLOWRATE AND TE/DC DILUTION RATIOS 244

FIGURE 4.40: RESPONSE SURFACE CURVE OF METHANE YIELD WITH VARIABLE OLR AND TE/DC DILUTION RATIOS 245

FIGURE 4.41: RESPONSE SURFACE CURVE OF TS CONTENT WITH VARIABLE POME FLOWRATE AND TE/DC DILUTION RATIOS 246

FIGURE 4.42: RESPONSE SURFACE CURVE OF TS CONTENT WITH VARIABLE OLR AND TE/DC DILUTION RATIOS 246

FIGURE 4.43: REGRESSION ANALYSIS OF NEURAL NETWORK FOR DISTINCT PHASES: TRAINING, VALIDATION, TESTING AND OVERALL PHASE..... 248

FIGURE 4.44: ERROR HISTOGRAM OF ANN MODEL 249

FIGURE 4.45: PERFORMANCE GRAPH OF ANN MODEL: MSE VERSUS EPOCHS..... 250

LIST OF ABBREVIATION

BOD	Biochemical Oxygen Demand
$BOD_{removal}$	Biochemical Oxygen Demand Removal Efficiency
CDM	Clean Development Mechanism
CER	Carbon Emissions Reduction
COD	Chemical Oxygen Demand
$COD_{removal}$	Chemical Oxygen Demand Removal Efficiency
CPO	Crude Palm Oil
CSTR	Continuous Stirred Tank Reactor
C/N	Carbon to Nitrogen
DO	Dissolved Oxygen
DOE	Department of Environment
EFB	Empty Fruit Bunch
FFB	Fresh Fruit Bunch
FiT	Feed-in Tariff
F/M	Food-to-Microorganisms
GHG	Greenhouse Gas
HRT	Hydraulic Retention Time
MLSS	Mixed Liquor Suspended Solid
MLVSS	Mixed Liquor Volatile Suspended Solid
NKEA	National Key Economic Area
NREPAP	National Renewable Energy Policy and Action Plan
OLR	Organic Loading Rate
O&G	Oil & Grease
POME	Palm Oil Mill Effluent

R&D	Research and Development
SRT	Solid Retention Time
SS	Suspended Solid
SVI	Sludge Volume Index
TA	Total Alkalinity
TN	Total Nitrogen
TS	Total Solid
TSS	Total Suspended Solid
TVS	Total Volatile Solid
UNFCCC	United Nations Framework Convention on Climate Change
VFA	Volatile Fatty Acid

CHAPTER ONE

INTRODUCTION

1.1 Overview of Palm Oil Industry in Malaysia

The palm oil industry has grown significantly in recent years and has been an essential economic contributor for countries like Indonesia, Thailand, Malaysia, Colombia, and other tropical developing regions (Liew et al., 2015). Figure 1.1 illustrates the global palm oil production data of various countries obtained from the Foreign Agricultural Services of United States Department of Agriculture (USDA, 2024). An overall uptrend is observed within the world production of palm oil from 2016 to 2023. Undeniably, the Southeast Asia region dominates the palm oil industry due to its higher yield rates and suitable regional climatic condition (Iskandar et al., 2018).

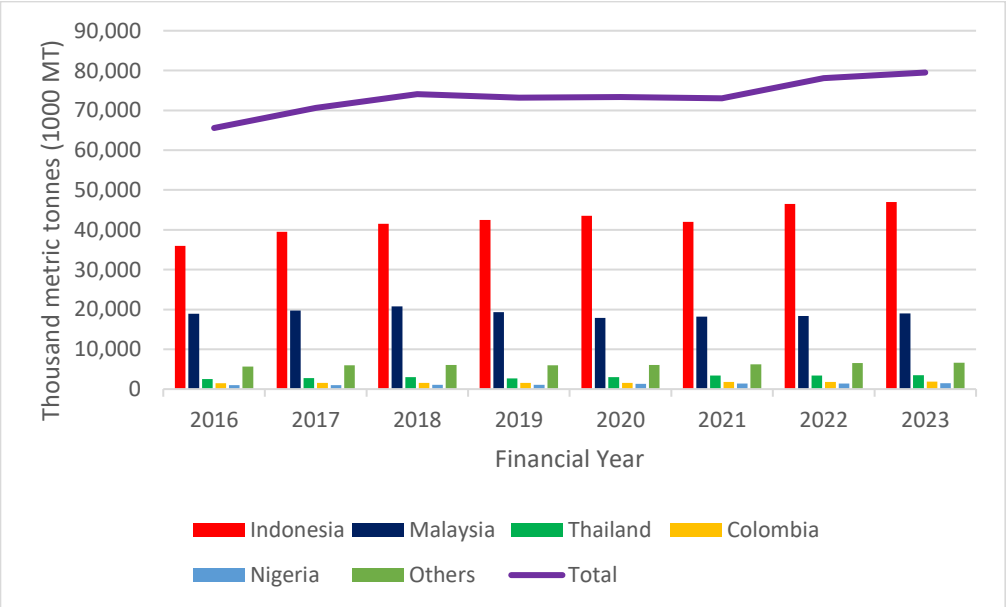

Figure 1.1: World palm oil production from 2016 to 2023 (USDA, 2024)

In Malaysia, the palm oil industry has been growing gradually over these past few decades, securing its position as one of the world's biggest palm oil producers. Figure 1.2 shows the global palm oil production in 2023 (USDA, 2024). As the world's largest palm oil producers, Malaysia and Indonesia contribute a total of 84% of the world's palm oil production. The palm oil industry has become one of the leading agriculture industries in Malaysia, with average palm oil production of over 13 million tons annually (Bala et al., 2015a). In 2023, Malaysia had produced 19.0 million tons of palm oil which contributed 24% of global production. Meanwhile, Thailand takes third place where it contributes 4% of the world's palm oil production and Indonesia is remain the largest producer to date with market share of 59% (USDA, 2024).

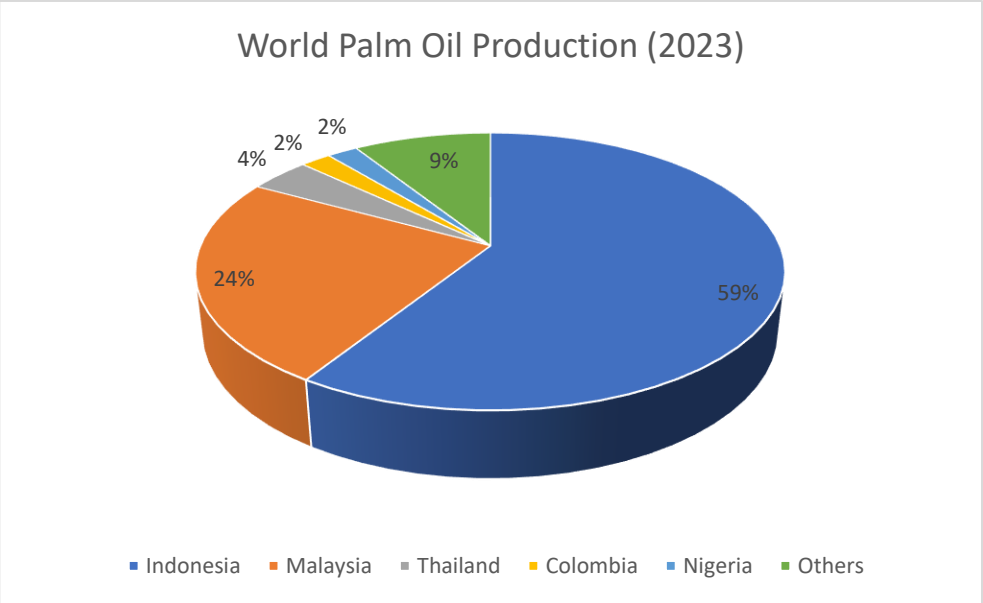

Figure 1.2: World palm oil production in 2023 (USDA, 2024)

In 2006, the Government of Malaysia released a National Bio-fuel Policy to utilise sustainable energy sources to reduce dependency on fossil fuels. There are a few other initiatives and policies, such as the National

Green Technology Policy (2009), National Renewable Energy and Action Plan (2010), Sustainable Energy Development Act (2011), and National Energy Efficiency Action Plan (2014). One of the objectives of these plans is to stabilise the palm oil industry (Wahab, 2020). The government aims to promote the demand for palm oil as the first option for bio-fuel production in Malaysia (S. Lim & Teong, 2010). Under the Renewable Energy Act, the Malaysian government established a feed-in-tariff (FiT) system to promote renewable energy generation. The implementation of such policy has re-positioned palm oil as a valuable renewable asset in Malaysia. Not only that, with the recent development on the National Energy Transition Roadmap, government have listed biogas and bioenergy as one of the key sectors towards generation of new economic model that will benefit the country. According to the roadmap, bioenergy sector will contribute towards clean energy development with few mechanism such as alternative fuel for power generation, rural electrification with micro grid, green transportation and green industrial applications (Ministry of Economy, 2023).

Nonetheless, Yule (2008) and Laurance et al. (2010) point out that the sustainability of palm oil production has always been questioned by non-government organisations (NGOs). They had claimed that further expansion of palm oil plantations would cause severe environmental impacts such as deforestation, destruction of habitat, and greenhouse gases (GHG) due to over-exploitation of peatland. However, the major setback in palm oil production is the wastes generated from palm oil mills and not really on the plantation expansion plan. According to Awalludin

et al. (2015b), the valuable oil extracted from the oil palm fruit only consists of 10 wt% while the remaining 90 wt% is discarded as waste. In addition to that, 452 palm oil mills are currently operating in Malaysia, producing a remarkable amount of crude palm oil and waste. Based on Sustainable Energy Development Authority (SEDA) Malaysia, waste generated from palm oil or landfill is the one of the key sectors that contributed towards energy transition plan in Malaysia (SEDA Malaysia, 2022a). With the new market being developed, waste generated from the palm oil industry will slowly become an asset for Malaysia and will bring a better image for the country.

1.2 Overview of Biogas Industry in Malaysia

A large quantity of POME treated in the open ponding system releases a significant amount of greenhouse gas (GHG) into the environment (Chin et al., 2013a). Under the Malaysia National Energy Plan 2022-2040, which was launched by the Prime Minister of Malaysia, the government is committed to strengthen the energy market in Malaysia. One of the initiatives is by promoting green energy through solar projects, hydro power plants and bioenergy sector. This effort is supported by a few prominent agencies under Ministry of Energy and Natural Resources. Sustainable Energy Development Agency (SEDA) is the responsible agency that has been given a mandate to administer and manage the implementation of Feed-In-Tariff (FiT) Mechanism in Malaysia. Through this mandate, SEDA introduced a platform for a biogas plant developer and mill owner to venture into renewable energy sector. As end of 2022,

SEDA reported in total of 262.88 MW from 144 biogas plant projects has been achieved under FiT mechanism (SEDA Malaysia, 2022a).

There are few types of biogas plant installation in Malaysia. Most common installation reported by SEDA Malaysia is by using anaerobic digester tank or in-ground lagoon anaerobic digester. Concord Green Energy Sdn Bhd (CGESB) is one of a biogas project developer in Malaysia and has built four biogas plants utilising a POME produced by four POMs owned by FGV Holdings Berhad. CGESB invest in all biogas plant under a mechanism of FiT. Generally, construction cost of the biogas plant with a capacity of less than 2 MW is capped below RM 20 million. This large amount of investment is demanding an optimum and efficient process, operation and maintenance (O&M) of biogas plant to ensure the investment returns as per initial prediction.

1.3 Palm Oil Mill Effluent (POME) Characteristics

POME is the thick brownish characteristic of POME from various sources and its standard discharge limit effluent that is typically discharged at a temperature between 80 °C to 90 °C with a pH of 4 to 5. According to Table 1.1, POME is a colloidal suspension that contains 95–96% water, 0.6– 0.7% oil and 4–5% total solids including 2–4% suspended solids, which is mainly the debris from the palm fruit mesocarp. Although POME is a non-toxic liquid waste as typically no chemicals were added during the oil extraction process (Saad et al., 2021a), it can still cause serious pollution and environmental problems to the river bodies if it is discharged untreated. Table 1.2 shows the physicochemical set by the Malaysia Department of Environment. POME has a fluctuating characteristic due

to various sources of wastewater, and POME collected from different mills, batches or days will give analytical results (Liew et al., 2015). Thus, the characteristics of POME are dependent on the efficiency of the operation and process control of the mill.

POME can cause significant water pollution due to high amounts of organic matter, which is closely related to high levels of COD and BOD. According to Table 1.2, POME has a COD value in the range of 50,000-150,000 mg/L-1 and the BOD value of 25,000-75,000 mg/L-1. POME also contains an average value of 4000 mg/L-1 oil and grease, 40,000 mg/L-1 of total solids, and 750 mg/L-1 of nitrogen. Besides, the acidic pH condition of POME is reported due to the presence of organic acids in complex form (Mohamad Anuar Kamaruddin et al., 2021a). The presence of degradable organic matters in the discharged POME will encourage the growth of microorganisms, in which these microorganisms will compete with aquatic life for the uptake of oxygen, consequently leading to depletion of dissolved oxygen in the water (Ehsan et al., 2015a; Khadaroo et al., 2019a). Thus, this phenomenon hinders the growth of aquatic creatures and endangers the marine ecosystem.

POME is made up from main elements such as carbon (C), oxygen (O), hydrogen (H), nitrogen (N), phosphorus (P), potassium (K), calcium (Ca), zinc (Zn), Copper (Cu) magnesium (Mg), iron (Fe), boron (B) and chromium (Cr) (Saad et al., 2021a). Table 1.3 shows the nutrients and heavy metals concentration in POME. (Izzah et al., 2017) and (Kamyab et al., 2018a) reported that these significant number of nutrient elements such as N, P, K, Mg and Ca are vital for plant growth while the dissolved

components such as carbohydrate, fat, protein, and minerals could be converted into valuable materials through microbial processes. Carbohydrates such as cellulose, starch and sugars make up the majority of biodegradable material, proteins are made up of long chains that contains large number of amino acids while lipids are made up from long chain of fatty acids (Kelleher et al., 2002a). Another chemical composition that could be detected from raw POME are ash and lignin. According to Awalludin et al. (2015b), lignin is an important chemical constituent in oil palm biomass, which acts as a binder that supports all the cells and microfibrils in lignocellulosic structure. While toxic heavy metals such as lead, mercury and manganese are not present in POME, which makes it a non-toxic wastewater, it still has potential to pollute the environment.

Table 1.1: Composition of POME (Igwe & Onyegbado, 2007; Lam & Lee, 2011a; Zinatizadeh et al., 2006)

Composition	**%**
Water	95–96
Solid	4–5
Oil	0.6– 0.7

Table 1.2: Characteristics of POME and discharge limits set by Malaysian Department of Environment

Parameters	(Bala, Lalung and Ismail, 2015)	(Alhaji et al., 2016a)	(Lee et al., 2019b)	(Akhbari et al., 2020a)	(Elvitriana et al., 2021)	(C. C. Yap et al., 2021)	Standard Discharge Limits
Temperature (°C)	-	85	90	85	65	-	45
pH	4.74	4.7	4.3	5	4.07	3.90	5-9
Oil and grease	191	4,000	4,000	4,000	-	4,633	100
Fatty acids	-	-	-	-	1,855	11,874	-
Biological Oxygen Demand (BOD5)	34,393	25,000	27,000	25,000	26,818	73,412	50
Chemical Oxygen Demand (COD)	75,900	50,000	57,500	50,000	60,396	146,824	100

(Bala, Lalung and(Bala et al., 2015)

Total solids	-	40,500	45,250	40,000	-	-	-
Total suspended solids	14,467	18,000	29,500	18,000	47,375	29,138	400
Total volatile solid	13,033	34,000	40,500	34,000	-	-	-
Total nitrogen	-	750	790	750	700	1126	150
Ammoniacal-nitrogen	-	35	42	35	-	-	-

a All parameters are in mg L-1 except temperature and pH.
B (Alhaji et al., 2016a; Lam & Lee, 2011a)

Table 1.3: Nutrients & Heavy metal in POME (A Aziz et al., 2020a; Alhaji et al., 2016b; Izzah et al., 2017; Lee et al., 2019a; Loh et al.,2017; Zainal et al., 2017)

Element	Unit	Average Concentration	Standard Discharge Limit
Carbohydrate	g/100g	1.5	-
Protein	g/100g	0.83	-
Fat	g/100g	0.71	-
Ash	g/100g	0.65	-
Lignin	ppm	4700	-
Carbon to Nitrogen (C/N) ratio	mg L^{-1}	49,000	-
Manganese	mg L^{-1}	2	10
Zinc	mg L^{-1}	2.3	10
Copper	mg L^{-1}	0.89	10
Iron	mg L^{-1}	46.5	50
Magnesium	mg L^{-1}	615	-
Boron	mg L^{-1}	7.6	-
Calcium	mg L^{-1}	439	-
Phosphorus	mg L^{-1}	180	-
Potassium	mg L^{-1}	2270	-
Chromium	mg L^{-1}	10.2	-

The characteristics of POME are largely dependent on the efficiency of the operation and process control of the mill. In Malaysia, the widely used method to extract palm oil from fresh fruit bunches (FFB) is by wet palm oil milling process (T. Y. Wu et al., 2010a). The unit operations used for extractions are a steriliser, a stripper, a digester, a press machine, a clarifier, a separator, an extractor, and a purification system (Ehsan et al., 2015a). By understanding the role of each unit operation in the extraction process, steps can be taken to optimize efficiency and reduce negative environmental impacts. The typical processes of wet Palm Oil Mill

(POM)s include sterilization of FFB, stripping, digestion, and pressing, clarification and kernel oil recovery.

1.4 In-ground Lagoon Anaerobic Digester Processes and Technology

The production of biogas from POME requires an anaerobic digestion process, which is a complex mechanism involving interactions between microorganisms through four successive stages, hydrolysis, acidogenesis, acetogenesis, and methanogenesis. Anaerobic digestion is widely used as a treatment system for industrial, agriculture and municipal wastes while producing renewable energy source, that involves the breakdown and stabilisation of organic matters in absence of oxygen which leads to the formation of a mixture of gases, mainly methane and a combination of solid and liquid effluents, known as the digestate (Anukam et al., 2019a; Y. Chen et al., 2007a; Kelleher et al., 2002a; L Chen & H Neiibling, 2014a). The general reaction for anaerobic digestion is shown:

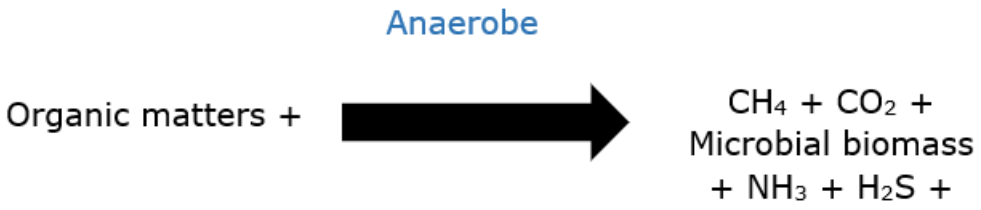

Figure 1.3: General reaction of anaerobic digestion

Several advantages of the anaerobic digestion of POME reported in various studies are reducing greenhouse gas emissions to the atmosphere. It eliminates most of the harmful pathogens, enables energy recovery through methane production, produces nutrient-rich fertiliser,

and efficiently treats the wastewater (Anukam et al., 2019a; Khadaroo et al., 2019a; L Chen & H Neiibling, 2014a). The chemistry of the four pivotal steps of anaerobic digestion is explained in the following subsections, and its reaction sequences in these critical steps are also depicted in Figure 1.3.

Generally, four main steps are involved in the anaerobic digestion process; hydrolysis, acidogenesis, acetogenesis, and methanogenesis. Figure 1.4 illustrates the complete steps of anaerobic processes:

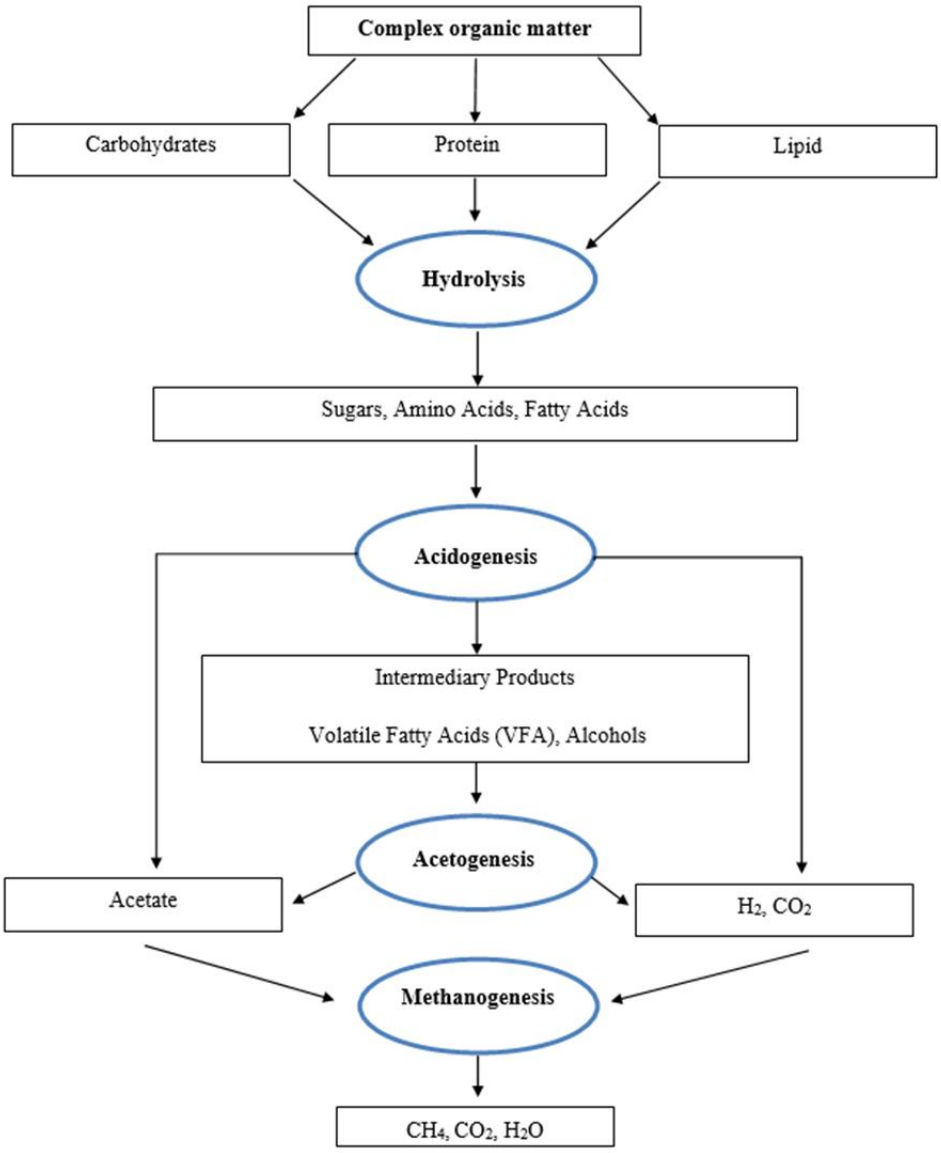

Figure 1.4: Anaerobic digestion processes

In the integrated system, four parameters are condemned to be crucial in the anaerobic digestion of POME: temperature, solid and hydraulic retention time, pH, and organic loading rate. This is due to the microbial community in the anaerobic digestion process being highly sensitive to the process parameters function in a favourable condition (Khadaroo et al., 2019a). Thus, the following subsections discuss the significant parameters needed to monitor the anaerobic digestion of POME:

1.4.1 Temperature

In anaerobic digestion process, temperature plays the most crucial role to maintain a healthy digester as any fluctuation that occurs could have a negative impact on the microbial community and biogas production. Temperature has a direct influence on the pH, solid and Hydraulic retention time as well as organic loading rate of the digestive system.

1.4.2 pH

pH also plays an important role in the anaerobic digestion process. Each of the microbial communities has a specific pH region for optimal growth and their adaptability in the anaerobic digestion (Appels et al., 2008a). The methanogens are highly sensitive to the pH with an optimum value of 6.5 - 7.2, while the fermentative microorganisms are less sensitive and can operate in a broader range of pH around 4 - 8.5 (Hwang et al., 2004a; Khadaroo et al., 2019a; Turovskiĭ & Mathai, 2006a).

1.4.3 Solid & Hydraulic Retention Time

Another characteristic that determines the effectiveness of an anaerobic digestion system is the solid retention time (SRT) and hydraulic retention

time (HRT). SRT is the amount of time solids spend in the digester, while HRT is the amount of time liquid sludge stays in the digester.

1.4.4 Organic Loading Rate (OLR)

The organic loading rate is defined as the amount of organic matter which is measured by COD of substrate treated by a specific volume of anaerobic digester in each amount of time. The OLR of a process closely related with the HRT.

1.5 Cooling Tower

Anaerobic digesters operate using either mesophilic bacteria optimized at around 35-40˚C or thermophilic communities over 55˚C. Mesophilic digestion forms the conventional standard allowing stable and resilient processing. However, thermophilic digestion accelerates reaction rate but demands stricter environmental controls. Although thermophiles enhance productivity potential via elevated temperatures, small fluctuation will risk stagnating its biochemistry. Meanwhile, mesophiles can tolerate large deviations in temperature before slowing down its activity (J. K. Kim et al., 2006a). The effectiveness of biogas plants in attaining targeted COD levels and biogas production rate is contingent upon properties of POME and temperature at which POME enters the anaerobic digester This parameter directly influences the percentage of COD removal, a critical factor in meeting the treated effluent discharge standards established by Department of Environment in Malaysia (Yong et al., 2023).

Conventional way for cooling POME is by utilizing cooling pond and mixing tank. Natural cooling in cooling pond is achieved through hydraulic retention time (HRT) while cooling in mixing tank is achieved by recirculation sludge which mixes with POME causing reduction in temperature (Mohammad et al., 2021). Mesophilic components are present in POME which are temperature sensitive. They play a significant role by converting organic waste to renewable gas (i.e., methane). However, since raw POME are usually discharged between 80-90 ˚C, this reduces mesophilic activity thus reducing biogas output and quality from anaerobic digester. Hence, a decent and stable temperature control system is required to maintain temperature of POME at optimum mesophilic temperature (30-40 ˚C) before feeding into anaerobic digester for quality biogas production (Sodri & Septriana, 2022; Yusof et al., 2024).

Utilizing cooling pond (CP) serves some drawbacks in the treatment plant. CP is an open space with a large body of water. With CP system, effluent or water can be lost through evaporation. Another drawback is the release of methane gas from CP which causes ozone layer to deplete. Finally, effectiveness of CP will also decrease over time due to the reduced HRT and capacity of pond as the scum and sludge tend to clump up with each other. Furthermore, based on the study conducted by Yusof et al. (2024), it is proven that this conventional method cannot efficiently control the temperature of POME. Hence, it is proposed to replace these CP and mixing tank with a cooling tower (CT) in this study. CT is a heat exchanger that is commonly utilized for reduction in process

effluent temperature by evaporation. A new technique used in POME treatment plant in recent times are also by introducing CTs for a more stable temperature control before feeding them into the anaerobic digester. There are two types of CTs, natural and mechanical cooling towers. Natural CTs are more commonly used in large power plants as they are bulky. Mechanical CT draws air into system with the aid of fans. Surrounding air drawn into tower will be used to cool down incoming effluent.

1.6 Decanter Cake

Palm oil as a ubiquitous global commodity, produce significant by-products which one of it is palm oil Decanter Cake (DC), within its production cycle. Palm oil DC is a residual biomass generated from the oil clarification process, holds the potential as a co-substrate for biogas production for its richness in organic matter. Through the anaerobic digestion (AD) of organic matter, in this case, anaerobic co-digestion (ACoD) of POME with palm oil DC. The biogas produced mainly composed of methane, CH_4 (55-70%), carbon dioxide, CO_2 (30-45%), hydrogen sulphide, H_2S (0.1-5%) and other trace compounds. It holds promise as a versatile energy reservoir applicable to electricity generation, heat production and transportation fuel.

Both DC and POME transcend mere waste, presenting an opportunity for waste-to-energy initiatives. Recent studies highlighted the ACoD tehcniques as an innovative pathway to enhance biogas production, significantly contributing to renewable energy portfolio (Mehariya S, Patel AK, Obulisamy PK, Punniyakotti E, 2018); (Mirmohamadsadeghi et

al., 2019). ACoD involves simultaneously co-digestion POME and DC within an enclosed tank, thus generate a higher methane yield in the biogas, owing to improved nutrient balanced and digestion rates. However, past studies have primarily operated on a laboratory-scale, focusing on and optimize parameters such as DC: POME mixing ratio, pH, organic loading rate (OLR), temperature and hydraulic retention time (HRT), in which may impact the ACoD performance.

1.7 Problem Statements

Despite implementing such advanced technologies to treat POME anaerobically, part of the problem persists in the palm oil mill domain, such as optimising the factors that affect the biogas production process and efficient effluent treatment aspects in the anaerobic digester. As it was observed that the main challenge lies within the characteristics of the POME itself as it depends on the efficiency of the palm oil extraction process, the quantity and the quality of FFB processed as well as the process control of the mill (Khadaroo et al., 2019b). The different equipment, processes and operational practices applied in the POM contributed to the complication in understanding the POME quality. Hence, the quality of POME is always unpredictable. Understanding the POME characteristics and its effect to the AD design and operational performance become crucial especially for biogas plant developer, who finance and developed the biogas plant for power generation purposes. Malaysia introduced Feed In Tariff (FiT) program in 2016. Initial FiT program introduced by Sustainability Environmental Development Agency (SEDA) was programmed for 16 years, in which the biogas plant

developer will sign a Renewable Power Purchase Agreement (REPPA) with Tenaga Nasional Berhad. Later at 2021, SEDA improved the program by introducing new FiT scheme with 21 years PPA period. Under this new scheme, biogas plant developer has to enter into e-bidding system to secure the FiT quota. Based on the reported data by SEDA Malaysia, the average FiT rate was reduced after the implementation of e-bidding system (SEDA Malaysia, 2022a). This scenario affected the biogas plant developer to maintain high and rising capital expenditure (CAPEX) year by year to develop good quality biogas plant. Apart from this, long term operational aspects of biogas plant are another challenge for biogas plant developer. To maintain its performance for 21 years throughout REPPA period, biogas plant developer must understand all aspects that will affect the AD performance. In this case, understanding of POM and AD is crucial aspects.

The performance of the anaerobic digester (AD) depends on a few critical factors, such as the characteristics of raw POME in terms of Chemical Oxygen Demand (COD), Biological Oxygen Demand (BOD), pH and temperature. The fastest way for the biogas plant developer to assess the performance is by comparing the revenue generation from each biogas plant that sells the green electricity to Tenaga Nasional Berhad (TNB) through FiT program. However, it is found that there is a gap in the performance evaluation of each biogas plant, even though the design of the covered lagoon and installed capacity are similar. Hence, this study aims to evaluate and compare the performance and efficiency of all four biogas plants owned by CGESB. This study would be able to identify and

compare the process and operation parameters that affect the performances of the biogas plants. The investigation started with evaluating raw POME quality entering the AD through the pretreatment process in the conventional cooling pond and mixing tank. The recirculation sludge is added to the mixing tank to increase the pH and decrease the temperature of raw POME entering the AD. The performance of the AD is studied by analysing hydraulic retention time (HRT), organic loading rates (OLR), bottom sludge quality and treated effluent quality. Concerning the biogas quality and quantity, comparison in terms of methane (CH_4), carbon dioxide (CO_2) and hydrogen sulfide (H_2S) composition, and total biogas produced is evaluated. The novelty of this study lies in its comprehensive evaluation and comparison of the performance and efficiency of the industrial size biogas plants, considering various process and operation parameters. By identifying the key factors that influence plant performance, this study contributes valuable insights to optimizing biogas plant operations and enhancing their overall efficiency.

Among few issues related to performance of AD are low biogas production and treatment capability that could be observed for several reasons, such as unbalanced nutrients due to low C/N ratio in POME, insufficient POME production for the anaerobic digestion, ineffective pretreatment process, imbalance of effluent recirculation ratio, and the case of diluted POME due to the processes practice and design in POM. The co-digestion of POME with various waste is widely reported to be able to enhance the production of methane (A Aziz et al., 2020b; Seekao

et al., 2021). One potential substrate that could be co-digest with POME is decanter cake due to its high COD, nutrient content, and biodegradability (Kaosol & Sohgrathok, 2014; Khairul Anuar et al., 2018). Thus, this study has been formulated to improve biogas production through anaerobic co-digestion of POME and decanter cake. To improve the pretreatment process especially on temperature control due to the limitation on the process control of using cooling pond and recirculation sludge in the mixing tank, cooling tower was introduced.

Among the various biogas capturing technologies available, the In-Ground Lagoon Anaerobic Digester technology is widely preferred for the POME treatment. It is simple, capable of tolerating a high OLR, has a stable operating system, and is easier to operate (Sharvini et al., 2020). However, there are some limitations, such as the necessity to maintain a mesophilic condition, lack of mixing element, and loss of effective volume due to sedimentation (Harris & McCabe, 2020). Therefore, an analysis of the economic performance is needed by conducting a techno-economic analysis to estimate the capital and operating cost as well as the selection of the optimal technology for the anaerobic digester. Subsequently, an effective POME treatment system is introduced using the In-Ground Lagoon Anaerobic Digester technology through new engineering design and operational practises with sets of optimum operating conditions.

1.8 Research Objectives

The general objective of the entire study is to determine the optimum operating parameters to improve the performance of the in-ground lagoon anaerobic digester. Optimisation strategies were implemented

after identifying the crucial parameters, and their effectiveness was assessed. This study was conducted in four different biogas plant locations in Malaysia. Despite the uniform engineering and technical principles underlying the design of these plants, variations in performance were observed. Hence, the entire study focused on detailed information about the effect of critical parameters, operation practices, and process control of the in-ground lagoon anaerobic digester. Additionally, the study explores the impact and correlation of different Palm Oil Mill Effluent (POME) qualities originating from four distinct palm oil mill (POM) processes and designs.

The specific objectives of this research are as follows:

a) To compile, analyse, and compare two years of operational and process data collected from four biogas plants and palm oil mills in Malaysia
b) To identify critical parameters affecting industrial anaerobic digester performances
c) To optimise industrial in-ground lagoon anaerobic digester performances by controlling incoming POME temperature via cooling tower application
d) To improve and optimise biogas quality and quantity via industrial anaerobic co-digestion (ACoD) of POME and decanter cake (DC)
e) To perform a techno-economic analysis of the optimisation plan

1.9 Research Scope

The following research scopes are carried out to ensure that the research objectives (Section 1.7) are achieved. In order to identify the critical parameters that affected performances of four in-ground lagoon anaerobic digesters, the profiling of palm oil mills and biogas plants was conducted. The data was gathered through physical interviews, and its authenticity was checked based on the Written Declaration Document submitted to the Department of Environmental Malaysia. Among the parameters recorded and investigated are the palm oil mill processes information, equipment used, and process control practices. As for the biogas plants, design data such as organic loading rate (OLR), sizing, hydraulic retention time (HRT), pre-treatment process, mixing mechanism and biogas collection and treatment process were collected. The monitoring instrument and equipment, such as flowmeters, transmitters, online and portable biogas analyser and SCADA system were also recorded and validated.

The first important milestones for this research were achieved with the POME Characteristics Study. The weekly data was collected for 2 years, from July 2019 to June 2021. Several important parameters were analysed such as COD, BOD, TSS, total solid, oil and grease, temperature, and pH. The POME produced for all four palm oil mills was compared to specific processes and effluent management practices involved in each palm oil mill. This study is critical because the in-ground lagoon anaerobic digester requires detailed information on POME characteristics. The study was conducted by collecting POME in the drain

after the cooling pond. This sampling point was chosen because of the existing intake point of POME to the biogas plant. The effluent drainage flows to the open pit, where the pumps were installed. Subsequently, POME is delivered to the mixing tank or cooling tower through piping.

In parallel with the POME characteristics study, the data on the in-ground lagoon anaerobic digester process were collected. The study on performance evaluation of AD was divided and focused into two main segments of AD, which are effluent and biogas. Under effluent segment, the pre-treatment process, bottom sludge quality and treated effluent quality were examined. While for biogas, its quantity and quality were researched. Under the pre-treatment segment, inlet and outlet POME temperature and pH were recorded. The mixing tank efficiency in controlling pH and temperature was evaluated by recording the amount of bottom sludge and treated effluent recirculated to the mixing tank. Then, the ratio of POME and recirculated effluent and sludge was calculated based on the reading recorded by the flowmeter. On the bottom sludge study, there are few parameters analysed such as pH, temperature, COD, TSS and total solid. The bottom sludge sample was collected by running a pump to withdraw the sample from the piping that connected at the bottom part of the anaerobic digester. This study was crucial because most of the methanogenic bacteria lives in the bottom sludge. Hence, this study will provide more clarity on the biogas production and its quality study. As for the treated effluent quality study, all the data collected was the same compared to the bottom sludge. Both study of bottom sludge and treated effluent was designed and conducted

to examine the efficiency of the in-ground lagoon anaerobic digester. Few crucial findings were derived and explained such percentage of total solid and COD removed, total COD loaded and removed, hydraulic retention time, and organic loading rate of the in-ground lagoon anaerobic digester. Whilst for biogas segment, few key parameters were recorded such as total monthly biogas production and biogas concentration focuses on quality of methane, carbon dioxide, oxygen, and raw and treated hydrogen sulfide. All these data were used to analyse methane and biogas yield and its relation to the COD loaded and removed, amount of biogas produced and its relation to OLR, biogas quality and its relation to the bottom sludge characteristics and finally to evaluate the biological scrubber efficiency.

In order to determine the most critical parameters and the significant differences between the operational data that affected AD performance from all four biogas plants, the two years of data were analysed in detail using various machine learning and statistical methods. The results are analysed using methods such as Analysis of Variance (ANOVA) and Statistical Analysis. Further analysis is also conducted by using a mathematical model, surface, interaction, and box plots. Once the critical parameters affected the AD performance was determined, the optimisation plan was introduced.

The first optimisation plan conducted is related to temperature control and its affect to the AD performance. The study was conducted in BGP A. Industrial twin packed crossflow induced draft cooling tower was designed based on the input POME characteristics and parameters such

as POME flowrate, POME inlet temperature, POME desired outlet temperature, relative humidity, and air inlet temperature. After completion of cooling tower construction, operational data were collected for a period of 6 months from January to June 2022. The six months operational data analysed in details such as the inlet and outlet cooling tower temperature, OLR of AD, bottom sludge and treated effluent pH and temperature, biogas production and biogas quality. The collected data were compared with two years operational data using various machine learning and statistical analysis such as Artificial Neural Network (ANN) and sensitivity analysis to understand the impact and effectiveness of the optimisation plan.

The second optimisation plan to further improve the performance of AD is by introducing co-digestion process. Decanter cake produced in the POM A was collected and analysed. The first step on this study is characterisation study of the decanter cake. Four tests consisted different ratio of dilution rate of decanter cake and distilled water (1:1, 1:5, 1:10 and 1:20) was designed. Each test was duplicated for 12 samples. Among studied parameters are pH, temperature, COD, BOD, TSS, total solid and volatile solid. The results were analysed by comparing its characteristics to POME. The field trial was conducted for a period of 6 months from July 2021 to December 2021. The decanter cake collected in POM A was introduced to the AD through temporary mixing facilities built in BGP A. Diluted decanter cake was transferred using pump and piping system to the inlet mixing tank before pumping into the AD. Throughout 6 months field trial, important parameters recorded and

analysed are daily POME feeding, POME COD, daily decanter cake feeding, daily biogas production and biogas quality, bottom sludge and treated effluent quality in terms of pH, temperature, COD, TSS and total solid. The data obtained for a period of six months field trial are compared with previous two years operational data without decanter cake co-digestion application. The collected data were further analysed by running simulation to predict its performance by using SuperPro Designer. The machine learning study using ANN was designed and studied to understand the long-term impact of decanter cake application in the AD. Both optimisation studies also focused on the economic analysis as part of final evaluation on the effectiveness of the proposed solution. Key parameters discussed in economic analysis are capital expenditure (CAPEX), operational expenditure (OPEX), internal rate of return (IRR), return of investment (RoI) and payback period.

1.10 Thesis Organisation

The summary of the entire research objectives and planning is illustrated in the Figure 1.5 below. This report consists of six chapters. Chapter One (Introduction) briefly explained the current status of palm oil industry in Malaysia, characteristics of palm oil mill effluent (POME), in-ground lagoon anaerobic digestion process, cooling tower technology, and palm oil decanter cake characteristics. This chapter also includes problem statements explaining the challenges of various POME characteristics and their effect on the anaerobic digester performance. Possible solutions, such as the application of a cooling tower and co-digestion of decanter cake into POME to optimize AD performance, were also

discussed. This was also followed by the objectives presented with the research scope. An organisation of this thesis was also summarised in the final section of this chapter.

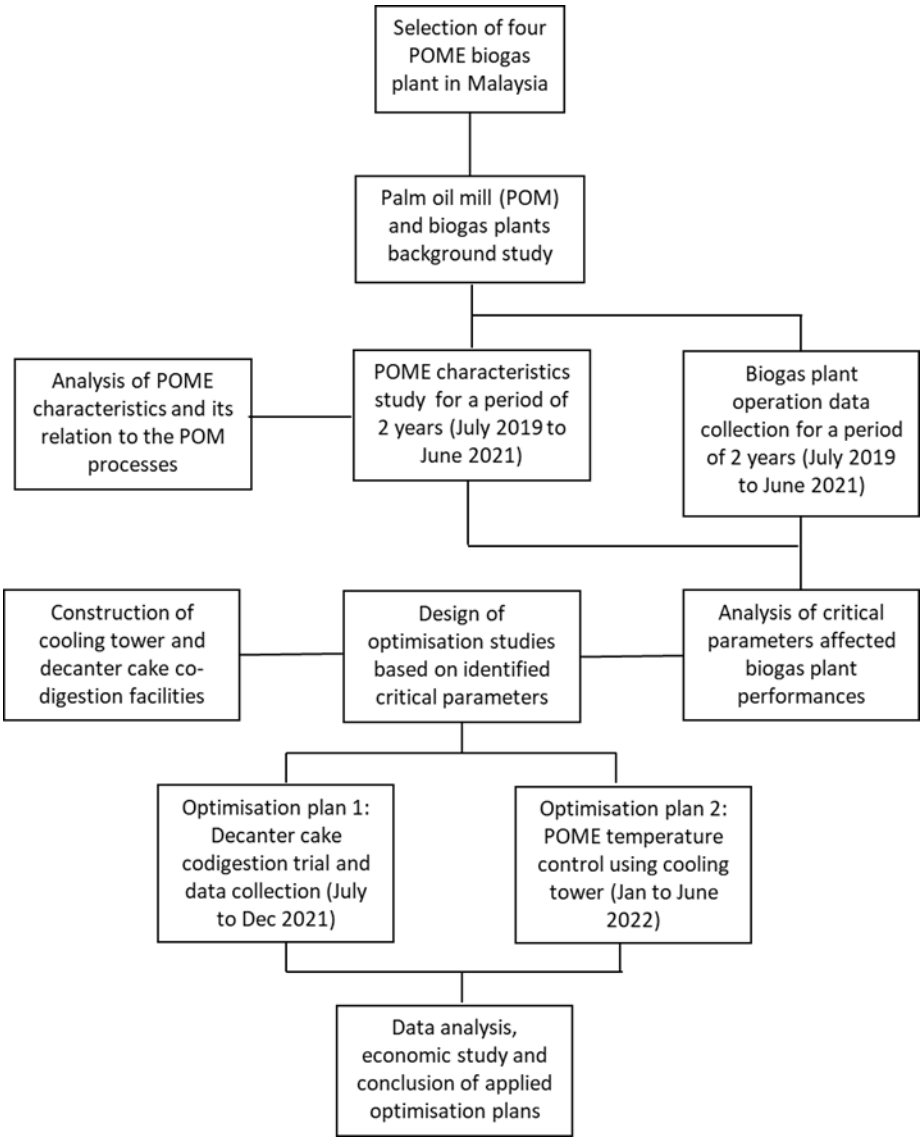

Figure 1.5: Summary of the entire research objectives and plan

Chapter Two (Literature Review) covers the review of Malaysia's palm oil industry, mainly focusing on the detailed processes and equipment in the mill, such as sterilisation, fruit stripping, digestion, clarification, empty fruit bunches (EFB) pressing, separation, and oil recovery. The source of effluent generated throughout the processes was thoroughly

investigated. Furthermore, this chapter presents an overview of the four stages of the anaerobic process. Then, there will be an in-depth explanation of one of the research core scopes; the anaerobic digester technology and important/critical parameters influencing its performance. The study explores the outputs of AD, such as biogas quality and quantity, as well as effluent characteristics, to understand its relations to the input of AD, which is POME quality. These aspects are also discussed by examining the impact of AD design parameters, including hydraulic retention time (HRT), organic loading rate (OLR), temperature control process and sludge management. A review of different methods of data analysis technique, machine learning and optimisation software used in the study were also discussed. Finally, the detailed concept of cooling towers co-digestion of POME and decanter cake were also presented.

Chapter Three (Materials and Methods) provides the list of site locations and all the materials, procedures, and analytical methods used to conduct the present study. This was followed by an experimental procedure including POME, effluent, biogas sampling analysis and procedures, and research parameters. Various data analysis techniques and methods used in this research were also discussed. The chapter meticulously details the methodology employed in the investigation's primary research scopes, namely the study of POME and decanter cake characteristics, the evaluation of AD performance, POME co-digestion, and the application of cooling tower technology. Each aspect is presented separately, offering a clear and systematic overview of the experimental

procedures. Lastly, an overall experimental flowchart was presented that illustrates a clearer picture of the experimental works involved.

Chapter Four (Results and Discussion) is the core of this thesis with three main studies. The first section of this chapter discussed the profile of all four palm oil mills and in-ground lagoon AD. The details of engineering design parameters, equipment used, and process data were compared and investigated. All information in the first section is crucial, which contributed to the analysis of results obtained from the process data of the AD. The second section discussed the AD's two-year operational data. The third section focused on the optimisation plan. There are two main scopes for this section: temperature control of incoming POME by cooling tower and co-digestion of POME with decanter cake (DC). Both studies were conducted based on the analysis results obtained from the second section and conducted in one of the plants (BGP A).

Chapter Five (Conclusions and Recommendations) concludes the work that has been carried out and the important outcomes obtained from this research study. The conclusions reflect the achievements of the listed objectives that were obtained throughout the study. Finally, the recommendations for future study were listed as well. These recommendations were presented in view of their significance and importance related to the current research.

Chapter Six (References) contained the list of references used for this study.

Chapter Seven (Appendices) contained the list of tables and figures that supports this study.

CHAPTER TWO

LITERATURE REVIEW

2.1 Palm Oil Industry in Malaysia

The abundant quantity of palm oil processing mills in Malaysia observed leads to that large amount of POME released annually during palm oil extraction. Based on the data on the amount of crude palm oil production each year, the quantity of POME production can be estimated. According to Chin et al. (2013), about 2.5-3.75 tons of POME are generated for every ton of crude palm oil production. By taking the average of 3 tons of POME generated for every ton of crude palm oil produced (Chin et al., 2013), the amount of POME generated from 2015 to 2020 is calculated and illustrated in Figure 2.1. It is estimated that about 59.88 million tons of POME were generated to produce 19.96 million tons of crude palm oil in 2015. Meanwhile, in 2020, with 19.0 million tons of crude palm oil, 57.42 million tons of POME were generated. POME is considered the most significant pollutant, and with a great amount of POME released from palm oil mills every year, it will have a severe impact on the environment if no proper waste management practices are enforced (Lam & Lee, 2011b).

Table 2.1**:** Composition of products/wastes from the production of FFB (Abdullah & Sulaiman, 2013)

Products/Wastes	Weight percentage to FFB composition on dry basis (%)
Palm oil	21
Palm Kernel	7
Fiber	15
Shell	6
Empty fruitbunches (EFB)	23
POME	28

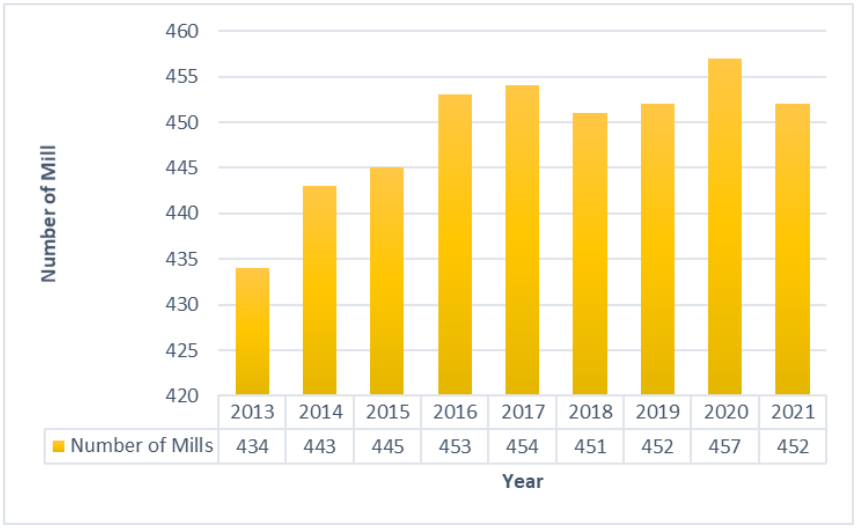

Figure 2.1: Number of palm oil mills operating in Malaysia from 2013 to April 2021

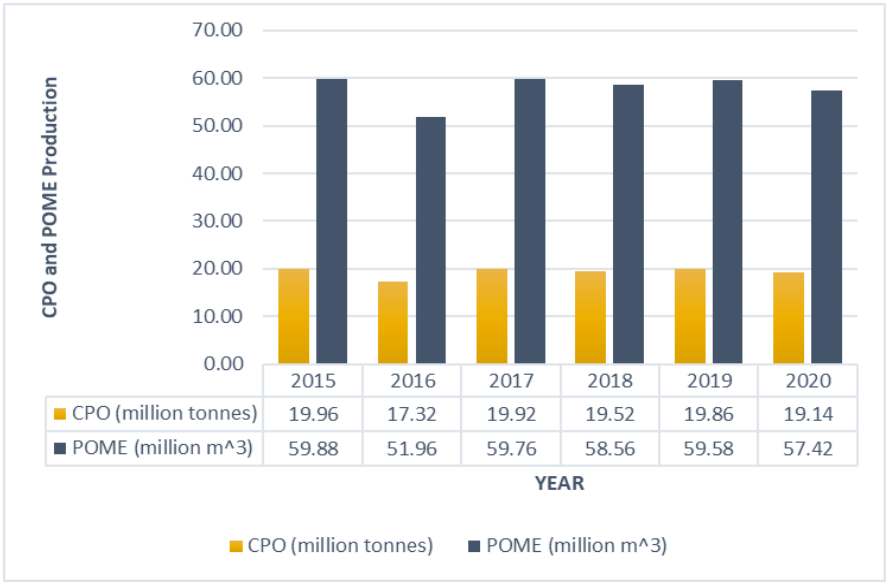

Figure 2.2: Estimated POME generation based on the CPO production in Malaysia

The effluent from palm oil mills is often treated through a series of ponding stages via waste stabilisation. (Genderen, 1995) defined waste stabilisation ponds as a lagoon with shallow dyked structures explicitly designed to treat wastewater by "self-purification" and utilising natural biological, chemical, and physical processes. It is a system which consists of a cooling pond, an anaerobic pond, a facultative pond, and

followed by a maturation pond (Chia et al., 2020). Furthermore, a waste stabilisation system is suitable for warm tropical countries due to their temperature and lengthy duration of exposure to sunlight which offers high efficiency and satisfactory performance of the treatment process (Kayombo et al., n.d.). The general POME treatment system by Palm Oil Mills (POM) in Malaysia is illustrated in Figure 2.3.

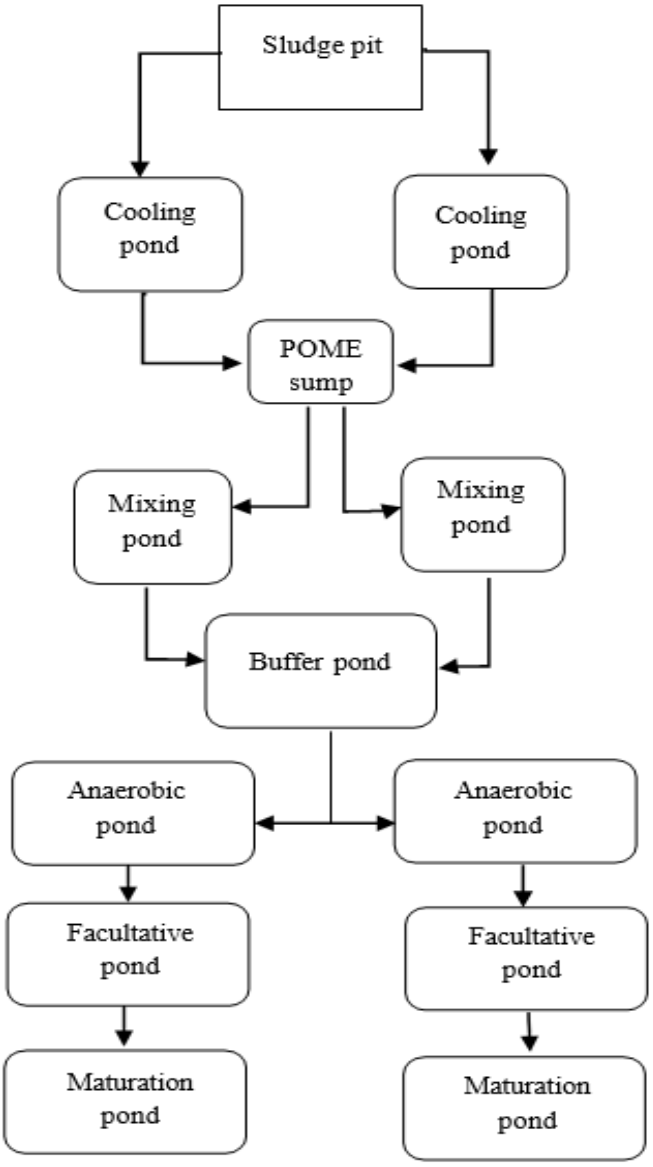

Figure 2.3: Process flow diagram of the palm oil mill effluents (POME) treatment system in mills

2.2 Biogas Industry in Malaysia

The rapidly and steadily growing biogas industry in Malaysia has been driven by many factors such as the increasing awareness of environmental sustainability and need for renewable energy. The Malaysian government plays a crucial role and remains as one of the main players in the industry, particularly through organizations like the Sustainable Energy Development Authority (SEDA). The mainly oversee the implementation of renewable energy policies and initiatives by implementing and administering programs like the Feed-in-Tariff (FiT), which acts as a financial support for biogas projects. Apart from the government authorities, private and agricultural companies particularly in the palm oil industry represent key players in the development of biogas projects. The installation of biogas projects typically depends on organic waste from palm oil mills, livestock farms and food processing plants through the process of anaerobic digestion.

The biogas installations in Malaysia primarily focus and consist of the lagoon and tank system. The lagoon system stores the effluent in a shallow underground basin where the effluent is left to settle. The tank system on the other hand stores the effluent in a sealed tank typically made of durable material like stainless steel to withstand the corrosive nature of the effluent and biogas being produced. Despite there being ample amounts of potential for biogas production in Malaysia, the industry is slower moving when compared to European countries due to lack of notoriety, technological constrains and limited infrastructure (SEDA Malaysia, 2022b). However, Malaysia has introduced the

Malaysia National Energy Plan 2022-2040, which is committed to strengthening the renewable energy market in Malaysia through introduction of the solar, hydro and also the biogas sector. As the prioritization of bioenergy in Malaysia increases alongside organizations like SEDA, the biogas industry is expected to play a significant role in the country's energy transition.

2.3 POME Characteristics and POM Processes

Palm Oil Mill Effluent (POME) is the thick brownish effluent typically discharged at a temperature between 80 °C to 90 °C with a pH ranging from 4 to 5. While POME is generally regarded as a non-toxic liquid waste since chemicals are not used during oil extraction (Saad et al., 2021a), its discharge without treatment can have significant environmental consequences, particularly for rivers, due to its high organic content and the large volume produced by palm oil mills. POME has fluctuating characteristics due to a combination of wastes from three main sources such as sterilisation of FFB, clarification of extracted crude palm oil, and hydro cyclone separation of cracked mixture of shell and kernel. It leads to 36%, 60%, and 4% of POME comprises steriliser condensate, clarification wastewater, and hydro-cyclone wastewater, respectively (Sethupathi, 2004a). Table 2.2 shows the psycho-chemical characteristics of POME from various sources.

Table 2.2: Characteristics of each source of effluent of POME in palm oil mills (Ahmed et al., 2015a)

Parameters	Units	Steriliser condensate	Clarification wastewater	Hydro cyclone wastewater
COD	mg/L	47,000	64,000	15,000
BOD	mg/L	23,000	29,000	5,000
Dissolved solids (DS)	mg/L	34,000	22,000	100
TSS	mg/L	5,000	23,000	7,000
Total Nitrogen (TN)	mg/L	500	1,200	100
Ammoniacal nitrogen	mg/L	20	40	-
Oil and grease (OG)	mg/L	4000	7,000	300
pH	-	5.0	4.5	-

The characteristics of POME are largely dependent on the efficiency of the operation and process control of the mill. In Malaysia, the widely used method to extract palm oil from fresh fruit bunches (FFB) is by wet palm oil milling process (T. Y. Wu et al., 2010a). The unit operations used for extractions are a steriliser, a stripper, a digester, a press machine, a clarifier, a separator, an extractor, and a purification system (Ehsan et al., 2015b). By understanding the role of each unit operation in the extraction process, steps can be taken to optimize efficiency and reduce negative environmental impacts. The typical processes of wet Palm Oil Mill (POM)s include sterilization of FFB, stripping, digestion, and pressing, clarification and kernel oil recovery.

The first step in extraction of crude palm oil is sterilization, where the FFB is subjected to heat treatment. The FFB is sterilized using pressurized steam at the pressure of 3×10^5 Pa and the temperature of 140°C for 60 to 90 minutes (Pratap Singh et al., 2010). The hot pressurized steam in the steriliser will force the kernel to detach from the shell wall. It is also used to deactivate hydrolytic enzymes and prevent rapid formation of free

fatty acids (Lam & Lee, 2011a; T. Y. Wu et al., 2010b). In the recent development, there has been increasing use of continuous steriliser, a moving conveyor with steam injection at atmospheric pressure (Chew, Ng, et al., 2021). This sterilisation process generates condensate, which contributes to one of the major sources of POME, where the latter produces more (Chew, Low, et al., 2021). The characteristics of steriliser condensate are shown in Table 2.2. As shown in Table 2.2, the total dissolved solids in steriliser condensate are significantly higher than hydro cyclone wastewater.

During stripping process, the sterilised palm fruits are separated from the bunches through a rotating cage (Chew, Low, et al., 2021) The empty fruit bunches (EFB) are collected and conveyed to the plantation ground to be used as raw fertilizers or fuel for the boiler (T. Y. Wu et al., 2010b). Meanwhile, the detached palm fruits are conveyed to the digester. In the digester, the fruits are mashed by a steam-heated cylindrical vessel fitted with a central rotating shaft at 80–90 °C (Lam & Lee, 2011a). During digestion, the fruit's mesocarp is loosened from the nuts and directed into the mechanical press machine to extract the crude palm oil out of the mesocarp (Harsono et al., 2014). After pressing, the palm fruits are separated into two parts: press liquor and press cake. Press liquors consist of mixture of oil, water and some solid impurities, while press cake consists of fiber and nut.

The purpose of clarification is to separate oil from the press liquor that contains high amount of non-oil component. Hot water is added into the clarifier to reduce oil viscosity and facilitate separation of the oil from the

insoluble solids (Harsono et al., 2014). The crude palm oil (CPO), at this stage, contains a mixture of palm oil (35-45%), water (45- 55%) and fibrous materials in different portions (Pratap Singh et al., 2010). The insoluble solids and water are settled to the bottom of the clarifier tank, while the crude palm oil is extracted from the top layer of the clarifier tank. The heavy oily sludge that settled at the bottom of the clarifier tank is sent to a decanter or a sludge separator to recover the remaining crude palm oil.

In the conventional clarification process, oil separation is achieved by settling tanks gravity separation. However, in a modern mill setup, two-phase or three-phase decanters are installed to further recover oil from clarifier underflow replacing continuous settling tanks combined with a sludge centrifuge. A two-phase decanter separates the press liquor into a heavy phase (decanter cake) and a light phase (oil and water) (Mamat et al., 2016). Meanwhile, a three-phase decanter separates the press liquor into three parts which are solid (sludge/decanter cake), heavy liquid (wastewater) and light liquid (oil). The recovered crude palm oil is recycled back to the clarifier. The wastewater is either returned to the clarifier to make up the dilution water or released as POME. As for the sludge, it is sent to the bio-composting plant for land application. According to T. Y. Wu et al. (2010b), 1.5 tons of sludge waste is obtained per ton of produced CPO.

In the kernel oil recovery process, press cake from the press machine consisting of nut and fiber is channelled to a nut/fiber separator. The separation process is accomplished through strong air current induced

by a suction fan (Lam & Lee, 2011a). The fiber is usually sent to the boiler as fuel while the nuts are sent to a nutcracker. During the cracking process, palm kernel is loosened from its shells. The cracked nut is then sent to winnowing for air separation to recovery the kernel. The residue of the shell and broken kernels are sent to a hydro cyclone for further kernel recovery (Harsono et al., 2014). The wastewater from the hydro cyclone is discharged as the final source of POME.

According to Wu et al. (2010b), approximately 0.1 tons of liquid effluent per ton of produced CPO is generated as POME. POME can cause significant water pollution due to the high contents of COD and BOD levels. As shown in Table 2.3, the characteristics of POME vary considerably, with COD value in the range of 50,000-150,000 mg/L^{-1} and BOD value of 25,000-75,000 mg/L^{-1}. POME also contains an average value of 4000 mg/L Oil and grease (OG), 40,000 mg/L of Total Solids (TS), and 750 mg/L of Total Nitrogen (TN). Besides, the acidic pH condition of POME is reported due to the presence of organic acids in complex form (Mohamad Anuar Kamaruddin et al., 2021b)

Table 2.3: Literature data of raw POME characteristics

Parameters	(Bala et al., 2015 b)	(Alhaji et al., 2016 a)	(Lee et al., 2019 b)	(Akhbari et al., 2020b)	(Elvitriana et al., 2021)	(A. Yap et al., 2021)	Average POME characteristics
Temperature (°C)	-	85	90	85	65	-	81.3
pH	4.74	4.7	4.3	5	4.07	3.90	4.5
OG	191	4,000	4,000	4,000	-	4,633	3364.8
Fatty acids	-	-	-	-	1,855	11,874	-
BOD	34,393	25,000	27,000	25,000	26,818	73,412	35,270.5
COD	75,900	50,000	57,500	50,000	60,396	146,824	73,437.7
Total Solids	-	40,500	45,250	40,000	-	-	41,916.7

TSS	14,467	18,000	29,500	18,000	47,375	29,138	26,080.0
Total Volatile Solid (TVS)	13,033	34,000	40,500	34,000	-	-	-
TN	-	750	790	750	700	1126	-
Ammoniacal-nitrogen	-	35	42	35	-	-	-

The environmental challenges posed by POME are significant due to its high levels of COD and BOD (Table 2.3), which can lead to water pollution. In order to comply with the discharge limits set by Department of Environment (DOE), POMs must adopt cost-effective and efficient processes to reduce POME's polluting strength. One possible solution is to use technologies such as three-phase decanters or sludge separators, which have proven to be effective. However, if POMs intend to construct an anaerobic digester to trap methane gas for power generation, such technologies may not be advisable since less COD will result in lower methane production and reduced power generation capacity.

2.4 In-ground Lagoon Anaerobic Digester Processes and Technology

2.4.1 Anaerobic Digestion

The production of biogas from POME requires an anaerobic digestion process, which is a complex mechanism involving interactions between microorganisms through four successive stages, hydrolysis, acidogenesis, acetogenesis, and methanogenesis. Anaerobic digestion is widely used as a treatment system for industrial, agriculture and municipal wastes while producing renewable energy source, that involves the breakdown and stabilisation of organic matters in absence of oxygen which leads to the formation of a mixture of gases, mainly

methane and a combination of solid and liquid effluents, known as the digestate (Anukam et al., 2019b; Y. Chen et al., 2007b; Kelleher et al., 2002b; L Chen & H Neiibling, 2014b). The general reaction for anaerobic digestion is shown in Figure 2.4:

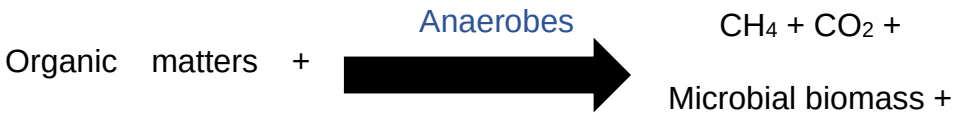

Figure 2.4: General reaction of anaerobic digestion

Several advantages of the anaerobic digestion of POME reported in various studies are reducing greenhouse gas emissions to the atmosphere. It eliminates most of the harmful pathogens, enables energy recovery through methane production, produces nutrient-rich fertiliser, and efficiently treats the wastewater (Anukam et al., 2019b; Khadaroo et al., 2019b; L Chen & H Neiibling, 2014b).

2.4.2 Anaerobic Digestion Stages

Generally, four main steps are involved in the anaerobic digestion process; hydrolysis, acidogenesis, acetogenesis, and methanogenesis. Figure 2.5 illustrates the complete steps of anaerobic processes:

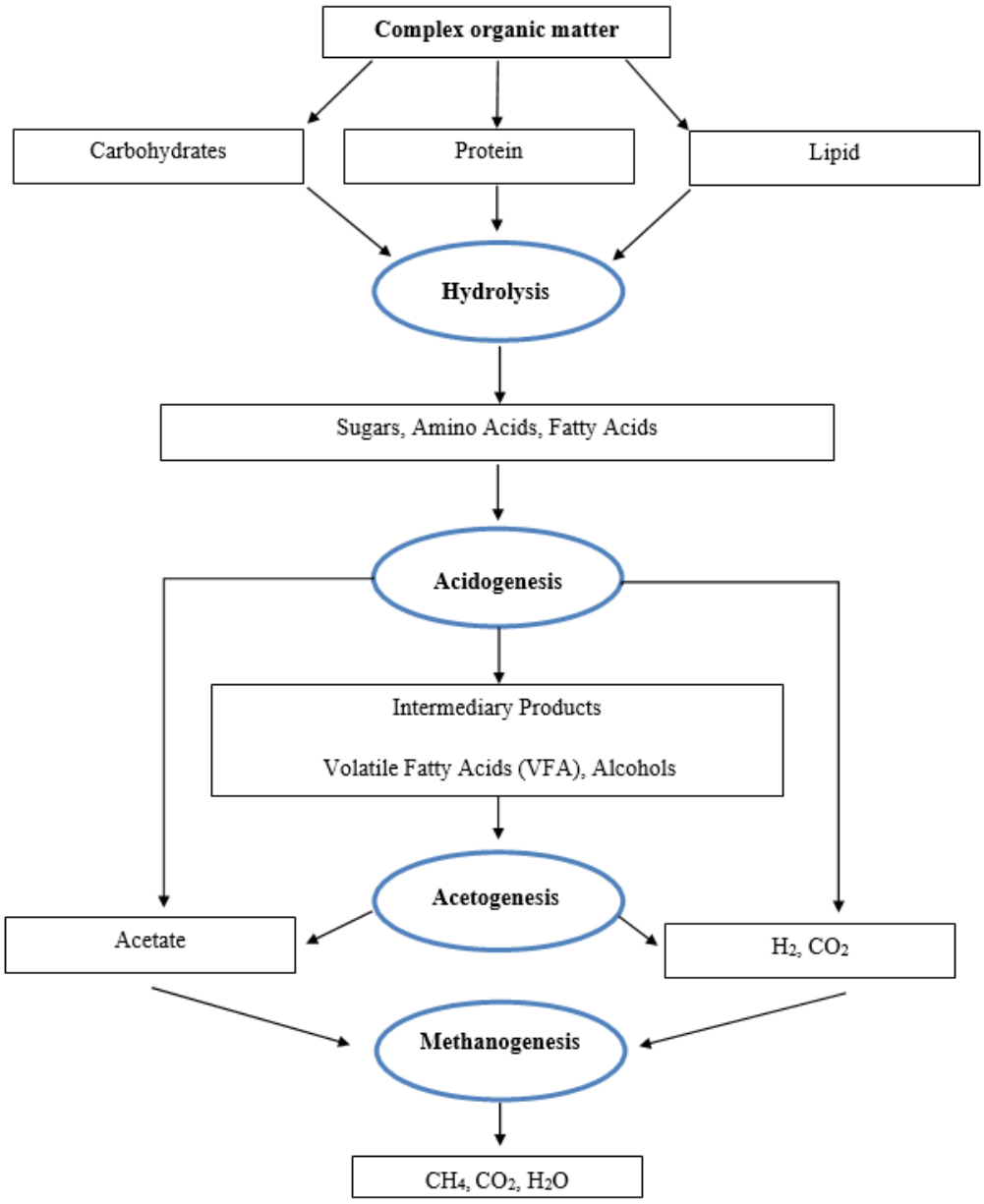

Figure 2.5: Anaerobic Digestion Processes

2.4.2.1 Hydrolysis

The first step in the anaerobic digestion process is hydrolysis, where the organic matter such as carbohydrates, protein, and lipids are hydrolysed from their complex form to their respective monomers. The reactions that occurred in this process are shown in Figure 2.6.

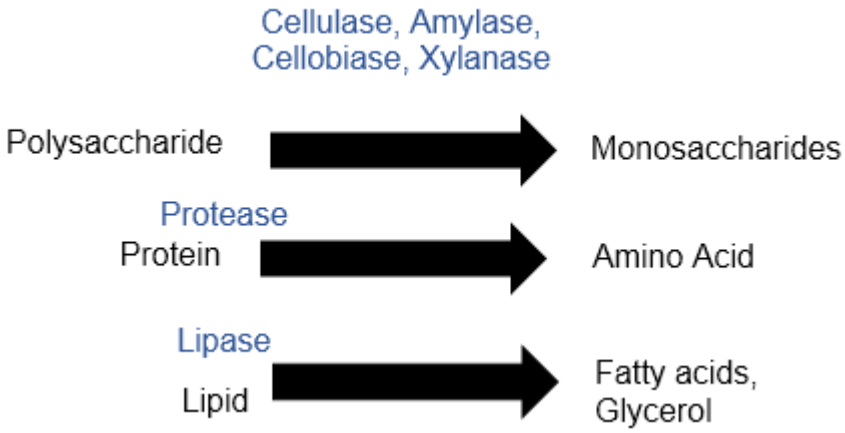

Figure 2.6: Hydrolysis Process

The hydrolysis process is conducted by a group of hydrolytic bacteria. Most of them are strict anaerobes such as Clostridia and Bifidobacteria and some facultative anaerobes such as Streptococci and Enterobacteriaceae (Weiland, 2009). Hydrolysis is carried out by several hydrolytic enzymes such as amylase, cellulases, lipase, and protease. The large complex substrate such as carbohydrates, proteins, and lipids are breakdown into smaller molecules of sugar, a long chain of fatty acids (LCFA), and amino acids, respectively. In this stage, all the raw materials will be converted into amenable forms for the further microbial activities to take place. According to Meegoda et al. (2018), the optimum temperature for the hydrolysis process ranges between 30–50 ◦C and with an optimum pH of 5–7.

Hydrolysis process is a rate-determining step with a relatively slow step which can limit the rate of the overall digestion (Anukam et al., 2019b) as certain substrates such as cellulose, lignin, and hemicellulose, are difficult to degrade, and can be inaccessible to microbes due to their complex structures (Meegoda et al., 2018a). In fact, the main constituent

of oil palm biomass is holocellulose which is composed of cellulose and hemicellulose (Awalludin et al., 2015a). POME as a lignocellulosic matter, needs to be properly treated before being used as a substrate for biogas production in order to increase the degradation rate of POME as well as to boost the biogas production (A Aziz et al., 2020b). Apart from that, the presence of high oil and grease and suspended solid fractions in POME are considered to be obstacles for anaerobic digestion, especially the hydrolysis process (J. Wang et al., 2015).

Thus, various pre-treatment processes are recommended and have been developed which includes mechanical, thermal, chemical and biological interventions to the feedstock in order to enhance the hydrolysis process and to reduce the substrate limitations in anaerobic digestion (Appels et al., 2008b; Roussel et al., 2014). Moreover, (Khadaroo et al., 2019b) also agreed that the biological pre-treatment processes such as ozonation, acidification, ultrasonication, microwave irradiation and alkali pre-treatment does enhance the hydrolysis process as the increase in methane production can be observed.

2.4.2.2 Acidogenisis

Acidogenesis, also known as fermentation process, is the second stage of the anaerobic digestion process, where the hydrolysed products from the first stage (hydrolysis) are degraded into much simpler products. Interestingly, all acidogenic bacteria are also able to participate in the hydrolysis process, but they are more dominant in the acidogenic phase (Deublein & Steinhauser, 2008). The hydrolysed molecules such as simple sugars, amino acids, fatty acids, and glycerol are degraded to

carbon dioxide, hydrogen, acetate, ethanol, volatile fatty acids (VFA) such as propionate acid, butyric acid, valeric acid and lactic acid as well as several inorganic compounds such as ammonia and hydrogen sulphide (A Aziz et al., 2020b; Gozan et al., 2018). VFAs are short-chain organic acids (C2–C6) and regarded as important intermediates for methane production (Deublein & Steinhauser, 2008). Acidogenic bacteria such as Syntrophomonas, Pseudomonas, and Flavobacterium will degrade the hydrolysed molecules to form intermediary compounds such as alcohols (aldehydes) and volatile fatty acids (Divya et al., 2015).

According to Deublein and Steinhauser (2008), acidogenic bacteria have a regeneration time less than 36 hours, which makes the acidogenesis process proceed at a faster rate than other stages of anaerobic digestion. By taking the rapidity of this stage into consideration, it is necessary to note that although the production of VFAs to be the precursors in the final stage of methanogenesis, it is widely reported that, VFA acidification could cause the failure of the digester (Meegoda et al., 2018a).

2.4.2.3 Acetogenesis

Acetogenesis, which is the third stage of anaerobic digestion process, converts the complex intermediary products and higher VFA that are yet to be made accessible in the methanogenesis process into acetate and hydrogen. This is due to some products from acidogenesis that cannot be directly used by the methanogens that include fatty acids longer than two carbon atoms, alcohols longer than one carbon atom, and branched-chain as well as aromatic fatty acids (Boe, 2006). Thus, Acetogenic bacteria such as Acetobacterium woodii, Clostridium acetium,

Desulfovibrio and Clostridium degrades these products (propionic acid, butyric acid, valeric acid, lactic acid, and ethanol) to form acetate, carbon dioxide, and hydrogen (A Aziz et al., 2020b; Deublein & Steinhauser, 2008; Weiland, 2009).

While acetogenic bacteria are mainly hydrogen producers, high concentration of hydrogen exhibits toxic effects towards them (Ali Shah et al., 2014). Thus, a syntrophic interaction between acetogenic bacteria and methanogenic bacteria (Meegoda et al., 2018a) is necessary in order to solve this problem. This syntrophic relationship is known as the syntrophic methanogenesis process which is achieved through interspecies electron transfer (IET) (M. Zhang & Zang, 2019).

According to Deublein & Steinhauser (2008), Acetogenic bacteria could only survive and grow at a very low hydrogen concentration for the acetogenesis process to be thermodynamically favourable ($\Delta G < 0$) while hydrogenotrophic methanogenic bacteria need higher hydrogen partial pressure to survive. The authors mentioned that the hydrogenotrophic methanogens could constantly eliminate the products of metabolism of the acetogenesis process and maintain a low hydrogen partial pressure for the acetogenic bacteria.

2.4.2.4 Methanogenesis

Methanogenesis is the most final and crucial stage for methane production. On the biochemical viewpoint, methanogenesis is considered as an intriguing microbial process as the methanogens are the only microorganisms with a specialised metabolism that are able to produce

large amount of methane while reducing carbon dioxide, hydrogen and cleaving acetate into methane and carbon dioxide (Stams et al., 2006). The regeneration time of methanogens are significantly slower compared to other microbial community in anaerobic digestion, in which they would generally take around 5 to 16 days to regenerate and they are also extremely sensitive to changes in environment, (Anukam et al., 2019b; Deublein & Steinhauser, 2008). The methanogens are strictly anaerobic, where they have acute sensitivity towards oxygen. According to a study done by Kiener & Leisinger (1983), 99% of *Methanococcus voltae* and *Methanococcus vannielii* are killed upon exposure to oxygen within 10 hours.

Methanogens are classified into two different groups of bacteria, which are Acetotrophic methanogens and Hydrogenotrophic methanogens. Acetotrophic methanogens convert and cleave acetate into methane and carbon dioxide, while Hydrogenotrophic methanogens use hydrogen and carbon dioxide to form methane. Hydrogenotrophic methanogens use H_2 as electron donor and CO_2 as electron acceptor to produce biomethane (Demirel & Scherer, 2008). According to Weiland (2009), only few species can degrade acetate into CH4 and CO2, e.g., *Methanosarcina barkeri, Metanonococcus mazei*, and *Methanotrix soehngenii*, whereas all methanogenic bacteria are able to use hydrogen to form methane. Despite the fact that only few species of methanogens are able to produce methane through acetate, A Aziz et al. (2020) reported that a vast majority of methane, which is around 70% formed through

ectotrophic methanogens pathway, while only 30% of methane is produced through hydrogenotrophic methanogens pathway.

2.4.3 Parameters Affecting Anaerobic Digestion

In the integrated system, four parameters are condemned to be crucial in the anaerobic digestion of POME: temperature, solid and hydraulic retention time, pH, and organic loading rate. This is due to the microbial community in the anaerobic digestion process being highly sensitive to the process parameters function in a favourable condition (Khadaroo et al., 2019b). Thus, the following subsections discuss the significant parameters needed to monitor the anaerobic digestion of POME.

2.4.3.1 Temperature

In anaerobic digestion process, temperature plays the most crucial role to maintain a healthy digester as any fluctuation that occurs could have a negative impact on the microbial community and biogas production. Temperature has a direct influence on the pH, solid and Hydraulic retention time as well as organic loading rate of the digestive system. Anaerobic digestion can be conducted at three different temperature regime, which are psychrophilic (<25 °C), mesophilic (35-42 °C) and thermophilic (45-60 °C) condition (El-mashad, 2004; Khadaroo et al., 2019b; Weiland, 2009). However, according to Engin (2017), only mesophilic and thermophilic ranges could provide optimum conditions for the anaerobic digestion process. The comparison of anaerobic processes done in thermophilic and mesophilic conditions is summarised in Figure **Error! Reference source not found.**2.4.

Throughout the research, thermophilic conditions have been reported as being superior to mesophilic conditions as it offers many advantages such as reducing pathogens at a higher rate, enhancing chemical and biological reaction rate as well as increasing biodegradation rate of organic matters up to 50% higher (El-mashad, 2004; Khadaroo et al., 2019b). As reported by Jeong et al. (2014a) and Weiland (2009), the increase in specific growth rates of microorganisms especially methanogens in thermophilic conditions, increases the production rate of biogas in anaerobic digestion of POME. On that note, in a study done by Fikri Hamzah, Md Jahim and Mohamed Abdul, (2019), it had been reported that thermophilic anaerobic digester could produce 20.0 day^{-1} of biogas which is higher than biogas produced in a mesophilic condition, 13.5 day^{-1} at organic loading rate (OLR) of 15 kg COD/m^3/d. Therefore, higher operating temperature provides a faster degradation and conversion process due to high microbial growth rate and diffusion rate of organic matters. Consequently, it is reported that, thermophilic digesters could provide a higher OLR or could be operated at a lower hydraulic retention time (HRT) compared to mesophilic condition, in which, typically only 7-14 days are required for the digestion to take place in thermophilic condition while for mesophilic condition, it takes around 30- 40 days to complete the digestion process (Alepu et al., 2016a; Weiland, 2009).

Additionally, in thermophilic conditions, the optimum operating conditions for anaerobic digestion are achieved faster as the oxygen becomes less soluble at a higher temperature (Deublein & Steinhauser, 2008).

Furthermore, thermophilic condition provides a slightly better COD removal rate efficiency with an average value of 91.16%, while the mesophilic condition was 84.49% (Engin, 2017). This is due to the insufficient biodegradation rate at low HRT in mesophilic temperature.

Despite having several significant advantages, thermophilic anaerobic treatments have a lower stability compared to mesophilic treatments (L Chen & H Neiibling, 2014b). According to Weiland (2009), the application of higher temperature could increase the concentration of free ammonia, which could adversely affect the microbial community as well as the treatment performance by inhibiting the role of microorganisms in anaerobic processes. Consequently, when the process is inhibited by ammonia, the concentration of volatile fatty acids (VFA) will increase to counteract the effect of free ammonia by decreasing the pH value (Weiland, 2009). Although the process remains stable, the methane yield is reduced as methanogens are inhibited at pH 7.6 under thermophilic condition (Appels et al., 2008b). Meanwhile, under mesophilic conditions, the inhibition of ammonia is reduced due to low concentration of free ammonia produced (Deublein & Steinhauser, 2008).

Moreover, thermophilic microorganisms are more sensitive towards temperature fluctuation compared to mesophilic microorganisms especially methanogens as they are sensitive to rapid changes of temperature (Deublein & Steinhauser, 2008; L Chen & H Neiibling, 2014b). Weiland (2009), reported that mesophilic microorganisms could still tolerate the temperature fluctuation of +/−3°C without significant reductions in methane production. As for the operating cost, although L

Chen and H Neiibling, (2014) stated that the cost to maintain thermophilic condition is higher. However, argued that it depends on the type of effluents, for instance, effluent from cannery, palm oil mill and coffee processing plant are typically discharged at a higher temperature. Hence, a costly pre-cooling system is necessary to treat these effluents under mesophilic conditions. Nevertheless, mesophilic condition is still preferable due to greater stability and robustness compared to thermophilic conditions.

Table 2.4: Comparison between mesophilic and thermophilic condition for anaerobic digestion

Condition	Mesophilic	Thermophilic	References
Optimum temperature	35 °C	55 °C	(Engin, 2017)
Hydraulic retention time (HRT)*	15-30 days	7-14 days	(A Aziz et al., 2020b; Alepu et al., 2016a)
COD removal rate	76.36 - 92.62 %	89.12 - 93.20 %	(Engin, 2017)
Degradation rate	lower	higher	(El-mashad, 2004)
Microbial growth rate	slower	faster	(Weiland, 2009)
Biogas production rate	lower	higher	(Jeong et al., 2014)
Pathogen destruction	lower	higher	(El-mashad, 2004)
Energy requirement	lower	higher	(Ruffino et al., 2015)
Size of reactor	larger	smaller	
Operation cost*	lower	higher	(L Chen & H Neiibling, 2014b)
Degree of imbalance	lower	larger	(Weiland, 2009)
Degree of ammonia inhibition	lower	higher	
Sensitivity towards temperature fluctuation	lower	higher	(Saad et al., 2021b; Weiland, 2009)

*Depends on the process effluent

2.4.3.2 pH

pH also plays an important role in the anaerobic digestion process. Each of the microbial communities has a specific pH region for optimal growth and their adaptability in the anaerobic digestion (Appels et al., 2008b). The methanogens are highly sensitive to the pH with an optimum value

of 6.5 - 7.2, while the fermentative microorganisms are less sensitive and can operate in a broader range of pH around 4 - 8.5 (Hwang et al., 2004b; Khadaroo et al., 2019b; Turovskiĭ & Mathai, 2006b). According to Boe, (2006), fermentative microorganisms tend to produce acetate and propionic acid at higher pH and acetate and butyric acid at lower pH. Therefore, the suggested optimum pH range is 6.5-7.5, to achieve a good stability and performance of anaerobic digestion system as both bacterial groups can function efficiently within this range.

Besides, it is widely reported that instability of pH level could also lead to microbial activity inhibition. Divya, Gopinath and Merlin Christy (2015) stated that the increase in pH over 8.5 could lead to the accumulation of ammonia. Meanwhile, the metabolism rate of methanogens is reported to deteriorate and causes the VFA conversion rate to decrease as the pH dropped below its optimum value of 6.5 (Akhbari et al., 2020a; Y. Chen et al., 2007b). Usually, the reduction of pH value is countered by the methanogens as they produce alkalinity in the form of carbon dioxide, ammonia as well as bicarbonate (Turovskiĭ & Mathai, 2006b). Furthermore, the authors also stated that the concentration of carbon dioxide in the gas phase and bicarbonate in the liquid phase control the pH of the digestive system.

However, while VFA is a key intermediate in anaerobic digestion process, it is capable of inhibiting methanogens at a high concentration (Khadaroo et al., 2019b; Weiland, 2009). Appels et al. (2008) outlined that the production of VFA is toxic to the microbial community, especially to methanogens at a concentration of 6.7–9.0 mol/m^3. Since methanogens

are unable to convert acetate, butyric acid, and hydrogen fast enough into methane and other by- products as the pH of the system is lower than their optimum pH range, the VFA will continue to build-up. Consequently, as the organic acid concentration increases, the pH level continues to drop and this acidic nature could also cause the hydrolysis and acetogenesis to be inhibited (Appels et al., 2008b). Therefore, it can be perceived that the inhibiting effect of VFA increases as the pH of the system is low. As pointed out by Zhai et al. (2015), the undissociated form of VFA moves spontaneously through the cell membrane where they dissociate, causing reduction in pH value, eventually interrupting the homoeostasis of the process.

Thus, the best way to increase pH and buffering capacity of the system is by adding buffer materials such as sodium bicarbonate, sodium nitrate, lime as well as ammonium bicarbonate (Saad et al., 2021b). According to Jun et al. (2009), the addition of ammonium bicarbonate in order to control the alkalinity of the system is reported to be able to maintain a pH close to neutral inside cells which is called ‘metabolism generated alkalinity’. Additionally, ammonium bicarbonate is also able to enhance the pH of raw POME (4 to 5) and sustain the pH of the digestion system to almost neutral (Akhbari et al., 2020a; Lin et al., 2011). Meanwhile, the addition of lime could also increase the bicarbonate alkalinity but it may result in the formation of scale (calcium carbonate) (Turovskiĭ & Mathai, 2006b). However, Sri et al. (2015) stated that there is no need to apply any alkaline additive for POME digestion system as treated effluent of POME contains buffer alkalinity from bicarbonate, thus by recirculating

the treated effluent and mixing it with the raw POME will able to maintain a neutral pH of the system.

Nonetheless, in several studies, it is mentioned that it is important to note that VFA accumulation can be taken as a response to a process imbalance occurring in the system such as variation in temperature, organic overloading, pH and presence of toxicants (Abdurahman et al., 2013; Akhbari et al., 2020a; Mechichi & Sayadi, 2005). Thus, VFA concentration could be a good indicator for the operators to monitor the pH value, the stability of the digestive system and to be able to take curative action in time.

2.4.3.3 Solid & Hydraulic Retention Time

Another characteristic that determines the effectiveness of an anaerobic digestion system is the solid retention time (SRT) and hydraulic retention time (HRT). SRT is the amount of time solids spend in the digester, while HRT is the amount of time liquid sludge stays in the digester. The SRT/HRT ratio can be adjusted by separating the solids and liquids downstream of the digester and recycling one of the separated streams (Appels et al., 2008b). Khadaroo et al. (2019) reported that SRT has a huge impact on the subsequent stages of anaerobic process, in which the decrease in SRT causes the decrease in the extent of anaerobic reactions.

This has something to do with the fact that is mentioned by Turovskiĭ & Mathai (2006b), that each time when the digested sludge is withdrawn, a fraction of bacterial population is also removed, thus to avoid the

declination of the bacterial population in the digester and to assure a steady-state system, the rate of cell growth must at least compensate the cell removal. Otherwise, it could lead to process failure. SRT should be long enough to allow microbial activity, especially the hydrolysis process of the sludge, to take place optimally (Y. Chen et al., 2018). Figure 2.5 summarises the influence of SRT on the breakdown efficiency that could be related to the biogas production. The recommended SRT values for the design are in the range 15 to 20 days (Turovskiĭ & Mathai, 2006b). Interestingly, according to a study that is conducted by Aznury et al. (2017) on POME anaerobic digestion, by extending the SRT through the application of recycle sludge able to achieve better volatile solid degradation rate and COD removal efficiency compared to the digester without recycle sludge.

In comparison to the SRT, the hydraulic retention time (HRT) works differently. HRT usually represents the digester's capacity. As stated by Khadaroo et al. (2019b), the shorter the HRT of a process, the smaller the size of the digester used. The formula to calculate the HRT for POME is shown in Figure 2.7 below.

$$\boldsymbol{HRT} = \frac{\boldsymbol{Volume\ of\ digester}\ (\boldsymbol{m^3})}{\boldsymbol{POME\ flowrate}\ (\frac{\boldsymbol{m^3}}{\boldsymbol{day}})}$$

Figure 2.7: HRT calculation formula

As a matter of fact, for a large-scale biogas plant, a shorter HRT is desired as it could reduce the capital cost of the system by reducing the volume of the digester as well as increases the net electrical energy recovery through an enhanced biogas production (Khadaroo et al.,

2019b; W. Zhang et al., 2017). Although a shorter HRT is reported to increase the process efficiency, longer HRT is necessary for the digestion of lignocellulosic waste such as POME (Meegoda et al., 2018a).

As one of the key parameters in biogas processes, HRT influences the degradation process efficiency, system stability, biogas production, biomass concentration as well as the composition of the microbial community (Schmidt et al., 2018; W. Zhang et al., 2017). Further to this, washing of microbes could happen when the microbial regeneration time is shorter than HRT, which could lead to process failure (Schmidt et al., 2018). Moreover, a shorter HRT could also lead to inhibitory effects as commonly it is associated with VFA acidification (Meegoda et al., 2018a). Therefore, the control of HRT for anaerobic digestion is crucial although it depends on the technologies used, process temperature as well as type of effluents (Lang, 2007).

Table 2.5: The influence of SRT on the breakdown efficiency (Khadaroo et al., 2019b)

SRT	Observation
<5 days	VFA concentration increases due to the loss of methanogens
5-8 days	VFA concentration was still slightly elevated as only partial disintegration of organic compounds occurred
8-10 days	VFA concentration decreases as lipids are solubilised
>10 days	The sludge has significantly solubilized

2.4.3.4 Organic Loading Rate

The organic loading rate (OLR) is defined as the amount of organic matter which is measured by COD of substrate treated by a specific volume of anaerobic digester in each amount of time. The OLR of a process closely related with the HRT. A shorter HRT would result in a

higher OLR as well as reduce the contact time between substrate and biomass (Meegoda et al., 2018a; Poh & Chong, 2009).While high OLR would reduce the anaerobic treatment efficiency, it is reported that increasing the OLR up to a certain extent would increase the production of biogas as the methanogens are functioning effectively (Saad et al., 2021b). However, after that certain extend when the methanogens are not able to convert acetic acid to methane at a fast rate, the biogas production deteriorate as the methanogens are inhibited by the accumulation of VFA and thus reduces the pH of the system (Poh & Chong, 2009; Saad et al., 2021b).

Nonetheless, according to Meegoda et al. (2018), following cost-benefit analyses of municipal wastes, it was discovered that digesters operating at a low OLR and a high HRT provide the highest benefit especially for the digestion process that is operating under mesophilic conditions.

2.4.4 Biogas

Biogas is a colourless and odourless gas which mainly consists of methane (CH_4), carbon dioxide (CO_2), a small amount of hydrogen sulphide (H_2S), hydrogen (H_2), nitrogen (N_2), and trace amounts of carbon monoxide (CO) and oxygen (O_2). It is about 20% lighter than air and has an ignition temperature between 650°C and 750°C (Sri et al., 2015). The production of biogas provides a versatile carrier of renewable energy, as methane can be used for the replacement of fossil fuels in both heat and power generation and as a vehicle fuel (Chin et al., 2013b; Weiland, 2009). The percentage composition of biogas produced from anaerobic process is often determined by the type of feedstocks and the

relative content of methane and carbon dioxide depends on several factors such as the degradability of organic matter, digestion kinetics, digester temperature as well as retention time (Dobre et al., 2014; Monnet, 2003). The general range of percentage composition of biogas is shown in Figure 2.6. The efficiency of the anaerobic digestion process is typically determined by the methane yield as it is the main energy carrier in biogas (Anukam et al., 2019b).

There are various kinds of feedstocks such as food waste, animal manure, municipal waste, sewage sludge and agriculture waste that could be used for anaerobic digestion to produce biogas (Divya et al., 2015). According to A Aziz et al. (2020b), biogas production from agro-industrial wastes is favourable, cheap and available in abundance compared to other waste effluents.

Table 2.6: The range of percentage composition of biogas (Sri et al., 2015)

Element	Composition (%)
Methane	50-75
Carbon dioxide	25-45
Water	2-7
Oxygen	0-2
Nitrogen	0-2
Hydrogen sulfide	0-2
Ammonia	0-1
Hydrogen	0-1

Table 2.7 shows comparisons of biogas and methane yields that can be produced from different types of feedstocks in relation to their methane compositions. POME is regarded as a potential substrate for biogas production as it generates a relatively higher value of biogas and methane yield compared to food, vegetable, and manure wastes.

According to several studies on POME treatment using anaerobic digestion system, the end products were consisted primarily of methane (63-75%) and carbon dioxide (35-37%) (A Aziz et al., 2020b; A. Yap et al., 2021). Yap et al. (2021) estimated that $1m^3$ of POME could generate 25 m^3 of biogas, resulting in the production of 14.35×10^8 m^3 of biogas in 2020. The estimated methane production from POME based on the CPO production of Malaysia in 2020 is calculated and summarised in Table 2.8. It is expected that more than 500k tons of methane could be produced as an energy source if all these POME are treated anaerobically.

Table 2.6: The range of percentage composition of biogas (Sri et al., 2015)

Element	Composition (%)
Methane	50-75
Carbon dioxide	25-45
Water	2-7
Oxygen	0-2
Nitrogen	0-2
Hydrogen sulfide	0-2
Ammonia	0-1
Hydrogen	0-1

Table 2.7: Comparison of biogas, methane yield and methane content from different potential feedstocks

Feedstock	Biogas yield (L/kg VS)	Methane yield (LCH_4/kgVS)	Methane content (%)	C/N ratio	Reference
Food waste	600	440	60-70	3–17	(Divya et al., 2015; R. Zhang et al., 2007)
POME	717	450–500	63-75	13.7	(A Aziz et al., 2020b; Samsu Baharuddin et al., 2013; A. Yap et al., 2021)
Cattle manure	400–450	200–250	49–55	16-25	(A Aziz et al., 2020b; Divya et al., 2015)
Vegetable waste	450	190–400	65	7–35	(A Aziz et al., 2020b; Divya et al., 2015)
Swine manure	400–450	250–350	65	6-14	(Chae et al., 2008; Divya et al., 2015)

Table 2.8: Estimated methane production from POME based on the CPO production of Malaysia in 2020

Parameter	Unit	Value
CPO production	Tons	19,140,000
POME generated[a]	m^3	57,420,000
Biogas produced[b]	m^3	143,550,0000
COD level in POME[c]	mg/L	51,000
COD converted[d]	Tons	2,342,736
Methane produced[e]	Tons	585,684
Energy rate[f]	MJ	29,284,200,000

[a]Assume that 3 m^3 POME generated per tonne CPO produced (Chin et al., 2013b)
[b] Assume that 25 m^3 biogas produced per tonne POME generated (A. Yap et al., 2021)
[c] CPO production and COD of POME based on mean value given by Malaysia Palm Oil Board (MPOB)
[d] Assume that digester efficiency is 80% (Chin et al., 2013c).
[e] Theoretical methane conversion factor is 0.25 kg CH4 per kg COD (Chin et al., 2013c)
[f] Calorific value of CH4 is 50 MJ/kg (Chin et al., 2013b)

2.5 Cooling Tower

2.5.1 Importance of Pre-treatment in Anaerobic Digester

POME is a lignocellulosic (plant dry matter) material (Maniruzzaman Aziz, Khairul Anuar Kassim, Moetaz ElSergany et al., 2019). This means

it must be adequately pre-treated before it can be used for biogas production. Various methods include mechanical, thermal, chemical and biological methods (Ariunbaatar et al., 2014). A different pre-treatment method is applied when treating the raw POME before allowing it to enter the anaerobic digester. The reason for the pre-treatment method is to enhance the anaerobic digestion process. Raw materials that have not been pre-treated take a long time to process. The pre-treatment part enhances or accelerates the hydrolysis step and improves the quality of valuable components (Ariunbaatar et al., 2014). Pre-treatment may also increase the quality of the output of the gas collected from the digester. This process also acts as a catalyst.

When choosing the pre-treatment method, it is important to know the type of substrate used for biogas production. Not all methods of pre-treatment can be applied to treating POME. The effects of pre-treatment are diverse and depend on the treatment's mechanism (Carlsson et al., 2012). Using the wrong method may lead to the formation of toxic products or can even ruin the microbes inside the material.

2.5.2 Sensitivity of Methanogenic Bacteria on Temperature

The gas formed from the anaerobic digestion of POME contains methane, carbon dioxide and hydrogen sulphide. The digester's temperature affects the anaerobic bacteria's activities and waste decomposition. Methanogenic bacteria present in the digester are responsible for converting CO2 to methane (Parry, 1999). Methanogenic bacteria are susceptible to temperature change. Thermal shock will reduce the level of methane production. Reducing the temperature by

10^0C will reduce the bacteria activity and growth rate by 50% (Cioabla et al., 2012).

A study by Mei et al. (2016) studied the effect of heat shock on the performance of the bacteria. Between 45^0C and 50^0C, methane production was not inhibited. Production was partially inhibited between 55^0C and 60^0C, but the microbes recovered. When the temperature was above 60^0C, the performance was inhibited, and there was no recovery. It was concluded that the heat shock increased in severity, and methane production started to reduce (Mei et al., 2016). Another study found that biogas production reduces rapidly as the temperature is reduced (S. Wang et al., 2019). As the temperature decreased by 5^0C (starting from 35^0C), the methane produced also reduced. At 30^0C, the amount of methane is 24% less than the initial. By dropping another 5^0C, the amount was significantly reduced until the activity was inhibited. Therefore, it is essential to monitor the temperature and retain the correct temperature window to prevent a reduction of performance in the digester.

2.5.3 Optimum Growth Temperature Range

For the mesophile to grow, there are conditions for it to produce an optimal result. Different researchers have indicated that the temperature for the microorganism to grow can be more than what is typically stated. The typical range for the mesophile to grow is around 20^0C to 45^0C, with an optimum growth temperature of 30^0C to 39^0C (Zuberer & Zibilske, 2021). Research by Moestedt et al., 2017 compared the usage of two other temperatures to the current 38^0C (Moestedt et al., 2017). This

research used mixed sludge obtained from a Swedish wastewater treatment plant. It was found that at 42^0C, gas yield reduced, the process became unstable and volatile fatty acid (VFA) accumulated. At 34^0C, the production of gas was low. Thus, 38^0C is the optimum condition. These researchers concluded that the anaerobic digester's operating range is around 34^0C until 42^0C.

Another study found that operating the bioreactor at the temperature of 37^0C is excellent for the mesophilic bacteria for POME (Choorit & Wisarnwan, 2007). Instability can be overcome by adjusting the OLR. The operation temperature varied due to the build-up of total VFA. It was found that for POME operating at 37^0C, to obtain satisfactory results. Instability can be adjusted by reducing the OLR. Table 2.9 provides the data collected by the researcher. The optimum temperature should be in the range of 37^0C to 42^0C.

Table 2.9: Operating temperature for mesophiles

Temperature Range (^{0}C)	Optimum Temperature (^{0}C)	Source
34-42	38	(Moestedt et al., 2017)
37-43	37	(Choorit & Wisarnwan, 2007)
35-42	-	(Aznury et al., 2017)
30-42	-	(Akhbari et al., 2020b)
25-34	31-34	(Babaei & Shayegan, 2020)

2.5.4 Design of CT

a) Sizing

The size of the tower is important when designing the column. The area of the CT will determine its size.

$$A = \frac{Q}{C_W}$$

A= area

Q= volumetric flowrate

Cw= concentration of water

The CT's length, width and height can be calculated using the Equation (1) below, by obtaining the area. The length of the CT must always be 1.5 of the width. The tower dimension will determine the size of the tower. This will also will provide the land area required for installing the tower.

$$L = 1.5W$$

$$A = L \times W$$

$$A = 1.5W \quad (1)$$

All the values are multiplied by 20%, which is the safety factor.

b) Basin Dimension

The basin is located below the CT. This is the part where the cooled liquid will be collected. Using the Equation (2) below, the sizing of the basin is obtained.

$$Basin\ Volume = Q \times holding\ time \quad (2)$$

$$Basin\ Height = \frac{V}{L \times W}$$

The length and width of the basin should be the same as the length and width of the CT. Length and width are obtained from the dimensions

calculated in the tower dimension. The factors that affect the basin volume are the holding time and flow rate of POME.

c) Fan Power required

In this section, the horsepower is typically provided by the supplier. An assumption of the tower performance is made before choosing the fan horsepower. The horsepower can then be obtained from this chart.

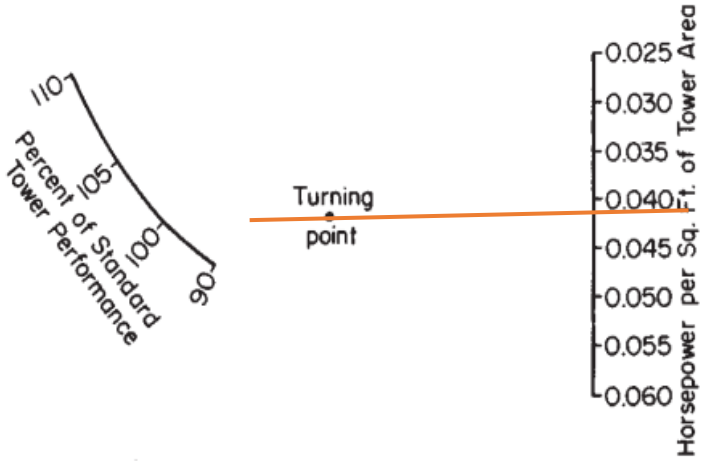

Figure 2.8: Horsepower required per square feet of tower area

Assuming the standard tower performance to be 100%, the horsepower of the fan would be 0.041 hp/ft^2. To find the power the fan uses, the tower's size is multiplied by the horsepower obtained, as in the Equation (3) below.

$$HP\ of\ fan = 0.041 hp/ft^2$$

$$Power = A \times HP\ of\ fan \quad (3)$$

Once the power of the fan required is obtained, the approximate efficiency of the motor is obtained. This is done by using the figure provided below.

Size(kW)	Efficiency (%)
5	80
15	85
75	90
200	92
750	95
>4000	97

Figure 2.9: Approximate efficiencies of electric motors

The motor's efficiency is obtained by relating it to the size of the motor which was calculated in the previous section. by dividing the efficiency by the fan's power, the actual horsepower used is obtained as in the Equation (4) below.

$$actual\ power = \frac{power}{\%efficiency} \quad (4)$$

d) Water Loss

Since CT uses water, it is important to know how much water is lost from the system. Water loss is calculated from the evaporation that is occurring, the drift that carries water droplet as well as the blowdown rate which all occurs inside the CT. By knowing this, the amount of water required can be determined. Evaporation loss (E) is the water evaporated for cooling duty. C is the amount of liquid circulating in the CT. Equation (5) derived the detail calculation of evaporation loss.

$$E = \frac{C \times (T_i - T_0) \times C_p}{\lambda} \quad (5)$$

Drift loss (Equation (6)) is the water droplet formed which is carried along in the air. These water droplets will result in water loss. It will also cause

corrosion or stain, or damage the structure of the CT. Circulating fluid can be in the range of 0.1% to 0.3%

$$D = \%\ of\ circulating\ fluid\ \times C \quad (6)$$

The cycle of concentration (COC) value ranges between 3.0 to 7.0 (Tjahjono et al., 2020). It specifies how often freshwater is added into the loop and used/pumped around before the water needs to be removed. The total dissolved solid increases over time as the tower operates. This is because as evaporation occurs, solid residue is left behind. The Equation (7) derived the detailed calculation of blowdown rate.

$$B = \frac{E}{(COC-1)} \quad (7)$$

Blowdown rate/draw-off is a discharge of a small amount of water to prevent scaling and corrosion (American Society of Heating & American Society of Heating, n.d.).

The total loss (Equation (8)) is the complete water loss from the CT to the environment. This is done by totalling the drift loss, evaporation loss and blowdown rate.

$$M = D + E + B \quad (8)$$

e) Cooling air requirements

Once everything is calculated, it is important to know the requirement for the cooling air. The amount of heat absorbed(Q) is calculated using the Equation (9) below.

$$Q = mCp\Delta T \quad (9)$$

From Mollier's chart, the enthalpy of dry air is obtained. In this case, the enthalpy of dry air is the same as the sensible heat of air. The specific humidity of dry air is also required to get the value.

Once this is done, the amount of cooling air required (Equation (10)) is calculated by dividing the amount of heat absorbed by the specific humidity of the air.

$$m = \frac{Q}{sensible\ heat\ of\ air} \quad (10)$$

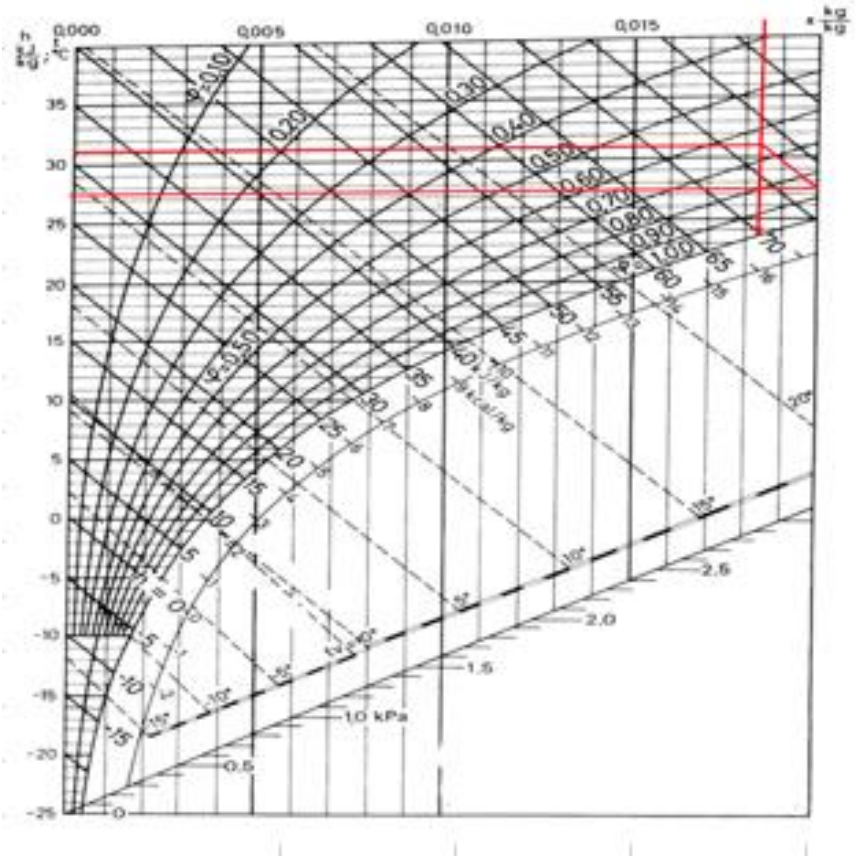

Figure 2.10: Mollier's chart

2.6 Decanter Cake

A large amount of biomass waste prompted concern about the palm oil industry's environmental consequences and sustainability. The sustainable waste management approach seeks to decrease waste by

turning it into high-value products. For each tonne of fresh fruit bunches (FFB), a typical palm oil mill produces 0.6-0.8 m^3 of palm oil mill effluent (POME), 23% of empty fruit bunch (EFB), 13.5% of palm mesocarp fibre (PMF) and 3.5% of palm oil DC (F. Y. Ng et al., 2011).

The DC is the solid residue that is retained from the decanting process of POME. Its high biodegradable organic content and nutrient-rich composition is an excellent feedstock for bioenergy generation such as biomethane and biohydrogen via fermentation. Over the past decade, most DC have been utilised as animal feed and fertiliser, as a raw material for cellulose, biobutanol and biodiesel production, and as a waste product (Kanchanasuta & Pisutpaisal, 2016a). Generally, the cost of producing bioenergy is heavily influenced by the cost of feedstocks. In view of this, agro-industrial wastes have been appealing as low-cost feedstocks for biogas generation by the palm oil mill sector since they can be used immediately on-site for biogas engines, among other purposes. Hence, the DC is a possible feedstock for biogas generation due to its high organic content and low cost.

2.6.1 Decanter Centrifuge

A decanter centrifuge, also known as a solid bowl centrifuge, constantly separates solid materials from liquids in a slurry and has become a vital component in wastewater treatment as well as the chemical, oil and gas drilling, industrial and food processing sectors. Various decanter centrifuges are used today, the most common types being vertical, horizontal, and conveyor centrifuges. The principle of gravitational separation governs the operation of a decanter centrifuge. A decanter

centrifuge's main inner component is a concentrically screw conveyor placed concentrically within a bowl. These two components allow for the mechanical separation of particles and liquids pushed outside the bowl (Anlauf, 2007).

2.6.2 Types of Decanter Centrifuge

Decanter centrifuges are widely used in various industrial applications due to their flexibility. The decanter is one of the most important mechanical inventions in the fruit oil extraction industry for separating the husk from the liquid phases (Tamborrino et al., 2015). It is utilised in a 2-phase or 3-phase configuration.

In a 3-phase decanter centrifuge, the waste is commonly carried to the conical side of the bowl into the centrifugal extractor by a variable flow-rate cavity pump. The two liquids, oil and process water, are discharged through two different liquid weirs on the cylindrical side, while the solids are discharged through husk holes on the opposite, conical side of the bowl (Leone et al., 2015). Adding warm water to the waste inlet at a variable composition of 10 - 30% facilitates the 3-phase sedimentation. The addition of water results in a considerable flow of wastewater and DC which contains 50 – 55% humidity (Dermeche et al., 2013).

2.6.3 Working Principle of POME 3-Phase Decanter Centrifuge

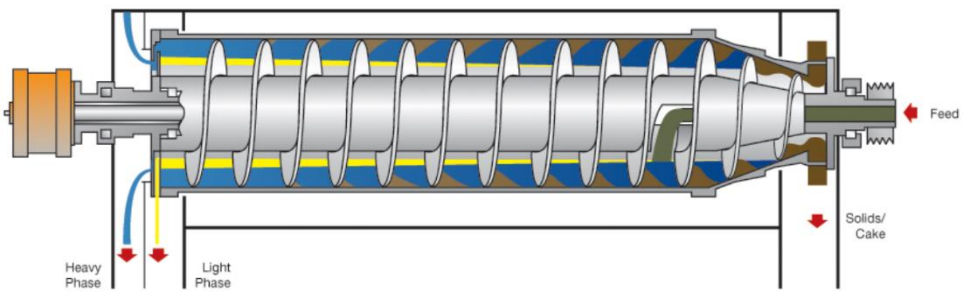

Figure 2.11: Illustration of a 3-phase decanter

In a horizontal cylindrical bowl fitted with a screw conveyor, the palm oil mill effluent (POME) is separated into dry solids (DC), mill effluent (water), and recovered oil fractions. The POME enters the decanter through the inlet feed, which offers practical and moderate acceleration, resulting in fewer emulsions and no plugging. The dry solids settle on the walls of the decanter instantly due to centrifugal force, while the liquid phases - heavy phase (water) and light phase (oil) – separate into two layers.

Ultimately, the 3-phase decanter separates the POME into three different phases – solids (DC), heavy phase liquid (water) and light phase liquid (recovered oil). The conveyor moves the solids to the conical end of the decanter, which rotates in the same direction as the bowl but at a different speed. Prior to being discharged into the collecting vessel, the solid DC is removed from the liquid and centrifugally dewatered. The liquid then overflows into the decanter's casing via an opening in the bowl's cylindrical end. Gravity flow through outlets under the machine allows both phases to exit the collecting chambers in the hood (High-performance Three-phase Decanter Centrifuges).

2.6.4 Characteristics of Palm Oil Decanter Cake

Table 2.10 shows the characteristics of the palm oil DC obtained from various studies. The DC has varying properties owing to the multiple waste sources collected from different mills during different seasons (Y. F. Lim et al., 2021a). As a result, the characteristics of the DC are

generally determined by a mill's operational efficiency and process control.

Water content is considered one of the most crucial parameters influencing the entire anaerobic digestion process. Thus, the total solids (TS) content of a medium is commonly used to define two types of processes; wet digestion, in which TS content is less than 15% and dry digestion or high solid, in which TS content is more than 15% to 20% (Karthikeyan & Visvanathan, 2013). Ultimately, the TS content should be optimised for efficient anaerobic digestion to take place, as reports have shown that TS content higher than 30% may inhibit the digestion performance and contribute to low methane production due to the accumulation of volatile fatty acids (VFAs) (Motte et al., 2013). Besides that, it is also important to identify the ratio of volatile solids (VS) to TS as this reflects the digestibility of the substrate, with a lower value signifying a longer retention time required for the anaerobic digestion (C. C. Yap et al., 2020).

The DC may also cause considerable water pollution due to high organic matter concentration, directly related to biological oxygen demand (BOD) and high chemical oxygen demand (COD) levels. As seen in Table 2.10, the amount of COD found in DC ranges from 270,000 – 1095,000 mg/kg. Additionally, BOD/COD ratio signifies the biodegradability of the wastewater and should exceed 0.5 to be deemed suitable for biological treatment (C. C. Yap et al., 2020).

The major portion of biodegradable material is composed of carbohydrates such as sugar, starch, cellulose, hemicellulose, proteins consisting of long chains of amino acids, and lipids, which consist of long chains of fatty acids. According to Table 2.10, the carbohydrates found in DC range from 8,000 – 427,000 mg/kg. More importantly, the digestion of cellulose and hemicellulose contributes to biogas production. It can be seen that the DC contains cellulose, ranging from 147,000 to 719,000 mg/kg, as well as hemicellulose 13,000 – 531,000 mg/kg, making it a viable source of biomass for bioenergy production.

Another significant characteristic detected is the presence of lignin, a chemical component in lignocellulosic feedstock that functions as a binder, supporting the cellulose and hemicellulose in the lignocellulosic structure (Awalludin et al., 2015a). In Table 2.10, the lignin content in DC ranges from 269,000 – 321,000 mg/kg. Due to the nature of lignin, its complex structure makes cellulose and hemicellulose inaccessible to be digested in the anaerobic digestion process. Hence, pre-treatment methods to remove the lignin to make the microorganisms more accessible to digest the cellulose and hemicellulose are important in ensuring a high biogas yield.

The biomass's total nitrogen content is important as nitrogen aids in the replication of microbial cells for protein synthesis. The total nitrogen content detected in DC ranged from 31.30 – 33,000 mg/kg. Although the nitrogen content is considerably lower, when the DC is added as a co-substrate in the digester system, it provides sufficient nitrogen content to make up the nutrients for sufficient microbial activity to occur (C. C. Yap

et al., 2020). The carbon to nitrogen C/N ratio is a significant parameter in determining the availability of nutrients to enable microbial development in the DC. As can be seen in Table 2.10, the C/N ratio detected in DC was from 9 to 25%. (Choong et al., 2018) proposed that the optimal C/N ratio is 20 – 30, as skewed values will negatively impact the anaerobic digestion. If the C/N ratio is too high, slow degradation of biomass occurs, and if it is too low, inhibitors such as ammonia will accumulate.

The ideal pH for the digestion of DC and POME is 6.8 – 7.2, which is the optimal range for methanogenesis. However, it can be seen from Table 2.10 that the pH detected in DC is around 5, which is lower than the ideal pH requirement. The pH must be enhanced and maintained during the anaerobic digestion since it influences the development of microbial cells and methanogen and the concentration of VFAs (C. C. Yap et al., 2020).

Table 2.10: Characteristics of palm oil decanter cake

Characteristics	(Chaiktkaew et al., 2015a)	(Suksong et al., 2015a)	(Kanchanasuta & Pisutpaisal, 2016b)	(Mamimin et al., 2019a)	(Tepsour et al., 2019a)	(Saraf et al., 2020a)	(Y. F. Lim et al., 2021b)	(Chan et al., 2021a)	(Kumar Mamindlapelli et al., 2022)
TS	94.1%	99.16%	754,480 mg/kg	297.5 g/kg	17.86%	210,000 mg/kg	260.8 g/kg	25.5 %	17%
VS	76.6%	80.74%	212,283 mg/kg	242.2 g/kg	15.51%	155,000 mg/kg	199.1 g/kg	81.9 %	15%
COD	-	-	508,810 mg/kg	-	-	270,000 mg/kg	1,095,000 mg/kg	834,110 mg/kg	100,000 mg/L
Cellulose	14.7%	32.78%	-	32.8 %	-	-	18.48%	14.79%	18%
Hemicellulose	53.1%	-	-	33.1 %	-	-	56.41%	46.59%	4.8%
Lignin	321,000	-	-	34.1 %	-	-	25.10%	38.62%	12%
Nitrogen	3.3%	31.30%	-	-	2.22 %	-	21.1 g/kg	2140 mg/L	2.4%
Lipids	11.5%	-	-	-	2.56 %	70 mg/kg	-	15.38%	-
Carbohydrates	11.9%	8.0%	-	-	42.7 %	-	189.4 g/kg	-	-
pH	4.71	-	-	4.7	427,000	5.1	4.8	4.8	3.8
C/N ratio	25%	-	-	-	19.23%	5.1	8.98	49.55	18

2.6.5 Anaerobic Digestion of Palm Oil Decanter Cake

A study on waste utilisation of DC for biogas fermentation showed promising results (Kanchanasuta & Pisutpaisal, 2016a). The DC was co-digested with anaerobic sludge seed in a batch fermentation system set up at 37oC and 150 rpm. It was reported that the DC functioned syntrophically in the presence of the sludge seed, which was inclusive of

methanogenic bacteria and indigenous microorganisms as the efficiency of biogas generation was greatly increased throughout the whole process. The highest methane generation of 418.9 mL/g was obtained with 2.5% total solids (TS) content after 72 hours of fermentation. The addition of sludge seed significantly enhanced the microbial cells and microbial groups which improved and maximised biogas production yield. It was concluded that the type of inoculum determined the type of fuel gases generated by the fermentation of the DC.

Another study by Saraf et al. (2020b) on biogas production from DC with a combination of solid and liquid state anaerobic digestion showed a significant decrease in Chemical Oxygen Demand (COD). The decanter cake was oven dried for 48 hours in a convection oven at 95^{o}C, prior to the anaerobic process. The DC characterised after the anaerobic digestion showed a COD reduction in 70 to 93%. It was also recorded that further increase in the reduction of COD resulted in an increase in biogas generation up to 93%, which corresponded to 0.120 m^3/kg. The study also highlighted the importance of the temperature of the anaerobic process on COD reduction and subsequent biogas production. As the temperature increased to 38oC, the COD reduction was at its highest, at 93%, with biogas production increasing up to 0.120 m^3. This inferred that an optimal temperature is needed for the anaerobic process in order to yield a higher production of biogas.

Furthermore, a study on the solid-state anaerobic co-digestion of Palm Oil Empty Fruit Bunches (EFB) and Palm Oil DC was done using 15% TS content under mesophilic conditions of 35oC (Tepsour et al., 2019b).

The mixing ratio of EFB to DC varied from 1:1 to 19:1, with a 5% addition of Palm Oil Ash (POA). The results showed that the highest methane yield was obtained at 414.40mL/g-VS, using an EFB:DC ratio of 1:1. This can be attributed to the synergistic effect between the two substrates in co-digestion due to the difference in C:N ratio between both substrates. The EFB is a carbon rich substrate with an 88.8 ratio while the DC is nitrogen-rich, with a ratio of 19.23. Since a C:N ratio of 20-30 is best suited for anaerobic digestion systems, the co-digestion of EFB with another low carbon substrate, such as the DC, balances the C:N ratio needed for the optimum anaerobic process. Even though a 1:1 ratio provided the highest methane yield, the other mixing ratios also provided relatively good methane yield, which concludes that the anaerobic co-digestion mesophilic operation is more flexible in adjusting mixing ratios according to the availability of substrates.

A similar study done by Chaikitkaew et al. (2015b) on the solid-state anaerobic digestion of DC exhibited comparable findings. The solid-state anaerobic digestion was carried out at a TS content of 25%, with palm oil biomass at mixing ratios ranging from 2:1 to 6:1. The experiments were conducted under mesophilic conditions of 37oC for 45 days. It was also found that the methane yield decreased as the mixing ratio increased. The highest methane yield was recorded at a ratio of 2:1, with the DC producing 130 mL/gVS. In terms of methane production, 41 m^3/ton-waste was obtained from the DC. This was inferred due to the high presence of lignin in the DC, which hinders enzymatic conversion of cellulase during the anaerobic process. The lignin inhibits cellulose accessibility to

enzymes, which in turn causes a lower methane yield. It was also noted that higher mixing ratios may cause organic overloading, which is the presence of organic acid at higher concentrations that contribute to the increase in volatile fatty acids (VFA). This hinders methanogens in the anaerobic digestion system resulting in lower biogas yield.

In addition, (Suksong et al., 2015b) research on anaerobic co-digestion of Palm Oil Mill Effluent (POME) and DC with different mixing ratios to produce biohythane, a combination of biomethane and biohydrogen, also showed exciting results. Thermophilic conditions of 60oC and 70oC at a constant pH 5.5 were used in the study to cultivate the inoculum needed in the first and second stages of the process. After 20 days of anaerobic digestion, the highest methane yield obtained from the second stage of the co-digestion was recorded at 391.62 mL/gVS, with a mixing ratio of 1:5. Also, the COD removal efficacy recorded for the same mixing ratio was higher than 58%, which subsequently led to a maximum methane production of 51.59 m^3/ton-waste. As the substrate ratio increased, there was a relative reduction in removal efficiency of VS, with the data being 60.4% for a mixing ratio of 1:5. Significantly, the study also proved promising results in terms of the removal efficiency of cellulose, hemicellulose, and lignin. With a 1:5 mixing ratio of POME to DC, the removal efficiency of cellulose, hemicellulose and lignin were the highest at 57.60%, 40.98% and 27.21%, respectively.

An identical study was done on the enhancement of biohythane production from two-stage thermophilic fermentation of POME and DC by (Mamimin et al., 2019b). The biogas production from co-digestion of

DC with POME was conducted with a variation of 5 to 20% TS content which corresponded to the initial VS loading of 48 to 72 g VS/L. In the second stage, the methane yield obtained from the co-digestion with the DC was 248 mL/gVS. Overall, the biohythane production recorded for the co-digestion of POME with the DC was 22.1 to 26.5 m^3/ton waste, with a 10% TS. This was considered suitable for biohythane synthesis as it was a 67% improvement as compared to the mono-digestion of POME. It was concluded that the co-digestion of POME with solid waste is favourable for biohythane generation and cost effective due to the interaction impact of the solid waste with POME having synergistic effects on methane generation, resulting in an increase in biohythane production.

Moreover, a study by Y. F. Lim et al. (2021a) also achieved strong potential regarding the anaerobic co-digestion technology. In this study, the DC was pre-treated with steam at 105^{o}C prior to the process. Mesophilic conditions were adopted in this study with a pH of 7. The results showed that the highest methane production was obtained at 1417.2 mL, which was 185.9% higher than mono-digested POME, with a DC to POME ratio of 0.8 (42.985 DC/L POME). It was also reported that methane generation decreased as the ratio exceeded 0.8, attributed to the increase in carbon sources due to the addition of substrate.

The pre-treated DC was easily accessible by the bacteria to hydrolyse the cellulose and hemicellulose. As a result, methane production increased. In terms of solids content removal, the co-digestion achieved an overall removal efficiency of 42.41% TS, 51.74% VS and 49.21% TSS. This indicated that the mixture ratio of 0.8 offered the most significant VS

reduction compared to other mixing ratios and mono-digested POME because it also produced the most methane. The COD removal efficiency was recorded at 90.20%, while the VFA was 94.44%.

The significance of this study was the analysis of electricity produced from methane production. It was reported that the co-digestion at an optimal ratio of 0.8 with steam pre-treatment of the DC was able to generate 4.82 MW of electricity, which was 5.13 times greater than mono-digested POME.

Table 2.11: Comparison of various literature on the anaerobic digestion of Decanter Cake

Substrate	Operating Conditions	Mixing Ratio (POME:DC)	Organic Matter Removal	Methane production/yield	Reference
DC	Mesophilic (37°C)	1:2	-	41m^3/ton-waste 130 mL/gVS	(Chaikitkaew et al., 2015a)
	Thermophilic (60°C, pH 5.5)	1:5	58% COD	51.59 m^3/ton-waste 391.62 mL/gVS	(Suksong et al., 2015a)
	Mesophilic (37°C, pH 7)	-	24% TS	-	(Kanchanasuta & Pisutpaisal, 2016b)
	Thermophilic (55°C)	10% TS	-	26.5 m^3/ton-waste	(Mamimin et al., 2019a)
	Mesophilic (37°C)	1:5 (DC:Water)	93% COD	0.120 m^3/kg decanter	(Saraf et al., 2020a)
	Mesophilic (35°C)	1:1 (EFB:DC)	-	414.40 mL/gVS	(Tepsour et al., 2019a)
DC + Empty Fruit Bunch (EFB) + 5% Palm Oil Ash (POA)					
Steam pre-treated DC	Mesophilic (pH 7)	1:0.8	90.20% COD 42.41% TS	1417.2 mL 0.515 L/gVS	(Y. F. Lim et al., 2021b)

2.6.5 Pre-treatment of Palm Oil Decanter Cake

As previously mentioned, it is found that DC has high contents of lignin, hemicellulose, and cellulose, which categorises it as a lignocellulosic feedstock. Cellulose and hemicellulose are types of carbohydrates that can be broken down into simpler sugars by hydrolytic bacteria, which become necessary in the production of biogas in an anaerobic digester. However, the presence of a complex organic polymer known as lignin that acts as a structure binder in the lignocellulosic structure reduces the degradation of DC, which may inhibit the conversion of biomass into biogas, and cause process instability in an anaerobic digester. Hence, it may be worth considering an investment in the pre-treatment of DC in order to reduce the recalcitrance of the lignocellulosic structure to increase its biodegradability, and, ultimately, the production of biogas in an anaerobic digester.

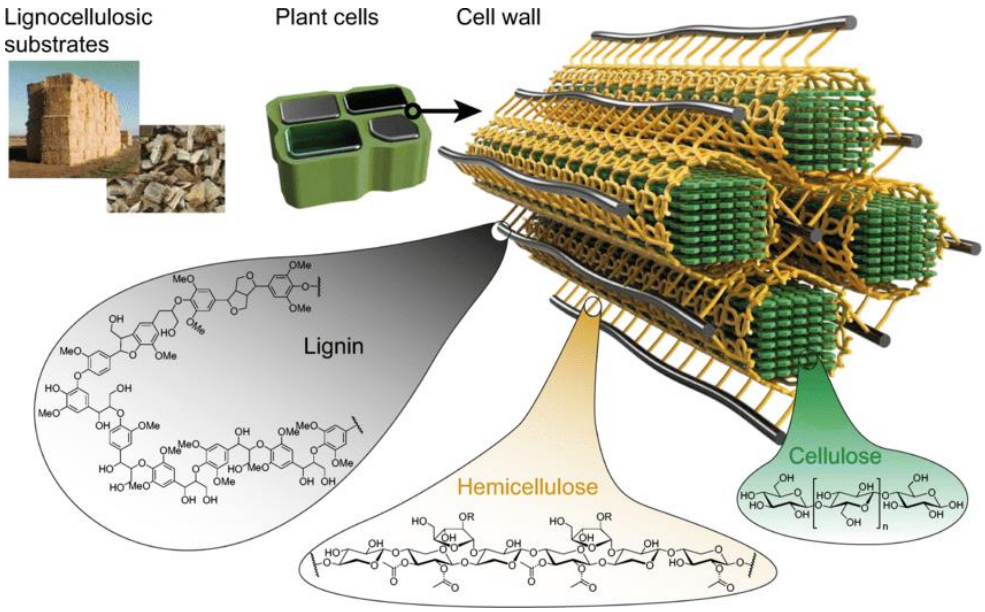

Figure 2.12: Components and structure of lignocellulosic plant cell walls (Brethauer et al., 2020)

Several methods of pre-treating lignocellulosic feedstocks have been documented in the literature. Feedstock size reduction through mechanical comminution (such as milling or grinding) has proven to be one of the most essential means of pre-treatment; it is present in most anaerobic digestion techniques, as it increases specific surface area while decreasing the crystallinity and degree of polymerisation of cellulose. Besides size reduction, other lignocellulosic pre-treatment methods include autohydrolysis (steam explosion), biological hydrolysis (fungal), chemical hydrolysis (acidic and alkaline), irradiation (microwave), thermal steaming, and ozonation. The types of lignocellulosic pre-treatment methods, their effects, and their limitations have been summarised below in Table 2.12.

Although there are several literatures on the pre-treatment of lignocellulosic materials, there seems to be a lack of research on palm oil mill DC as of 2022. It is imperative to note that despite being a lignocellulosic material, DC is unique in that it contains trace amounts of oil and grease, which may yield different results if it undergoes conventional lignocellulosic pre-treatment methods. Hence, it is important to refer to studies that focus on DC or any other substrates that are similar. The following analyses focus entirely on the pre-treatment of DC for biogas production, and they have been summarised in Table 2.13.

A comparative study by Chan et al. (2021b) investigated the effects of oven drying DC at 80°C for one day before grinding into powder form, as well as oven steaming DC at 90°C for 16 hours, as pre-treatment methods for the use of biogas production through the anaerobic co-

digestion of DC and POME with a 0.3:1 ratio under mesophilic conditions. The study found that using steam pre-treated DC in anaerobic co-digestion with POME increased methane yield by 1.7 when compared to using untreated DC, implying that steaming DC could reduce lignocellulosic structural recalcitrance and expand internal surface area. The removal efficiency of the co-digestion of steam pre-treated DC and POME with a 0.3:1 ratio was recorded to have a 97.7% reduction in COD, 16.9% in BOD, 78.8% in TS, and 94.1% in VS. The study also discovered that the methane yield from DC pre-treated with drying and grinding is higher than that of steaming due to the effective mechanical disruption of the lignin complex. However, more research is needed to validate this because the higher yield could be due to a higher mixing rate.

Additionally, the effects of partial ozonation pre-treatment with an O3 loading of 250 mg/h for 20 to 60 minutes, and thermal pre-treatment using a heated water bath at 100°C for 30 to 90 minutes for biogas production via the anaerobic mono-digestion of DC under mesophilic conditions were studied by Rongwang et al., 2017a. It was found that the fermentation of DC that was ozonated for 60 minutes resulted in a highest methane yield of 580.63 mL CH4/g TSadded, while the untreated DC had a highest yield of 382.38 mL CH4/g TSadded; this equated to a 52% increase in methane yield. On the other hand, the fermentation of DC that was thermal pre-treated for 60 minutes resulted in a highest methane yield of 417.65 mL CH4/g TS added, which is only a 9% increase in methane yield. According to the analysis on the total sugar content in DC after pre-treatment, the O3 loading of 250 mg/h for 60 minutes achieved

a 67% increase in the release of total sugars in comparison to untreated DC, which implied that ozonating DC increased the surface area of cellulose and hemicellulose that was accessible for hydrolysis. It was also found that amount of lignin decreased between 40 and 60 minutes of O3 loading. The removal efficiency of the fermentation of DC that underwent ozonation pre-treatment for 60 minutes was observed to have a 33% reduction in TS.

Another study by Kaosol & Rungarunanotai (2016a) investigated the effects of microwave pre-treatment on the Biochemical Methane Potential (BMP) of DC. In this study, DC was pre-treated with microwave irradiation at a power of between 160 and 800 watts for 2 to 8 minutes. It was found that the microwave pre-treatment of DC using a capacity of 160 watts for 8 minutes was most effective as its fermentation resulted in the highest methane yield of 309.9 mL CH4/g COD removed. Whereas the fermentation of untreated DC obtained a methane yield of 248.7 mL CH4/g COD removed, which is a 24.61% increase in methane yield. The removal efficiency of the pre-treated DC at 160 watts for 8 minutes was recorded to have a 18.9% decrease in TS, 10.3% in TDS, 27.8% in TVS, and 27.2% in Total COD.

Table 2.12: Pre-treatment methods of lignocellulosic materials, their effects, and limitations

Pre-treatment method	Effects	Limitations	Reference
Size reduction	Increased surface area Larger pore size Lower crystallinity	High energy consumption High equipment cost May require additional pre-treatment	(Mayer-Laigle et al., 2018; Mustafa et al., 2017)
Steam explosion	Increased surface area Larger pore size Solubilisation of hemicellulose	Incomplete degradation of lignin-carbohydrate complex	(Ramos, 2003; Yunos et al., 2012; Zhou et al., 2016)

		Inhibitor generation at higher temperatures Risk of destruction of hemicellulose	
Acid	Hydrolysis of hemicellulose Disruption in cellulose structure Increased surface area	Corrosive to equipment Expensive	(Solarte-Toro et al., 2019)
Alkali	Lignin cleavage Increased internal surface area Reduction in degree of polymerisation	Less effective if content is high in lignin Requires high temperatures	(Mirahmadi et al., 2010)
Fungal	Removal of lignin Partial hydrolysis of hemicellulose Disruption in lignocellulosic structure	Very slow rate Partial consumption of carbohydrates	(Kainthola et al., 2021); (Vasco-Correa & Shah, 2019)
Oxidation	Removal of hemicellulose and lignin Exposure to cellulose	Expensive High energy consumption	(García-Cubero et al., 2010)
Microwave	Chemical bond cleavage Increased surface area	Uneven distribution of microwaves on material due to non-homogeneity Leads to local overheating (heat spots)	(Hoang et al., 2021)

Generally, the pre-treatment of DC has shown results in increasing methane yield and removal efficiency during the AD process. Even though almost all of the previously reported research was done on a lab scale, it is proven that co-digestion of DC will increase the biogas yield. However, due to differences in operating conditions and DC characteristics, the effectiveness of the studied DC pre-treatment methods cannot be directly compared.

Table 2.13: Comparison of various literature on the pre-treatment of Decanter Cake

Substrate	Digestion method	Pre-treatment method	Inoculum type	Temp.	pH	Fermentation period	Non-pre-treated biogas yield	Pre-treated biogas yield	Biogas yield increase	Ref.
POME:DC (ratio of 1:0.3)	Batch co-digestion, mesophilic, with mixing at 145 rpm	Drying for 24 hours at 80°C, followed by grinding	Anaerobic sludge from POME digestion	35°C	6.8-7.2	35 days	-	~370 mL CH_4/g VS	-	(Chan et al., 2021a)
	Batch co-digestion, mesophilic, with mixing at 110 rpm	Steam (thermal) for 16 hours at 90°C					~100 mL CH_4/g VS	~270 mL CH_4/g VS	~170%	
DC	Batch mono-digestion, mesophilic, with rotary shaking at 100 rpm	Steam (thermal) for 60 minutes at 100°C	Anaerobic sludge seed from beverage processing wastewater	37°C	7.0	-	382.38 mL CH_4/g TS added	417.65 mL CH_4/g TS added	9.22%	(Rongwang et al., 2017b)
		Ozonation for 60 minutes with O_3 loading of 250 mg/h						580.63 mL CH_4/g TS added	51.85%	
DC	Batch mono-digestion, mesophilic, with manual shaking twice a day	Microwave irradiation at 160 watts of heating power for 8 minutes	Anaerobic sludge from POME treatment	35°C	7.2	45 days	248.7 mL CH_4/g COD removed	309.9 mL CH_4/g COD removed	24.61%	(Kaosol & Rungarunanotai, 2016b)

CHAPTER THREE

MATERIALS AND METHODS

This chapter are divided into 4 main categories which are material and methods for POM profiling and POME characteristics study, biogas plants profiling and AD performance study, temperature control by cooling tower and co-digestion of decanter cake with POME. The summary of overall study plan for this research are summarized in Figure 3.1 below.

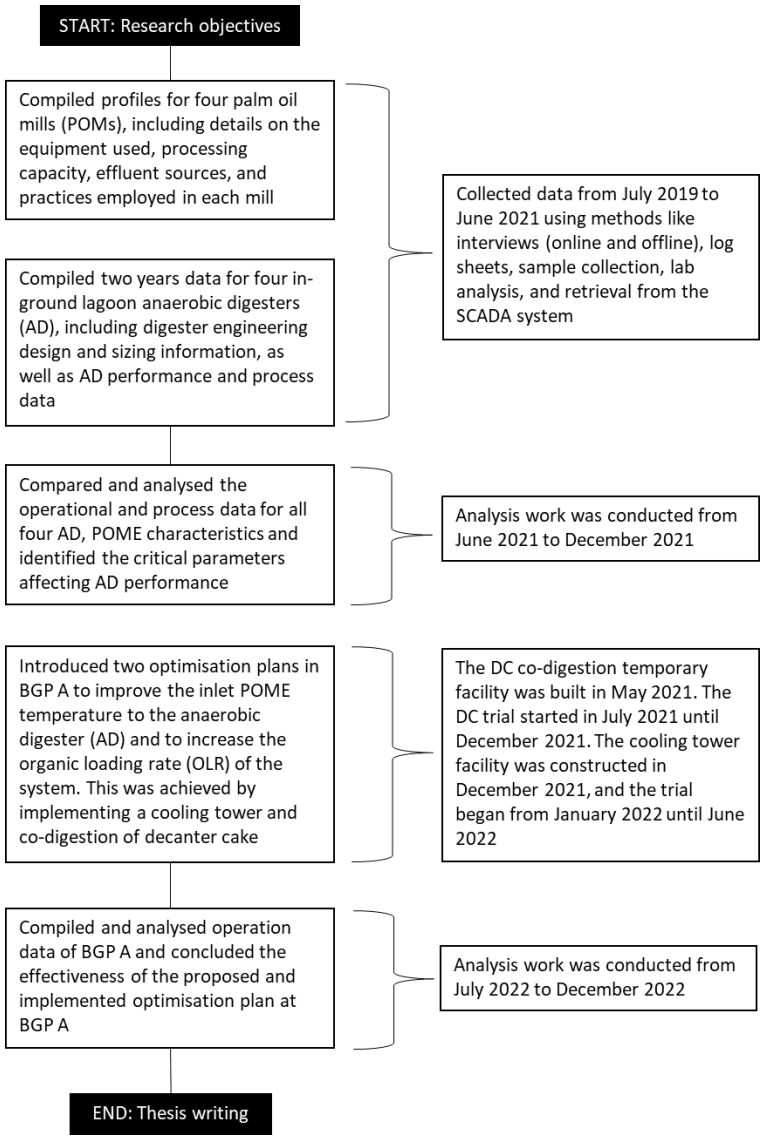

Figure 3.1: Summary of overall research methodologies

3.1 POM Profiling and POME Characteristics Study

This section explained the site location of the study and detailed processes involved in completion of the POME characteristics study. The first step involved in this study is gathering of POM data.

3.1.1 Site Locations

For on-site sampling and sample collections, 4 mills were selected from mills available in Malaysia. The 4 selected mills as illustrated in the Figure 3.2 were as follows: Kilang Sawit Lepar Hilir, 26300 Kuantan, Pahang (POM A); Kilang Sawit Adela, 81930 Bandar Penawar, Johor (POM B); Kilang Sawit Keratong 2, 26900, Bandar Tun Razak, Pahang (POM C); Kilang Sawit Lok Heng, 81930 Kota Tinggi, Johor (POM D).

Figure 3.2: Palm oil mills location

3.1.2 POMs Processing Information

Mills operation data and processing information were collected through semi-structured interviews with the person in charge assigned by the mill manager. The group of operators, lab technicians, and mill management team (mill managers or assistant palm oil managers) were selected and interviewed in the focus group discussion. The qualitative data obtained from the focus group and semi-structured interview discovered the reason for particular issues or problems and actual operation practices in the specific stations and processes plant inside the POM. This technique is in line with the Iterative Research Process presented by Busetto et al., 2020. The design information related to effluent generation factor for the POM, processing capacity and effluent treatment plant design data were obtained from Written Declaration submitted to Department of Environmental (DOE). All of the questions are prepared and used for this study are shown in Appendix 1.

3.1.3 Sampling Method of POME

For POME, grab samples of POME were taken from each mill every week for two years, starting from July 2019 to June 2021. The samples were collected from the drainage line after a cooling pond in each POMs, as in Figure 3.3 below. POME samples taken were stored in the chiller at 4 deg C to prevent excessive deterioration, which will change its characteristics. The lab analysis work is conducted within 48 hours of post-sampling time. This sampling technique is based on the DOE Malaysia Standard Methods for Analysis of Rubber and POM Effluent (4th Edition, 2019).

Figure 3.3: POME sampling point

3.1.4 Parameters for the Characteristic Study of POME and Analytical Methods

On-site parameters such as temperature, volumetric flowrate and appearance of the collected sample in a vial were recorded. The COD, BOD, TS, SS, pH, oil, and grease were analyzed, and the average monthly results were recorded from July 2019 to June 2021. Table 3.1 illustrates the list of parameters and standards used in this study.

Table 3.1: Methodologies implemented in analysing POME characteristics parameters

Parameters	Methodology
BOD_3	3-day BOD test at 30 °C
COD_{Cr}	HACH method 8000[a]
TS	APHA 2450 B
SS	HACH method 8006 (photometric)
OG	APHA 5520 B
pH	In situ test using pH meter (Mettler Toledo)

[a] HACH methods that comply with the APHA standards

All analysis were performed in duplicate and the average values were presented in tables and figures. Analysis of variance (ANOVA) was performed to determine if there is a statistically significant difference between the studied parameters.

3.2 Biogas Plant Profiling and In-ground Lagoon AD Performance Study

This section explained the detailed study conducted in understanding the factors affecting AD performance. The analysis of impact of POME characteristics to the AD performance in terms of effluent treatment capability and biogas generation performance were assessed.

3.2.1 Site Locations

The four selected biogas plants (BGPs) were as follows: Lepar Hilir Biogas Plant, 26300 Kuantan, Pahang (BGP A); Adela Biogas Plant, 81930 Bandar Penawar, Johor (BGP B); Keratong 2 Biogas Plant, 26900, Bandar Tun Razak, Pahang (BGP C); Lok Heng Biogas Plant, 81930 Kota Tinggi, Johor (BGP D). All of the biogas plants owned by Concord Green Energy Sdn Bhd (CGESB) and constructed side by side to each palm oil mills. CGESB is the biogas plant developer and owner. The biogas plants were developed for Feed-In-Tariff (FiT) program. These four plants were chosen because they share a similar in-ground lagoon AD design, despite variations in the characteristics of the POME they process. This targeted selection allows for a more in-depth analysis of the critical parameters affecting AD performance within this specific design framework.

3.2.2 Biogas Plant Profiling

The data related to all biogas plants were gathered based on the Focused Group Discussion (FGD) with CGESB. The Biogas Plant Profiling Form (Appendix 2) was prepared in advance before the discussion and filled up during the session. There are few key personnel involve during the FGD session, where mainly all of them are CGESB staff. The key departments involve during the session are Engineering Design, Project Management and Operation and Maintenance. Among the key personnel involved such as Engineering Manager, Project Manager, Site Engineer, Operation and Process Manager and Maintenance Manager. The representatives from all BGPs are also involved during the discussion and meeting.

3.2.3 Biogas Plant and AD Data Collection

There are two main components for inground lagoon AD, which are the effluent and biogas line. Hence this section explained both methods and parameters recorded and analysed for the AD performance study from June 2019 to July 2021. A composite sample collection method was used for inlet POME, bottom sludge, and treated effluent. Each composite sample is a combination of three grab samples that was taken at different times. Lab analysis was conducted on collected samples to determine pH, temperature, chemical oxygen demand (COD), biological oxygen demand (BOD), total solids (TS), and total suspended solids (TSS) as shown in Table 3.2. Analytical determinations of all parameters were carried out in accordance with the Standard Methods for the examination of water and wastewater (Chan et al., 2021b).

Table 3.2: Methods implemented in analysing effluent and sludge parameters

Parameters	Methodology
pH	
Temperature	
BOD_3	3-day BOD test at 30 °C
COD_{Cr}	HACH method 8000[a]
TS	APHA 2450 B
TSS	HACH method 8006 (photometric)

[a] HACH methods that comply with the APHA standards

The Supervisory Control and Data Acquisition (SCADA) installed in all four plants were used to record all operation data, which includes effluent, sludge and biogas flow rate, biogas temperature and pressure, biogas quality (methane, carbon dioxide, hydrogen sulphide, and oxygen), pump operation and status, etc as shown in Figure 3.4. The quality of biogas produced from the plants was determined using a portable and an online gas analyser, as shown in Figure 3.5. The reading obtained from the portable biogas analyser was manually recorded by the BGP operator, while the SCADA system captures the online biogas analyser reading. All of the data extracted from SCADA were further validated and verified on site by manually checking each instrument's reading. The log sheet and checklist were prepared for the operator to fill up (Appendix 3). Apart from this, interviews with focus groups consisting of plant heads from each biogas plant were conducted to understand each plant’s operational practises and issues.

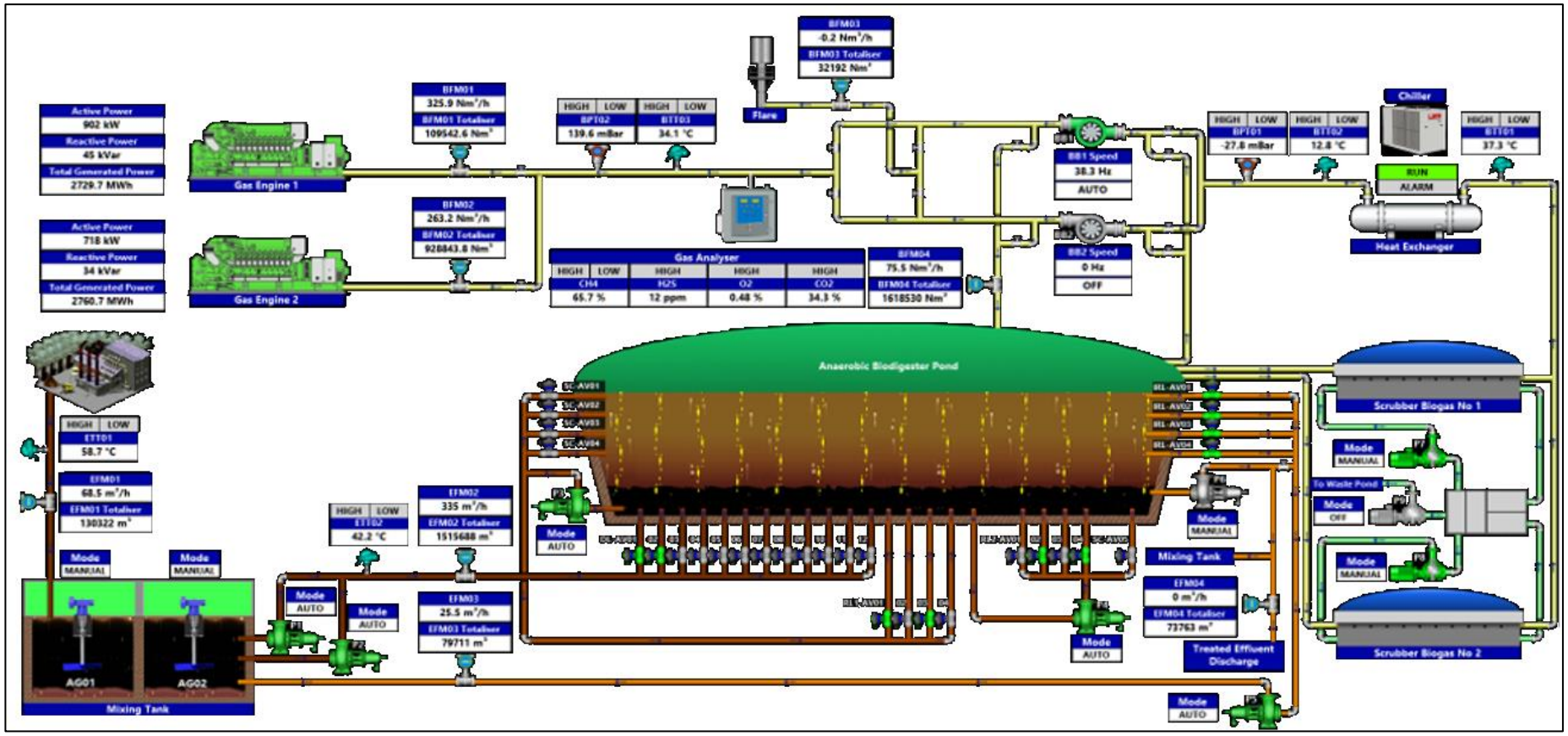

Figure 3.4: SCADA system for biogas plant

Figure 3.5: Online and portable biogas analyser

3.2.4 AD Process Data Analysis Methods

As shown in the process flow diagram in Figure 3.6, this data analysis processes consists of five stages. The first stage is to identify the problem through various literature resources to plan the process flow. Next, data is collected from each set of experiments consisting of different variables on two responses: COD removal and biogas production. The results are analysed using methods such as ANOVA and Statistical Analysis. Further analysis is also conducted by using a mathematical model, surface, interaction, and box plots. These methods are represented graphically and are easier to comprehend. Furthermore, optimisation of the model is performed, and sensitivity analysis is conducted to identify the crucial parameters affecting the responses before a conclusion is made. To identify the crucial parameters that affected the output/results of AD performances (COD removal efficiency, biogas production and methane yield), several input parameters were identified and analysed. The input and output parameters were explained as in the Table 3.3. All

of the input parameter were compiled and analysed from the study of POME characteristics and biogas plant and AD data collection.

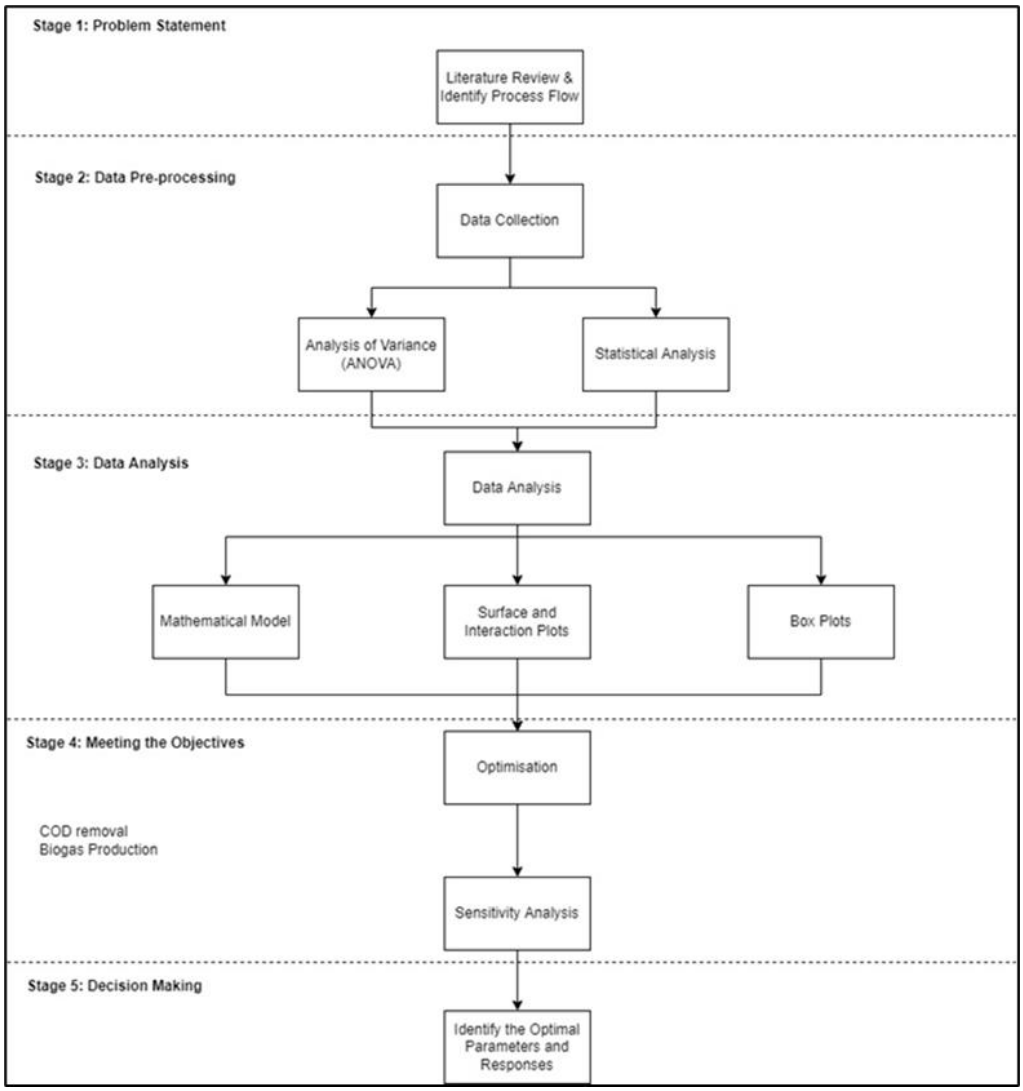

Figure 3.6: Process flow diagram of AD process data analysis

Table 3.3: Parameters analysed for the AD performance study

Input parameters	Output parameters
OLR, HRT, pH and temperature of AD	COD removal
TS, TSS, BOD, COD, OG of POME, treated effluent and bottom sludge	Biogas production
Recirculation ratio	Methane yield
Location	
Mixed liquor suspended solid of bottom sludge	

3.2.4.1 Analysis of Variance (ANOVA)

The statistical analysis was carried out using Design Expert software version 13 to investigate potential differences among the studied parameters. In this study, data were collected from four distinct biogas plants, each with unique conditions and characteristics. Despite using the same in-ground lagoon anaerobic digester, these plants are not traditional replicates due to substantial operational differences. As a result, assumptions related to replicative data, such as normality of residuals and variances equality were not applied. This approach accurately reflects the variations in operational parameters among different plants. While it may limit the generalizability of the findings beyond the specific plants studied, it mirrors the real-world conditions of biogas production, where variations among plants are common. These assumptions impact the scope of generalization but are crucial for maintaining the authenticity and applicability of the research within the industrial context.

ANOVA analyses the parameters using an F-test to determine the significant change in quality standards in a certain design of experiment. The ratio of mean square and residual error is applied to evaluate the significance of a factor among the parameters in the F-test tool. The mathematical equation representing the average of the test is expressed below as in the Equation (11).

$$SS_T = \sum_{i=1}^{n} (\eta_i - \eta_m)^2 \quad (11)$$

Where SS_T denotes the total sum of squared error, n is the number of datasets, η_i is the mean of signal to noise (S/N) ratio of the test, η_m is the total average S/N ratio.η_m is the total average S/N ratio.

3.2.4.2 Development of Mathematical Model and Statistical Analysis

Statistical analysis is conducted on the output parameters includes coefficient of determination (R^2), mean absolute error (MAE) and mean square error (MSE) (Jahed Armaghani et al., 2018; Uzuner & Cekmecelioglu, 2016). The statistical analysis shows the correlation of output variables on the input parameters with the aim of evaluating the representation of response parameters on the calculated mathematical equations. The equations for statistical analysis are denoted in below equations (Equation (12), Equation (13) and Equation (14)).

$$R^2 = 1 - \frac{\sum_i (y_{i,actual} - \hat{y}_i)^2}{\sum_i (y_{i,actual} - \bar{y})^2} \quad (12)$$

$$MAE = \frac{1}{N}\sum_{i=1}^{N} |y_i - \hat{y}| \quad (13)$$

$$MSE = \frac{1}{N}\sum_{i=1}^{N} (y_i - \hat{y})^2 \quad (14)$$

By utilising Design Expert software for ANOVA studies, it is possible to predict the regression coefficients and equations that correlate to the historical data from the four biogas plants. The expression that satisfies the polynomial equation will be fitted in the Equation (15) below (Passos et al., 2014; K. Wang & Lam, 1999),

$$F(x_1, x_2, .., x_m) = b_0 + \sum_{j=1}^{m} b_j x_j + \sum_{\substack{i=1}}^{m-1} \sum_{\substack{j=2 \\ i<j}}^{m} b_{ij} x_i x_j + \sum_{j=1}^{m} b_{jj} x_j^2 \quad (15)$$

Where b_0, b_j, b_{ij}, and b_{jj} are regression coefficients for intercept, linear coefficient, interaction coefficient and quadratic coefficient respectively; x_i and x_j are input variables in the regression function; m=7 represents the total number of variables; and $F(x_1, x_2, .., x_m)$ is the output variables.

3.2.4.3 Optimisation Model for each BGP

The objective function of the optimisation model in the below Equation (16) is to estimate the COD removal rate $f_1(x)$ and biogas production rate $f_2(x)$ for each BGP. The weighting sum (w_i) is calibrated as 0.5 for each output parameter indicating that each output represents an equal magnitude in the study.

$$\text{maximum } f(x) = \sum_{i=1}^{m} w_i f_i \quad (16)$$

To solve the multi-objective optimisation model, upper (x_j^U) and lower limits (x_j^L) are defined for the prominent parameters (x_j) including OLR, Temperature and RR. The upper and lower boundary limits are enumerated from the maximum and minimum operating conditions of the historical data. The inequality constraints of the prominent parameters as specified in below Equation (17) are typically represented by the low and high bounds and certain penalties for a more consistent optimised expression. Regarding the operating capability of the anaerobic digester, the lower boundary limit for RR is defined as well as the upper limit of operating temperature to construct a more feasible optimal solution for the stability of the system.

$$x_j^L \leq x_j \leq x_j^U \quad (17)$$

3.2.4.4 Application of Theoretical Models for Prediction of Methane Production

Numerous predictive models of methane productivity are proposed by researchers based on the feedstock's organic composition (Ali et al., 2018). It is important to identify the organic composition of the feedstock to predict the methane productivity and the design parameters of the anaerobic digester during commissioning to improve the plant's performance (Nielfa et al., 2015). The BMP test is associated with a respirometry test to estimate the amount of methane generated under anaerobic conditions where the amount, composition of waste, temperature and pressure are defined (Lesteur et al., 2010). Numerous BMP test protocols have been developed over the years such as BMPthCOD, BMPthAtC and BMPthOFC). Figure 3.4 summarises the overview of the BMPth models.

Table 3.4: Overview of the BMPth models

Models	Advantages	Disadvantages	References
BMPthCOD	Could be used on different types of feedstocks Saves time and cost Provides details on important parameters (i.e., COD concentration) of the feedstock	Complete biodegradation or anaerobic process did not carry out successfully leading to inaccuracies	(Nielfa et al., 2015; Raposo et al., 2011)
BMPthOFC	Better theoretical estimates on feedstock originating from animal manure and agri-food waste	The model provides recommendations with high lipid content where excess lipid concentration will inhibit the methanogenesis process	(Lesteur et al., 2010; Nielfa et al., 2015)
BMPthAtC	The model emphasises more on the atomic composition of the feedstock to predicts the methane production. The understanding on atomic composition gives a good estimation based on the stoichiometric equation of the anaerobic process.	The model is presented assumes that methanogen bacteria break down the N, C, O and H atoms	(Nielfa et al., 2015; Raposo et al., 2011)

BMPthCOD test estimates the methane potential from the quantity of the feedstock and COD concentration. The equation used is shown in below Equation (18) (Angelidaki et al., 2011).

$$BMP_{thCOD} = \frac{n_{CH_4}RT}{pVS_{added}} \quad (18)$$

where BMP_{thCOD} represents the theoretical value of methane at laboratory conditions, T is the temperature of the operating conditions, p is the operating pressure, R is the universal gas constant, VS_{added} denotes the volatile solids of the substrate and n_{CH_4} which is the quantity of methane in terms of mol can be derived from below Equation (19).

$$n_{CH_4} = \frac{COD}{64(g/mol)} \quad (19)$$

Since the total solid (TS) and solid fraction (Equation (20)) of the inoculum and substrate can be measured using the thermogravimetric method, the volatile solid (VS) added can be assumed (Sluiter et al., 2010).

$$Solid\ fraction = \frac{VS_{added}}{TS} \quad (20)$$

3.3 Methods and Parameters of Optimisation Study 1: Cooling Tower

In the following section, several factors are studied to understand the effect of using a CT to cool down the POME and positively impact anaerobic digestion. The POME entering and leaving the CT was investigated to observe the temperature change. The impact on bottom sludge and treated effluent were studied to observe the effectiveness of

the optimisation plan. The raw biogas quality was checked to understand the effect of controlling the temperature of POME entering the AD. Several analysis methods were used to study the effectiveness of the CT. All of these aspects were compiled and summarised in Figure 3.7.

The design starts in Stage 1 where scope identification is carried out through background research and literature reviews. In Stage 2, data collection from biogas plant is obtained such as input parameters, output parameters, and cooling tower design datasheet. Data standardization is also employed with the aid of MS Excel. Moving into Stage 3 where the algorithm of ML model (ANN) and cooling tower design are conducted. In the ML modelling section, performance evaluation is performed by obtaining the highest coefficient of determination, R^2 and the lowest mean square error (MSE). After the design of cooling tower, process simulation and techno-economic analysis are executed using SuperPro Designer V9 to examine the economic feasibility of incorporating cooling tower into the treatment plant, enhancing on payback period and internal rate of return (IRR). Model optimization is performed by searching the optimal parameter value and response which yields the highest methane yield and biogas production in Stage 4. In stage 5, the process is then concluded with a sensitivity analysis of the obtained optimal parameters.

3.3.1 Site Location

The trial of the first optimisation plant was introduced at BGP A. Only one site was selected for the optimisation plan based on the discussion with CGESB in order to check its effectiveness before introduce to the rest of BGPs.

3.3.2 CT Unit Design Parameters

CT is placed in the pre-treatment process line. The POME passes through the CT before it is delivered to the digester. The CT replaces the mixing tank where POME was initially cooled down with. For this study, the POME was collected before entering the cooling pond. This sampling point was decided based on the worst case scenario if cooling pond is not functioning. Hence the inlet temperature chosen for CT design was higher compared to the average temperature of POME analysed in POME characteristics study. The data in Table 3.5 provides the basic data used to design the CT. Twin-packed crossflow induced draft CT was chosen for the installation at BGP A decided by CGESB, as illustrated in Figure 3.8. While, the industrial CT constructed at BGP A after completion of the design process can be found in Figure 3.9.

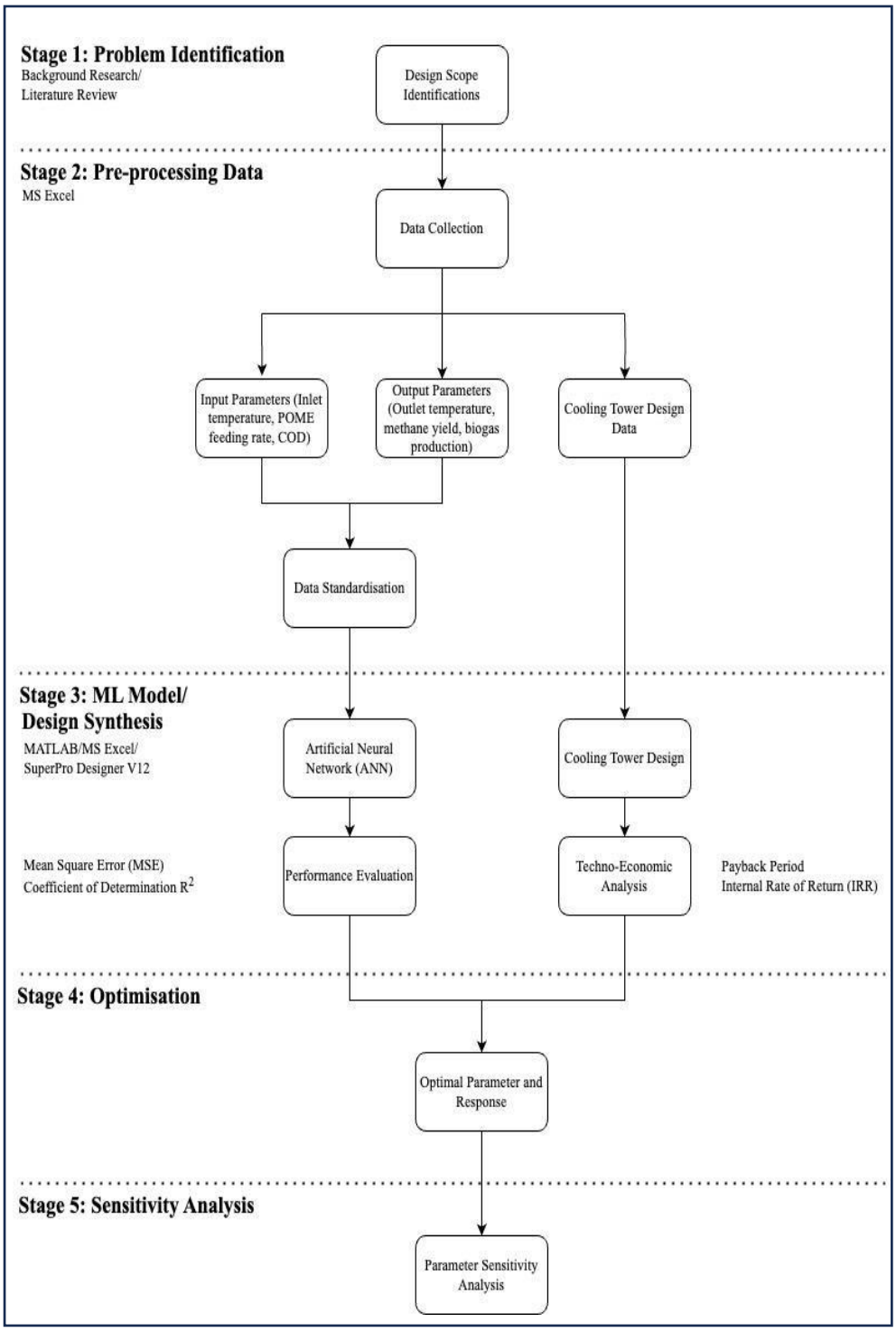

Figure 3.7: Summary of overall CT study

Table 3.5: Cooling tower database design

Parameter	Value	Unit	Reference
POME Volumetric Flowrate	60	m^3/hr	Biogas Plant
Inlet Temperature	80	˚C	-
Outlet Temperature	40	˚C	-
Air Inlet Temperature	31	˚C	Relative to Location
Relative Humidity	77	%	Relative to Location
Web Bulb Air Temperature	28	˚C	Psychometric Chart
Wet Air Specific Humidity	0.022	Kg/kg	Psychometric Chart
Water Concentration	0.95	$Gal/min.ft^2$	Perry's Chemical Engineering Handbook, 7th Edition
Safety Factor	20	%	-
Holding Time	1	hr	Assumed for Cooling Tower Dimensions

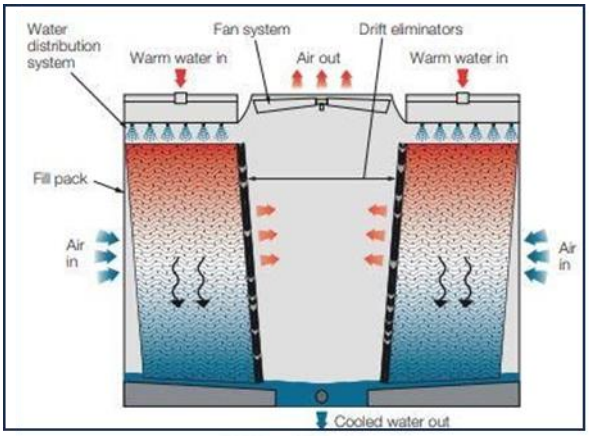

Figure 3.8: Concept of twin-packed crossflow induced draft CT

Figure 3.9: CT installed at BGP A

3.3.3 Methodology of Effluent and Sludge Data Collection for CT Study

The sample was collected to check the temperature change of the raw POME before entering and after leaving the CT. Its impact on the anaerobic digester performance was studied by analysing the bottom sludge, treated effluent and biogas composition quality. The samples were collected daily for six months, from January 2022 until June 2022. The data collected was then compared with the BGP A previous two years historical data.

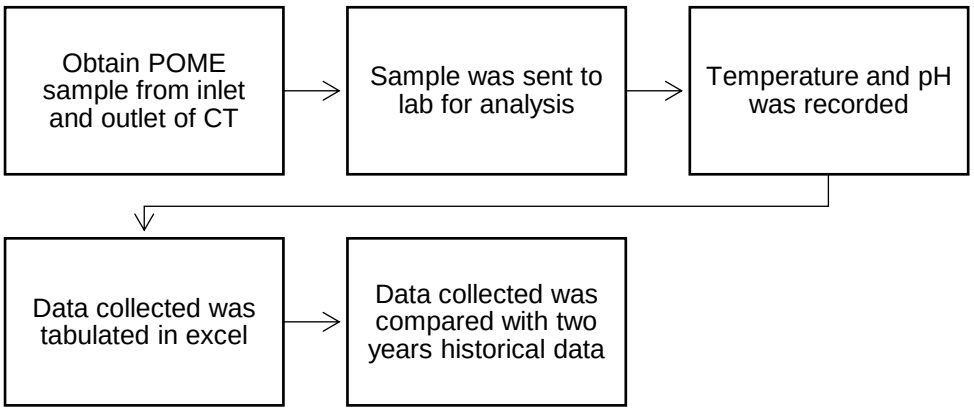

Figure 3.10: Summary of POME temperature and pH data collection

The sampling point for temperature and pH change of POME was collected at two points. For the inlet temperature and pH, a raw POME sample was tapped directly from the mill at the inlet of the cooling pond, as illustrated in Figure 3.10. For the outlet readings, the sample was collected at the outlet of the CT. The sample was directly and immediately transferred to the lab for analysis. As for the sample of bottom sludge

treated effluent and biogas production, the data were collected from the AD as explained in the AD profiling and performance study.

Figure 3.11: Sampling point of inlet CT temperature at inlet of CP

3.3.4 CT Process Data Analysis Methods

There are a few steps involved in the detailed data analysis works such as data standardisation, Artificial Neural Network (ANN) performance evaluation, optimisation process and sensitivity analysis.

3.3.4.1 Data Standardisation

Data standardisation (normalisation technique) is employed as a step in Stage 2 (Pre-processing data). This is a crucial step to determine the significance of independent variables to dependent variables. Data normalization is especially important in machine learning to convert

different parameters into ananalogous scale which in turns improve the training stability of the model (Google Developers, 2023).

Table 3.6: Statistical data value used in ANN modelling

Parameters	Units	Class	Max	Min	Average	Standard Deviation
Temperature	˚C	Input	42.0	32.5	39.3	1.60
POME Feeding Rate	m^3/day	Input	859.0	8.0	449.3	168.2
Biogas Production Rate	m^3/day	Output	14588.0	760.0	11054.2	2275.1
Methane Yield	Nm^3/kg $COD_{removed}$	Output	1.07	0.09	0.32	0.15

Data normalisation technique can be expressed as shown in Eqn (1).

$$Z = \frac{X-\mu}{\sigma} \quad (1)$$

where X = actual data

μ = sample mean value

σ= standard deviation

3.3.4.2 Artificial Neural Network (ANN)

Artificial Neural Network (ANN) is a computational model which was inspired to work like the human nervous system (Y. Wu & Feng, 2018). ANN consists of several layer of nodes interconnecting to each other known as neurons. Nodes comprises of input layer, hidden layer(s), and output layer. Connection between nodes is linked with bias weights that determines its connection strength (Walczak & Cerpa, 2003). Input data undergoes randomization and subsequently partitioned into three sets mainlytraining, validation, and testing. The setup designates 80% of the datasets for training the model, while 10% is allocated to both validation

and testing for accessing model accuracy. MATLAB R2022a programming is employed to create the ANN model.

In this ANN model generation, there are two input layer which is the temperature and POME feeding rate, 20 hidden neurons (basis from MATLAB) and two output later which is biogas production rate and methane yield. Levenberg-Marquardt network training algorithm, specifically the“trainlm” function is chosen for forecasting methane yield and biogas production in ANN (Kumaraswamy, 2021). This algorithm operates through iterative modification of weight vectors in ANN to minimize disparity between predicted outputs and actual observed outputs. During each epoch,errors are retroactively propagated through the network. Weights assigned to each input and node are proportionally updated to reduce overall error. This iterative process continues, with residual error being back propagated through the network and weights are readjusted strategically. Across each epoch, readjustments progressively diminish total error across all training data points until the ANN model achieves a high level of predictive accuracy (Udoka, 2016).

3.3.4.3 Performance Evaluation of ANN

To access reliability of the model in POME treatment plant, its projected performance will be compared against key benchmarks (Treve et al., 2022). By quantifying metrics of accuracy and precision between observed and predicted parameters, the model’s strengths and limitations can be examined in real-world plant conditions. Additionally, the model’s proficiency in capturing dynamic phenomena related to POME properties, such as variation in effluent composition over time, will

be scrutinized. Systematic measurement of model performance on relevant process attributes will determine whether the developed model is a suitable surrogate for studying the POME system, particularly for potential optimization, design, and control applications (Najib et al., 2020).

The primary indices calculated included the coefficient of determination, R^2, and mean square error (MSE). R^2 shows the proportion of total variance in the test data that can be elucidated by the model's predictions (Johnson & Schielzeth, 2017) while MSE quantify deviations as the average squared differences (Wallach & Goffinet, 1989). Collectively, these indices enable an evaluation of whether the model exhibits robust generalization capabilities beyond the training data or if it encounters significanterrors and uncertainty when applied to unseen data samples. Eqn (21) and (22) shows the equation to obtain R^2 and MSE respectively.

Prediction model with the most favorable statistical performance (i.e., highest R^2 and lowest MSE) is made to pinpoint the optimal operating conditions that result in the highest biogas productionrate and methane yield.

$$R^2 = 1 - \frac{\sum(\mathrm{yi,actual} - \hat{\mathrm{y}}\mathrm{i})^2}{\sum(\mathrm{yi,actual} - \mathrm{y})^2} \quad (21)$$

$$\mathrm{MSE} = \frac{1}{N}\sum_{i=1}^{N} (\mathrm{y}_i - \hat{\mathrm{y}}_i)2 \quad (22)$$

where $\hat{yi}$ = predicted value of yi

$\bar{y}$ = mean value of yi

N = total number of datasets

3.3.4.4 Optimisation Analysis of Cooling Tower Study

The objective of this optimisation model is to pinpoint the input and output variables that adhere to constraints and boundary limits while maximizing outcomes. Formulated using the MATLAB R2022a programming language, the optimization problem employs built-in MATLAB functions to discern optimal operating conditions and output values. The generation of 135 datasets utilizes the linearly spaced vector function linspace(), and the determination of the largest output value is achieved through the max() function applied to an array. Subsequently, a while() loop within a control flow statement is employed to execute the code until a Boolean condition is met. Specifically, the function identifies the dataset row providing the maximum values for both output variables and optimal input parameters.

Methane yield (Equation 23) represents methane composition percentage within total biogas generated, normalized per unit COD removed. Accordingly, higher absolute biogas output directly elevates its methane constituent linearly as well, explaining the high R2 fit to a straight-line trend. So, optimizing one parameter inherently enhances the other to a proportional degree. Therefore, exploring these two target variables together may offer limited additional optimization and sensitivity insights beyond investigation either one independently (D. Chen & Li, 2020).

$$\text{Methane Yield} = \frac{\text{CH4 quality} \times \text{Biogas Production Rate}}{POME\ Feed\ Rate \times (CDin - CODout} \quad (23)$$

3.3.4.5 Sensitivity Analysis of Cooling Tower Study

Sensitivity analysis is a quantitative technique used to assess the impact of variations in input parameters on the outcomes of a model. It helps to understand how changes in values of certain factors influence the results, providing insights into the robustness and reliability of the model (Kenton, 2023).

This analysis is employed to determine how input parameters (temperature and POME feed rate) would affect the output parameters (biogas production and methane yield) when its key parameters are altered by 80% and 120% from optimized values. MS Excel software is utilized as a platform to execute the sensitivity analysis calculations and visualize the results. Excel allowed implementing data manipulation scripts to efficiently automate parameter variations. Overall, conducting analysis through Excel balanced algorithmic control, output management, and visualization tools for flexible sensitivity screening (Zebra BI, 2023).

3.3.4.6 Techno-economic Analysis of Cooling Tower Study

Techno-economic analysis (TEA) evaluates the commercial viability of technologies across their life cycle by holistically assessing technical performance, cost, and revenue opportunities. Implementing TEA entails progressive modeling and quantification modules covering process simulation, equipment specifications, capital/operating expenses estimation, and financial analysis. Unlike narrow evaluations focused solely on engineering optimizations, TEA adopts an interconnected methodology spanning project development phases from concept to

commissioning. This approach provides vital insights accounting for complex real-world independencies affecting the operational, environmental, and fiscal outcomes from an engineering managerial perspective (Chai et al., 2022).

By employing SuperPro Designer, it becomes possible to simulate a comprehensive process flowsheet for the entire palm oil mill effluent (POME) treatment plant. This simulation facilitates the utilization of built-in functions within the software to generate an economic analysis report with the incorporation of cooling tower, replacing cooling pond and mixing tank. Furthermore, the simulated flowsheet allows for a thorough comparison between the results obtained from simulated data and real-world industrial data. This in-depth comparison aims to ascertain the reliability of utilizing simulation in the assessment of the POME treatment process.

3.4 Methods and Parameters of Optimisation Study 2: Decanter Cake

The following sections of this study explained the potential of DC as a co-substrate to improve the AD performance particularly in the biogas production aspect. The raw DC from the POM A was studied to evaluate their biodegradability, suitability and applicability in the AD. The production and quality of biogas from anaerobic digestion were also studied to better understand the performance of the AD during the co-digestion of DC with POME.

3.4.1 Characteristic Study

DC sample collection and overall study was carried out at BGP A. This location was selected based on the availability of DC production. The samples for raw POME were taken between the cooling pond and the anaerobic digester, while the samples for raw DC were taken directly after the 3-phase decanter centrifuge, as in Figure 3.12. 12 raw DC samples were taken from the 3-phase decanter centrifuge over the course of one month. The raw DC samples were diluted with distilled water at different dilution ratios of 1:20, 1:10, 1:5 and 1:1. To study their characteristics, the laboratory examination was conducted to assess pH, COD, BOD, TS, and SS. The lab analysis standard as explain in the Table 2.4. The dilution ratios were then compared to find the ideal ratio used for the co-digestion with POME. Figure 3.13 shows the flowchart of the DC characterisation study.

Figure 3.12: Decanter cake produced at POM A

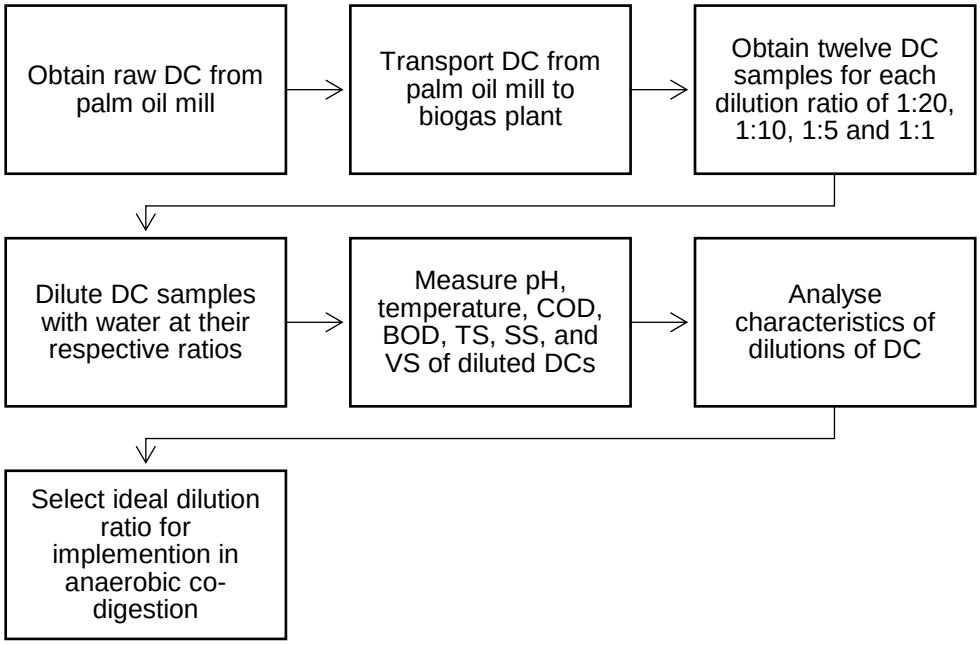

Figure 3.13: Flowchart of the DC characterisation study

3.4.2 Operation of Biogas Plant for Co-digestion of POME with DC

The feeding rate of POME was kept constant at 350 m^3/day with a co-digestion of 10 m^3 DC, during the first stage of study period from July to September 2021. This decision was made by the BGP A plant owner. The main objective of this first trial is by fixing the feeding rate is to check the suitability of DC co-digestion in the AD and to ensure no process disruption of the plant which will affect its performance, which subsequently will affect the revenue generation from BGP A. After first trial, CGESB agreed to proceed with three more months (October to December 2021) of study with random amount of DC ranging from 5m^3/day to 20 m^3/day. The POME amount also was not control during the entire period of second trial. This resulted the variety of OLR of the AD.

The raw DC was transported from the 3-phase decanter centrifuge from the palm oil mill to the biogas plant using a truck with a maximum load of one tonne, as shown in Figure 3.14 below. Figure 3.15 shows a temporary mixing facility consisting of an HDPE-lined pond installed between the treated effluent discharge line and the existing mixing tank to dilute DC with treated effluent. The DC was diluted at a ratio of 1:10. This ratio was selected based on the analysis from the characterisation study. The diluted DC was introduced into the mixing tank and mixed with POME before entering the anaerobic digester. The SCADA which was installed in the biogas plant, was used to record operational data, including effluent flow rate, biogas flow rate, effluent and biogas temperature, biogas quality (methane, carbon dioxide, hydrogen sulphide, and oxygen), and pump operation. Figure 3.16 summarises the DC application processes conducted at BGP A.

Figure 3.14: Collection of decanter cake from palm oil mill

Figure 3.15**:** Dilution of decanter cake in temporary mixing facility

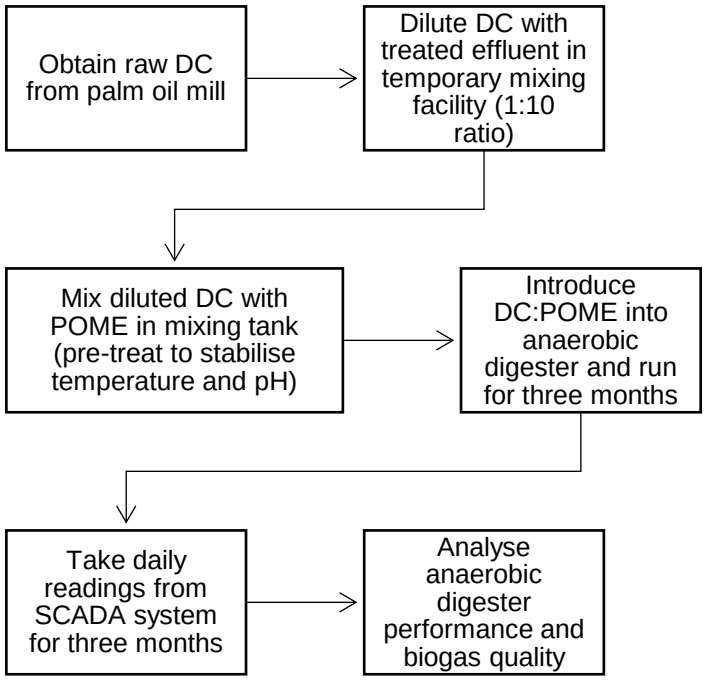

Figure 3.16: DC application and data collection processes

3.4.3 Anaerobic co-digestion (ACoD) performance analysis methodology

The effects of co-digestion on biogas yield were studied by comparing the theoretical maximum potential biogas yield from POME with the total actual volume of biogas recorded by the flowmeter in the biogas plant during the co-digestion of POME with DC. The theoretical maximum

potential biogas yield from POME was calculated based on past operational data from July 2019 to June 2021, using the average POME COD of 67 kg/m^3, the maximum COD removal rate of 85%, the COD to the methane conversion rate of 0.315. The daily biogas quality data from the anaerobic digester was measured and recorded in the SCADA system. POME COD value was verified once a week during three months of study duration and was consistent with two years of historical data. Various analysis techniques used for this study explained in the below subtopic. Figure 3.17 explained the detailed analysis carried out for ACoD study.

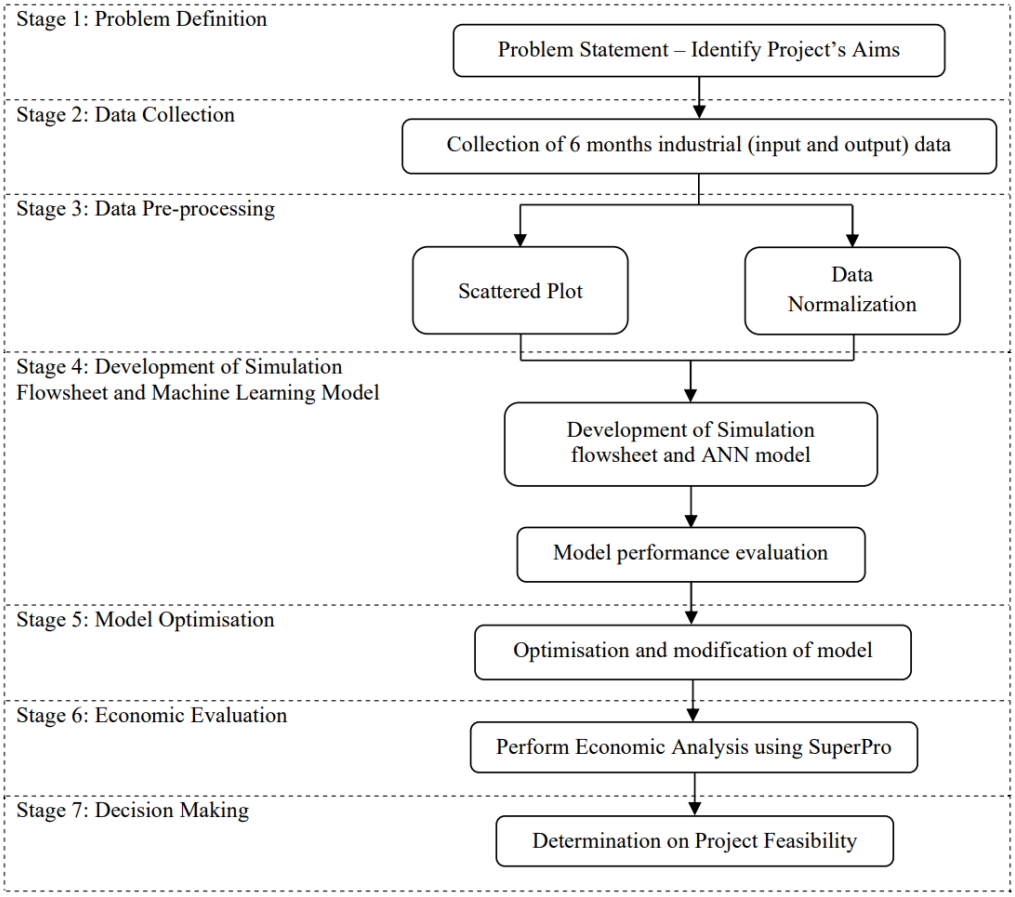

Figure 3.17: Summary of overall ACoD study

3.4.3.1 Machine learning using Neural Networks

Machine learning (ML) algorithms play a crucial role in predicting the biogas production and methane yield by leveraging complex relationships with diverse datasets. ANN method was used to predict the future performance under different conditions, enabling optimization strategies for DC: TE dilution ratios, DC: POME mixing ratios, process parameters adjustments and digester design modifications. In this study, ANN is developed using MATLAB R2020b, to predict methane yield and TS content for the ACoD of POME and DC. TS was selected as one of the key parameter due to the characteristics of DC, which is high with impurities such as sand, fiber etc.

3.3.3.2 Parameter Selection of ACoD

Careful selection and optimization of process parameters are vital in ACoD, significantly influencing the synergistic effects that dictate biogas production. Precise parameter choice is pivotal for accurately predicting and enhancing the ACoD process performance in biogas generation. Temperature regulation in the ACoD process is a critical determinant of microbial activity and subsequent biogas production dynamics. The OLR stands as another critical parameter in ACoD process, directly impacting digestion performance and system stability (H. Zhang et al., 2023).

The neural network toolbox in MATLAB 2020b provides few statistical analyse metrics to evaluate the performance of ANN model, including model performance metrics, gradient, Mean Squared Error (MSE), regression plots, coefficient of determination (R^2) and error histograms. Among these metrics, MSE, coefficient of determination (R^2) and error

histograms are employed to evaluate the performance of the ACoD process. Table 3.7 below shows the statistical analysis used for the performance evaluation of ANN model.

Table 3.7: Equation of error functions for performance evaluation of ANN model

Error Function	Equation	References
Mean Squared Error (MSE)	$MSE = \frac{1}{n}\sum_{i=1}^{n}(o_i - p_i)^2$	(Betiku & Taiwo, 2015)
Coefficient of Determination (R^2)	$R^2 = \frac{\sum_{i=1}^{n}(p_i - o_i)^2(p_i - \bar{p})}{\sum_{i=1}^{n}(o_i - \bar{o})^2 \sum_{i=1}^{n}(p_1 - \bar{p})^2}$	(Aklilu & Waday, 2023)

3.4.4 Economic analysis of ACoD

A comprehensive economic assessment is conducted to evaluate the financial feasibility and profitability of anaerobic co-digestion of DC and POME, by employing the integrated economic evaluation tool within SuperPro Designer v9.0. Through the analysis, potential financial risks and uncertainties associated with the project are systematically identified. Table 3.8 summarises the cost indicators and their equations. Total capital investment encompasses the fixed costs of the ACoD process, the summation of direct fixed capital cost, working capital, startup and validation cost, up-front research and development (R&D) cost and up-front royalties (Intelligen Inc., 2023). Moreover, the calculation of operating costs incorporates optimized process parameters, encompassing expenses associated with materials, labour, air emissions treatment, utilities, and transportation.

Table 3.8: Cost indicators for economic evaluation

Cost Indicator	**Equation**
Gross Profit	$Gross\ Profit = Total\ Revenues - Operating\ Cost$
Net Profit	$Net\ Profit = Gross\ Profit - Taxes$
Gross Margin	$Gross\ Margin = \frac{Total\ Capital\ Investment - Gross\ Profit}{Total\ Capital\ Investment} \times 100\%$
Return On Investment (ROI)	$ROI = \frac{Total\ Capital\ Investment - Net\ Profit}{Total\ Capital\ Investment} \times 100\%$
Payback Time	$Payback\ Time = \frac{Total\ Capital\ Investment}{Net\ Profit}$
Internal Rate of Return (IRR)	$IRR = \frac{Future\ Value}{Present\ Value}^{1/Periods} - 1$
Net Present Value (NPV)	$NPV = \frac{Cash\ flow}{(1+i)^t} - Initial\ Investment$

$i = Discount\ rate\ (7\%)$

$t = Number\ of\ time\ periods$

CHAPTER FOUR

RESULTS AND DISCUSSION

4.1 POMs Profiling and POME Characteristics Study

This section discussed the profile of each palm oil mill, focusing on its design and operation principle, equipment used, and specific processes that affected POME characteristics. Detailed POME characteristics and analysis from two years of collected data are also presented and discussed.

4.1.1 POMs Profile

All four POMs studied in this research vary in a few aspects, such as mill capacity and processing principle. Table 4.1 summarizes the specific key operational aspects of the selected POMs in different processing units, including a frontline system, a steam and power generation system, a clarifier system, an EFB plant, a kernel crushing plant, and a conventional treatment of open ponding system. Figure 4.1 is the general process flow chart of all four POMs. The operational differences are depicted in the rectangle box.

Table 4.2 shows the primary difference among the mills lies in their clarifier system. Specifically, POM A is the only mill with a three-phase decanter unit. In contrast, the other three mills have conventional sludge separators to remove oil from the high solid concentration of sludge in the wastewater. Using a three-phase decanter improves oil, solids, and oil-free wastewater separation, reduces water consumption by 10-30%, and produces solids with lower moisture (50-55%) (Dermeche et al.,

2013). The decanter treats the clarification tank underflow by separating the remaining CPO from the sludge before feeding it into the purification tank (Saad et al., 2021b). Therefore, the usage of a decanter reduces the sludge separator capacity. POM B's total sludge separator capacity is the highest due to its higher mill capacity and the absence of a decanter. While POM A has a higher overall capacity (54 tons/hr) than POM D (40 tons/hr), both have the same total sludge separator capacity of 40 tons/hr, indicating a lower necessity for sludge separation in POM A due to the presence of a three-phase decanter.

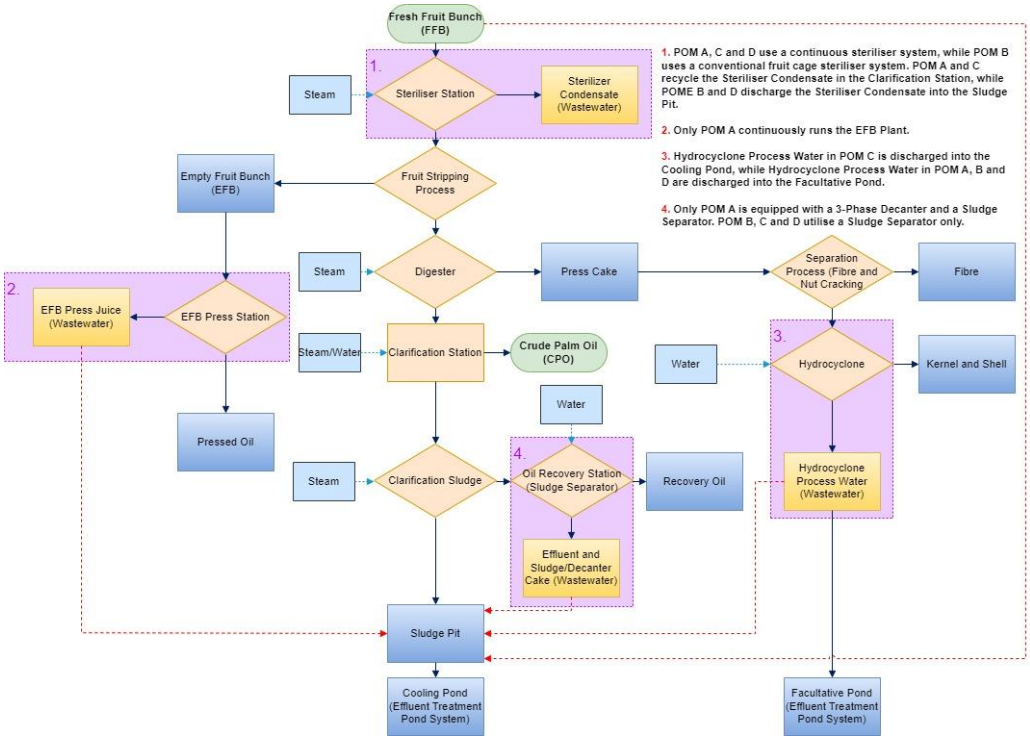

Figure 4.1: General flow chart of all POMs

Table 4.1: Summary of the processing units of mills

Mill Information					
Mill Name	**Units**	**POM A**	**POM B**	**POM C**	**POM D**
Address	-	Kilang Sawit Lepar Hilir	Kilang Sawit Adela	Kilang Sawit Keratong 2	Kilang Sawit Lok Heng
		26300 Kuantan	81930 Bandar Penawar	26900 Bandar Tun Razak	81930 Kota Tinggi
		Pahang	Johor	Pahang	Johor
Operation Information					
Capacity	tons/hr	54	54	40	40
A) Frontline system					
Conventional cages			X	-	-
Indexing system			-	-	-
Continuous steriliser		X	-	X	X
Vertical steriliser			-	-	-
Number of screw press	unit	6	6	4	4
B) Steam and power generation					
Boiler capacity	tons/hr	45	40	40	45
Number of boilers		1	1	1	1
Turbine capacity	kW	1600	1600	1600	1200
C) Clarifier system					
Three-phase decanter	unit	1 (30 ton/h)	N/A	N/A	N/A
Sludge separator	unit	5 (8 ton/h)	4 (15 ton/h)	4 (6 ton/h)	4 (10 ton/h)
Sludge pit	unit	2	2	2	2
Sludge handling		To sludge pit then to the cooling pond	To sludge pit then to the cooling pond	To sludge pit then to the cooling pond	To sludge pit then to the cooling pond
Steriliser condensate handling		Recycle to CCT[1], sludge from CCT to the sludge pit	To sludge pit then to the cooling pond	Recycle to CCT, sludge from CCT to the sludge pit	To sludge pit then to the cooling pond
Number of pre-cleaners	unit	6	4	4	4
Waste of pre-cleaner handling		To sludge pit then to the cooling pond	To sludge pit then to the cooling pond	To sludge pit then to the cooling pond	To sludge pit then to the cooling pond
D) EFB plant					
Number of EFB shredded	unit	3	3	3	3
Number of EFB press	unit	3	3	3	3
EFB pressed juice handling		Recycle to CCT & settling tank	Recycle to CCT & settling tank	Recycle to SPO[2] tank	Recycle to VCT[3] no. 3
E) Kernel crushing plant					
Number of hydro cyclones	unit	4	4	4	2
Hydro cyclone wastewater handling		To facultative pond	To facultative pond	To hydro pond then overflow to the cooling pond	To facultative pond
F) Conventional treatment of open ponding system					

Capacity of cooling pond		2,000 m^3	2,000 m^3	3,639 m^3	650 m^3
Capacity of mixing pond		4,000 m^3	2,800 m^3	-	N/A
Capacity of anaerobic pond		51,824 m^3	56,000 m^3	81,720 m^3	17,231 m^3
Capacity of facultative pond		22,804 m^3	20,000 m^3	37,736 m^3	6,994 m^3
Capacity of algae pond		20,250 m^3	24,000 m^3	17,017m^3	1 unit of 3,737 m^3 & 1 unit of 13,547 m^3
Capacity of polishing plant		NA	1 unit & 50 m^3/hr	NA	NA

[1]CCT: Continuous clarifier tank; [2] SPO: Sludge palm oil; [3] VCT: Vertical clarifier tank

Regarding FFB sterilisation, the conventional POMs use a “triple-peak sterilisation” process, which affects the performance of the threshing machine as the fruits may be inadequately heated, resulting in poor seeds stripping from the bunches. This, in turn, can cause an adverse effect on the oil extraction rate (Akhbari et al., 2020b). As shown in Table 4.1, only POM B utilises the conventional cages sterilisation. Newer sterilisation systems, such as the continuous sterilisation (CS) system, utilise saturated steam at a lower pressure of 1 atm and a temperature of 100°C, with a cooking time of about 80 minutes. This system provides efficient and effective heat transfer to each fruit bunch, and the continuous flow of sterilised fruit to the thresher at a constant speed reduces oil loss during the CS process and facilitates excellent separation of fruits from the bunch (Sivasothy et al., 2005). As a result, more conventional mills, including POMs A, C, and D, have been focusing on utilising the CS system. The discharge condensate and water from the sterilisation process are treated differently in each mill, and this difference in arrangement will have an impact on COD content in the

POME. In POM B and D, the steriliser condensate is sent to the sludge pit then to cooling pond, whereas in POM A and C oil is recycled back to oil room and a continuous clarifier tank (CCT) respectively, before sending it to the sludge pit. The POM A has 2 more pre-cleaners than the rest of the mills and all mills send the pre-cleaner handling waste to sludge pits except for POM C and D where the waste is sent to cooling ponds subsequently.

Besides, the handling of pressed juice in the EFB plant varied among the mills to recover the remaining oil in sludge. EFB, a by-product of POMs, is characterized by high moisture content of up to 70% and high organic matter, including carbon of about 490 kg/ton dry weight of EFB as well as nitrogen of about 7 to 9 kg/ton dry weight of EFB (Purnomo et al., 2018). In POM A and B, the EFB juice was recycled to the CCT and settling tank, and the oil recovery process was optimized through two steps of clarification processes. The extracted data from the mills showed that the oil content in EFB is about 2 to 4%, and it was collected as EFB juice and recycled back to the clarifier and settling tanks in POM A and B. Conversely, in POM C and D, the EFB juice was recycled back to the sludge palm oil (SPO) tank and vertical clarifier tank (VCT). According to the focus group interview, only POM A ran the EFB plant continuously, while the remaining POMs did not operate their EFB plant due to cost control.

In the effluent treatment plant, the overall capacity of cooling ponds, facultative ponds, and algae ponds for the mills is in descending order, i.e., POM C, B, A, and D. Only POM A and B have mixing ponds, with

respective capacities of 4,000 m^3 and 2,800 m^3, which are designed to adjust the pH and temperature of the effluent overflowing from the cooling ponds before it enters the anaerobic ponds. The capacity of anaerobic ponds for the mills is in descending order from POM C, B, D, and A, while the polishing plant is only present in POM B with a capacity of 50 m^3/h. The different sizing and number of ponds installed in all POMs are based on the DOE's theoretical BOD reduction and mass balance approval. Apart from that, the differences are also attributed to research and development activities planned and executed by the mill owners.

4.1.2 POME Characteristics for all POMs

The utilization of different types of equipment and process flows in the milling process may lead to variations in the quality of POME as discussed in Section 4.1.1. This section summarizes and compares the average characteristics of the POME based on two years of data collected from the mills. The summary of two years POME characteristics data was presented in the Table 4.2. The ANOVA analysis showed that the POME characteristics, including COD, BOD, TS, OG, SS, and pH, demonstrated statistically significant differences among the various mills ($p < 0.05$). This provides evidence that the factors or processes contributing to the generation of POME differ between mills and necessitate customized treatment approaches for effective management. These findings emphasize the need to develop mill-specific POME treatment strategies that consider the distinctive POME characteristics generated by each mill.

Table 4.2: Two years of POME characteristics data

Month/ Year	POME QUALITY-LEPAR HILIR (POM A)						POME QUALITY-ADELA (POM B)					
	COD (mg/L)	pH	TS (mg/L)	SS (mg/L)	BOD (mg/L)	Oil & Grease	COD (mg/L)	pH	TS (mg/L)	SS (mg/L)	BOD (mg/L)	Oil & Grease
Jul-19	65,012 ± 3,240	4.45 ± 0.19	24,500 ± 5,780	12,300	28,858		78,230 ± 10,987	4.52 ± 0.19	38,690 ± 9,760	20,620	32,100	1,615
Aug-19	59,002 ± 4,679	5.23 ± 0.22	21,033 ± 3,093	17,065	23,261		77,230 ± 8,965	4.61 ± 0.15	42,386 ± 7,650	25,580	37,000	2,053
Sep-19	55,957 ± 2,890	5.20 ± 0.25	25,276 ± 3,145	12,683	23,700	3,450	79,820 ± 11,908	4.43 ± 0.17	45,114 ± 2,356	28,600	33,560	1,827
Oct-19	72,442 ± 3,870	5.10 ± 0.28	27,543 ± 2,020	13,635	29,573		76,230 ± 11,802	4.38 ± 0.20	49,900 ± 7,230	24,829	36,700	1,587
Nov-19	63,473 ± 7,800	4.90 ± 0.29	25,870 ± 225	13,655	30,233		81,713 ± 15,320	4.45 ± 0.17	42300 ± 12,729	28,313	40,600	1,878
Dec-19	63,195 ± 7,788	4.65 ± 0.27	28,000 ± 3,101	14,500	23,027		75,340 ± 9,967	4.29 ± 0.19	46,500 ± 8,797	20,984	33,240	1,473
Jan-20	64,300 ± 3,190	4.67 ± 0.20	24,540 ± 4,747	18,600	22,650		82,950 ± 5,661	4.37 ± 0.20	51,100 ± 9,603	25,875	41,200	2,460
Feb-20	69,800 ± 4,320	4.84 ± 0.00	23,670 ± 345	14,434	26,900		85,500 ± 8,975	4.34 ± 0.15	49,100 ± 2,390	23,450	39,730	1,570
Mar-20	69,200 ± 8,970	4.74± 0.24	28,500 ± 3,456	16,500	22,500		86,300 ± 13,450	4.20 ± 0.16	46,780 ± 8,921	29,300	44,890	
Apr-20	68,900 ± 2,876	4.38 ± 0.17	32,520 ± 902	15,430	23,829		90,550 ± 18,760	4.40 ± 0.14	45,600 ± 8,902	35,460	43,080	
May-20	67,300 ± 3,490	4.60 ± 0.12	21,610 ± 989	16,980	25,400		79,600 ± 11,008	4.59 ± 0.90	40,500 ± 8,820	26,500	40,100	
Jun-20	68,000 ± 6,256	4.73 ± 0.18	23,470 ± 6,540	15,670	28,900		78,100 ± 7,620	4.57 ± 0.10	49,700 ± 2,378	24,000	43,200	
Jul-20	67,500 ± 6,650	4.90 ± 0.24	27,500 ± 8,400	16,510	33,576		81,900 ± 3,454	4.61 ± 0.17	47,830 ± 908	29,030	39,000	

Aug-20	68,819 ± 4,580	5.00 ± 0.20	20,148 ± 5,631	15,700	34,476		88,600 ± 8,720	4.42 ± 0.15	42,800 ± 8,721	26,303	45,780	
Sep-20	72,838 ± 3,400	4.90 ± 0.11	30,630 ± 1,290	20,420	27,378		85,000 ± 9,600	4.59 ± 0.13	48,900 ± 902	22,340	44,760	
Oct-20	67,700 ± 2,840	5.00 ± 0.11	28,420 ± 1,172	17,600	30,400	7,855	83,600 ± 8,881	4.51 ± 0.10	44,560 ± 8,762	29,700	35,700	2,255
Nov-20	69,583 ± 6,609	4.80 ± 0.15	31,100 ± 1,902	18,954	32,900	9,654	81,900 ± 2,670	4.53 ± 0.10	48000 ± 3,498	33,260	39,020	2,135
Dec-20	71,000 ± 1,540	4.80 ± 0.13	22,750 ± 905	16,700	29,800	5,529	80,100 ± 6,449	4.57 ± 0.17	53,700 ± 9,081	29,430	44,780	3,975
Jan-21	65,012 ± 2,765	4.45 ± 0.20	25,670 ± 1,802	19,640	28,858	8,148	80,150 ± 4,320	4.43 ± 0.14	41,906 ± 1,209	25,400	33,450	2,880
Feb-21	70,790 ± 4,110	4.60 ± 0.21	24,100 ± 1,933	17,065	23,261		81,140 ± 3,590	4.43 ± 0.13	44,780 ± 1,099	27,820	39,600	2,110
Mar-21	69,800 ± 3,890	4.80 ± 0.16	25,276 ± 2,092	12,683	23,700		80,560 ± 8,721	4.46 ± 0.10	51,340 ± 1,972	28,500	42,300	2,600
Apr-21	72,442 ± 6,494	5.10 ± 0.21	27,543 ± 443	13,635	29,573		89,820 ± 6,180	4.71 ± 0.11	46,200 ± 8,809	28,760	44,320	4,720
May-21	65,400 ± 3,475	4.90 ± 0.18	25,870 ± 8,124	13,655	30,233		82,430 ± 9,993	4.65 ± 0.12	44,320 ± 2,376	28,040	37,640	4,320
Jun-21	69,230 ± 2,270	4.65 ± 0.10	25,480 ± 7,624	13,670	23,027		80,920 ± 3,526	4.58 ± 0.10	41,200 ± 2,795	26,450	41,890	
AVG 2019	63,177 ± 4,496	4.98 ± 0.25	24,844	13,868	27,125	3,450	78,645 ± 11,796	4.48 ± 0.18	43,678 ± 7,945	25,588	35,992	1,792
AVG 2020	68,745 ± 4,560	4.78 ± 0.15	26,238	16,958	28,226	7,679	83,675 ± 8,771	4.47 ± 0.21	47,381 ± 6,074	27,887	41,770	2,479
AVG 2021	68,779 ± 3,834	4.75 ± 0.18	25,657	15,058	26,442	8,148	82,503 ± 6,055	4.54 ± 0.12	44,958 ± 3,043	27,495	39,867	3,326

Month/ Year	POME QUALITY-KERATONG 2 (POM C)						POME QUALITY-LOK HENG (POM D)					
	COD (mg/L)	pH	TS (mg/L)	SS (mg/L)	BOD (mg/L)	Oil & Grease	COD (mg/L)	pH	TS (mg/L)	SS (mg/L)	BOD (mg/L)	Oil & Grease
Jul-19	64,025 ± 12,017	4.59 ± 0.22	27,760 ± 4,460	21,340	34,476		89,800 ± 17,650	4.65 ± 0.26	56,420 ± 13,450	45,240	44,320	
Aug-19	61,300 ± 8,903	4.61 ± 0.16	32,390 ± 3,908	24,300	35,110	4,266	78,645 ± 13,054	4.77 ± 0.16	54,283 ± 11,096	39,850	40,800	2,431
Sep-19	60,233 ± 2,409	5.00 ± 0.08	27,385 ± 2,808	16,783	25,389		92,844 ± 12,164	4.68 ± 0.11	49,378 ± 9,399	37,144	45,780	3,490
Oct-19	60,546± 6,243	5.14 ± 0.15	25,460 ± 4,932	12,987	28,683	10,887	81,788 ± 14,603	4.73 ± 0.13	45,000 ± 12,300	38,442	40,700	2,837
Nov-19	53,654 ± 4,590	4.76 ± 0.07	27620 ± 3,489	15,760	22,900		77,340 ± 16,582	4.49 ± 0.07	43,000 ± 10,890	29,943	36,500	2,638
Dec-19	56,330 ± 4,870	4.84 ± 0.12	21,450 ± 5,714	17,210	23,587		78,400 ± 8,642	4.50 ± 0.12	53,214 ± 4,703	38,871	40,380	1,608
Jan-20	56,179 ± 7,521	4.63 ± 0.08	29,100 ± 1,820	16,926	25,430		83,400 ± 17,300	4.70 ± 0.00	44,300 ± 13,100	56,450	39,800	2,820
Feb-20	55,900 ± 2,309	4.75 ± 0.08	32,520 ± 3,098	18,900	24,800		87,200 ± 5,790	4.50 ± 0.23	48,000 ± 2,354	57,650	41,290	
Mar-20	68,354 ± 18,902	4.87 ± 0.08	34,110 ± 11,190	19,856	29,800		82,300 ± 9,876	4.50 ± 0.07	55,505 ± 5,678	34,600	40,540	
Apr-20	60,000 ± 1,436	4.73 ± 0.15	34,800 ± 908	23,900	29,650		84,000 ± 12,400	4.55 ± 0.10	41,474 ± 11,092	26,900	44,100	
May-20	65,603 ± 10,900	4.74 ± 0.08	33,500 ± 9,802	23,450	26,780		88,700 ± 1,450	4.79 ± 0.10	42,738 ± 980	22,250	46,700	
Jun-20	61,200 ± 6,782	5.02 ± 0.06	31,820 ± 8,235	19,000	27,100		85,600 ± 14,482	4.96 ± 0.10	48,625 ± 4,160	29,458	45,600	
Jul-20	59,340 ± 3,820	4.78 ± 0.07	32,171 ± 4,819	25,600	36,504		84,200 ± 8,199	4.73 ± 0.10	41,105 ± 3,081	29,175	44,440	
Aug-20	62,300 ± 11,908	4.76 ± 0.17	21,300 ± 8,709	18,700	36,700		88,300 ± 8,777	4.76 ± 0.05	48,635 ± 8,710	27,900	40,800	

Sep-20	55,700 ± 14,909	4.82 ± 0.26	27,152 ± 9,980	17,174	28,900		88,700 ± 470	4.76 ± 0.05	53,170 ± 203	32,733	43,560	
Oct-20	59,900 ± 7,834	4.72 ± 0.20	29,913 ± 7,540	19,000	27,650	9,332	86,300 ± 9,087	4.48 ± 0.10	51,700 ± 3,470	30,145	38,790	
Nov-20	55,300 ± 2,560	4.81 ± 0.13	30139 ± 2,490	21,000	29,000	5,814	85,400 ± 2,789	4.71 ± 0.13	49,300 ± 908	25,623	39,760	7,790
Dec-20	56,900 ± 7,620	4.75 ± 0.15	25,413 ± 3,476	21,000	27,430	4,241	79,300 ± 10,200	4.70 ± 0.15	46,740 ± 3,510	36,012	41,450	3,450
Jan-21	58,300 ± 7,100	4.51 ± 0.03	24,320 ± 4,519	18,902	27,885	4,100	72,648 ± 8,095	4.70 ± 0.10	50,333 ± 2,376	28,963	38,760	3,155
Feb-21	59,000 ± 10,893	4.65 ± 0.07	28,563 ± 8,051	20,100	33,462	5,039	75,205 ± 7,080	4.67 ± 0.05	44,125 ± 5,616	28,073	42,310	2,190
Mar-21	64,375 ± 8,519	4.63 ± 0.07	33,017 ± 5,463	21,450	28,760	10,769	92,400 ± 17,650	4.94 ± 0.22	37,700 ± 7,196	24,978	47,520	5,235
Apr-21	53,450 ± 4,071	4.60 ± 0.07	30,607 ± 2,309	16,540	27,885	8,478	91,113 ± 9,627	4.81 ± 0.06	44,517 ± 6,315	30,027	41,290	4,595
May-21	57,890 ± 7,187	4.55 ± 0.07	28,600 ± 5,024	18,650	25,857	6,746	78,667 ± 6,559	4.69 ± 0.15	38,105 ± 5,678	26,519	44,670	4,665
Jun-21	61,300 ± 13,063	4.61 ± 0.05	29,780 ± 4,642	23,450	28,710		90,800 ± 5,222	4.78 ± 0.08	49,800 ± 8,000	30,600	43,290	
AVG 2019	59,952 ± 6,832	4.82 ± 0.14	28,123 ± 3,919	18,234	29,312	7,577	84,083 ± 14,810	4.66 ± 0.15	49,616 ± 11,427	38,124	41,620	2,849
AVG 2020	59,723 ± 7,974	4.78 ± 0.13	30,162 ± 6,006	20,376	29,145	6,462	85,283 ± 8,485	4.68 ± 0.10	47,608 ± 4,770	34,075	42,236	4,687
AVG 2021	59,053 ± 8,472	4.59 ± 0.06	29,148 ± 5,032	19,849	28,760	7,026	83,472 ± 9,039	4.77 ± 0.11	44,097 ± 5,864	28,193	42,973	3,968

Figures 4.2, 4.3 and 4.4 summarize the average characteristics of raw POME from the four mills (the error bars are the standard deviations). Based on the literature data in Table 4.3, the COD level of POME is found to be in the range of 50,000 to 146,824 mg/L. This range is comparable to POM A and C, with an average COD of 66,900 mg/L and 59,576 mg/L, respectively. However, POM B and D have COD levels of 81,608 mg/L and 84,280 mg/L, slightly higher than the average COD concentration reported in the literature. These data are consistent with the solid contents in both POMs. It shows that low solid content will affect the COD content of POME. Overall, POM C COD is the lowest. This is due to high water usage in the POM. Eventhough the dilution is more than double comparing to POM A, B and D, but COD result is not reduced two times. This is contributed by the highest oil and grease content.

The presence of high organic content in POME leads to high BOD as the oxygen demand to degrade organic matter increases. The amount of BOD can also be affected by excessive FFB processing that exceeds regular processing hours (Akhbari et al., 2020b). Similar to COD concentration, POME in POM A and C have BOD levels within the average literature value of BOD, whereas POM B and D have slightly higher BOD levels than other mills. BOD level of POM A is the lowest, followed by POM C, B, and D being the highest. Besides, BOD/COD ratio ranges from 0.4075 to 0.5016, where POM A has the lowest and D has the highest value. This indicates that the raw POME from POM D is more easily treatable by the anaerobic microorganism compared to other POMs.

TS is a form of organic matter abundantly present in POME, contributing to increased BOD and COD content. Referring to the literature (Table 4.3), the TS concentration ranges from 27,645 mg/L to 52,355 mg/L. It can be observed that POM B, C, and D are within the concentration range, which is 45339 mg/L, 29,114 mg/L, and 47,107 mg/L, respectively. Meanwhile, POM A has the lowest TS content, which falls below the lower limit of the concentration range, mainly due to the installation of a three-phase decanter. As for SS, the result shows similar trend to TS. POM D recorded highest SS due to direct discharge of effluent from sludge separator or steriliser station which may carry foreign materials like dirt, mesocarp fibre etc. After various stages of milling process (i.e. sterilization, stripping, digestion, pressing, and clarification), there is often a fraction of uncovered palm oil in the POME known as Oil and Grease (OG). Typically, fresh POME contains OG with 130 to 18,000 mg/L (Kamyab et al., 2018b). These oil droplets are present in two phases, floating in the supernatant of POME and suspended in the solids of POME. About 2,000 mg/L residue oil is emulsified in the supernatant of POME. Oil removal or recovery from the effluent is difficult as POME has an extremely high concentration of surfactant compounds that help to stabilize the oil droplets. Residue oil in the effluent is one of the main parameters that affect the COD and BOD values of POME (Sethupathi, 2004b). Adela Bukhari & Kheang Loh, 2013 also stated that the value of OG content in POME could be influenced by the amount of volatile fatty acids. Based on Figure 4.3, it can be observed that POM B and POM D have lower average OG content in POME compared to the other two

mills, with values of 2,532 mg/L and 3,835 mg/L, respectively, which fall within the average literature value range of 3364.8 mg/L shown in Table 4.3. On the other hand, POM C had the highest average OG content of 7,022 mg/L, while POM A had an average value of 6,426 mg/L. The results suggest that the OG content in POME can vary depending on the source, and factors such as the amount of volatile fatty acids present can also influence the OG content. Therefore, it is important to consider the source of POME and the treatment processes employed to reduce the OG content in the effluent.

POME is typically an acidic effluent with a pH range from 3.2 to 5.2 due to the presence of organic acids in complex forms that can be used as a carbon source. POM B has the most acidic POME, with an average pH value of 4.5. POM A is the least acidic, with an average pH of 4.8. POM C and POM D have the same pH value of 4.7. However, these pH values are still acceptable, as shown in Figure 4.4.

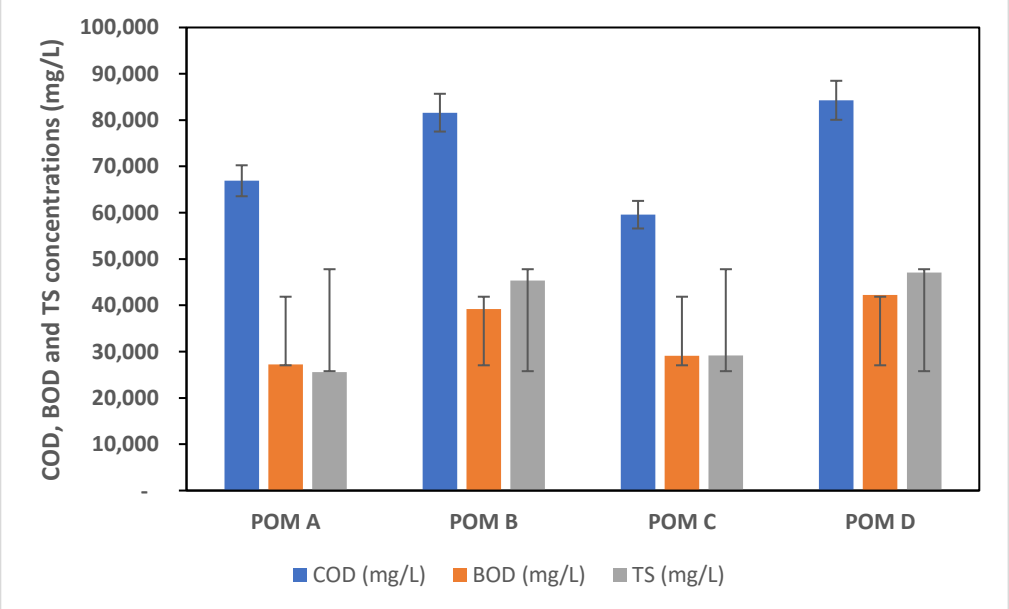

Figure 4.2: Average COD, BOD levels, and TS content of raw POME

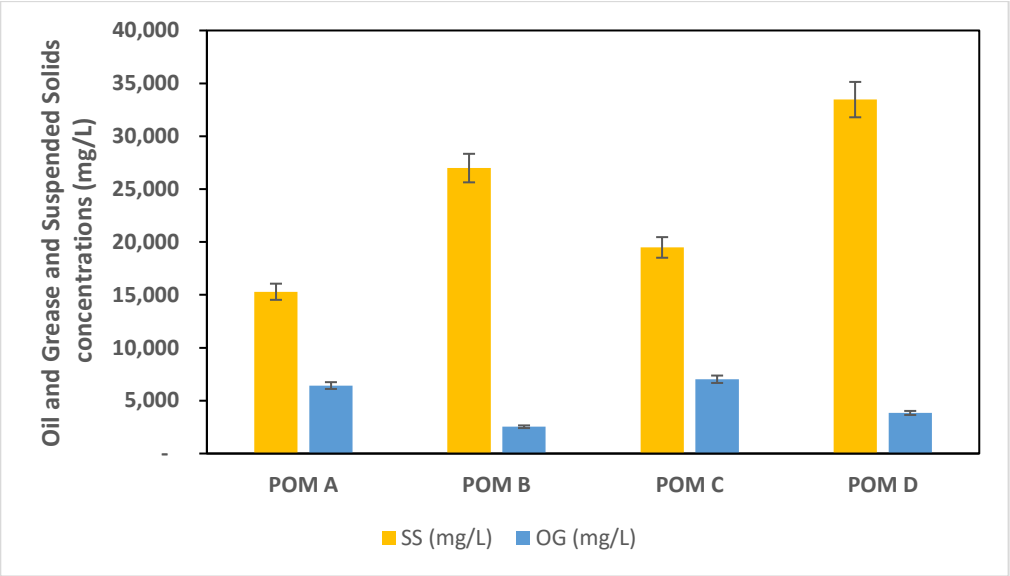

Figure 4.3: Average OG and SS content in raw POME

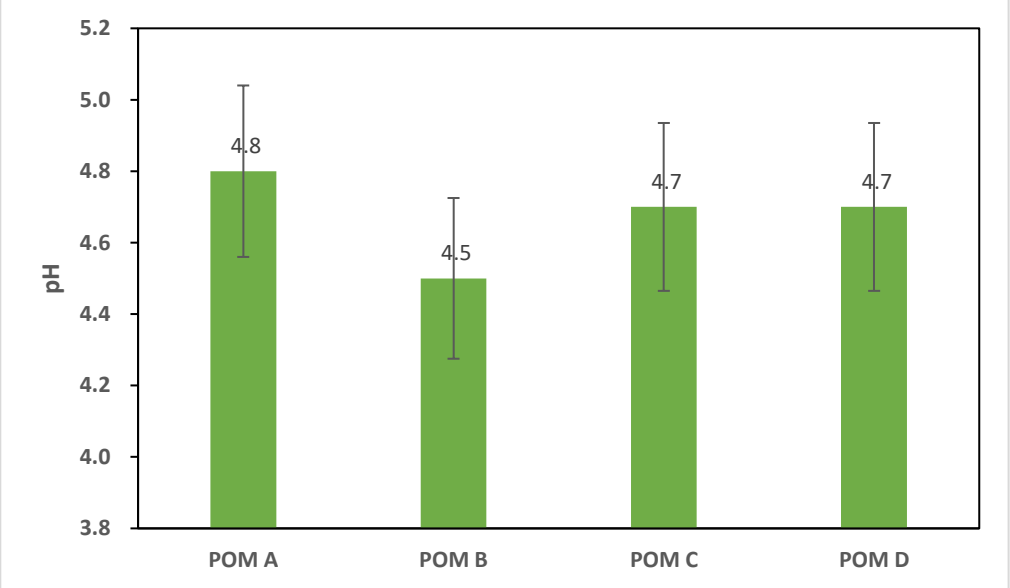

Figure 4.4: Average pH content in raw POME

4.1.3 Factors affecting the quality of POME in different mills

Identifying the factors that determine the POME characteristics is crucial so that the resulting POME can generate sufficient biogas to safeguard the profitability and sustainability of the POME-based biogas plants.

4.1.3.1 Selection of Clarifier System

The two most common technologies used in POM to treat the underflow sludge from the clarifier system are a three-phase decanter or a sludge separator. A three-phase decanter is valuable as it is cost-effective, has high throughput capacities for a continuous process, and can produce drier solids than a sludge separator. On top of that, it can recover the remaining oil from the sludge channeled from the bottom of the oil clarification tank. It also generates low solids concentration in wastewater, and low water consumption is used to ease the oil separation. On the other hand, a sludge separator only removes oil from the sludge, but the separation process is relatively ineffective compared to a decanter. Therefore, a three-phase decanter proves to be more efficient than a sludge separator in terms of effectiveness, oil losses, and water consumption. This is evident from the results obtained from the mills, where POM A has the lowest TS content of 25,580 mg/L (Figure 4.2) due to the use of one three-phase decanter and five sludge separators in the clarifier station. Furthermore, the use of a three-phase decanter reduces the TS content, which should lower the COD of POME. However, this is not the case for POM A due to the high COD addition from EFB juice produced in the EFB plant, which balances out the reduction of COD by the three-phase decanter and sludge separators. Therefore, the choice of technology for treating underflow sludge should take into account the specific conditions of each POM, such as the amount of EFB juice produced in the EFB plant.

4.1.3.2 Amount of Water Consumed

The quality of POME is greatly affected by the amount of water consumed during the extraction process. As reported by Ahmed et al. (2015b), a huge amount of water is used in the crude palm oil extraction process, with approximately 1.5 m^3 of water being used to process one tonne of fresh fruit bunch, and half of the water exits as wastewater, known as POME. The effluent generation factor (EGF) for all POMs ranges from 0.6 to 1.3 m^3/TFFB, with POM C having the highest EGF range between 1.0 and 1.3 m^3/TFFB, while POM D has the lowest range between 0.6 to 0.8 m^3/TFFB.

Dilution is a common practice used in mills to improve oil separation from solids and sludge, which results in increased efficiency of oil extraction. The high water usage during extraction enables better oil recovery and reduces the amount of total solids (TS) in POME. This is demonstrated in POM C, where the water used for separation was nearly double compared to POM A, B, and D, as shown in Figure 4.5. This resulted in a lower content of TS in POME in POM C as illustrated in Figure 4.2, which is almost comparable to that of POM A, where a three-phase decanter was used. Furthermore, POME in POM C was further diluted by hydrocyclone wastewater and cleaning water, which resulted in the lowest COD level (Figure 4.2) among all POMs. Therefore, it can be concluded that separation is enhanced by the massive consumption of water. However, it is important to note that high water usage can lead to an increase in the volume of POME generated, which can result in environmental pollution. Therefore, mills must balance water

consumption with the need for efficient oil extraction while ensuring environmental sustainability.

Apart from this, the operation of the desanders unit after the clarifier is also critical in removing impurities such as sand and fiber trapped by the clarifier. To achieve this, operators must flush the desander with a high amount of water, which can further dilute the POME in the sludge pit. This practice can help to reduce the concentration of TS and COD in POME, which improves the quality of the effluent and reduces the environmental impact of POME. As mentioned in Section 4.1.2, the reduction of TS in POME for POM A and C resulted in lower levels of COD and BOD compared to POM B and D (Figure 4.2). Additionally, it was expected that the OG content in POME for POM A and C would be lower due to the trapping of OG in solids. However, this was not the case as the OG content in POME for both POMs was also high (Figure 4.3). The reason behind this is poor operation control by the operator in the clarification station.

One of the issues is with the manual sludge discharge process, which is not easy to operate as the oil can be carried out together with the sludge if the discharge valve is not carefully controlled. Furthermore, the continuous and fluctuating flow of sludge into the clarifier mixed the settled sludge and floated oil. This inconsistency is due to the incoming flow rate to the clarifier tank, which stirs the top and bottom parts of the clarifier whenever the flow rate is too high. To address these issues, it is crucial to improve the operation control in the clarification station. The operators should be trained to discharge the sludge properly and control

the discharge valve to avoid carrying oil out with the sludge. Moreover, the incoming flow rate to the clarifier tank should be regulated to maintain consistency, ensuring that the settled sludge and floated oil are not mixed. These improvements would result in lower OG content in POME, which can further reduce the COD and BOD levels.

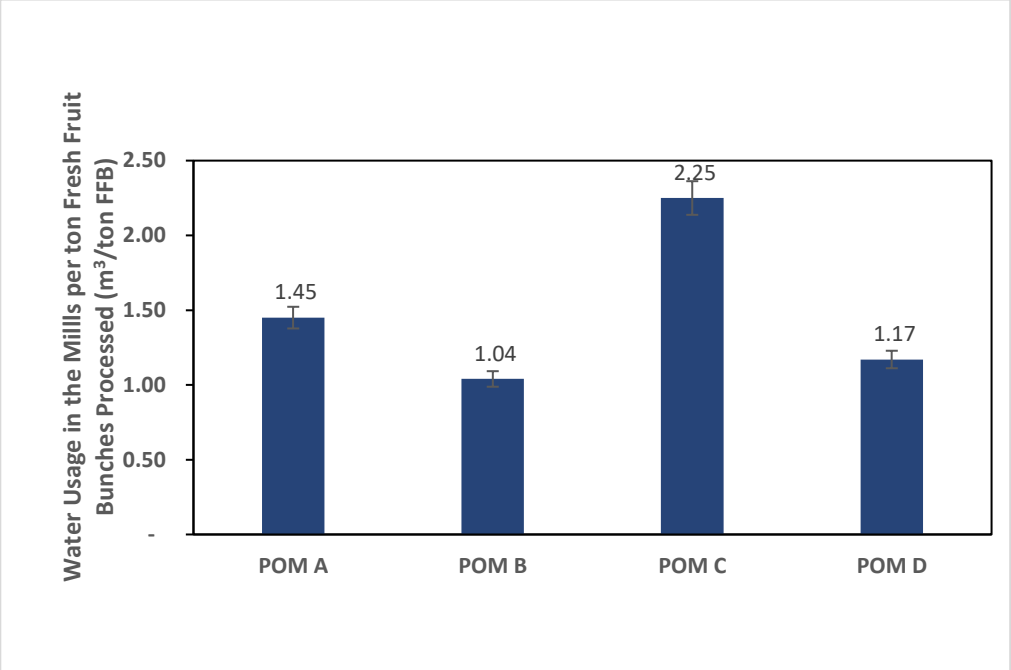

Figure 4.5: Water usage in the mills. The error bars are the standard deviations

The high water usage in the POMs processes is not a sustainable solution. The water source for mill operations typically comes from a nearby river or state clean water provider. Some POMs have to pay a substantial cost for this matter. POMs must be accountable for their high water usage consumption, especially for dilution purposes during processing palm fruit, because it affects the overall water footprint around the palm oil mill area (Subramaniam et al., 2014). Furthermore, the reduced water usage in POM B has resulted in a decreased dilution effect

of organic acids in POME. This may explain why POM B has the lowest pH level, as depicted in Figure 4.4. It is imperative that POMs consider sustainable alternatives to water consumption to mitigate their environmental impact and reduce their operational costs.

4.1.3.3 Installation of EFB Press Station

Despite all mills being equipped with EFB plants, only POM A conducts EFB pressing operations continuously and efficiently, while POMs B, C, and D do not. This is due to the high maintenance cost of the screw press, which often experiences wear and tear and requires regular replacements. Therefore, POM A recovers additional oil from EFB pressing, resulting in more oil being recycled back to the clarifier station, and ultimately leading to higher OG levels in the POME (Figure 4.3), despite the use of a three-phase decanter for better separation. According to Akhbari et al. (2020b), about 4% of oil remains in EFB, further contributing to the high OG levels in POM A's POME. However, the EFB pressed juice also increases the COD content of POME in POM A, which explains why even though POM A recorded the lowest TS, the COD reading is still considered high (Figure 4.2. The COD content of the EFB juice produced in Lepar Hilir was found to be 72,400 mg/L based on laboratory analysis data. This value is slightly lower than the reported value by Boe (2006), which is 74,750 mg/L. Not many studies report the COD value of EFB pressed juice characteristics, with most focusing on the physical characteristics of EFB and its suitability for co-digestion with POME for biogas generation or composting business. Therefore, despite the advantages of EFB pressing, the high maintenance cost and

increased COD content of POME should be taken into account before implementing EFB pressing operations.

4.1.3.4 Selection of Steriliser Type

POM B is the only mill equipped with a conventional cages system to sterile the FFB. This mill recorded the lowest OG content (Figure 4.3). It proved that a conventional cages system with an application of steam is able to reduce the oil losses that might trap in the steriliser condensate. On the other hand, POMs A, C, and D recorded higher OG content in POME, which can be attributed to the sterilizer condensate handling principle and the amount of water used in the mills. In POM C, excessive water is used in the separation process in the clarification tank, which leads to the mixing of bottom sludge with the floating oil. This results in some oil flowing out with the underflow sludge to the cooling pond. In POMs A and D, the high OG content is related to poor handling at the clarifier station. Moreover, the direct discharge of sterilizer condensate to the sludge pit without clarification in POM B and POM D resulted in higher COD content in both POMs. The use of bunch splitter cutters in the CS system prior to sterilization, as based on the input from the mill manager experience, could potentially increase oil losses in the condensate. However, this finding could benefit the biogas plant project developer, as higher COD content in POME results in more biogas production and maximizes power generation capacity.

4.2 Inground Lagoon AD Profiling and Performance Study

This section will explain the findings of design parameters of all AD and its performance in terms of effluent, sludge, and biogas production. The AD profile is summarised in Table 4.3. The historical data from July 2019 to June 2021 of OLR, HRT, pH, temperature, recirculation ratio, TS, SS, BOD_3, COD and biogas production collected from the biogas plants were analysed and summarised in Table 4.3 before conducting the ANOVA analysis for each parameter. Table 4.3 provides a comprehensive overview of the variability observed in the measured parameters. Detailed monthly data was compiled in the Appendix 4. The standard deviations offer insights into the extent of variation within each performance indicator and help to assess the consistency of the digester performance. The subsequent ANOVA analysis delves deeper into identifying significant differences or similarities between groups, providing valuable insights into the factors affecting the digester performance. By utilizing both the standard deviations and ANOVA analysis, a comprehensive understanding of the consistency of the digester performance can be obtained, and any significant differences among the studied variables can be determined. This approach enables the drawing of robust conclusions regarding the factors influencing the digester operation and their impact on performance indicators.

4.2.1 In-ground Lagoon AD Profile

All of the AD utilised the in-ground lagoon AD system based on the decision made by the CGESB management. The main reason for choosing this technology is the bigger biogas storage underneath the AD

cover, allowing them to optimise biogas engine operation to generate electricity consistently without interruption of gas supply. According to CGESB, the selection was made based on the advice of FGV engineers managing different types of AD technologies. FGV experienced inground lagoon AD has better process control than the tank system. Generally, all of the AD was designed using the same value of OLR, which is at 2.1 kgCOD/m^3.day. The in-ground lagoon AD was equipped with a series of pipelines: POME feeding, POME mixing in the AD, bottom sludge piping system to handle accumulated sludge at the bottom part of AD, treated effluent pipeline, biogas pipeline surrounding the AD (underneath the cover) to collect the biogas and also for gas flaring facilities. The mixing of POME in the digester was done by the pumps connected to the mixing tank. This tank is the pre-treatment facility for all BGPs to control the pH and temperature of POME entering the AD by mixing the recirculation of bottom sludge and treated effluent with POME. Mixing tanks, pumps, and piping sizes for all BGPs are identical. However, the AD capacity sizing varied due to the POM processing capacity. CGESB assessed and analysed at least five years of historical and projection data of FFB processed for each mill before designing the AD. Table 4.4 below is the summary of the design data of each BGP.

Table 4.3: Profile for all in-ground lagoon AD

BIOGAS PLANT INFORMATION					
PLANT NAME		BGP A	BGP B	BGP C	BGP D
ADDRESS		26300 Kuantan	81930 Bandar Penawar	26900 Bandar Tun Razak	81930 Kota Tinggi
		Pahang	Johor	Pahang	Johor
BIOGAS PLANT BACKGROUND					
SEDA FEED-IN-TARIFF (FiT) INFORMATION					
Net Export Capacity	kW/hr	1500	1500	1300	1300
Installed Capacity	kW/hr	1800	1800	1500	1500
Commissioning Year		Dec-18	Jun-19	Feb-19	Jun-19
DESIGN INFORMATION					
AD Capacity	m^3	37000	39000	33000	30000
Type of AD		In-ground lagoon digester	In-ground lagoon digester	In-ground lagoon digester	In-ground lagoon digester
Type of Feedstock		POME	POME	POME	POME
OLR	$kgCOD/m^3.d$	2.1	2.1	2.1	2.1
HRT	days	> 29	> 37	> 33	> 45
Mode of AD Condition		Mesophilic	Mesophilic	Mesophilic	Mesophilic

POME Pretreatment Information		80m^3 mixing tank, POME to mix with recycle sludge	80m^3 mixing tank, POME to mix with recycle sludge	80m^3 mixing tank, POME to mix with recycle sludge	80m^3 mixing tank, POME to mix with recycle sludge
Post AD Treatment Information		Not available; after the AD, the treated effluent is delivered to an open ponding system for further conventional effluent treatment (facultative and algae open ponds)	Not available; after the AD, the treated effluent is delivered to an open ponding system for further conventional effluent treatment (facultative and algae open ponds)	Not available; after the AD, the treated effluent is delivered to an open ponding system for further conventional effluent treatment (facultative and algae open ponds)	Not available; after the AD, the treated effluent is delivered to an open ponding system for further conventional effluent treatment (facultative and algae open ponds)
Mixing Mechanism		By hydraulic mixing using pumps	By hydraulic mixing using pumps	By hydraulic mixing using pumps	By hydraulic mixing using pumps
Sludge Handling		By pumps; inlet suction pipe at the bottom of AD	By pumps; inlet suction pipe at the bottom of AD	By pumps; inlet suction pipe at the bottom of AD	By pumps; inlet suction pipe at the bottom of AD

Table 4.4: Summary of two years AD process parameters

Analysis parameters		Units	BGP A			BGP B		
Pre-treated POME			Min	Max	Average	Min	Max	Average
	Temp.	$°C$	35.9	45.2	41.39±2.35	37.6	43.2	40.41±1.37
	pH	-	6.91	7.40	7.08±0.10	6.8	7.1	6.97±0.08
	RR	-	0.18	2.28	0.99±0.47	1.24	4.42	2.39±0.74
Operating parameters	OLR	-	0.91	1.51	1.12±0.17	0.98	1.62	1.30±0.15
	HRT	days	40.26	74.13	61.4±9.55	49.87	87.92	64.04±7.83
Treated Effluent	T	$°C$	37.8	42.5	40±1.3	36.7	41.0	39±1.3
	pH	-	7.1	7.4	7.19±0.07	7.3	7.7	7.45±0.10
	COD	mg/L	10330	20800	14814±2589	14500	19340	17546±1283
	BOD	mg/L	2356	4440	3579±524	3450	5670	4562±552
	TS	mg/L	7505	16540	12639±2192	11150	21480	15932±2569
	TSS	mg/L	8769	16660	12663±1931	8460	19900	12576±2523
Performance indicators	Biogas Production Rate	$Nm^3 /month$	64731	483126	276956.94±86073	223490	468521	378874.72±67967
	Methane Yield	Nm^3 CH_4 / kg COD removed	0.135	0.364	0.221±0.053	0.191	0.360	0.250±0.040
	Methane content	%	60.80	63.91	62.75±0.94	55.74	62.38	58.62±1.32
	H_2S	mg/L	2	1073	653.92±280	805	1887	1291.3±236
	COD removal	%	68.0	83.8	78.6±0.04965	75.5	81.4	78.7±0.01755
	COD Removal Rate	$\mathrm{kgCODr}/\mathrm{month}$	300935.9	1137195	767063.8±186550.9	369942	1209674	906847±179807
	BOD removal	%	81.32	91.14	86.85±2.72	82.77	92.31	88.47±2.30
	TS removal	%	66.8	85.0	77.69±0.0486	54.8	77.3	64.78±6.0

Analysis parameters		Units	BGP C			BGP D		
Pre-treated POME			Min	Max	Average	Min	Max	Average
	Temp.	$°C$	37.9	44.2	41.71±2.23	37.8	48.7	43.08±2.91
	pH	-	6.78	6.98	6.88±0.05	6.75	7.1	6.89±0.08
	RR	-	0.76	3.06	1.32±0.64	0.55	3.07	1.39
Operating parameters	OLR	-	0.85	1.78	1.29±0.23	1.22	1.77	1.46±0.15
	HRT	days	34.04	65.81	47.62±8.55	50.48	67.97	57.92±4.70
Treated Effluent	T	$°C$	35.8	42.5	39.8±2.3	35.3	44.5	39.6±2.7
	pH	-	7.0	7.2	7.11±0.05	7.15	7.55	7.32±0.10
	COD	mg/L	9200	18300	13313±2404	13450	23670	18197±3195
	BOD	mg/L	1990	5780	816	2680	4560	3428±504
	TS	mg/L	8570	19700	12048±2417	10100	25652	16925±4186
	TSS	mg/L	386	11659	7542±3863.36	8700	21300	13917±3366
Performance indicators	Biogas Production Rate	$Nm^3/month$	173153	424648	320825.07±68541	18320	396169	272378.47±100745
	Methane Yield	$Nm^3\ CH_4$ / kg COD removed	0.173	0.292	0.246±0.032	0.037	0.316	0.237±0.062
	Methane content	%	57.82	64.02	61.09±1.23	57.90	62.53	60.47±0.97
	H_2S	mg/L	535	1680	1167.29±278	246	1797	1167.29±269
	COD removal	%	70.7	83.6	78.3±0.04195	69.9	84.8	79.0±0.0449
	COD Removal Rate	$\mathrm{kgCODr/month}$	417221	1098279	806224±184258	266099	1102973	640250±207357
	BOD removal	%	79.8	93.3	88.3±3.40	89.00	93.81	91.80±1.36
	TS removal	%	31.0	74.0	57.36±11.0	45.1	77.4	63.44±10.8

4.2.2 Analysis of Pre-treated POME at the Mixing Tank

The outlet mixing tank temperature trend in all BGPs is inconsistent. Figure 4.4 shows the monthly average mixing tank outlet temperature, pH and recirculation ratio data in the four different BGPs. Figure 4.6(a) shows that the temperature entering the AD is fluctuates between 36 to 49 ^{0}C. There was a huge drop in the temperature of BGP A between Oct-19 to Feb-20. An abnormal temperature trend for BGP B's mixing tank from July-19 to Dec-19 is observed. For BGP C, the outlet temperature of the mixing tank from t-19 to Apr-20 and Nov-20 to Feb-21 experienced a major decline. As for BGP D, it is seen that the outlet temperature of the mixing tank is not only high but also fluctuates most of the time and reached the highest at 49 ℃ in Oct and Nov-19. This is mainly due to the high loading of POME and poor control of the re-circulation ratio (56-58%). Based on the data obtained (Table 4.5), the BGP B has the closest outlet temperature of 40°C compared to the literature data of 37°C. As for BGP A and C, they have comparable outlet temperatures at 41°C and were slightly higher than BGP B. This is because of a few factors, such as the poor efficiency of the cooling pond to reduce the raw POME temperature consistently, sudden environmental changes such as extreme temperature drops during rainy days, and recirculation amount is not easily controlled due to the limitation of the pump flowrate and the manual operation, which requires skilled operators. A high amount of recirculation, an average of 250%, reduced the mixing tank's temperature outlet, as proved by BGP B. Hence, BGP B shows the most stable and the lowest temperature outlet from the mixing tank compared to the

remaining BGPs. BGP A, BGP C, and BGP D's average recirculation ratio are below 120%.

The pH of each biogas plant is considered consistent in the data, as shown in Figure 4.6(b). The average pH recorded in all BGPs are between 6.9 to 7.1. This value is considered good for the pre-treatment section. Recirculation ratio from treated POME is prevalent to maintain the alkalinity of the pH level to 7.0. While specific alkalinity measurements are not carried out in this study, the understanding of the relationship between alkalinity and pH supports the justification for maintaining high alkalinity levels to ensure a desired pH of 7.0 in the system (Fikri Hamzah et al., 2019a). The preservation of high total alkalinity that acts as pH buffer for the anaerobic digestion system. With the presence of pH buffer, it can prevent notable change in pH and able to eliminate the remaining volatile fatty acids during the AD. Unstable pH causes the methanogens not being able to carry out neutralisation of volatile fatty acids properly in the anaerobic digester (Fikri Hamzah et al., 2019)Click or tap here to enter text.. However, the methanogens favour the pH conditions as it is near the neutral condition. The minimum pH recorded was 6.75 in BGP D on Nov-19. A pH spike in BGP could be observed from Jul-19 to Aug-19 where the pH increased by 0.7. However, pH for BGP B and D is relatively more stable than BGP A and C as the pH values were well maintained within the margin of ±0.5.

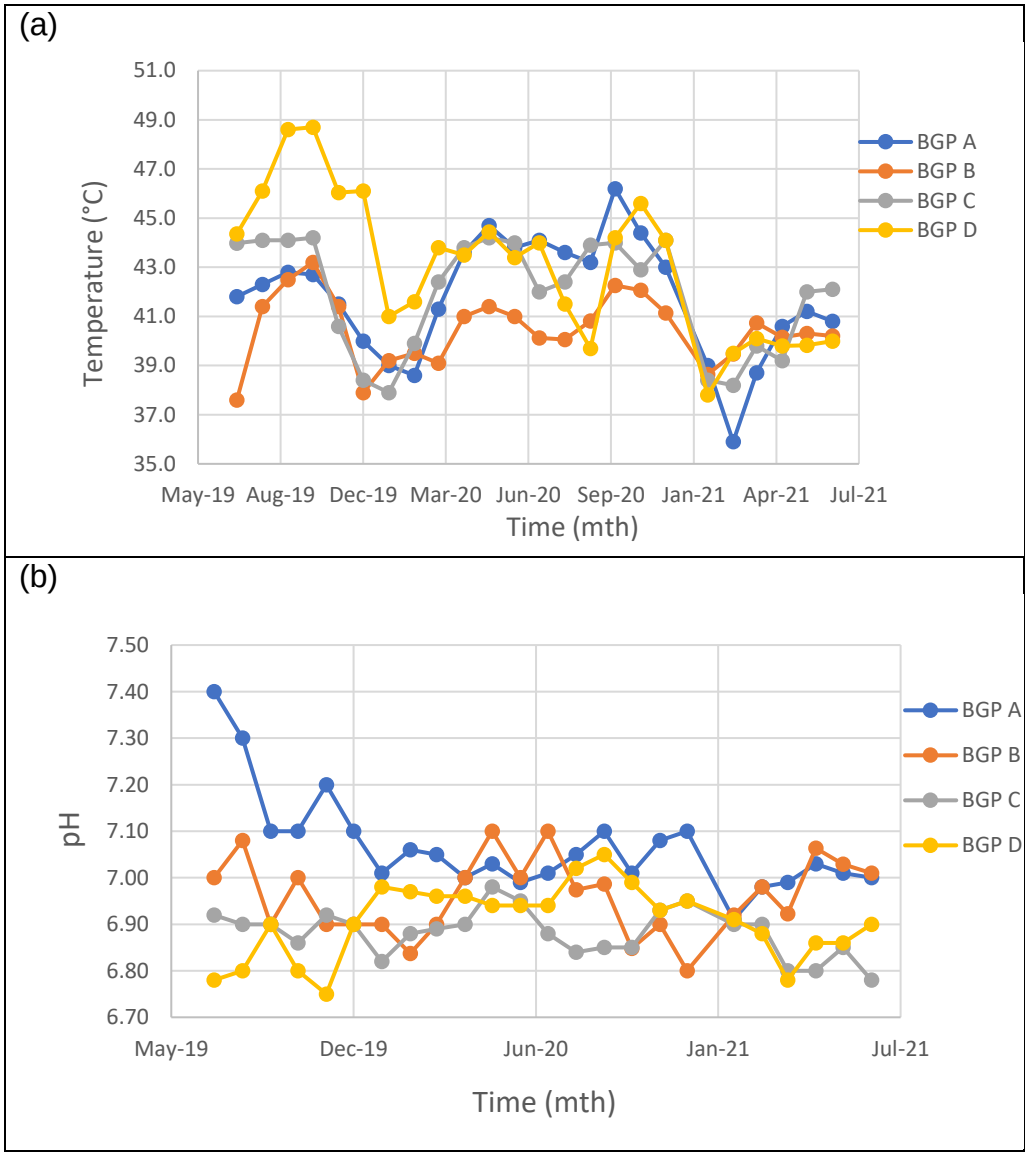
(a)
51.0
49.0
47.0
45.0
43.0
41.0
39.0
37.0
35.0
Temperature (°C)
May-19
Aug-19
Dec-19
Mar-20
Jun-20
Sep-20
Jan-21
Apr-21
Jul-21
Time (mth)
BGP A
BGP B
BGP C
BGP D
(b)
7.50
7.40
7.30
7.20
7.10
7.00
6.90
6.80
6.70
pH
May-19
Dec-19
Jun-20
Jan-21
Jul-21
Time (mth)
BGP A
BGP B
BGP C
BGP D

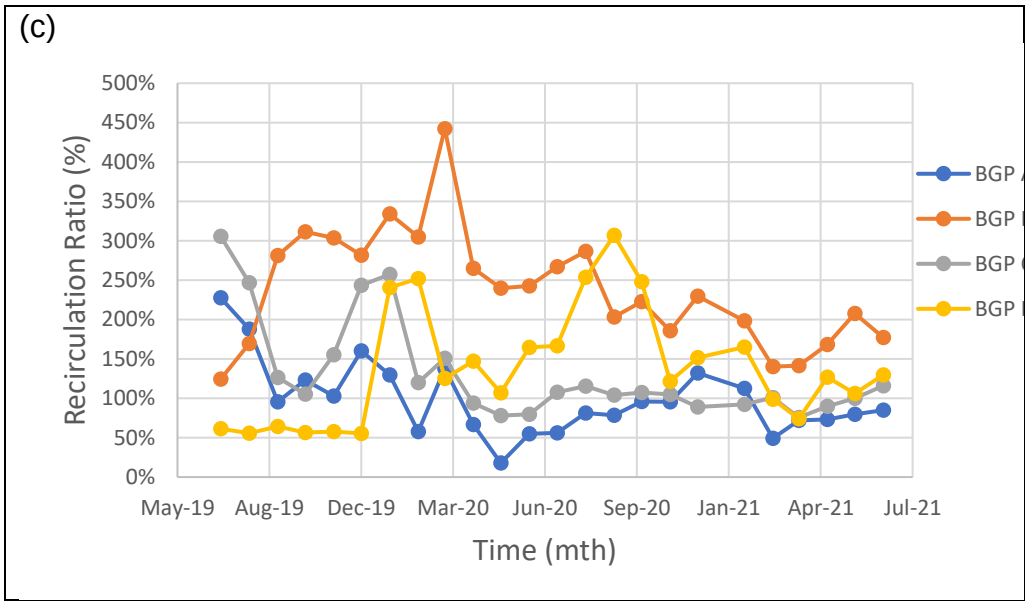

Figure 4.6: Analysis of mixing tank outlet (a)temperature, (b)pH and (c)RR of biogas plants from July-19 to Jun-21

Generally, the fluctuations in the recirculation ratio can be attributed to the manual operation of the recirculation process in the biogas plants. The recirculation of bottom sludge to the mixing tank is carried out manually using a centrifugal pump connected to a pipe that reaches the bottom part of the anaerobic digester. In this manual mode, the flow rate of the pump cannot be precisely controlled by the operators. The recirculation process relies on the operators manually turning on the pump whenever POME is pumped into the mixing tank. Due to the manual nature of this operation, inconsistencies in the flow rate of the bottom sludge occur (between 15 m^3/hour to 40 m^3/hour), leading to fluctuations in the recirculation ratio. Furthermore, difficulties may arise with the airlock inside the piping, resulting in pipe clogging. These incidents can significantly reduce the flow rate during such occurrences. Conversely, when the bottom sludge is diluted, typically containing fewer total solids, the flow rate tends to increase.

As shown in Figure 4.6(c), BGP A shows the highest ratio of recirculation of treated effluent and bottom sludge to POME from July-19 to Sep-19. In July-19, the recirculation ratio recorded is 228% and it eventually drops to 96% with an increasing POME load. The huge decrease in the recirculation percentage greatly reduces the pH but not the temperature. The increase in outlet temperature of the mixing tank could be because of the high POME load which makes it difficult to maintain the temperature.

As for BGP B, a significant increase in the ratio of recirculation to POME can be seen in Figure 4.6(c) from July-19 to October-19. This change has not much effect on the pH but on the outlet temperature which can be seen increasing. This clearly show that the inlet temperature of the mixing tank (i.e. raw POME from the cooling pond) was the disturbance that causes the temperature rise. Although, the data shows that the treat effluent and the bottom sludge from the lagoon have low temperature, yet it could not do much to the outlet temperature of mixing tank. Apart from that, there was a sudden rise in Feb-20 to Mar-20 (305% to 442%) but no significant change in the temperature and pH was observed. Temperature and pH were well maintained as the POME loading (approximately 1.0 kg COD_{in}/m^3 day) is quite low.

For BGP C, there is a massive drop in the recirculation ratio, though a consistent temperature and pH was recorded based on the data in Figure 4.6(c) from Jul-19 to Oct-19. Another relationship can be seen from Jan-20 to May-20 when the recirculation percentage drops from 254% to

78%. The pH is well maintained but the temperature is increased resulting from the high inlet mixing tank temperature.

Similarly, for BGP D, a huge rise in the recirculation ratio from May-20 to Sep-20 does not affect the pH much but a temperature drop was observed. Although the inlet temperature was high, yet it is stable, and the outlet temperature can be easily controlled through the recirculation ratio. The only attention that needs to be focused on is the POME loading as low loading of POME might require a high recirculation ratio. This is because a lower POME loading means there is a reduced amount of fresh POME entering the system. To ensure optimal performance and maintain the desired operational conditions, a higher recirculation ratio is often implemented to compensate for the lower POME input and sustain the required levels of substrate and microbial activity within the anaerobic digester.

4.2.3 Analysis of Treated Effluent at Anaerobic Digester

The temperature of all the treated effluent ranges from 35.3°C to 44.5°C. Figure 4.7(a) presents the temperature trend of treated effluent from BGP A, B, C and D. All the temperatures obtained show a similar trend with pre-treatment inlet temperature readings. As for the temperature, many factors such as the temperature from the bottom sludge and treated effluent, inlet mixing tank temperature and POME loading can greatly influence the process of anaerobic digestion. BGP C demonstrates the least stability among all the other BGPs while BGP B shows the most stable temperature readings. These temperature readings heavily influenced by the processing of FFBs, which led to the quality of raw

POME. This is because the maximum specific methanogenic activity was affected by daily upward temperature fluctuations rather than daily downward temperature fluctuations (El-mashad, 2004).

As shown in Figure 4.7(b), the pH values of all treated POME ranges from 7.0 to 7.68. It can be deduced that the pH obtained for all the treated POME in all the BGPs are satisfactory and within the standard discharge limit set by DOE (5-9). The pH fluctuations were due to inconsistent POME feeding, which resulted different loading rate every day. It can be concluded that most biogas plant can control the pH well by adjusting the ratio of the total recirculation to POME.

(a)

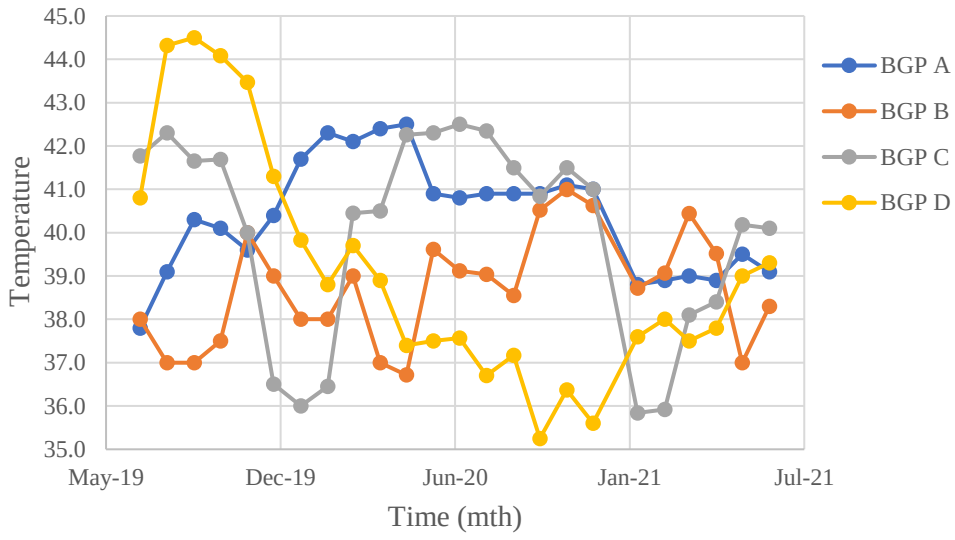

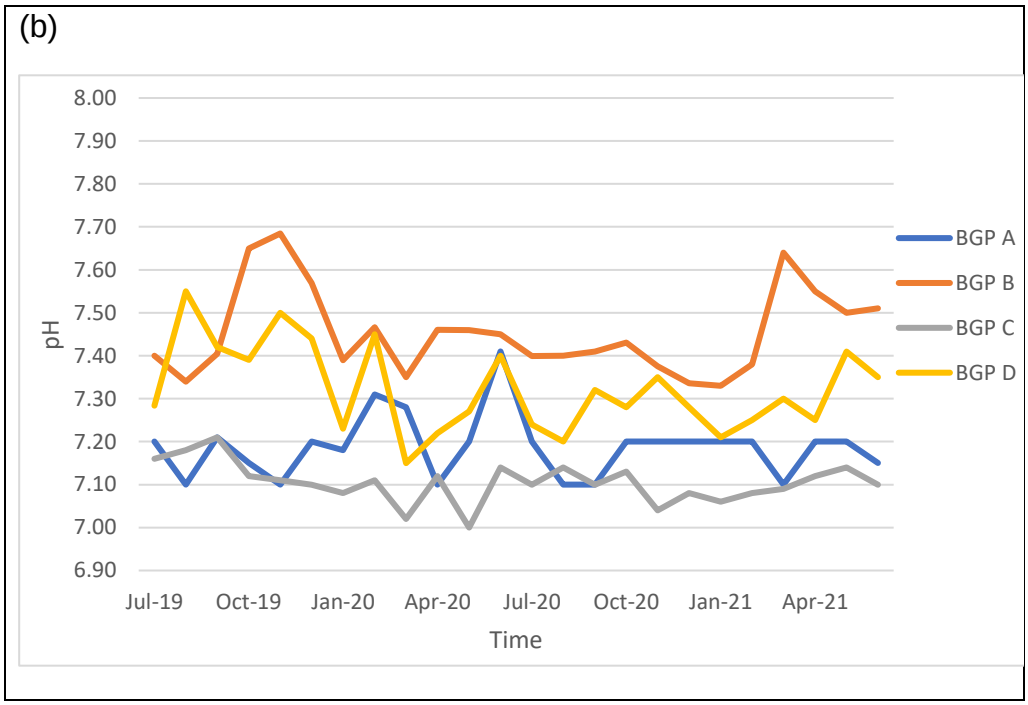

Figure 4.7: a) Temperature and b) pH of the treated effluent in biogas plants from July-19 to Jun-21

Figure 4.8 shows the monthly average BOD, COD and TSS concentrations of the treated effluent. Referring to Figure 4.8(a), BGP C and D has a comparable average BOD content of about 3,400 mg/L which have also the lowest BOD content in the treated effluent. BGP A has a slightly higher BOD content (3,579 mg/L) as compared to BGP C and D. The highest BOD concentration in treated effluent was recorded as 4,562 mg/L at BGP B. According to the DOE, the BOD contents of the treated effluent of all BGPs have yet to meet the discharge standard limit of 20 mg/L (Mohammad et al., 2021). Hence, further treatment like aerobic pond which helps to reduce BOD is mandatory (Chin et al., 2013).

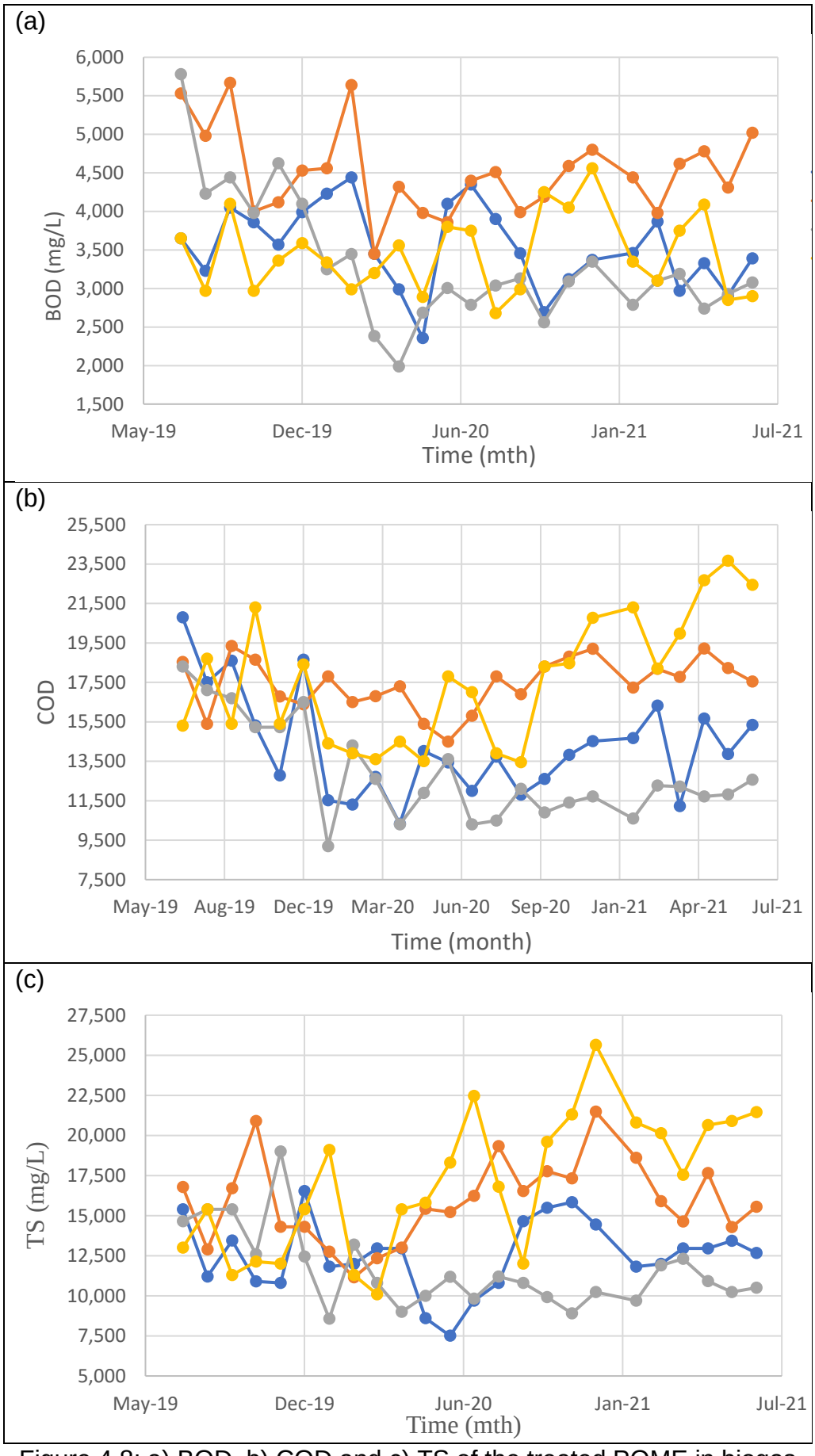

Figure 4.8: a) BOD, b) COD and c) TS of the treated POME in biogas

plants from July-19 to Jun-21

Figure 4.8(b) shows the COD trend of treated effluent of BGP A, B, C and D. The average COD level in BCP D (18,197 mg/L) is the highest followed by BGP B (17,546 mg/L), BGP A (14,814 mg/L) and lastly BGP C (13,313 mg/L) in a decreasing order. By comparing the influent COD with the effluent COD of the anaerobic lagoon, it shows all BGPs have achieved the desired COD content at the treated effluent. About 80% of the COD is said to be successfully removed from the untreated POME to produce methane gas for power generation. However, 20% of the COD is remained in the treated effluent which is still high as seen in the Figure 4.8(b) ranging from 10,000 to 20,000 mg/L. Thus, the COD value of the treated effluent must be lowered and further treated. This treated effluent will be conveyed to the facultative ponds, algae ponds and finally discharge to waterways.

Figure 4.8(c) shows the total solids concentration at the treated effluent of all BGPs. BGP C has the lowest total solids concentration (12,048 mg/L) followed by an increasing solids content at BGP A (12,639 mg/L), then BGP B (15,932 mg/L) and lastly BGP D (16,925 mg/L) having the highest concentration. In BGP D, there is an increasing trend of total solids due to the high total solids in the raw POME from POM D. This will cause some drawbacks to the AD as it is unstable and low methane yield would be formed due to the high concentration of inactive biomass.

4.2.4 Operating Parameters and Performance Indicators of Anaerobic Digester

The designed loading rate of each covered lagoon digester for the plants is 2.1 kg COD_{in}/m^3 day. Alexiou & Mara (2003) claimed that the best COD removal efficiency can be achieved when the operating OLR of the pond is lower than the designed loading rates. Figure 4.9 shows the OLR, HRT and TS of the bottom sludge of the anaerobic digester while Figure 4.10 shows the COD removal of the anaerobic digester. Figure 4.11 shows the total biogas production of four plants. Referring to Figure 4.9(a), OLR of all the BGPs are lower than designed loading rate. The average OLR for BGP A, B, C, and D ranges from 1.13 to 1.47 kg COD_{in}/m^3 day. These results are satisfactory and acceptable as methane production can be accomplished. However, the design loading for the covered lagoon can be optimised to achieve higher OLR as increase in OLR would increase COD removal, and thus higher methane production.

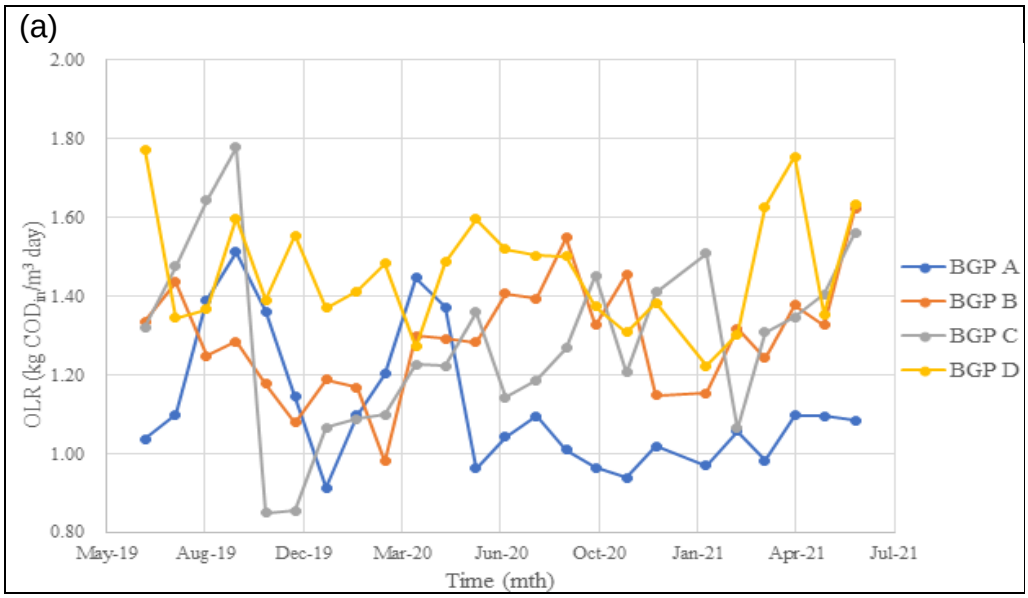

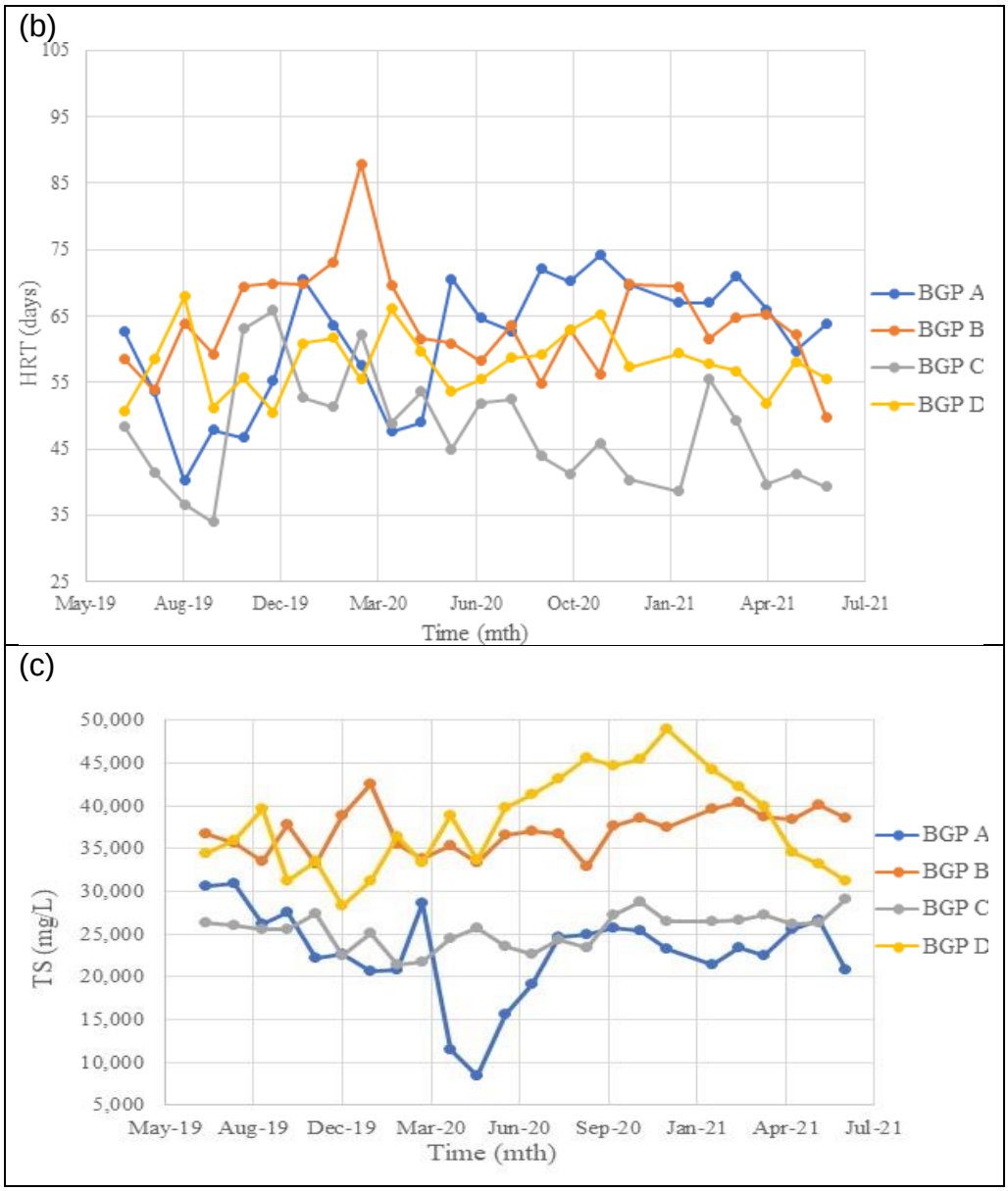

Figure 4.9: a) OLR, b) HRT and c) TS of bottom sludge in biogas plants

(a)

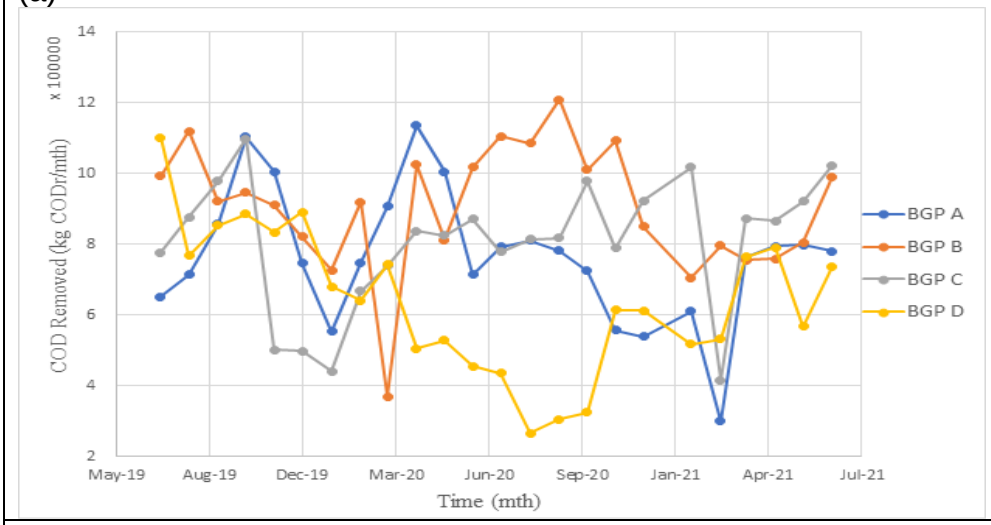

(b)

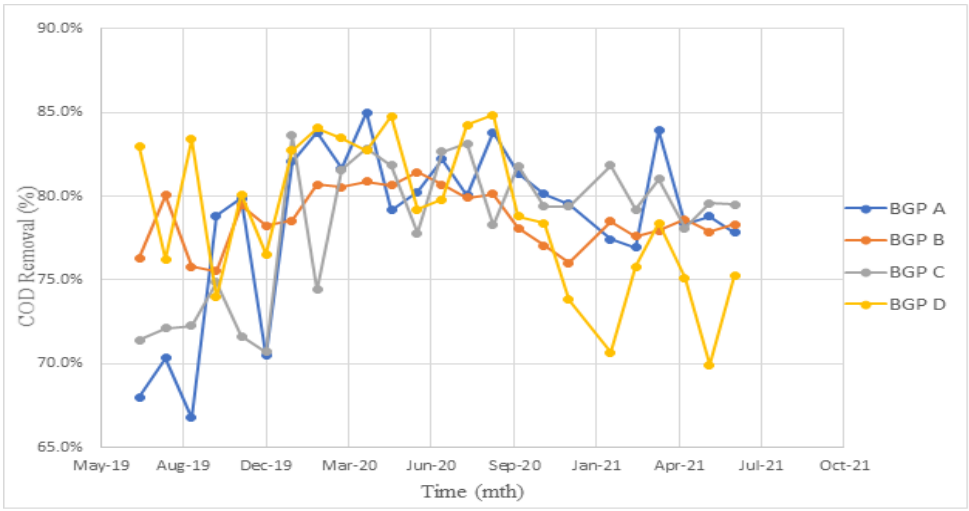

(c)

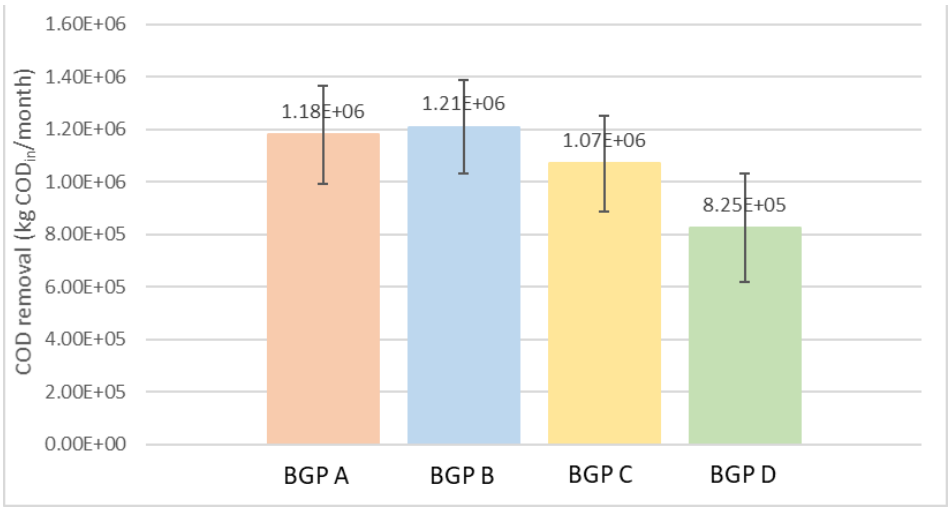

Figure 4.10: a) Total COD removed b) COD removal (%) c) Maximum COD removal for each biogas plant

(a)

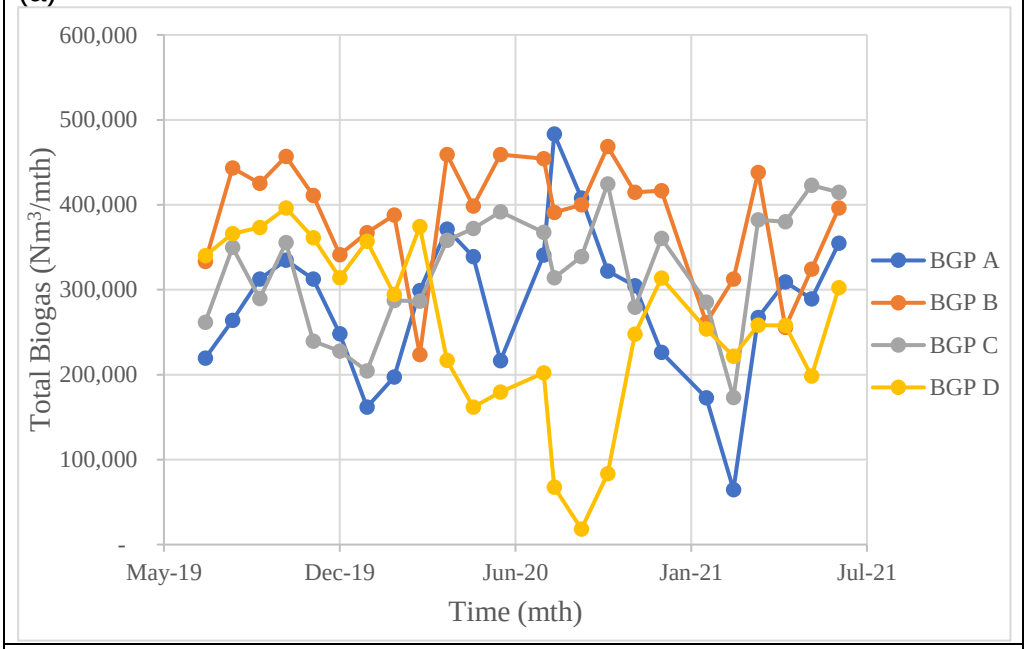
600,000
500,000
400,000
300,000
200,000
100,000
-
Total Biogas (Nm3/mth)
May-19
Dec-19
Jun-20
Jan-21
Jul-21
Time (mth)
BGP A
BGP B
BGP C
BGP D

(b)

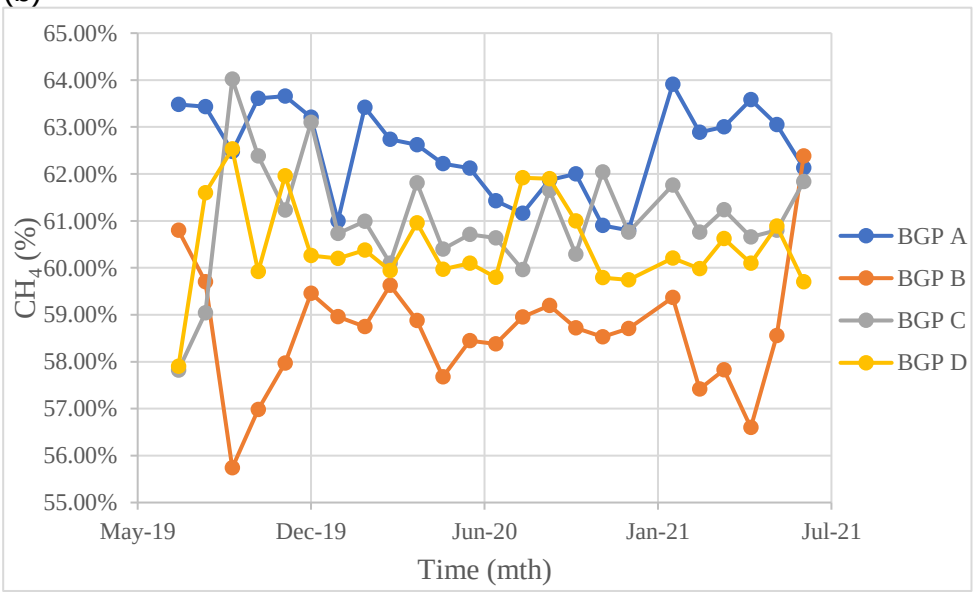
65.00%
64.00%
63.00%
62.00%
61.00%
60.00%
59.00%
58.00%
57.00%
56.00%
55.00%
CH4 (%)
May-19
Dec-19
Jun-20
Jan-21
Jul-21
Time (mth)
BGP A
BGP B
BGP C
BGP D

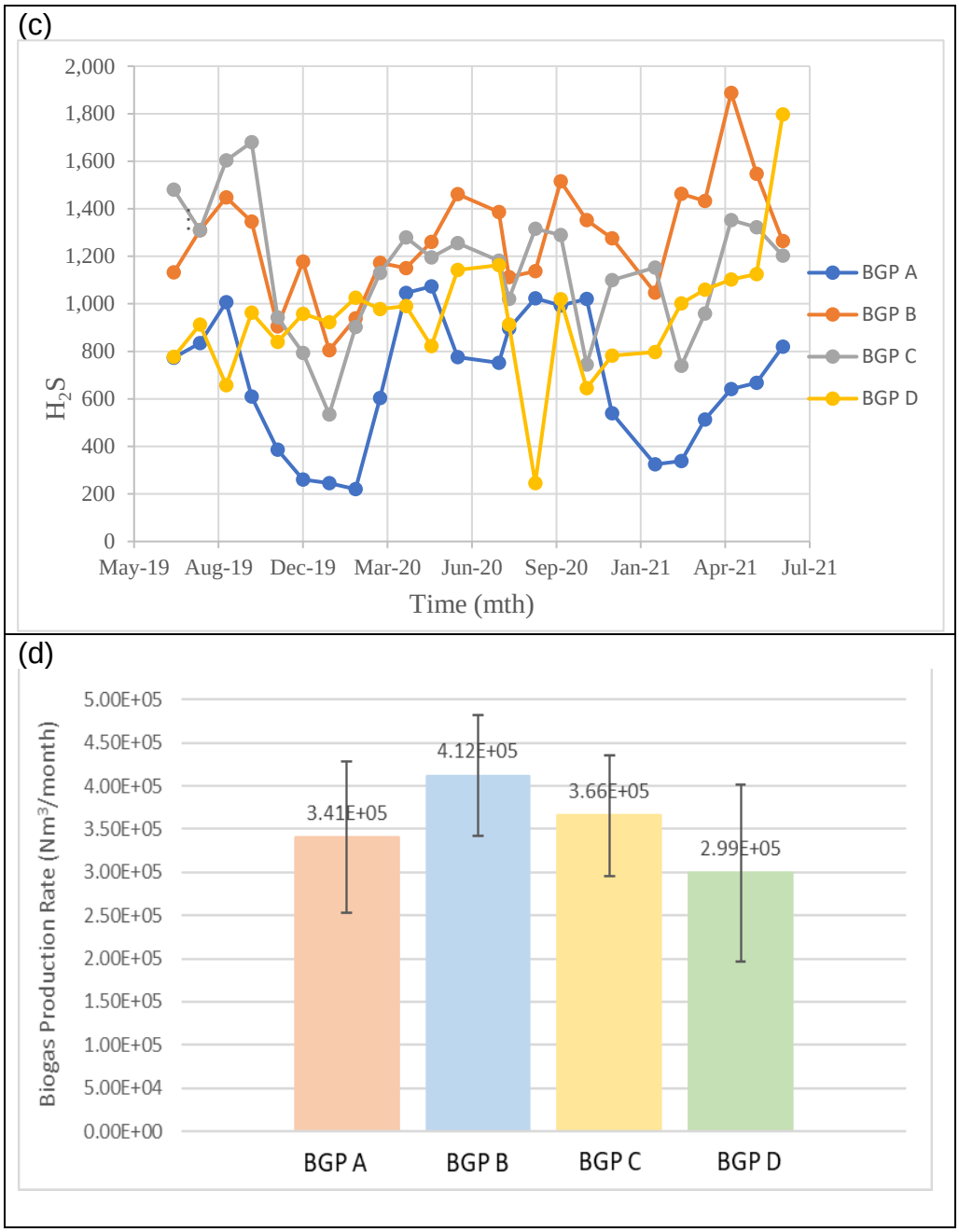

Figure 4.11: a) Total biogas production b) Methane composition c) H_2S concentration of biogas d) Maximum Biogas Production rate for each plant

Between the month of July-19 to Oct-19 in BGP A, an increase of OLR from 1.04 to 1.51 kg COD_{in}/m^3day (Figure 4.10(a)) has improved the COD removal rate from 652,039 to 1,103,369 kg CODr/mth (Figure 4.11(a)). Similar trend is observed with all the other BGPs where OLR content is directly proportional to the total COD

removed. This result is consistent with studies conducted by Musa et al. (2018), where it was determined that high COD removal as well as decrease in volatile solids concentrations in the treated effluent would indicate a successful substrate consumption to generate methane in anaerobic digestion. The factor underlying the increase in OLR with increase in COD removal is that the methanogens have adjusted and adapted to the new environment effectively, and thus they become more active in digesting organic materials (Kanimozhi & Vasudevan, 2010). Moreover, the increase in substrates in the anaerobic digestion can improve methanogenic growth which gradually increases the substrate conversion to methane by methanogens. Subsequently, high OLR can result in a highly productive and efficient performance of anaerobic digestion. On the contrary, excessively high OLR could lead to failure of AD as it could cause low COD removal and VFA accumulation. It could reduce biogas productivity due to high food to microorganism ratio (F/M), leading to inhibition of methanogens growth, and hence low methane yield (Hamzah et al., 2020). Referring to Figure 4.10(a), highest OLR was recorded in BGP C and BGP D amounting to 1.78 and 1.77 kg COD_{in}/m^3 day respectively. However, there was no overloading of organic matter during anaerobic digestion at the highest OLR as no significant reduction of methane yield could be observed for all plants. Based on the results obtained for the COD removal (Figure 4.11 (b)), the optimum range of OLR to achieve COD removal of above 80% for BGP A, B, C and D

is 1.10 to 1.45, 1.28 to 1.43, 1.00 to 1.51, and 1.27 to 1.49 kg COD_{in}/m^3 day, respectively.

The performance of digester with respect to COD removal was found to be influenced by HRT. This was verified using the ANOVA analysis. Figures 4.10(b) and 4.11(b) indicates that COD removal in BGP A increases from 82.1% to 85% as HRT decreases from 70 to 40 days. This could be due to soluble biodegradable matters in the effluent increase with the rise of OLR as Figure 4.10(a) shows that an increase of OLR from 0.91 to 1.45 kg COD_{in}/m^3 day during this period. This also indicates that the anaerobic digester of BGP A is performing efficiently to achieve COD removal of above 80% with high OLR and low HRT. A similar trend can be observed in BGP C between Jul-19 to Oct-19 where HRT decreases from 48 days to 34 days with increasing COD removal from 71.4% to 74.8% as well as increase in OLR from 1.32 to 1.78 kg COD_{in}/m^3 day. BGP D also depicts the same trend in Jan-21 to Apr-21 where COD reduction efficiencies increases with increasing OLR and decreasing HRT. These findings are consistent with the results obtained by Wong et al. (Wong et al., 2013) where HRT of anaerobic digestion was inversely proportional to COD removal efficiency and OLR. It can be concluded the performance of digester during these times are productive as most of the operational parameters are within appropriate range and able to yield methane.

Overall, BGP A has the lowest average total solids in the bottom sludge followed by BGP C (25719 mg/L), while BGP B and D have comparable TS of 37251 mg/L. Figure 4.10(c) shows BGP A starting from Mar-20 to

May-20 experienced a sharp drop in total solids which also implies that there is a decline in suspended solids. BGP A is shown to have the lowest total solids (23,616 mg/L) among all BGPs. However, BGP A is said to be quite stable except during the desludging process which results in a decreased in total solids. BGP D shows an increasing trend in 2020 indicating that there is accumulation of solids in the digester where the COD removal experienced a sharp drop to 70% (Figure 4.11(b)) due to the high total solid content (TS of 49,000 mg/L) found at the bottom sludge. This will reduce the treatment capacity and HRT due to the accumulation of inactive sludge, leading to insufficient time for the methanogens to digest the POME. Therefore, desludging was conducted from Jan-21 to Apr-21 to remove the excess total solids from the digester. This remediation was successful as the COD removal increased gradually to 75% in Jun-21.

A relationship is seen between total COD removed which is directly proportional to the total COD load. Similarly, COD removed per month is dependent on the HRT, OLR and COD removal efficiency of the system. Figure 4.11 (a) depicts that BGP A has inconsistent COD removed in each month which could be due to different amount of COD load, recirculation ratio and raw COD POME supplied into the digester. In BGP B, as shown in Table 29, the COD removed is the highest (906,847±179807) and quite consistent except that in Mar-20 when it is the lowest (369,942 kg CODr/mth) due to low COD load and total feed to the digester as the plant operates 12 days only in that month. This leads to low biogas production, but high COD removal efficiency was

maintained with high HRT of 88 days. This is because high HRT with low feeding can help to increase the contact time between the substrates (COD) and microorganisms to maintain high COD removal efficiency (Wong et al., 2013). As for BGP C, COD removed increases from Jan-20 to Apr-20 along with increasing OLR from 1.07 to 1.23 kg CODin/m^3.day (Figure 4.10(a)). Although there was a significant drop in COD removal efficiency in Feb-20, it was then increased to more than 80%. In BGP D, the COD removed increases from Aug-20 to Nov-20. The OLR decreases with increasing HRT which leads to low content of VFA that is insufficient for the methanogens to produce methane gas (Wong et al., 2013). Consequently, this caused low biogas production as well as decreasing efficiency of the COD removal. Other than that, the operating days in Aug-20, Sep-20 and Oct-20 was very low which could also lead to low biogas production as compared to Nov-20.

Referring to the recorded data in Table 4.5, the average COD removal efficiency of all BGPs are almost comparable to each other of about 78%. Judging on the data obtained, BGP A with the lowest COD removal efficiency was observed in Feb-21. A decreasing trend is also seen in Figure 4.11(b) from Sep-20 to Feb-21. This is because of the different total feeding into the digester that based on the number of operational days in that particular month. The decreasing COD removal efficiency has negative impact on the biogas production. Hence, COD removal efficiency is proportional to the biogas production.

As shown in Figure 4.11(b) and 4.11(c), BGP B has the most consistent COD reduction efficiency compared to other BGPs with the least standard deviation (Table 4.5). As a consequence, BGP B also has the highest average biogas production (378,874 Nm^3/mth) (Figure 4.12(d)). BGP C has the lowest COD removal efficiency in 2019 but it gradually increased to about 80 % efficiency in 2020 and 2021. The data shows that there is sufficient POME feeding in 2019 as compared to year 2020 and 2021. The performance and stability of the digester is seemed operating at optimum condition of the pH (around 7) and temperature (<40). However, the biogas production keeps fluctuating and this might be due to the mixing intensity. According to Singh et al. (2020), intense mixing has a negative impact on the biogas generation resulted from low methanogenesis rate caused by low presence of methanogens. Besides, it was found that the COD of the treated effluent in 2019 was very high due to high OLR which obviously indicate there is high content of VFA in the digester and hence low removal of COD efficiency (Wong et al., 2013).

In BGP D, a decreasing trend is observed from Sep-20 to Jan-21 (84.7% to 70.7%). The digester efficiency (COD removal) reduced with an increase in the COD effluent, implying that a high VFA content present in the digester. Meanwhile, a high total solid content is found at the bottom sludge which could be one of the factors affecting the efficiency of the digester. An abnormal trend can be seen from Sep-20 to Oct-20 and Dec-20 to Jan-21 with POME feeding at about 4000 m^3/mth and 10000m^3/mth, respectively. From the data, despite having reduction in

COD removal with almost the same feeding amount (4000 m^3/mth) yet the biogas production is seen increasing from Sep-20 to Oct-20. However, for the case of Dec-20 to Jan-21, further COD reduction occurred at POME feeding of 10000 m^3/mth but there is a decreasing in the biogas production as well as methane yield which agrees to a report by Fikri Hamzah et al. (2019). Consequently, high COD in the effluent is noticed due to the low consumption of substrate concentration and hence producing low methane yield as shown in the results.

Despite BGP B fed with high COD of POME (Table 4.3), which contributed to higher OLR, it achieved the highest COD removal rate as shown in Figure 4.11(d). This is probably due to their lower oil and grease concentration of POME (2,477$\pm$975 mg/L) (Table 4.3) as compared to other BGPs, which led to efficient biodegradation of POME in the anaerobic digester with minimum operational problems. Besides, this might be associated to the efficient mixing process in the anaerobic digester of BGP B, which conforms to the contact of bottom sludge and POME. Apart from this, the TS of the bottom sludge in BGP B is stable and has fewer fluctuations than other BGPs. The TS content was maintained at an average of 35,000 mg/L. This might give a better environment for the bacteria to perform digestion activity. Sludge management is important because it can increase solids hydrolysis process and methane generation (Young et al., 2012).

Figure 4.12(a) shows that low biogas production experienced in BGP D. Although, the BGP D has long HRT which is 80 days, but it still did not

increase the biogas production. This result did not match the study done by Alepu et al. (Alepu et al., 2016), as high HRT will increase the biogas production. This could be due to methanogens being incompletely acclimatised to the optimal conditions required for the anaerobic digester (Fikri Hamzah et al., 2019) especially high temperature and low pH can be observed from the pre-treated POME entering the digester in BGP D.

The stability of the digester plays a vital role in determining the performance of the digester as parameters such as pH and temperature will affect methanogenesis process significantly. From the data obtained on the parameters (pH and temperature), it was observed that BGP D was unstable as it fluctuates a lot, compared to the other BGPs. On Sep-20, the lowest biogas production is generated with low OLR as only a small portion of POME (4060 m^3/mth) is fed into the digester. However, high ratio of recirculation (bottom sludge and treated effluent) to POME is carried out to gradually increase the biogas production which can be seen from Figure 4.7**Error! Reference source not found.**(c) after Sep-20. According to Fikri Hamzah et al. (2019), the increased in biogas production is also contributed by high microbial activity and stability in digester, hence accelerating the decomposition rate.

As for BGP A, a drop in biogas production is observed from the Figure 4.12(a) in Feb-21. Based on the findings obtained, the pH and temperature are in the optimal conditions of AD. From the biogas composition, about 63% is methane which indicates that there are no issues with the pH and temperature as these parameters are the main factors that affect the biogas production rate. The HRT in this month is

also quite long (167 days) which allows microorganism to interact with the substrates efficiently. However, the concern in the historical data is the critically low OLR value which is the main reason of the decline of the biogas production. Microorganism requires food to perform microbial growth which is associated with the OLR supplied into the digester (Meegoda et al., 2018). The pH result during this month is close to neutral pH which is seemed to be normal as this means that no excess food was supplied into the digester. Although, the OLR is low, yet the methane yield is still satisfactory with that amount of biogas produced.

BGP A shows an obvious result of high average methane content (62.8%) generated from POME digestion in Figure 4.12(b). This is followed by BGP C (61.1%), BGP D (60.5%) and lastly BGP B with the lowest (58.6%). These averaging values are indeed within the literature range from Table 4.5, which implies that the anaerobic digester is operating optimally at its best efficiency (Shakib & Rashid, 2019). However, high methane composition does not imply high biogas production as this is seen from the recorded data showing that BGP A has the second lowest biogas production (276956.9 Nm^3/month) in average compared to BGP B and C.

Table 4.5: Composition of biogas components in all biogas plants and literature values

Component	Biogas in BGP A	Biogas in BGP B	Biogas in BGP C	Biogas in BGP D	(Shakib & Rashid, 2019)	(Bharathiraja et al., 2018)	(Huertas et al., 2020)
CH_4 (%)	60.80 – 63.91	55.74 – 62.38	57.82 – 64.02	57.90 – 62.53	50 – 75 %	40 – 75 %	–
CO_2 (%)	31.81 – 36.42	32.88 – 43.57	31.94 – 35.80	32.92 – 38.20	24 – 45 %	15 – 60 %	–
O_2 (%)	0.26 – 0.59	0.01 – 1.04	0.02 – 0.15	0.34 – 0.75	< 2 %	< 2 %	–

H_2S (ppm)	220 – 1073	805 – 1887	535 – 1680	246 – 1797	< 2 %	0 – 5000 ppm	100 – 30,000 ppm

In Figure 4.12(b), a sudden drop in methane content to 61% is seen in BGP A in Jan-20. This is probably due to a reduction in organic loading rate (OLR) to 0.91 kg COD_{in}/m^3.day, lowest OLR in BGP A. Besides, the total COD removed during this period is also the lowest which concludes why there is a reduction in methane content in Jan-20 (Hamzah et al., 2020).

BGP B shows a decreasing trend of methane composition from July-19 to Sep-19 but there is an increase in the methane production per COD removed or supplied. Other factors like carbon dioxide increment in biogas can also cause the decreased in methane composition but this does not imply that the methane production decreases as the recorded data shows high methane generation in Sep-19.

From Figure 4.12(b), the lowest methane composition (57.8%) is seen in Jul-19 at BGP C. Perhaps, this is due to the low removal of total solids (TS) and COD at 47% and 71.4% respectively. Low TS removal indicates that the removal of volatile solids (VS) is low as well. A low removal of VS and COD implies that methanogenesis was inhibited by the presence of high VFA concentration in the digester (Wong et al., 2013).

It is observed BGP D has the lowest methane composition (57.9%) in Jul-19 as well. This is resulted from the low methane generation per COD supplied or removed in the anaerobic digester. However, in Jul-19 the total biogas produced is relatively high. Since methane generation is low

but with high biogas production rate, this deduce that carbon dioxide increment is due to the acetogenesis process (Wong et al., 2013). Therefore, if methanogens are weak during that period, this carbon dioxide will not be consumed leading to high carbon dioxide concentration and low methane content in biogas.

Referring to the data presented in Table 4.5 and Figure 4.12(c), H_2S content in raw biogas increases from 773 to 1,007 ppm between the months of Jul-19 to Sept-19, as CH_4 concentration decreases from 63.48% to 62.48%. This trend can also be seen in BGP B during the same period where methane content decreases from 60.8% to 55.74% H_2S which increasing from 1,132 to 1,448 ppm. It can be concluded that the methane concentration in biogas from POME is inversely proportional to H_2S content. From data of H_2S content in raw biogas obtained, the average H_2S obtained for all the plants ranges from 653.91 to 1291.30 ppm. The highest H2S readings were recorded in POM B and D. This is probably related to microorganism activity in the AD. Sulphur-reducing bacteria can inhibit methanogenesis due to the competition for a wide variety of organic and inorganic substrate which resulted lower methane content and higher H2S content in POM B and D. This is also possibly related to high total solid content in the bottom sludge of POM B and D which reduced the efficiency of mixing and slower down methanogenesis process in the AD. The H_2S content for all the plants is comparable to the literature data showed in Table 4.5. Other than that, the data calculated for H_2S concentration in treated biogas for all the BGPs is rather optimal. This is because the data of H_2S content in treated biogas for all the plants

is less 500 ppm. Concentrations exceeding 500 ppm in a closed environment can lead to death within 30–60 min, while concentrations exceeding 1000 ppm is instantly fatal. Therefore, H_2S concentration in for all the BGPs in treated biogas is acceptable for the environment.

Figure 4.12(d) shows that BGP B has the highest maximum biogas production rate, which is consistent with the results obtained in COD removal rate (Figure 4.11(d)). This is mainly due to the appropriate COD concentration of POME (81,987±2149 mg/L) and adequate bottom sludge concentration (32,736±5115 mg/L) in the anaerobic digester. POME with higher COD (>84,000 mg/L) is not a guarantee to produce optimum biogas production. In particular, BGP D has the highest COD concentration of POME (Table 4.2), but its biogas production rate is the lowest as compared to other BGPs.

Overall, the results show that the standard deviations for the observed parameters are relatively low (<20%) except for the biogas production rate, suggesting a consistent and stable performance of the digesters. The observed fluctuations in the digester performance are mainly due to the normal operational fluctuations (OLR, HRT, recuirculation ratio), raw POME quality, variations in the environmental conditions (temperature, bottom sludge quality, etc.) and desludging activities. Nonetheless, the deviations remained within an acceptable range, indicating an overall consistent performance of the digesters.

4.3 Statistical Analysis of AD Performance Study

In the literature, there are many operating parameters reported to have significant effects on biogas production and COD removal, though it does not applicable to all biogas plants as shown in the history data analysis (Section 4.1). Therefore, ANOVA studies was carried out using the Design Expert software to identify the most critical parameters that have statistically significant effects on biogas production and COD removal.

Table 4.6 shows the descriptive statistics of the input and output parameters for AD process with their responses. ANOVA studies was carried out using Design Expert software to identify the most critical parameters that have statistically significant effects on biogas production and COD removal. The regression coefficient and the equations that correlates to the historical data from the four biogas plants were predicted (Table 4.7 and 4.8).

Table 4.6: Descriptive statistics of the AD data utilised in the four POME treatment plants

Parameter	Unit	Category	Min	Max	Average	Standard Deviation
Temperature (A)	$°C$	Input	31.98	44.10	39.35	2.12
OLR (B)	$kgCOD_{in}/m^3month$	Input	0.981	1.685	1.305	0.134
Recirculation Ratio (RR) (C)	-	Input	0.1784	4.44	1.52	0.8424
Biogas Production Rate	$Nm^3/month$	Output	18840	484225	3.114E+05	95492.44
COD Removal	$kgCOD_{in}/month$	Output	276208	1.22967E+06	7.921E+05	2.109E+05

Table 4.7: ANOVA and significance test of each model term for COD removal

Source	Sum of Squares	df	Mean Square	*F*-value	*p*-value
Model	3.322E+12	21	1.581E+11	13.35	< 0.0001
A-OLR	1.151E+12	1	1.151E+12	89.48	< 0.0001

D-Temp (C)	5.525E+10	1	5.525E+10	4.71	0.0302
F-RR	1.249E+11	1	1.249E+11	9.71	0.0028
L-Location	1.639E+12	3	5.464E+11	46.57	< 0.0001
AD	9.459E+09	1	9.459E+09	0.8061	0.3722
AF	1.402E+10	1	1.402E+10	1.19	0.1789
AL	5.524E+10	3	1.841E+10	1.57	0.1080
DF	3.876E+08	1	3.876E+08	0.0330	0.7469
DL	1.229E+11	3	4.097E+10	3.49	0.0185
FL	1.986E+11	3	6.621E+10	5.64	0.0012
A²	1.412E+10	1	1.412E+10	1.20	0.2874
D²	7.777E+08	1	7.777E+08	0.0663	0.6975
F²	8.704E+10	1	8.704E+10	7.42	0.0085
Residual	8.683E+11	74	1.173E+10		
Cor Total	4.189E+12	95			
R^2	0.8023				
Adjusted R^2	0.7749				
Predicted R^2	0.7123				

Notation: df is degree of freedom.

Table 4.8: ANOVA and significance test of each model term for Biogas Production

Source	Sum of Squares	df	Mean Square	*F*-value	*p*-value
Model	5.919E+11	21	2.915E+10	7.58	< 0.0001
A-OLR	1.581E+10	1	1.581E+10	4.21	0.0321
D-Temp (C)	9.961E+10	1	9.961E+10	26.70	< 0.0001
F-RR	3.325E+10	1	3.325E+10	8.85	0.0032
L-Location	2.091E+11	3	6.971E+10	18.62	< 0.0001
AD	6.806E+07	1	6.806E+07	0.0172	0.7935
AF	1.579E+10	1	1.569E+10	4.18	0.0442
AL	1.792E+10	3	5.941E+09	1.49	0.1878
DF	1.814E+09	1	1.804E+09	0.4816	0.4874
DL	1.976E+10	3	6.554E+09	1.75	0.1622
FL	5.887E+10	3	1.959E+10	5.23	0.0015
A²	2.898E+10	1	2.894E+10	7.73	0.0049
D²	3.445E+07	1	3.438E+07	0.0092	0.9245
F²	3.771E+10	1	3.764E+10	10.05	0.0018
Residual	2.784E+11	74	3.548E+09		
Cor Total	8.664E+11	95			
R^2	0.8907				
Adjusted R^2	0.7912				
Predicted R^2	0.7042				

Notation: df is degree of freedom.

The statistical analysis conducted using the Fisher test (F-value) and a 95% confidence level for probability (p-value) demonstrates the statistical significance of both models. Specifically, the model focusing on COD removal as the response variable yields an F-value of 13.35 with a p-

value of <0.01, indicating an extremely low likelihood (0.01%) of such an extreme F-value occurring due to random chance (Table 4.7). Additionally, the p-value <0.01 suggests the significance of model terms A, D, F, L, DL, FL, and F^2. Conversely, values greater than 0.1 imply the insignificance of model terms, prompting consideration for model reduction. In this context, terms AD, AF, AL, DF, A^2, and D^2 are considered insignificant. The adjusted R^2 of 0.7749 and predicted R^2 of 0.7123 reflect a robust correlation with COD removal.

For the model focusing on biogas production, it exhibits an F-value of 7.58 and accompanied by a low p-value of <0.01. This indicates that there is only 0.01% chance for such an F-value to occur due to noise, otherwise the model is significant (Table 4.8). In this model, terms A, D, F, L, AF, FL, A^2, and F^2 are considered significant model terms, while AD, AL, DF, DL, and D^2 are regarded as insignificant. To enhance the model, model reduction is recommended. The adjusted R^2 of 0.7912 and predicted R^2 of 0.7042 indicate a strong correlation with biogas production. Overall, the key parameters that accurately represent both responses with $p<0.05$ are A (OLR), D (Temperature), F (RR), FL and F^2 with $p<0.05$. Notably, OLR (A) emerges as the most influential parameter, highlighting its critical role in shaping both wastewater treatment and biogas production outcomes. The effects of these parameters on the biogas production and COD removal will be discussed in detail in Section 4.3.3.

Subsequently, 3D surfaces and contour plots obtained from the equations are used to study the individual and interactive effects of the observable parameters on both responses (Section 4.3.2). This approach

is important to determine the optimal input parameters that will maximize the theoretical biogas production and COD removal by employing numerical and point prediction methods.

4.3.1 Box Plot Analysis

The most significant input parameters obtained in Section 4.3 including OLR, temperature, and RR are evaluated by using the box plots as shown in Figure 4.12. From Figure 4.12(a), the OLR for BGP A has the lowest median with a relatively low interquartile range. This can infer that the OLR for BGP A is the lowest overall, with an average value of 1.12±0.17 $kgCOD_{in}/m^3.day$.

For temperature, the ranges of BGP A, B, and C are rather consistent with each other (32.3^oC-44.0^oC) as described in Figure 4.12(b). Conversely, BGP D shows higher data spread with average value of 43.08±2.91 due to the inefficiency of the cooling pond. According to the previous studies, mesophilic conditions are fundamental to in-ground lagoon type anaerobic digester compared to thermophilic conditions. The temperature of the digester should be maintained in a narrow range to prevent a sudden increase in temperature.

Figure 4.12(c) shows that the RR of BGP B is relatively higher than that of BGP A, C, and D, with an average value of 2.39±0.74, while the others have average values of 0.99 – 1.39. It is found that a controlled recirculation system potentially increases methane yield from the anaerobic digestion of citrus waste in a two-stage process at high OLRs (Lukitawesa et al., 2018). However, D. Chen & Li (2020) have also

discovered that an RR of 0.6 performed better in continuous dry anaerobic digestion for biogas production and methane yield than a lower RR of 0.5. Conclusively, a high RR is favourable in sustaining biogas production by the anaerobic digester. However optimal conditions must be prioritised considering the operational costs as well as the efficiency of the anaerobic process.

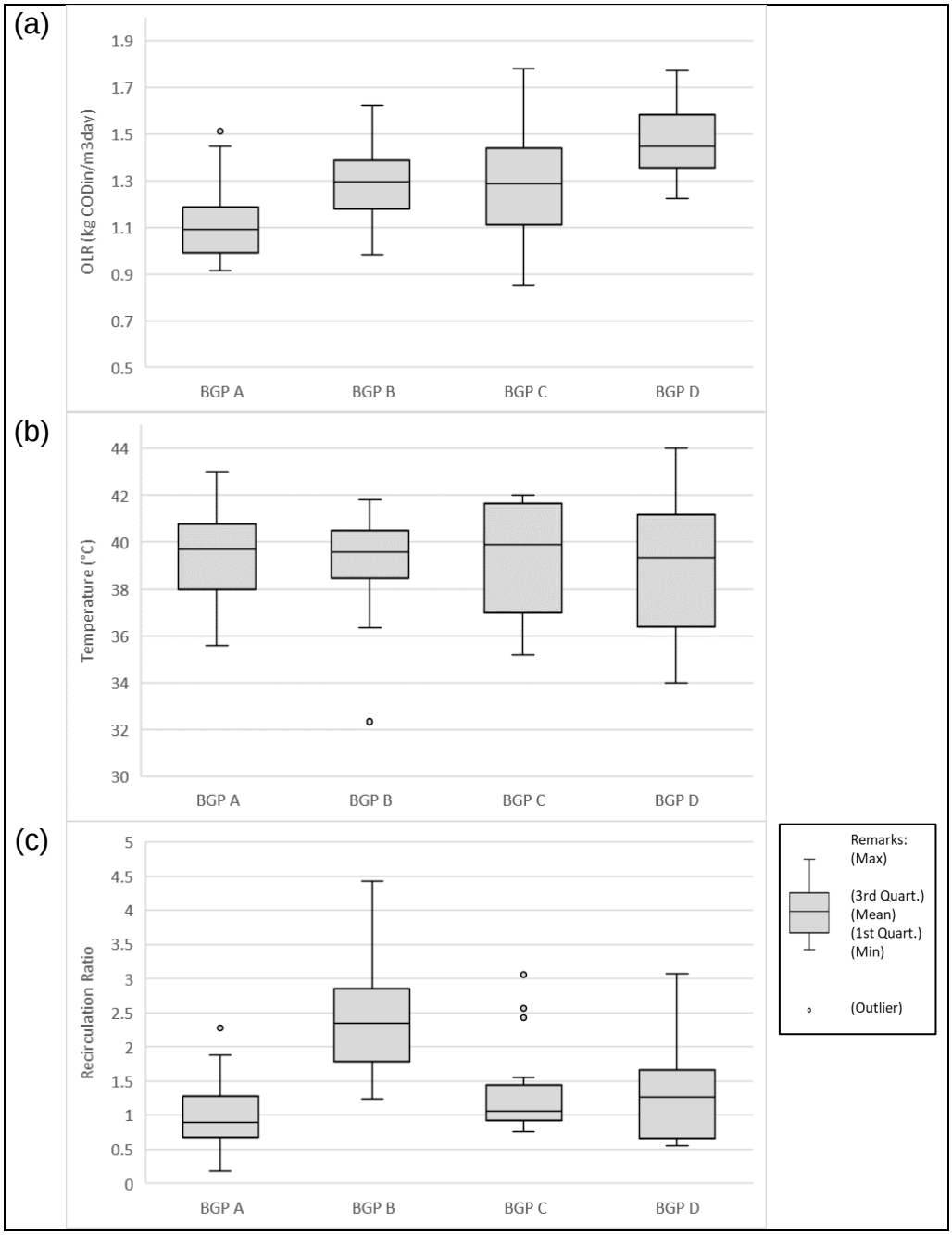

Figure 4.12: Box plots of the studied input parameters for each biogas plant (a) OLR (b) temperature (c) recirculation ratio.

Figure 4.13 shows the responses of each biogas production plant in the form of box plots, these parameters are the COD removal of wastewater and the biogas production in BGP A, B, C and D. Figure 4.13 shows that the COD removal for BGP A, B and C fluctuates relatively less compared to BGP D, which has a larger range of intermediate values (2.66×10^5-1.11×10^6 kg CODr/mth). This means that the instability of BGP D's performance in removing COD from the wastewater due to various issues such as long hydraulic retention time and high variation in temperature (Figure 4.13(b)) (Shi et al., 2017). Nonetheless, results obtained from BGP B with an average value of 7.67×10^5kg CODr/mth is significantly higher than that from BGP A, C, and D. This correlates with the higher efficiency of wastewater treatment by the plant amongst the others.

Figure 4.13(b) depicts the biogas production per month for each plant because of anaerobic digestion whose product is a form of energy. Among the data obtained, BGP B has an overall higher biogas production, ranging from 2.23×10^5 to 4.69×10^5 Nm^3/mth, which also signifies stability due to its smaller range compared to BGP A, C and D. It also has the highest median of all at 3.99×10^5 Nm^3/mth, and an interquartile range of 3.35×10^5 to 4.42×10^5 Nm^3/mth. When placed among other BGPs, BGP B shows the most cost-effective performance as it is the most efficient in biogas production as well as COD removal.

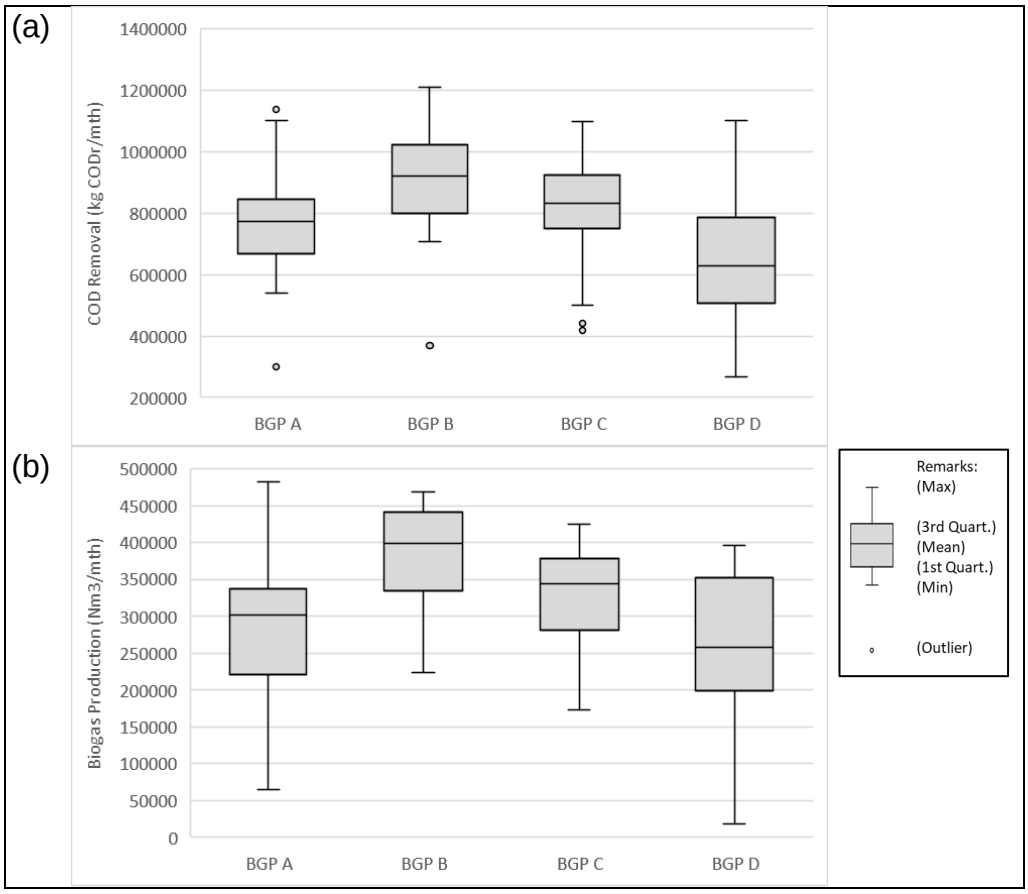

Figure 4.13: Box plots of the studied response parameters for each biogas plant (a) COD removal (b) biogas production.

4.3.2 Development of Mathematical Model

Each mathematical model is a four-level factor which includes three numerical factors (OLR, T and RR) and one categorical factor (mill location: BGP A, BGP B, BGP C and BGP D). The main effects and interaction effects on $COD_{removal}$ and biogas production are illustrated in Equation (24) and Equation (25). Referring to both equations, HRT, pH, MLSS, TS, SS, BOD as well as the concentration of oil and grease are excluded from the equations since they have p-value greater than 0.05, indicating that these parameters do not exhibit a significant effect on the outputs (Di Leo & Sardanelli, 2020).

$$COD\_removal\ (kg\ COD_{in}/month) = 755500 + 275000A + 56237.11D - 289900F + 226600L[1] + 52453.36L[2] + 8243.04L[3] - 98480.48AD - 188900AF + 173900AL[1] - 30054.52AL[2] - 20347.48AL[3] + 19998.97DF - 175700DL[1] + 40250.36DL[2] - 17808.55DL[3] + 413100FL[1] + 4366.24FL[2] - 240200FL[3] - 87519.67A^2 - 18661.58D^2 - 356300F^2 \quad (24)$$

$$Biogas\ prodcution\ (Nm^3/month) = 268500 - 32526.03A + 112900D - 194200F + 138800L[1] + 36877.81L[2] - 138500L[3] - 8353.94AD - 199900AF + 106600AL[1] - 6155.22AL[2] - 98278.93AL[3] + 43140.95DF - 85243.42DL[1] - 9532.7DL[2] + 67002.49DL[3] + 248900FL[1] - 20124.72FL[2] - 221100FL[3] - 125300A^2 - 3923.65D^2 - 234300F^2 \quad (25)$$

Where A represents organic loading rate (kg COD_{in}/m^3 day), D denotes the anaerobic temperature (^oC) whereas F is the recirculation ratio. The main effect of mill location namely BGP B, BGP C, BGP A and BGP D are in the form of $L[1]$, $L[2]$ and $L[3]$ respectively.

The boundary limits for temperature (^oC) (Equation 26) and recirculation ratio (Equation 27) are determined based on the previous studies conducted in the biogas plant.

$$Temperature\ (^oC) < 40 \quad (26)$$

$$ecirculation\ ratio > 1.0 \quad (27)$$

The coefficient of determination (R^2) for COD removal is 0.7927. This indicates the high correlation between the actual and the estimated output variables, hence, there is a substantial accuracy for the reduced order quadratic model to study the COD removal (Henseler et al., 2009).

On the other hand, the predictive ability of the reduced polynomial order for biogas production was confirmed by the R^2 value of 0.6807. By adhering to the rule of thumb when deducing the strength of correlation between the predictive model based on the R^2 values, the value is generally regarded as moderate effect size (Leysieffer, 1999).

Additional performance evaluation analysis is employed to understand the historical data of four different mills. Root means square error is accessed as it is widely applied to define the errors for numerical predictions (Christie & Neill, 2022). Generally, low RMSE values indicate low errors, meaning that the predicted values are close to the actual values. In this study, the RMSE values for COD removal and biogas production are 9.51E+4 kg COD_{in}/month and 5.37E+4 Nm^3/month respectively. This provides insights that the errors are considerably high for both models. The large errors are also reflected by the measurement of mean absolute error (MAE), quantifying at 6.97E+4 kg COD_{in}/month and 4.16E+4 Nm^3/month for COD removal and biogas production respectively.

4.3.3 Effects of Process Parameters on the Studied Output Variables

4.3.3.1 Effect of OLR on COD Removal

Based on the results generated in the surface and contour plots shown in Figure 4.14 and the interaction plot shown in Figure 4.15, the increase in OLR shows a positive impact on the COD removal of the raw POME, regardless of the variation in temperature. Ramanathan et al. (2022) concluded that OLR is an important factor that affects the production of

biogas in anaerobic digestion, particularly in a continuous flow process. They proposed that the ideal value for OLR ranges from 0.5 to 2 kg for entire volatile solids in a unit volume of digester per day with regards to hydraulic retention time, temperature, and feedstock. Nevertheless, the increase in OLR reaches a plateau after peaking at the maximum allowable range. This is supported by findings where excess OLR will result in the inhibition of COD removal, subsequently reducing the biogas production rate (Hussain et al., 2021). This is because the increase in OLR increases the acidity of the digester which will affect the microbial growth in the digester (Periyasamy et al., 2022). However, when the recirculation ratio is on the higher side (4.42), the COD removal will become less sensitive to the OLR due to the high dilution factor caused by the high flow rate of treated effluent.

4.3.3.2 Effect of Temperature on COD Removal

Temperature is often regarded as one of the important parameters for COD removal and biogas production. High temperature increases the metabolic rate of the microorganisms, thus improving the anaerobic performance. This claim was supported by Hu et al. (2018) where high temperature produces satisfactory results for COD removal and biogas production. Referring to Figure 4.16(a) and Figure 4.16(b), the COD removal slightly increases with the constant value of OLR. Moreover, an increment of COD removal could be visible in Figure 4.16(a) for the increase in temperature and recirculation ratio. However, only the BGP B plant decreases in COD removal with the rise of mesophilic

temperature whereas temperature has positive effects on BGP A, BGP C and BGP D (Figure 4.16(b)).

4.3.3.3 Effect of Recirculation Ratio and Location of the Plant on COD Removal

The recirculation ratio of effluent is defined as the ratio of recycling treated substrate against the incoming untreated substrate in the mixing tank. The unrecycled treated wastewater will be transported from the anaerobic digester to the setting pond and discharged as treated effluent. The purpose of recirculation from a methanogenic lagoon is to increase the alkalinity of the reactor for optimal anaerobic digestion. Recycling treated POME further increases the pumping of healthy microorganisms into the system, leading to better COD removal efficiencies in the anaerobic digester (Y. Zhang et al., 2009). Hence, a supervised recirculation ratio increases the COD removal efficiencies in the digester. Figure 4.17 illustrates that the optimal range of recirculation ratio differs for each plant. This is because each plant has different capacities and POME sources. Therefore, the location factor in the interaction plots demonstrated in Figure 4.16 (b) and is averaged over to produce generalized projections for better statistical evaluation of the impact of each parameter. However, each location displayed that there is a maximum point for COD removal for the recirculation ratio. The general optimal range for the recirculation ratio of BGP A, BGP B, BGP C and BGP D is in the range of 1.2 -2.3 (Figure 4.17).

4.3.3.4 Effect of OLR on Biogas Production

As shown in Figure 4.18 (a), the gradual increase of OLR will contribute to the surge of biogas production where it will reach a maximum value. Biogas production from the methanogenesis process is correlated to the mass density of methanogenic archaea bacteria (Eslami et al., 2018). The active bacteria will produce a byproduct namely volatile fatty acids (VFA) when decomposing the organic matter in the POME effluent. These VFA are a source of nutrient for archaea, and it is the key reactant to produce biogas and COD removal (Dinh et al., 2014; Kwon & Nakasaki, 2015; Palatsi et al., 2011). However, excess OLR will result in organic load shock to the anaerobic digester, inflicting a negative effect on the biogas production rate. Thereafter, the accumulation of VFA and Oxidation-revival Potential (ORP) will surge. The acidic environment will lead to stunted growth of archaea bacteria, leading to lower biogas production output (Kwon & Nakasaki, 2015).

4.3.3.5 Effect of Temperature on Biogas Production

Figure 4.19 (a) shows the biogas production as a function of temperature and OLR. When the OLR is constant, it is visible that the biogas production increase with increasing temperature. Kim et al. (2006b) elaborated that the effect of temperature increases the kinetics of the process, leading to better digestion of the raw POME in the digester. Since literature studies reviewed that mesophilic temperature ranges from approximately 35^{o}C to 40^{o}C (depending on sources), the results from the surface plots support the claim of the past literature (Sánchez et al., 2001). However, Bouallagui et al. (2004) suggested the

implementation of thermophilic temperatures as it is more effective for biogas production compared to existing mesophilic temperature, but the former is more sensitive to environmental changes (Ahn & Forster, 2002; El-Mashad et al., 2003; M. Kim et al., 2002).

4.3.3.6 Effect of Recirculation Ratio and Location on Biogas Production

The recirculation ratio acts as a buffering agent to maintain the pH level of the anaerobic digester to regulate and stabilize the pH level within the anaerobic digester, which is an essential aspect of alkalinity control in anaerobic digestion (Gottardo et al., 2017). Moreover, the recycling of treated effluent will increase the degree of degradation of the POME (Aslanzadeh et al., 2013). The optimal recirculation ratio is configured to increase the biogas production from the AD performance. However, the optimal recirculation ratio is not a one-size-fits-all solution; instead, it is intricately tied to the specific characteristics of the feedstock and the microbial community within each biogas plant. Based on the interaction plots of the biogas production for recirculation ratio for each location, it is deduced that each plant has a different optimal ratio for maximum biogas production which has a similar scenario when evaluating the COD removal. BGP B proposed the highest recirculation ratio range, spanning from 2.5 to 3.0. Studied mills such as BGP A, BGP C and BGP D have lower recirculation ratio ranges, with 1.0-1.5, 0.2-0.7 and 1.3-1.8 respectively (Figure 4.20). Since recirculation could potentially enhance AD performance by increasing the alkalinity and speeding up the nutrient uptake by the microorganisms, the optimal ratio is highly dependent on

the number of substrates and VFA concentration in the raw feedstock (Lukitawesa et al., 2018).

One key consideration is the diversity of substrates present in the raw feedstock. Different palm oil mills may receive POME with varying compositions, which can result in different alkalinity needs. A higher recirculation ratio can help buffer pH in cases where the influent POME has a lower alkalinity. This is particularly relevant in situations where POME characteristics may fluctuate seasonally or due to variations in palm oil production practices.

Moreover, the concentration of volatile fatty acids (VFAs) in the influent can significantly impact the alkalinity balance within the digester. VFAs are intermediates in the breakdown of organic matter and can lower pH if their accumulation surpasses the buffering capacity of the system (Lukitawesa et al., 2018). An optimal recirculation ratio should consider the potential VFA concentrations in the raw feedstock. In cases where VFAs are prevalent, a higher recirculation ratio may be required to counteract their acidifying effects and maintain stable pH conditions.

In light of these complexities, optimizing the recirculation ratio is not a one-time endeavour but an ongoing process that considers the dynamic nature of POME characteristics and microbial dynamics (Hwu et al., 2013). This highlights the need for continuous monitoring and adjustment of recirculation ratios in biogas plants to ensure consistent and efficient AD performance. Additionally, it highlights the importance of site-specific studies to tailor AD processes to the unique conditions of each palm oil

mill, ultimately maximizing biogas yield and wastewater treatment efficiency.

(a)

Factor Coding: Actual

COD removal

266099 1.20967E+06

X1 = A

X2 = D

Actual Factors

B = 60.9811

C = 4.715

E = 26880

F = 2.08304

G = 38284

H = 34975

J = 35010

K = 6180

L = Average over

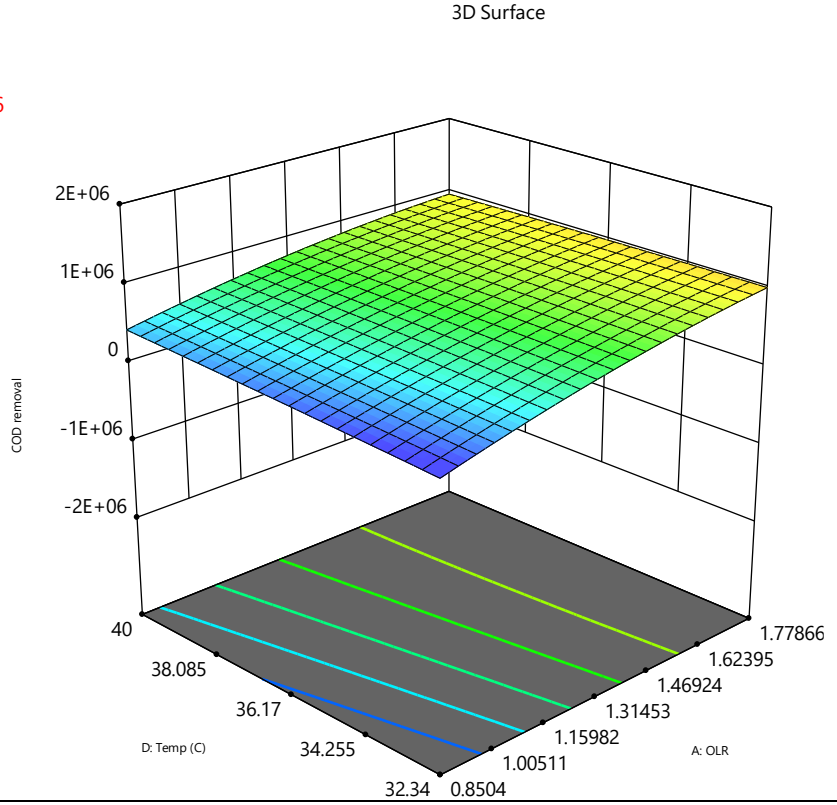

(b)

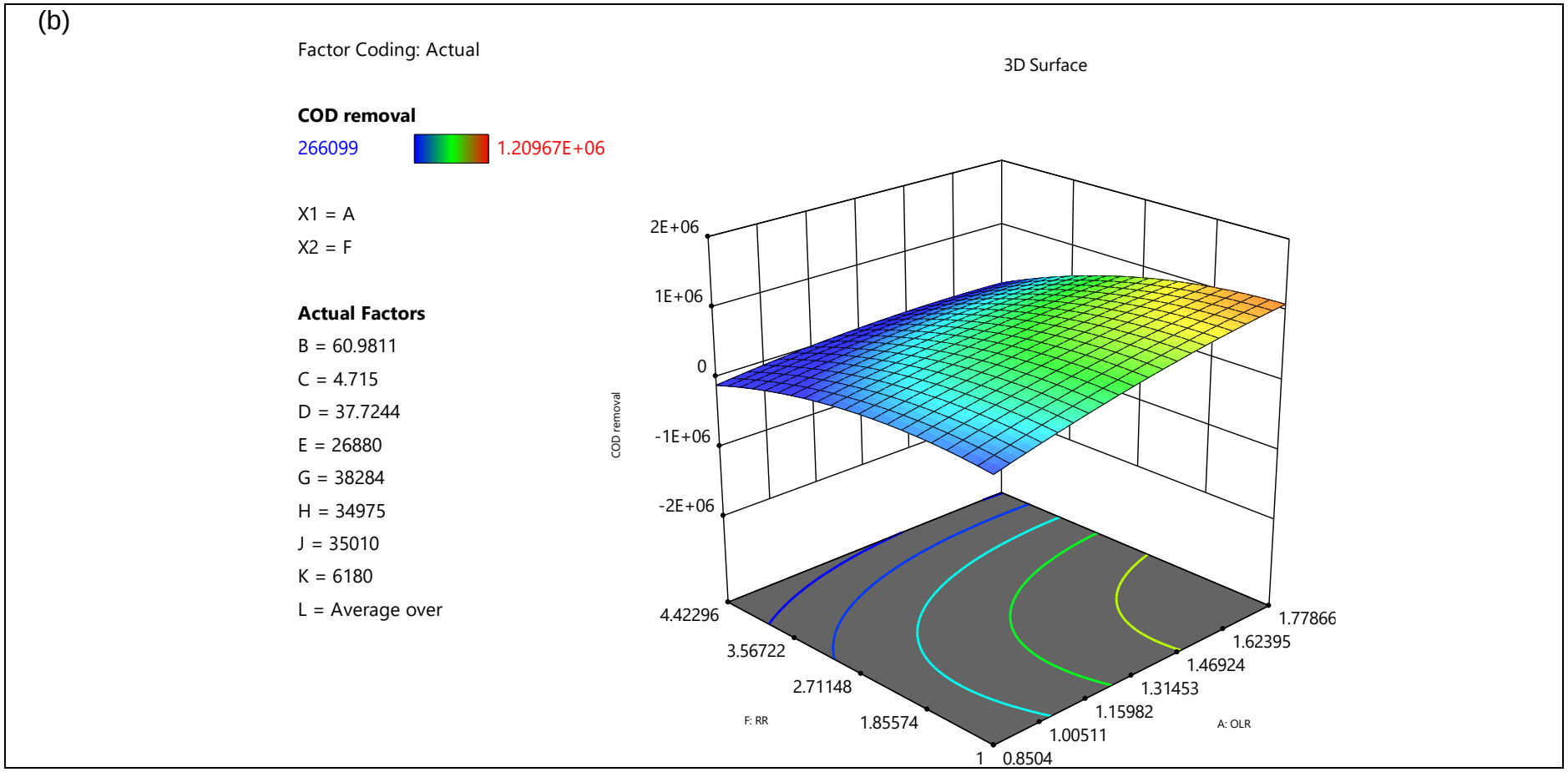

Figure 4.14: (a) Surface and contour plot for COD removal as a function of OLR and temperature; (b) Surface and contour plot for COD removal as a function of OLR and recirculation ratio.

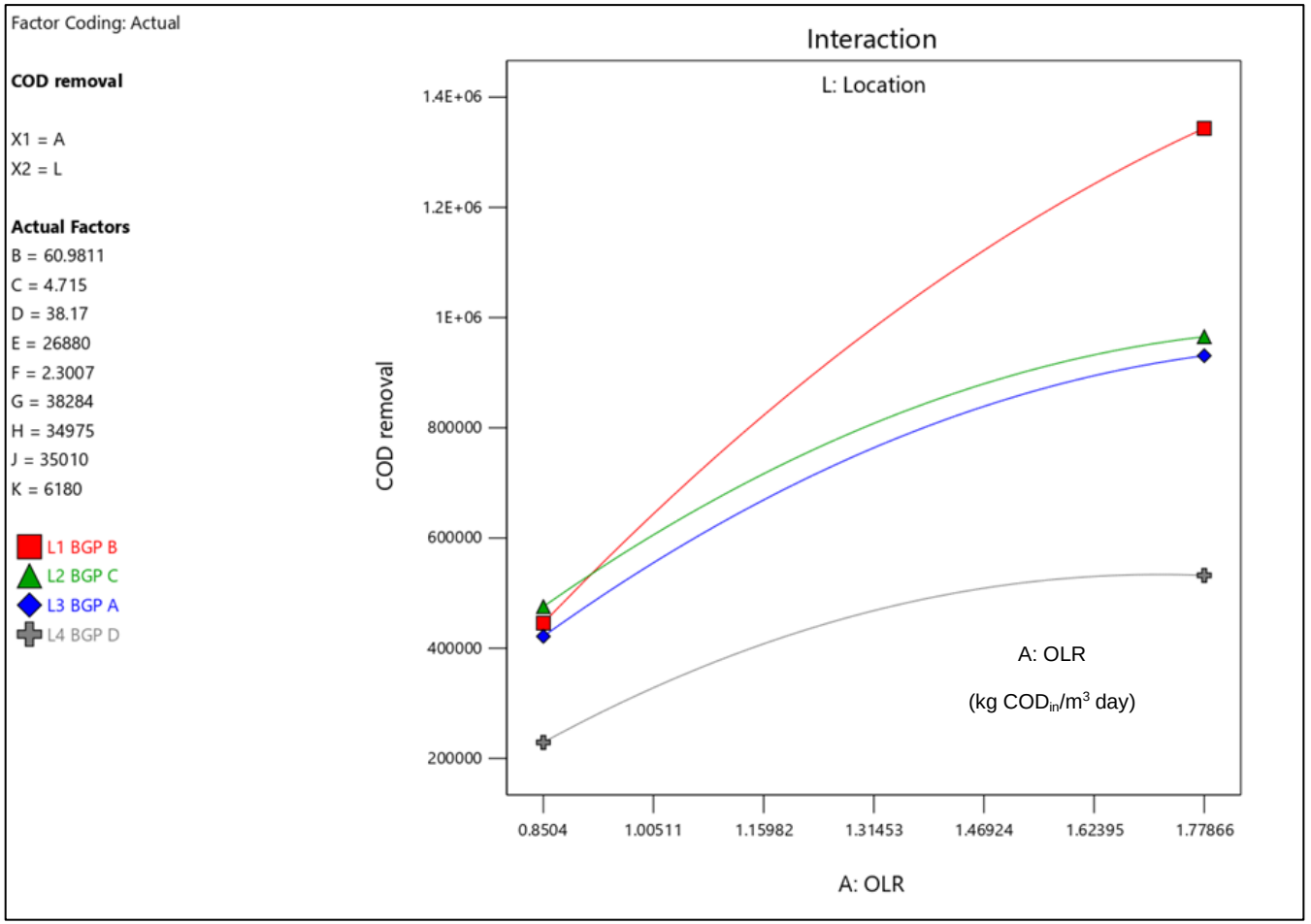

Figure 4.15: Interaction plot for COD removal as a function of OLR and location

(a)

Factor Coding: Actual

COD removal

266099 1.20967E+06

X1 = D

X2 = F

Actual Factors

A = 1.56932

B = 60.9811

C = 4.715

E = 26880

G = 38284

H = 34975

J = 35010

K = 6180

L = Average over

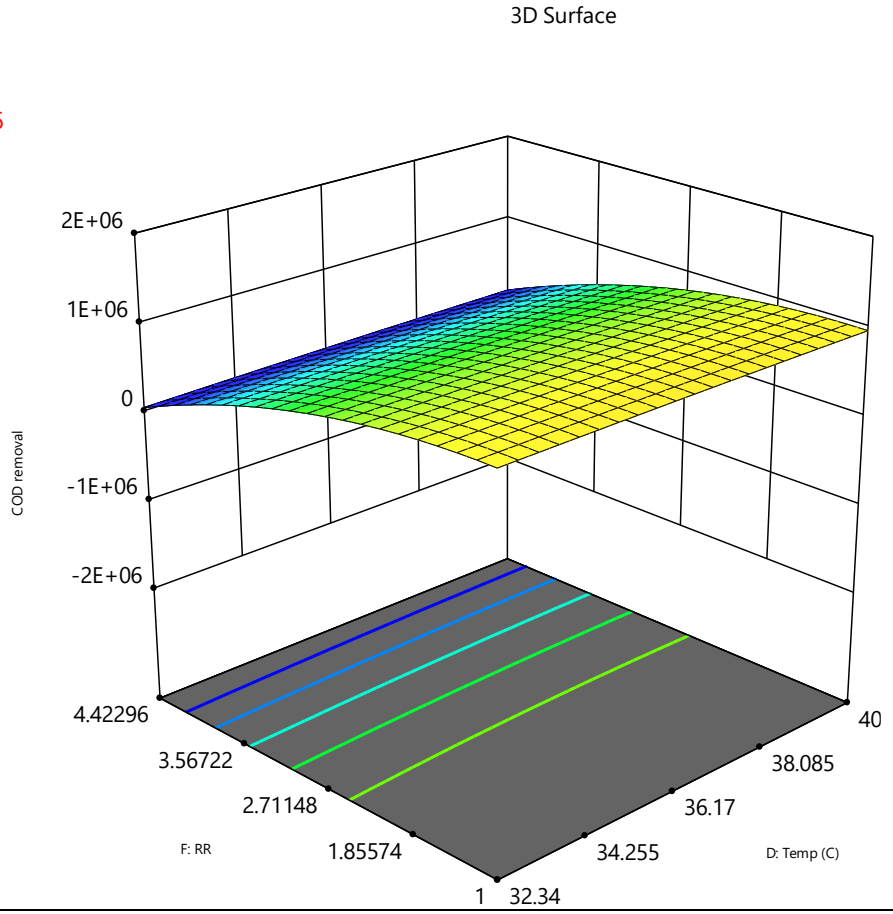

(b)

Factor Coding: Actual

COD removal

X1 = D
X2 = L

Actual Factors
A = 1.31453
B = 60.9811
C = 4.715
E = 26880
F = 2.3007
G = 38284
H = 34975
J = 35010
K = 6180

L1 BGP B
L2 BGP C
L3 BGP A
L4 BGP D

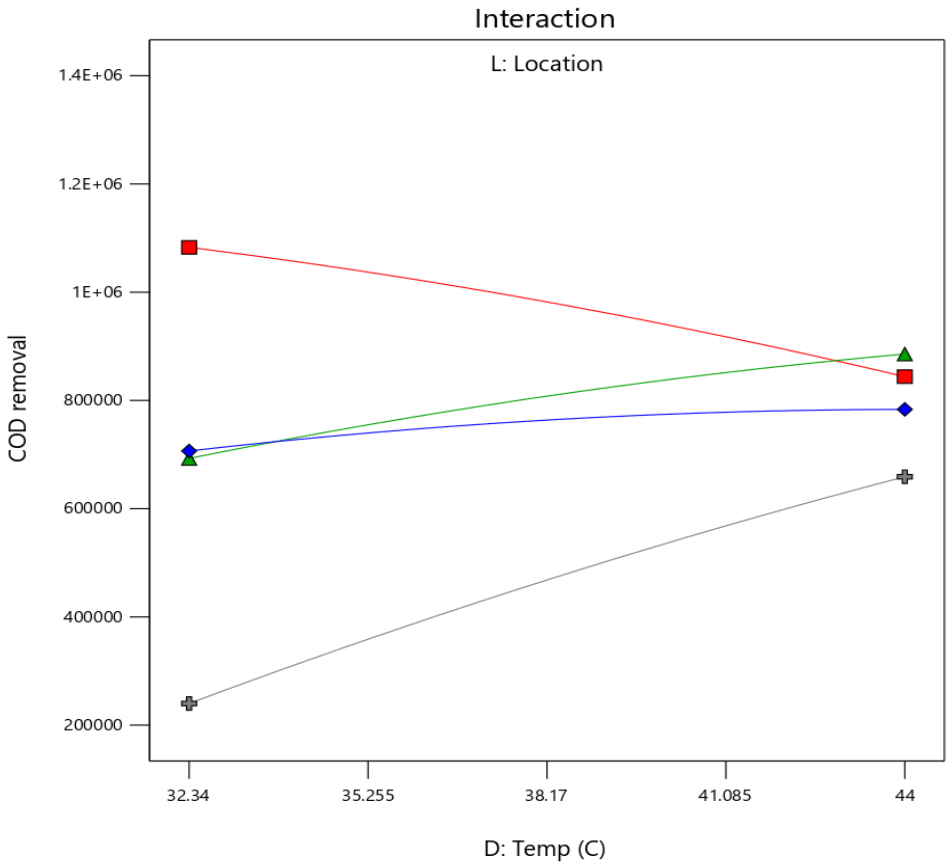

Figure 4.16: (a) Surface and contour plot for COD removal as a function of temperature and recirculation ratio; (b) Interaction plot for COD removal as a function of temperature and location

Factor Coding: Actual

COD removal

X1 = F
X2 = L

Actual Factors
A = 1.31453
B = 60.9811
C = 4.715
D = 38.17
E = 26880
G = 38284
H = 34975
J = 35010
K = 6180

L1 BGP B
L2 BGP C
L3 BGP A
L4 BGP D

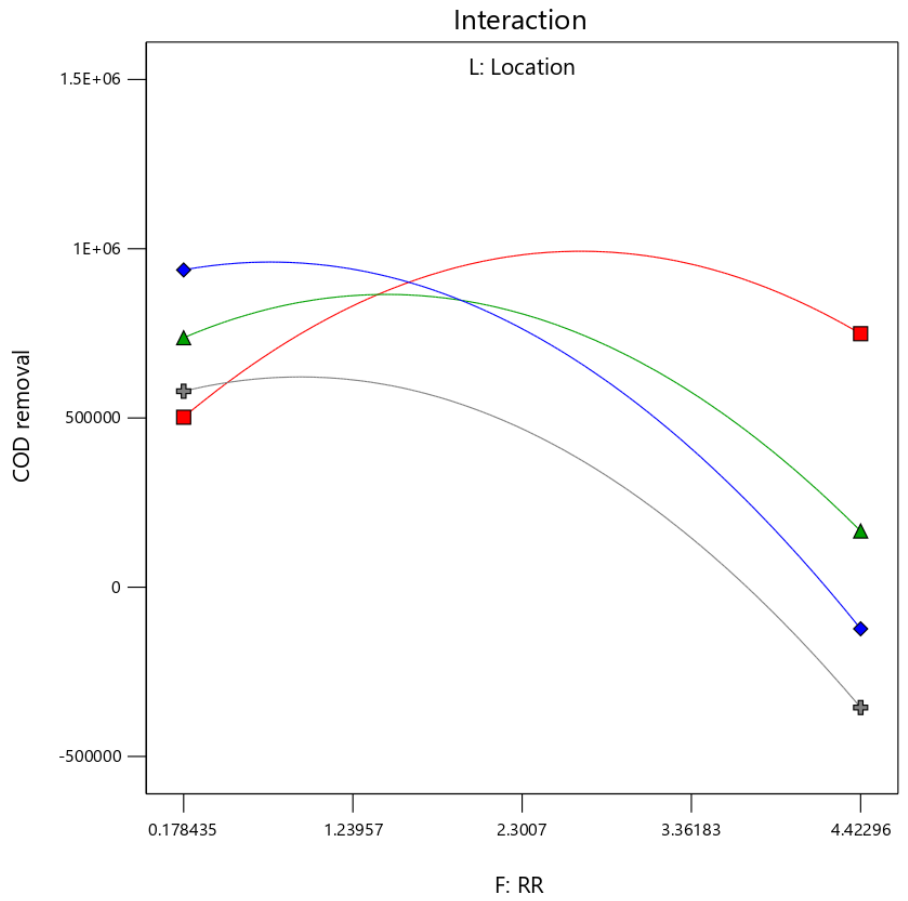

Figure 4.17: Interaction plot for COD removal as a function of recirculation ratio and location

(a)

Factor Coding: Actual

Biogas production

18320 483126

X1 = D

X2 = A

Actual Factors

B = 60.9811

C = 4.715

E = 26880

F = 2.08304

G = 38284

H = 34975

J = 35010

K = 6180

L = Average over

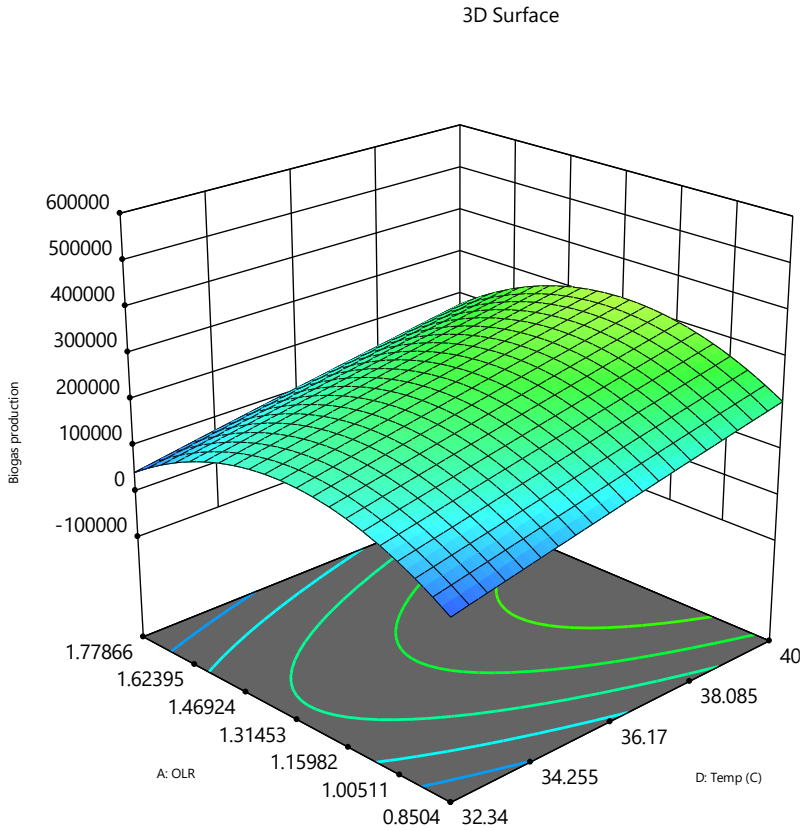

(b)

Factor Coding: Actual

Biogas production

18320 483126

X1 = F

X2 = A

Actual Factors

B = 60.9811

C = 4.715

D = 37.7244

E = 26880

G = 38284

H = 34975

J = 35010

K = 6180

L = Average over

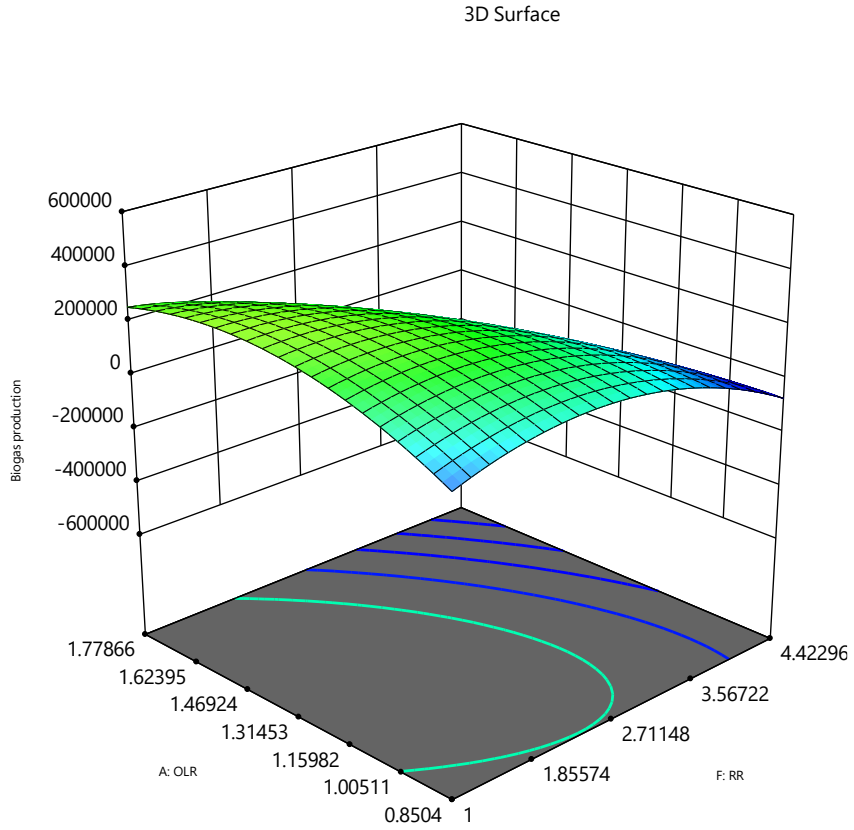

(c)

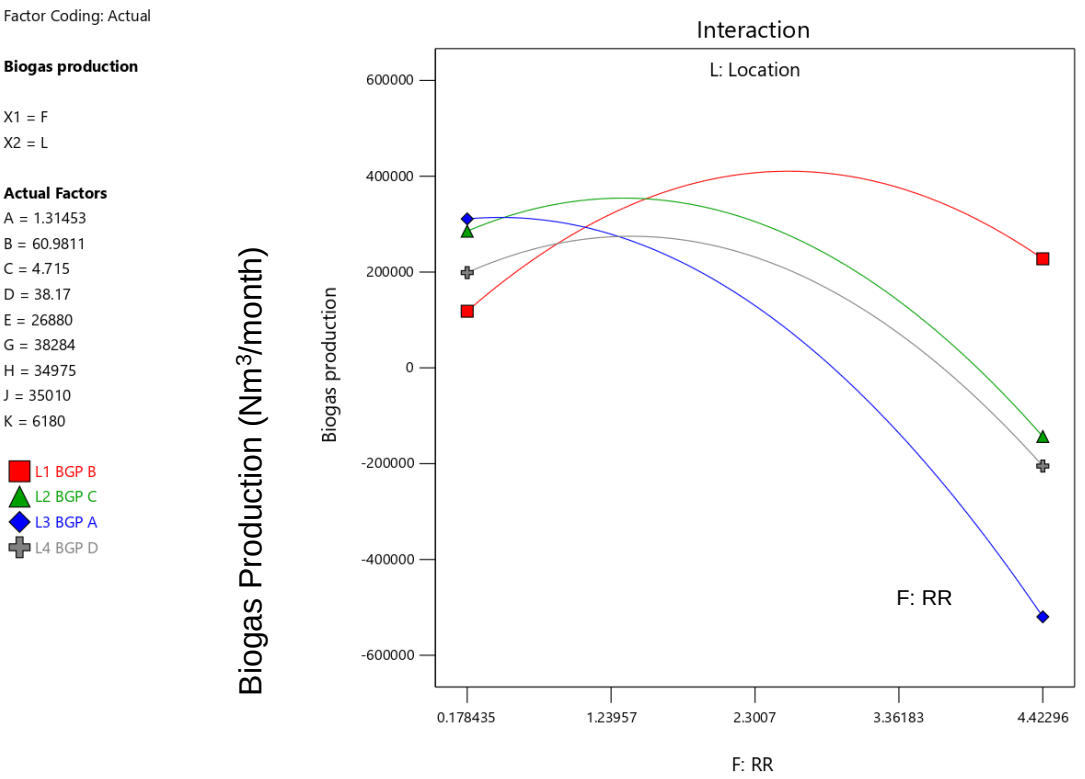

Figure 4.17: (a) Surface and contour plot for biogas production as a function of temperature and OLR; (b) Surface and contour plot for biogas production as a function of recirculation ratio and OLR; (c) Interaction plot for biogas production as a function of recirculation ratio and location.

(a)

Factor Coding: Actual

Biogas production

18320 483126

X1 = F

X2 = D

Actual Factors

A = 1.56932

B = 60.9811

C = 4.715

E = 26880

G = 38284

H = 34975

J = 35010

K = 6180

L = Average over

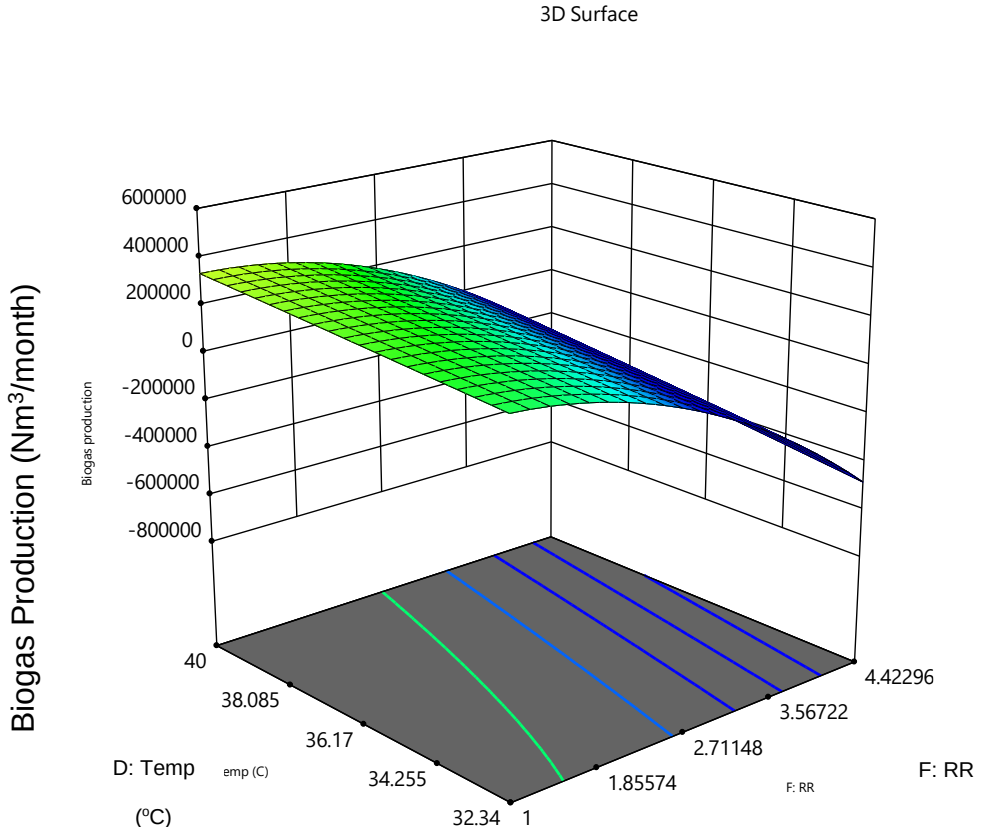

(b)

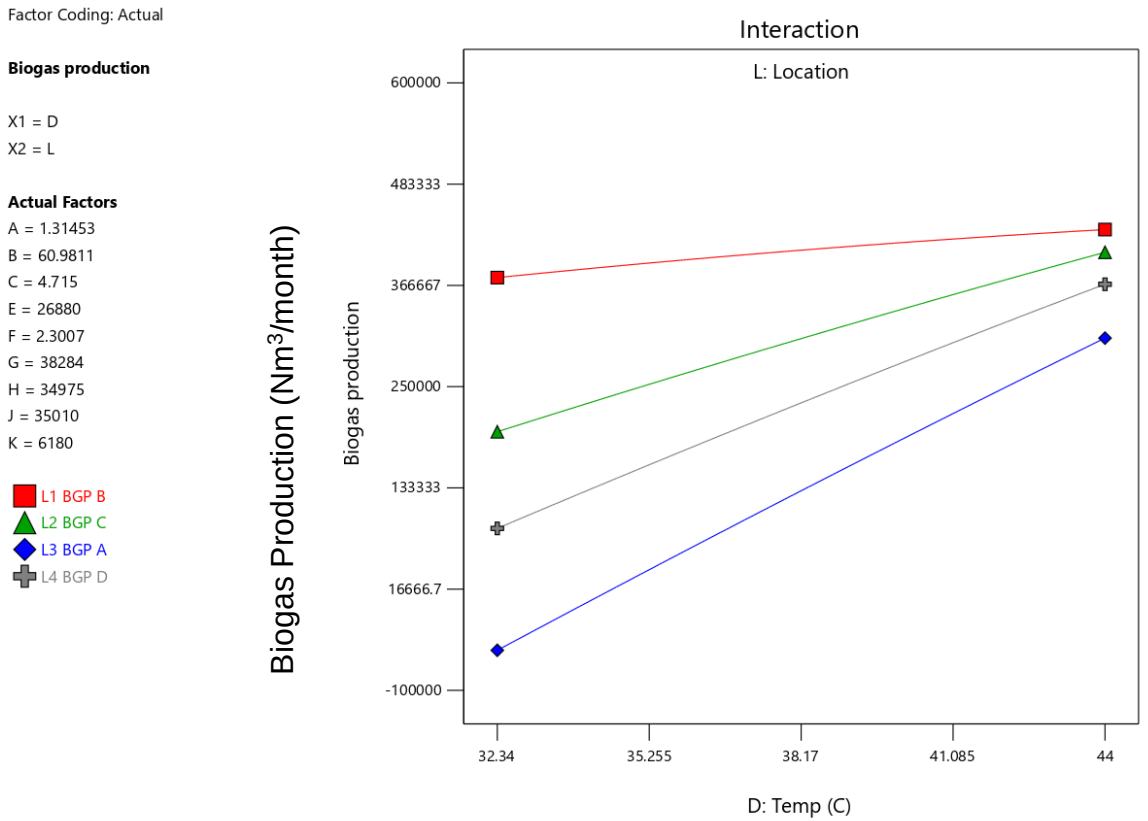

Figure 4.18: (a) Surface and contour plot for biogas production as a function of recirculation ratio and temperature; (b) Interaction plot for biogas production as a function of temperature and location.

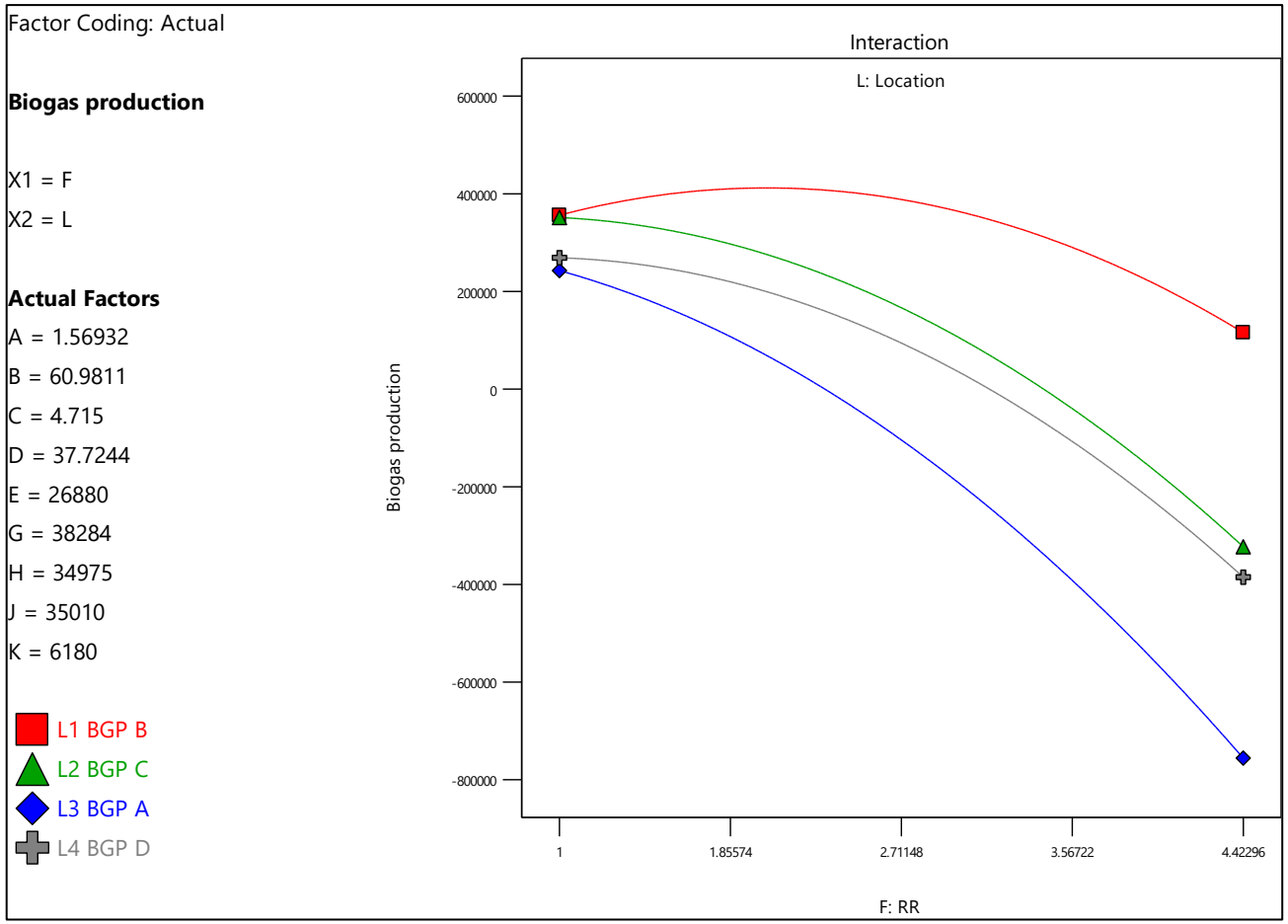

Figure 4.19: Interaction plot for biogas production as a function of recirculation ratio and location

4.3.4 Optimisation and Sensitivity Analysis of AD Performance Study

A comprehensive optimization study was conducted on the operating conditions to achieve efficiency of 85% removal of COD, BOD and TSS removal in compliance with the effluent discharge limit and production of methane gas with a purity of 60% with good stability by considering the trade-off between capital cost, operating cost and revenue. The optimization study under mesophilic conditions was conducted by using Design Expert 13 software on a nonlinear multiple regression model.

Both outputs (COD removal and biogas production) are calibrated whereby both weights are equally as important to achieving maximum value. The parameters that are considered statistically significant for both responses are only altered in the study. Table 4.9 illustrates the optimal conditions of the biogas plants with the objective to maximise COD removal and biogas production. BGP B can achieve the highest COD removal (1.21 X 10^6 kg COD_{in}/month) as well as biogas production rate (4.12 X 10^5 Nm^3/month), with a corresponding methane yield of 0.28 Nm^3 CH_4/kg $COD_{removed}$ when the optimal operating parameters for OLR, temperature and recirculation ratio are configured at 1.60 kg COD_{in}/m^3 day, 37.7 ^oC and 2.08 respectively.

Table 4.9: Optimised values for each BGP plant

Location	OLR (kg COD_{in}/m^3 day)	Temperature (^oC)	Recirculation ratio	COD removal (kg COD_{in}/month)	Biogas production (Nm^3/month)
BGP A	1.49	40.0	1.00	1.07 X 10^6	3.23 X 10^5
BGP B	1.60	37.7	2.08	1.21 X 10^6	4.12 X 10^5
BGP C	1.64	40.0	1.00	1.06 X 10^6	3.69 X 10^5
BGP D	1.60	40.0	1.00	7.94 X 10^5	3.07 X 10^5

A series of sensitivity analyses are performed on each of the plants to evaluate the effect of an independent variable on the dependent variables of a process under a given set of assumptions. The advantage of sensitivity analysis is that it identifies important areas to improve the performance of the model and that the crucial parameters can be monitored once identified (Kaplan Financial Limited, 2020). The independent variables are the input parameters of the process which are OLR, temperature and RR. While the response by which analysis is conducted is the COD removal. The results obtained are normalised and represented in pie charts (Figure 4.21).

Firstly, BGP A is analysed according to the database provided on OLR, temperature and RR. The percentage change of COD removal when each of the input parameters (OLR, temperature, and RR) is brought upon a change of ±10% based on its original mean value. It is found that OLR plays a major role in contributing to the removal of COD, making up about 71% of the three parameters evaluated (Figure 4.21 (a)). From the results, an increase of 10% in the OLR amounts to a decrease of approximately 12% in COD removal. This indicates that the model is sensitive to OLR change compared to temperature and RR. Although the effects of temperature and RR on the COD removal efficiency on the plant are both rather low, the temperature still impacts the responses more than RR, implying that temperature is a relatively sensitive parameter compared to RR. However, being the most sensitive input, OLR must be monitored from time to time to ensure its stability for efficient COD removal.

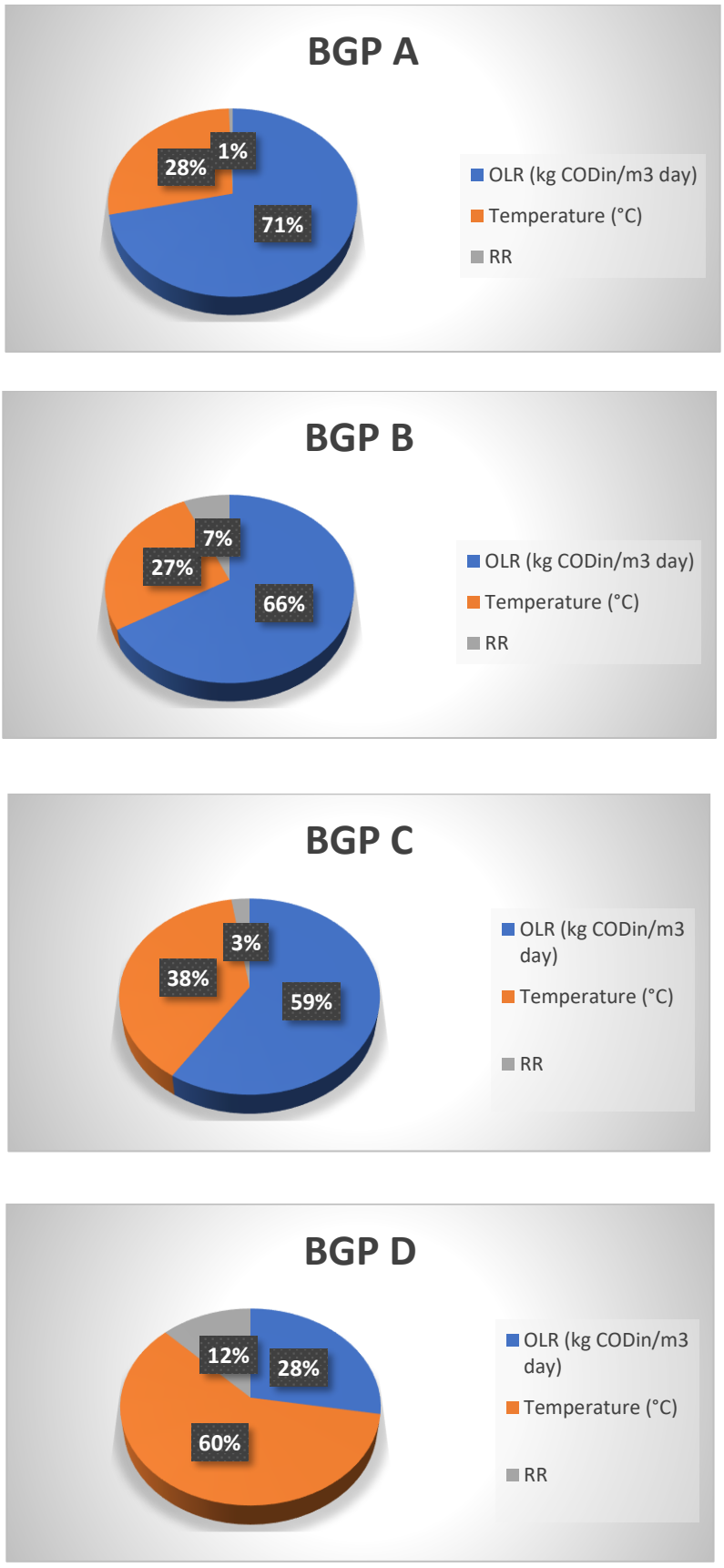

Figure 4.20: Sensitivity analysis of OLR, temperature and RR on a) BGP A, b) BGP B, c) BGP C, d) BGP D

BGP B is like BGP A for its trend of OLR being the most sensitive parameter, followed by temperature and finally RR (Figure 4.21 (b)). With an increase in 10% of OLR, the percentage of COD removal has decrease by approximately 12%. While the increase in 10% of temperature and RR of BGP B has increased 9.5% and decreased 0.77% of the initial COD removal respectively. In BGP B, OLR has occupied 66% of the pie chart followed by 27% of temperature and 7% of RR. Overall, the sensitivity trend observed in BGP B is same as BGP A.

Similar to BGP A and BGP B, it can be observed that BGP C follows the trend of decreasing sensitivity from OLR to temperature and RR (Figure 4.21 (c)). However, it is also found that the percentage change in COD removal due to OLR is gradually decreasing compared to the previous BGPs, while OLR makes up to only 59% of the pie chart. This indicates decreasing sensitivity of OLR and increasing sensitivity of temperature and RR to 38% and 3% respectively.

Finally, the trend previously observed among the parameters for BGP A, B and C are not representative of BGP D. Temperature makes up the largest portion of the pie chart following normalising, occupying up to 60% of the pie chart (Figure 4.21 (d)). Hence, the temperature has a relatively high sensitivity contributing to the COD removal of the wastewater by the treatment plant. This means that a small change in temperature may inflict a major change in COD removal. This is possibly due to the smaller cooling pond size in BGP D which results in lower cooling efficiency. Thus, the optimum temperature must be maintained and monitored from time to time to prevent sudden temperature fluctuations in BGP D.

4.3.5 Theoretical Models for Prediction of Methane Production

The first type of theoretical bio-methane productivity model is implemented in this study. The methane potential calculated by the BMP test is an important input variable and it is applied to study cumulative methane production. The calculated theoretical BMPth results provide a higher methane production than the actual data since the model provides an assumption where 100% of the organic materials are digested anaerobically by the system. However, the estimation is considered accurate if the difference remains below 15% (Nielfa et al., 2015; Raposo et al., 2011). Despite that the model can be applied for homogeneous or heterogeneous feedstocks, physiochemical parameters such as pH, temperature, total suspended solids, total alkalinity, dissolved oxygen etc are often disregarded (Ali et al., 2018).

Figure 4.22 illustrates the average methane productivity of the experiments for each plant. Based on the outcomes, BGP A is projected to generate the highest productivity values (0.655 $mLCH_4/gVS$). This is followed by mills in BGP B, BGP C and BGP D valued at 0.647 $mLCH_4/gVS$, 0.496 $mLCH_4/gVS$ and 0.478 $mLCH_4/gVS$ respectively. Hence, it is concluded that BGP A has the highest productivity, despite using a similar type of substrate. This is because bio-methane productivity is estimated as a function of volatile solids (VS), and BGP A has the lowest average VS in the effluent compared to the other mills.

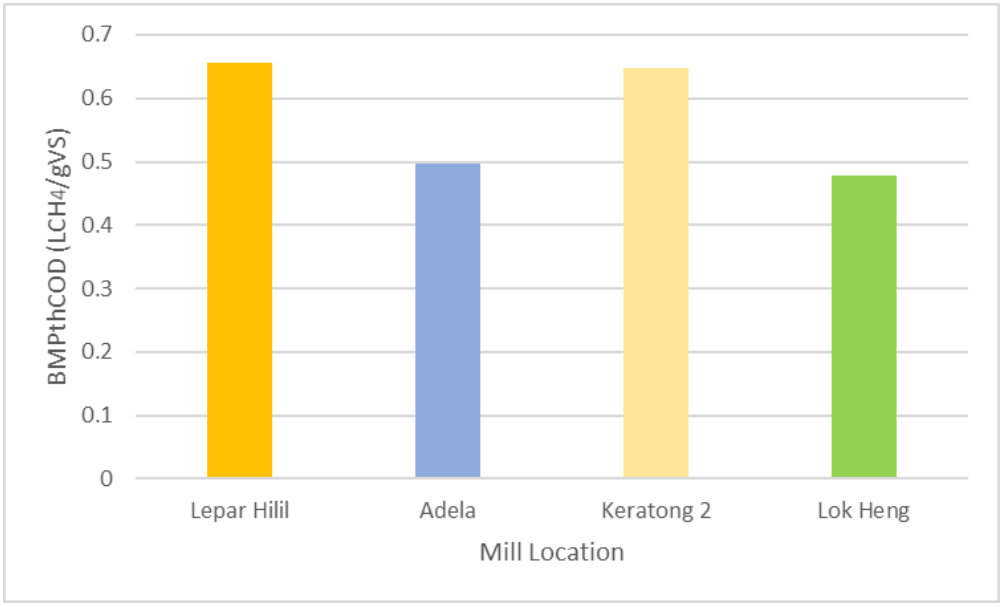

Figure 4.21: Average methane productivity of each biogas plant.

4.3.6 Limitations and Further Improvements of AD Performance Study Analysis

Due to the dependency on the quality and flow rate of raw POME inlet affecting the anaerobic performance of palm oil mills, the incoming capacity of POME is often irregular due to the harvest season of the FFB. Therefore, there are uncertainties which affect the generation prediction model using the plants' historical data. In addition, since the performance monitoring is conducted monthly, any spike would not be captured in the data as it only reflects the mean operating conditions during the uptime of the mill. This would reduce the prediction range as the process parameters are only controlled in a certain desirable range.

The low R^2 values would also cause several complications when estimating the biogas and COD removal. Moreover, the design models implemented for the study are reduced quadratic models. This is because there is insufficient data to represent the prediction model to a higher

order polynomial equation. In addition, the development of mathematical model from the given number of datasets are surreal (K. H. Ng et al., 2020). This is because most responses could not be defined using polynomial equations and the development of polynomial model without validation steps are generally unreliable.

Prediction models could be applied to accurately estimate the anaerobic performance of the biogas plant. Supervised machine learning models such as Support Vector Regression (SVR), Adaptive Neuro-Fuzzy Inference System (ANFIS), and Artificial Neural Network (ANN) can be employed in this scenario. SVR has the capability to minimise prediction errors by assuming the shortest distance between the actual and estimated output values (López-Martín et al., 2020). It is particularly suitable in this historical dataset as statistical evaluation witnesses a high MAE and RMSE for both reduced order quadratic output models.

ANN machine learning model has been extensively employed in the prediction of biogas using different types of substrates (Ghatak & Ghatak, 2018a). Furthermore, the application of ANN machine learning model in biogas prediction has been further improved by coupling optimisation algorithms such as Genetic Algorithm and Particle Swarm Optimisation. This approach can troubleshoot various complex mathematical modelling that requires huge computational operations (Z. Zhang et al., 2018). ANN modelling could be implemented since the anaerobic digestion exhibit several complex reactions such as hydrolysis, acidogenesis, acetogenesis and methanogenesis. Similarly, ANFIS has been adopted in the palm oil mill industry to study the effect of pH, COD, TTS and

methane composition (Tan et al., 2018a). Literature findings support the usage of ANFIS as it had successfully maximised the biogas production from AD after optimising the input process parameters (Zareei & Khodaei, 2017a).

4.4 Six Months Operation Data Analysis of Cooling Tower Application

Based on the overall result analysis presented in the Section 4.3, temperature control is one of a key parameters to optimise AD performance. Hence, cooling tower study was introduced and its effect was analysed.

4.4.1 Analysis of the Temperature and pH Change

4.4.1.1 Analysis of the Effect of Applying CT on the Temperature Inlet and Outlet

Temperature is one of the main factors which affects biogas production. The initial temperature is collected from the POME entering the CT, and the outlet temperature is data recorded from the POME leaving the CT before entering the anaerobic digester. In this section, the temperature change before and after CT can be observed.

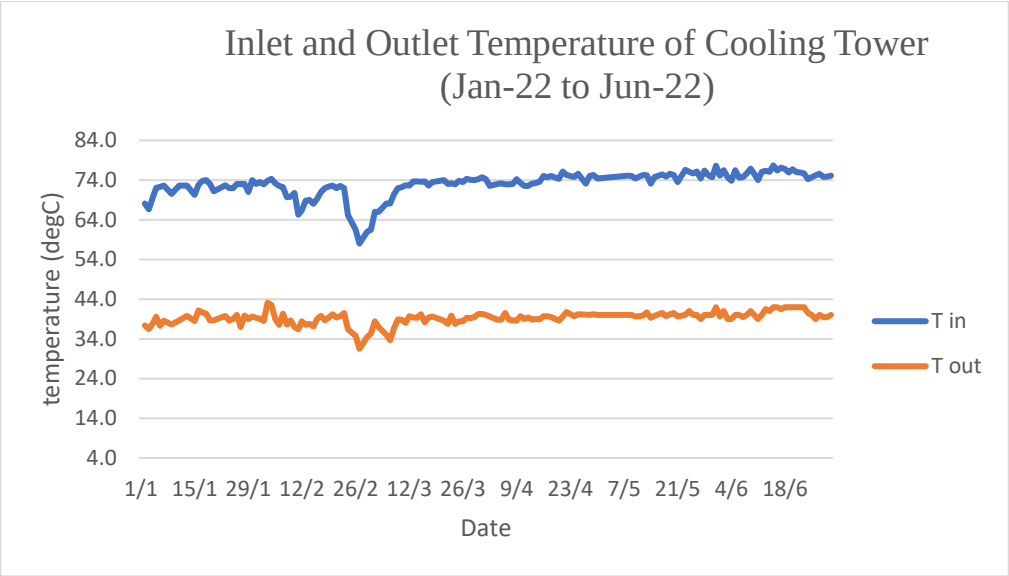

Figure 4.22: Inlet and outlet temperature of CT from January 2022 until June 2022

The usage of CT has successfully reduced the temperature of the POME by at least 46%. The average temperature of POME entering the CT is 73.06°C, and exiting is at 39.3°C. This is within the target range of the operating temperature of mesophilic bacteria. From Figure 4.23, on 27/2, the lowest outlet temperature recorded was 31.5°C. This is due to the inlet temperature being at its lowest, which is 58.0°C compared to the average of 73.06°C. The outlet temperature's standard deviation is low, indicating that the data does not deviate from the average. It can be seen that there is minimal fluctuation in the reading of the outlet temperature. Despite a high fluctuation in the inlet temperature reading, the outlet temperature reading is stable and does not fluctuate by much. This proved that the CT could reduce the inlet temperature while controlling the fluctuation of the POME at the outlet. Hence, a better quality of POME entered the AD.

Table 4.10: Comparison between inlet temperature and outlet temperature from 2019 until 2022

	Inlet Temperature (°C)				Outlet Temperature (°C)			
	Min	Max	Average	Dev	Min	Max	Average	Dev
2019	53.00	56.00	54.32	1.09	40.00	42.80	41.85	1.04
2020	52.20	58.00	55.54	1.71	38.60	46.20	42.96	2.25
2021	52.90	56.20	54.83	1.19	35.90	41.20	39.37	1.98
2022	69.95	75.64	73.04	2.26	38.28	40.55	39.29	0.91

The data collected from 2019 until 2021 was when a CT was not installed in the pre-treatment section of raw POME. During this period, the CP and mixing tank was used to cool down the POME before releasing it into the AD. From Table 4.10, it can be seen that the inlet temperature is between the range of 52°C to 58°C. The inlet temperature recorded in 2022 is between 69.95°C and 75.64°C. This is because the inlet temperature from 2019 until 2021 was sampled from the entry point into the mixing tank in the biogas plant compound, where the POME generated from the mill has passed through the CP. Meanwhile, the temperature recorded in 2022 was tapped directly from fresh raw POME generated from the mill. This was done to study the optimum performance of the CT.

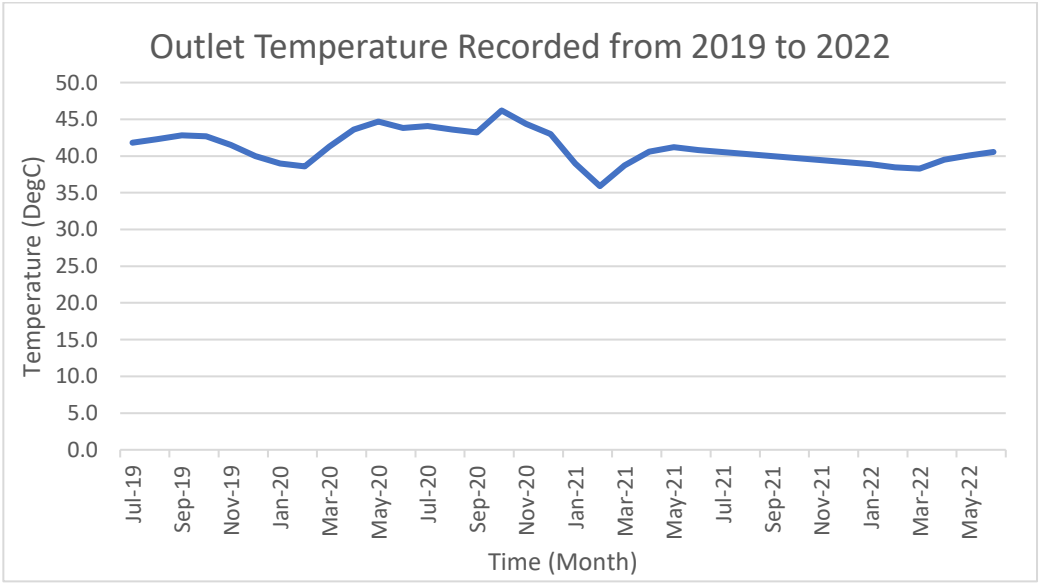

Figure 4.23: Outlet temperature recorded from July 2019 to June 2022

From Table 4.10, the deviation recorded for 2019 until 2021 is high in each respective year, between 1.04°C to 2.25°C. This shows that the combination of the mixing tank and CP is not able to control the temperature properly. It also indicates that the outlet temperature fluctuates. On the other hand, the deviation of the outlet temperature recorded after applying the CT is below 0.91°C, which is lesser than previously recorded. This shows that the outlet temperature of POME leaving the CT is stable, as shown in Figure 4.23. The average outlet temperature recorded in 2019, 2020 and 2021 is 41.85°C, 42.96°C and 39.37°C, as seen in Table 4.10. This outlet temperature is higher than the one recorded in 2022, where the outlet temperature is 39.29°C. Despite having a higher inlet temperature, the outlet temperature recorded when using the CT is lower than when a combination of CP and mixing tank was used. From Figure 4.23, Figure 4.24 and Table 4.10 show that the CT can reduce the temperature of POME much better than a CP and mixing tank. Another finding observed is that the CT can provide a stable outlet temperature despite being fed a range of temperatures that fluctuate significantly.

4.4.1.2 Analysis of the Effect of Applying CT on the pH Outlet

A CT is used only to reduce the temperature and does not alter the pH of the effluent. As stated in Section 4.1.1, the sample was tapped directly from raw POME generated by the mill. The POME provided by the mill is typically in the acidic range. Thus, the pH value should be between 4 and 5. As seen in Figure 4.24 and Figure 4.25, the inlet pH of the POME that enters the CT ranges from 4.40 to 5.68. There appears to be no change

in the range of the pH reading recorded on both sides. The average pH inlet and outlet are constant at 4.57. This proved that the CT function is for temperature reduction. No chemical or biochemical processes occurred to adjust the pH.

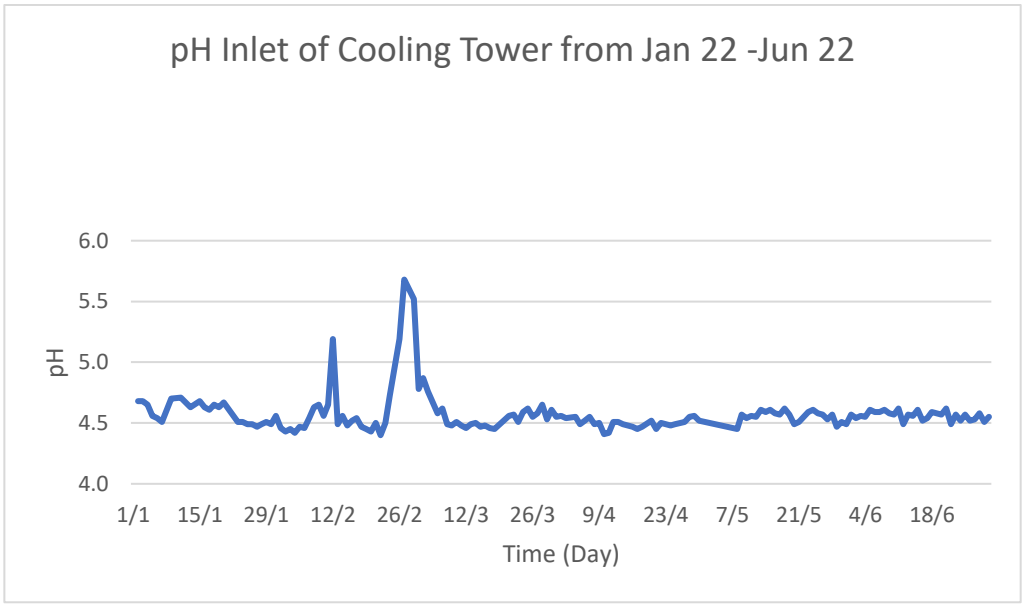

Figure 4.24: pH Inlet of CT from January 2022 until June 2022

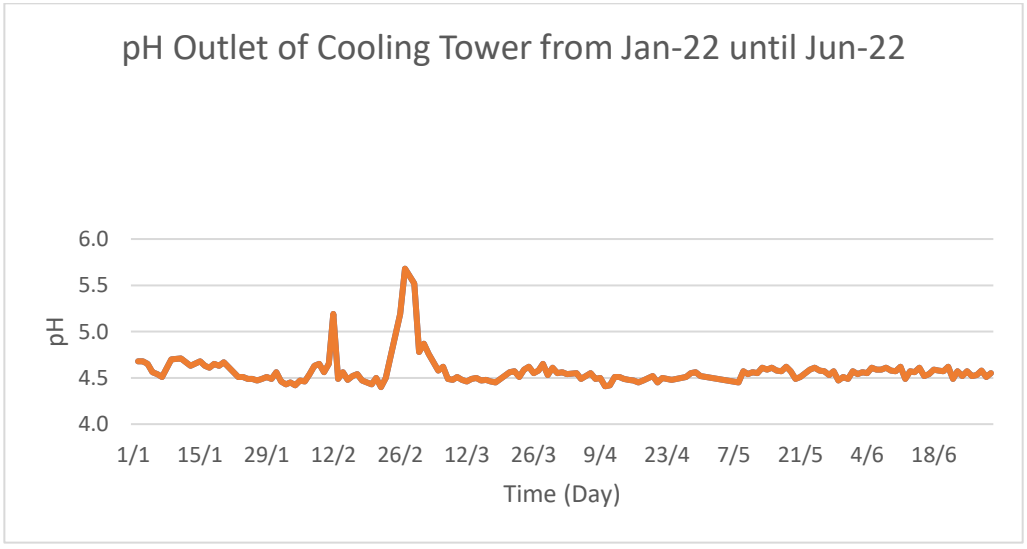

Figure 4.25: pH Outlet of CT from January 2022 until June 2022

4.4.2 Analysis of Bottom Sludge

4.4.2.1 Temperature change of Bottom Sludge

Bottom sludge is formed and sedimented in the digester during gas formation processes. The sludge would be recirculated back to the mixing tank to reduce temperature and adjust the pH of effluent before entering the AD. The recorded temperature is 32.5°C to 35°C, with an average reading of 33.1°C. Figure 4.26 shows that for the first 13 days of January, the temperature fluctuates between 32.5°C and 33°C. The second anomaly was between 24/6 and 30/6, with the temperature at 35°C. Despite this, the data is still within the operating range of the mesophile. This anomaly may be due to the input temperature of the raw POME, which causes a difference in the values with the previous days. Despite this, the values do not fluctuate by much and are still within the operating range of mesophiles.

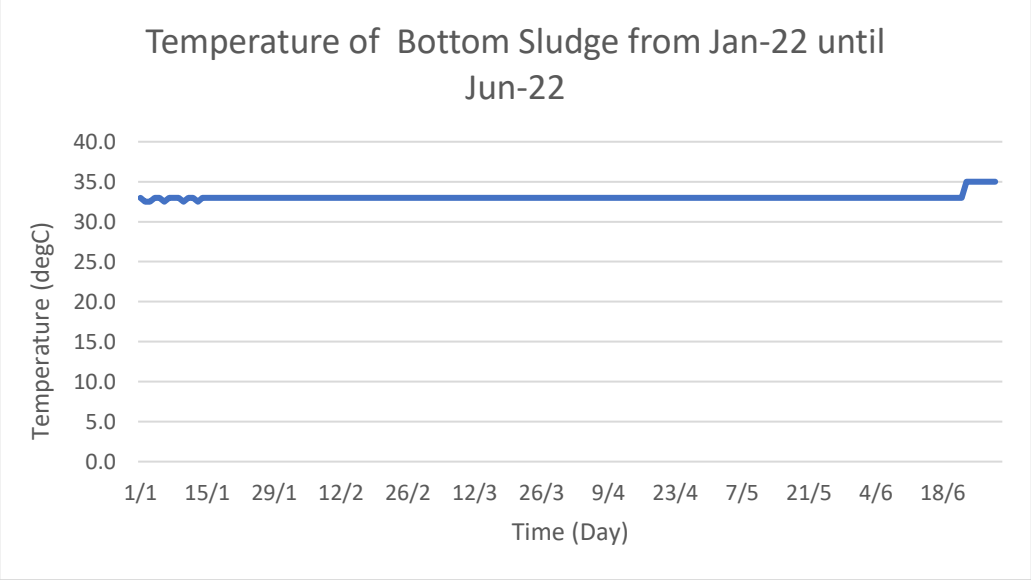

Figure 4.26: Temperature of bottom sludge recorded from January 2022 until June 2022

The average temperature of the bottom sludge recorded before applying the CT is greater than the average reading recorded after using CT in the pre-treatment process. Compared with the data collected from 2019 until 2021, the deviation recorded is higher than in 2022. This is because the temperature is not adequately controlled in the mixing tank, which increases the bottom sludge's temperature, as seen in Table 4.11 below. In 2022, the average temperature for bottom sludge was 33.1°C compared to the average recorded in 2019, 2020 and 2021, which gives a reading of 39.9°C, 39.9°C and 37.8°C respectively. This proves that applying the CT reduces the bottom sludge's temperature fluctuation, allowing for a more controlled environment for the mesophiles to nurture.

Table 4.11: Temperature of bottom sludge from 2019 until 2022

Temperature of Bottom Sludge (°C)				
	2019	**2020**	**2021**	**2022**
Min (°C)	38.8	36.0	35.6	32.9
Max (°C)	41.0	43.0	39.5	33.5
Average (°C)	39.9	39.9	37.8	33.1
Dev	0.744	2.109	1.438	0.202

4.4.3 Analysis on Treated Effluent

4.4.3.1 Temperature of Treated Effluent

The temperature of the treated effluent is between the range of 31.0°C to 32.5°C with an average reading of 31.9°C, as shown in Figure 4.27. The temperature does not deviate by much, which is only 0.2°C. It can be assumed that there appears to be little to no difference in the temperature of the treated effluent. From Figure 4.27, the reading is stable because the temperature was controlled during the pre-treatment phase. The reading of the temperature is within the operating range of mesophiles.

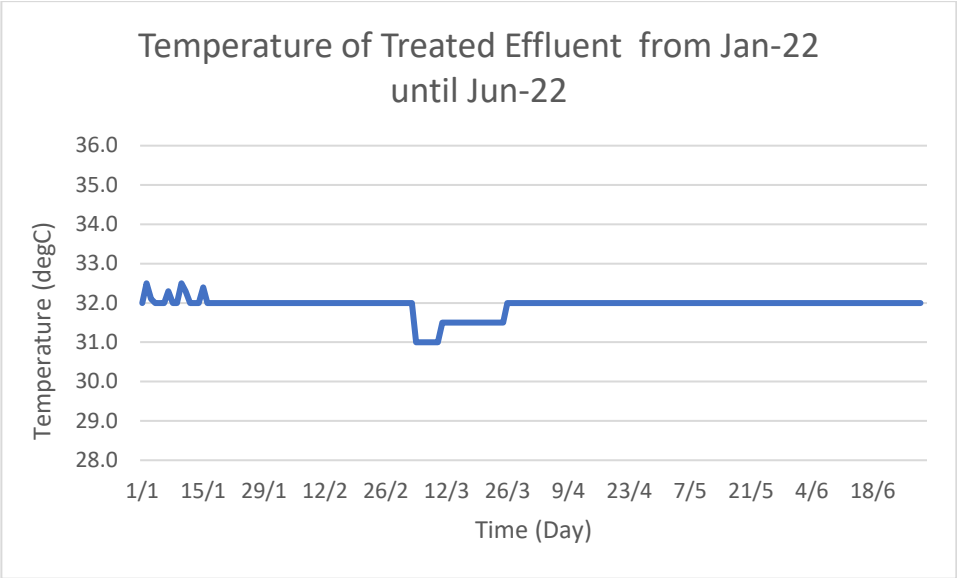

Figure 4.27: Temperature of treated effluent from January 2022 until June 2022

Table 4.12: Temperature of Treated effluent from 2019 until 2022

	Temperature of Treated Effluent (°C)			
	2019	**2020**	**2021**	**2022**
Min	37.8	40.8	38.8	31.6
Max	40.4	42.5	39.5	32.1
Average	39.6	41.5	39.0	31.9
Dev	0.985	0.686	0.25	0.187

Table 4.11 summarised average reading recorded in 2019, 2020 and 2021. The reading are 39.6°C, 41.5°C and 39.0°C, respectively, while in 2022, the average reading is much smaller, which is only 31.9°C. The deviation recorded in 2022 is the lowest compared to the previous three years. This proves that by controlling the inlet temperature to the AD, the temperature fluctuations in the AD will be reduced and improved.

4.4.4 Analysis on Raw Biogas Quality in Lepar Hilir

4.4.4.1 Analysis of Gas Quality from January 2022 until June 2022

In the raw quality of biogas, four main gaseous were examined and checked. These gases are methane (CH_4), carbon dioxide (CO_2), oxygen

(O_2) and hydrogen sulphide (H_2S). The gaseous quality was compared from 2019 to 2022 to check and compare the effect of temperature control on the biogas quality.

The average percentage of CH_4 present in the biogas was at least 65.91%. The CH_4 produced was around the range of 60% to 70%. Figure 4.28 shows that CH_4 produced in the biogas does not fluctuate by much, and the values are stable. The reading of CO_2 recorded is within the range of 25.5% to 86%, which is not in the standard range. On 20/5, there was an abnormal reading of CO_2, which is at 86%. This is due to an error caused by the biogas analyser. The rest of the reading recorded is within the optimal range of CO_2 recorded, and the deviation is also relatively small.

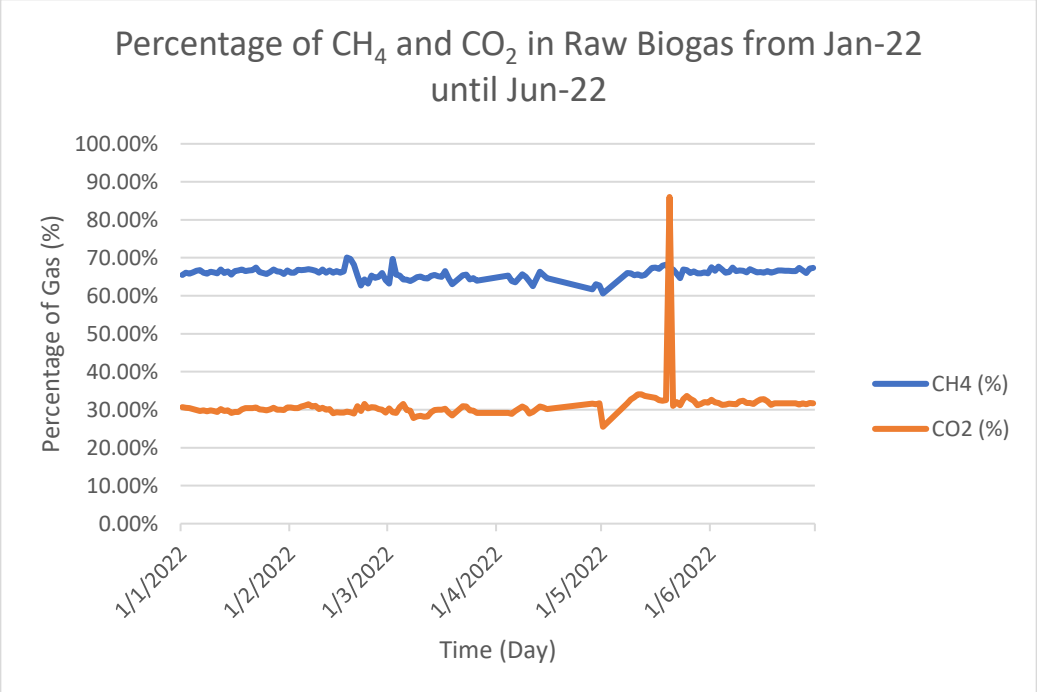

Figure 4.28: Percentage of CO_2 and CH_4 in Biogas from January 2022 until June 2022

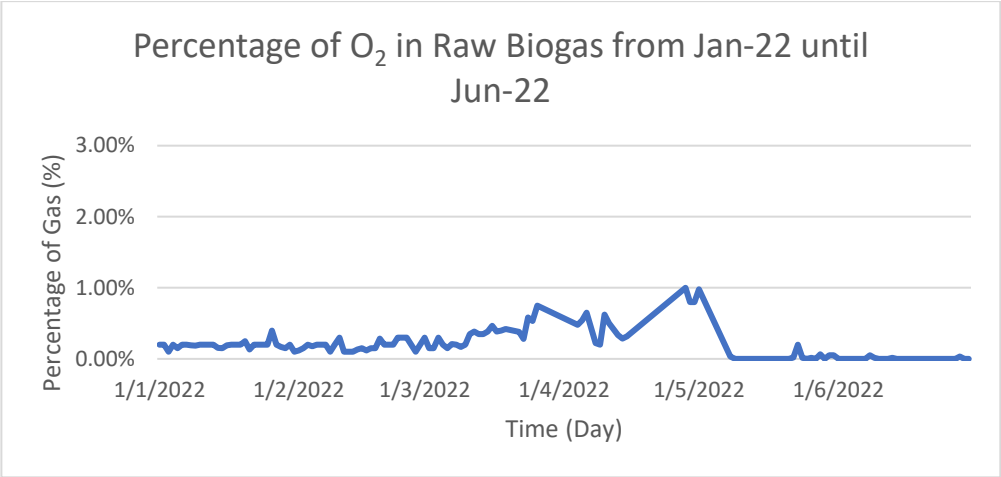

Figure 4.29: Percentage of O_2 inside biogas collected from January 2022 until June 2022

There were traces of O_2 inside the biogas due to recycling the gas from the biological scrubber. However, the O_2 presence is less than 1%, as seen in Figure 4.30. The highest amount of O_2 present in the raw biogas was on 28/4 where the reading collected 1% of O_2 present inside the biogas. From January until June, the reading showed that there were little to no traces of O_2 in the biogas collected.

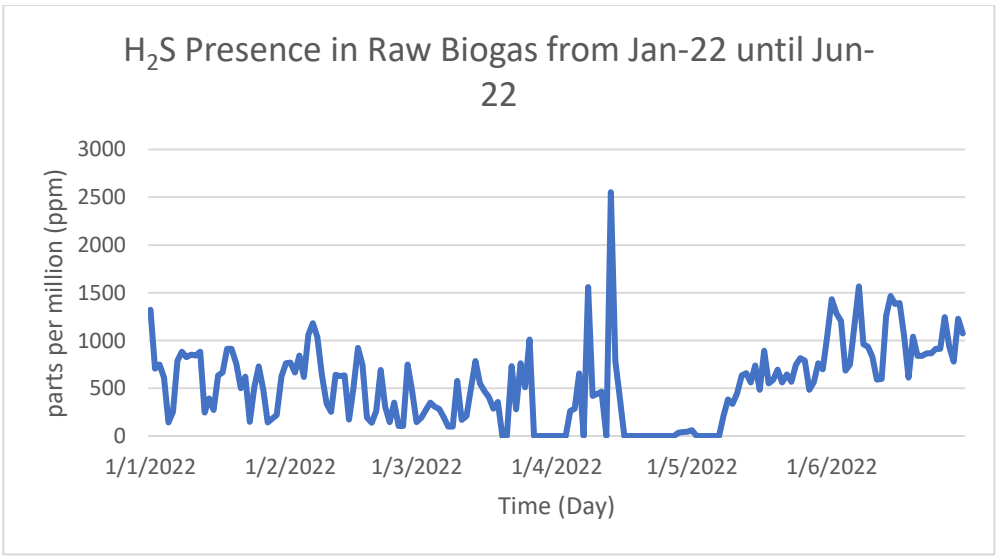

Figure 4.30: Presence of raw H_2S inside biogas collected from January 2022 until June 2022

The average amount of raw H_2S detected is 641ppm. The amount of H_2S inside the gas is within the range of 35ppm to 2553ppm, as seen in Figure 4.31. These values show that the amount of H2S is within the expected range. The highest amount of H2S detected occurred on 13/4, where the reading was 2553 ppm.

4.4.4.2 Comparison of CH4 Quality (Pre and Post-CT Installation)

The production of CH_4 is essential because this will determine the amount of energy generated by AD. The percentage of CH_4 in biogas is typically 50% to 75% (Lok et al., 2020). A high CH_4 rate proved that the application of CT provides a positive output. As long as the reading of the methane percentage is not below previous years' reading, the usage of CT will prove beneficial.

Table 4.13: Percentage of CH_4 in raw biogas from 2019 until 2022

	Methane Percentage in Raw Biogas (%)			
	2019	**2020**	**2021**	**2022**
Min	62.48%	60.80%	62.13%	64.12%
Max	63.66%	63.42%	63.91%	66.64%
Average	63.31%	61.86%	63.09%	65.71%
Dev	0.44	0.82	0.61	0.97

A higher methane percentage inside the raw biogas is obtained by using a CT to control the temperature of the POME entering the digester. The average percentage of CH4 produced in 2022 is 65.71%. This average is much higher than the ones recorded in 2019, 2020 and 2021; the readings recorded are 63.31%, 61.86% and 63.09%, respectively. From Table 4.13, it can also be seen that the lowest amount of methane detected in the raw biogas is 64.12%. This value is still much higher than the maximum value recorded from the previous three years. The mixture

of using CP and mixing tank provides less amount of CH_4 compared to using a CT to control the temperature.

4.4.4.3 Comparison of CO2 Quality (Pre and Post-CT Application)

The amount of CO_2 in the biogas reduces after applying a CT. Before using the CT, the amount of CO_2 ranged from 29.95% to 36.42% from 2019 to 2021, as seen in Table 4.14. After using the CT, the average CO_2 percentage was 31.04%. This average is much lower compared to the previous years. The average reading for 2019, 2020 and 2021 was 33.47%, 34.25% and 32.25%, respectively. The highest amount of CO_2 present inside the biogas is 34.42%. Overall, the reading of CO2 is not much different compared to the previous years

Table 4.14: Percentage of CO_2 present in biogas from 2019 until 2022

Carbon Dioxide Percentage in Raw Biogas (%)				
	2019	**2020**	**2021**	**2022**
Min	32.90%	31.81%	29.95%	29.55%
Max	34.06%	36.42%	33.38%	34.42%
Average	33.47%	34.25%	32.25%	31.04%
Dev	0.60	1.50	1.24	1.82

4.4.4.5 Comparison of Hydrogen Sulphide Quality (Pre and Post CT)

H_2S is often produced from the microbial breakdown of organic matter in the absence of oxygen. This occurs when the sulphate present in the material is broken into gas. H_2S is corrosive and poisonous. The amount of H_2S presence should be in the range of 50 ppm to 5000 ppm for crude biogas (Konkol et al., 2021). H_2S will cause corrosion to the equipment that will use this biogas.

Table 4.14: Presence of Hydrogen Sulphide in Biogas from 2019 until 2022

	Hydrogen sulphide detected in biogas (ppm)			
	2019	**2020**	**2021**	**2022**
Min	261	220	325	397
Max	1007	1073	819	1022
Average	645	765	550	628
Dev	282	304	195	209

It can be seen that the amount of H_2S present in the gas after the usage of CT fluctuates in the same way as before a CT is applied. The amount of H_2S present inside the gas after using the CT ranged from 397 ppm to 1022 ppm. The amount of H2S present in the raw biogas in 2019, 2020 and 2021 are between 261 ppm to 1007 ppm, 220 ppm to 1073 ppm and 325 ppm to 819 ppm, respectively, as seen in Table 4.15 The average amount of H_2S detected from the raw biogas in 2022, at 628 ppm, is within the acceptable range, as stated earlier. The reason for the amount of H_2S to be high may be due to the amount of POME being fed into the digester.

4.4.5 Optimisation of AD by Cooling Tower Application

4.4.5.1 Performance Evaluation of Biogas Plant Using Artificial Neural Network (ANN)

The statistical data for the biogas production rate and methane yield used for ANN training, validation, and tests is presented in Table 3.6 in the methodology section. Temperature input data has a relatively low standard deviation (± 1.60˚C) and averages around 39.3˚C which is at optimal range for mesophilic temperature condition for biogas production plant. However, the input data for POME feeding rate varies (± 168.2 m^3/day) due to availability of Fresh Fruit Bunches (FFB) and the milling

operations in the mill. Since measurements are taken daily, biogas production rate cannot be observed directly from the daily POME feeding rate as there is accumulation of POME feed from the previous days. So, the measurements will consider the total amount of POME feed rate per month and biogas production rate per month. Hence, this shows the large variation in biogas production rate ($\pm$ 2275.1 m^3/day) as there are accumulation in biogas when measurements are taken daily. However, methane yield shows moderate variation ($\pm$ 0.15 Nm^3/kg $COD_{removed}$) with an average value of 0.32 Nm^3/kg $COD_{removed}$. With these variables, an ANN model will be implemented to provide high accuracy prediction to improve the palm oil industry processes. Figure 4.32 depicts the regression model plot for training, validation, and testing. All the datasets undergo randomized evaluation and testing to generate output parameters, including biogas production rate and methane yield. Table 4.16 shows the attributes of neural network utilized in system.

The forecasting model employs a multi-layer feedforward neural network trained with Levenberg-Marquardt (trainlm) algorithm. The network architecture comprises 2 input layer, two intermediary hidden layers, each containing 20 neurons and a linear output layer featuring 2 neurons representing desired output parameters. Non-linear association within the data are captured by hyperbolic tangent sigmoid activation function applied to hidden layers. This function introduces non- linear transformations to weighted sum inputs received by each hidden unit. Signals from the second hidden layer are then transmitted to the output layer, which utilizes linear activation functions, offering flexibility in

modeling potential output ranges without constraints (Won-Kee Hong, 2023). This enables reasonably accurate predictions of end-parameters based on a given set of initial inputs. Figure 4.32 displays outstanding outcomes with an R^2 more than 0.9. This suggests that the neural network model establishes a strong linearity with targeted values.

Table 4.15: Attributes of neural network utilized

Characteristics	Value
Network Type	Feed-forward
Neuron Count in Input Layer	2
Neuron Count in Hidden Layer(s)	2
Neuron Count per Hidden Layer	20
Neuron Count in Output Layer	2
Training Function	Tangent Sigmoid
Transfer Function	Levenberg-Marquardt (trainlm) Algorithm
Performance Function	MSE

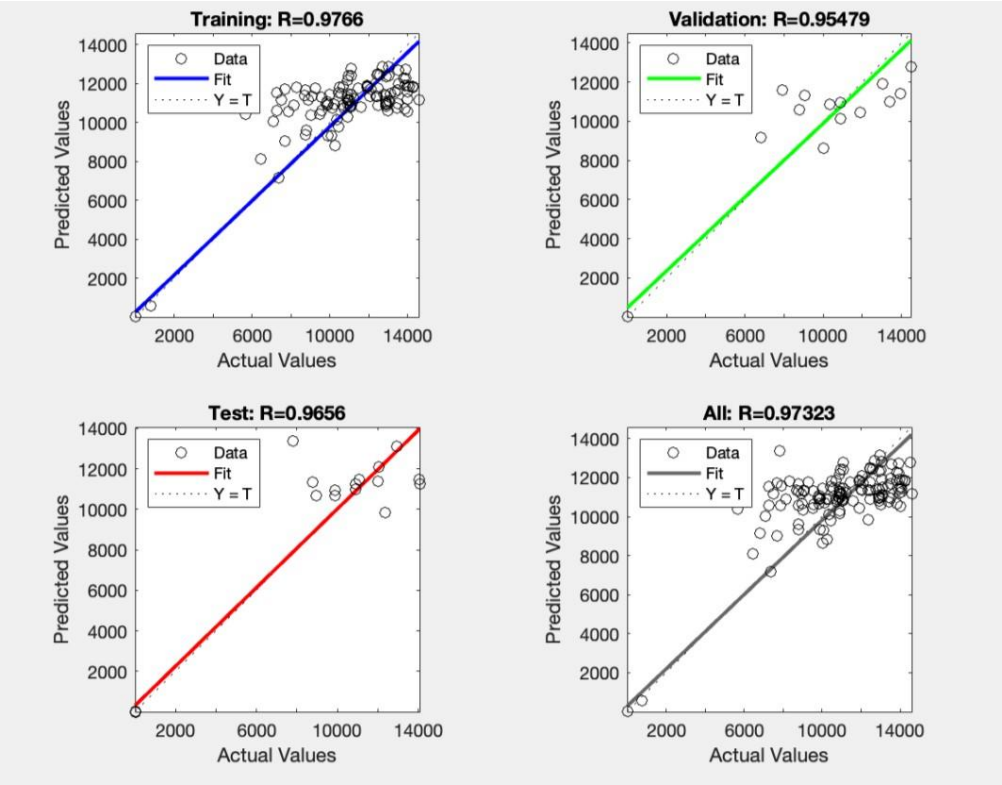

Figure 4.31: Regression plot from training, validation, test and overall phase in neural network

As illustrated in Figure 4.33(a), the mean squared error (MSE) plotted against training iterations(Epochs) which reveals a minimum validation error at 0.20959 at epoch 4. This signifies the neural network's robust generalization capability on unseen data. MSE serves as a metrics to evaluate model performance by averaging the squares of deviations between actual and predicted outcomes across data instances. Smaller MSE value indicates higher predictive accuracy with minimal variability in errors. The Levenberg-Marquardt algorithm facilitates automated weight adjustments over successive epochs to attain the lowest validation of MSE, halting further training to prevent overfitting beyond optimal point. Furthermore, the coefficient of determination R^2, representing the percentage ofvariance in the validation response value, corroborates the superiority in epoch 4. By considering multiple evaluation metrics on different datasets, the optimal trained network architecture is selected based on comprehensive evidence of its ability to generalize rather than merely fit training data. The resulting neural network can effectively predict unknown outcomes within the given problem domain when presented with new input combinations (Taghi Sattari et al., 2012).

The error histogram presented in Figure 4.33(b) represents the distribution of deviations betweenactual and model predicted values on the training dataset. It is divided into 20 vertical bars, each representing bins across numeric ranges. An error histogram provides insight into the frequency of data points experiencing various levels of errors, facilitating an analysis of predictive variability. Positive and negative errors indicate over and underestimation, respectively, in comparison to true values.

The highest bin, with count exceeding 100 instances, reveals error concentrated at around +67.94. This suggests that majority of output deviations in the training data falls within a narrow biasof +67.94, with fewer instances at significantly higher or lower errors. Overlapping between lowest error bin and the zero-error x-axis reference line confirms the near elimination of zero deviation, indicating a close alignment between numerous predictions and targets (MathWorks, 2023) . In summary, the error histogram illustrates the trained neural network's ability to centralize most outputsaround a tight error margin.

Coefficient of determination, R^2, metric expresses the proportion of variance in the target parameter captured by the model, with values close to 1 indicating greater predictive power (Figure 4.32). As anticipated, MSE reaches its lowest point during training when connection weights are calibrated on the same dataset. However, MSE increases when tested on previously unseen data, revealing unmodeled variations in new samples. Despite this, consistently accepted R^2 scores during validation tests underscore the network's ability to generalize learnings beyond the training cases with reasonable accuracy (Chicco, Warrens, et al., 2021). The process of refining the model involved running it 20 times, each iteration adjusting the architectural configuration. The most effective network architecture found the optimal balance—minimizing validation error while preserving generalization ability, as evidenced by a high R^2 approaching 1 (Stangierski et al., 2019).This indicated that the model effectively explains a significant portion of the actual output variance rather than merely fitting the training data. A reasonable correlation

extending from training to validation suggests suitability for accurately forecasting outputs with novel inputs within the domain.

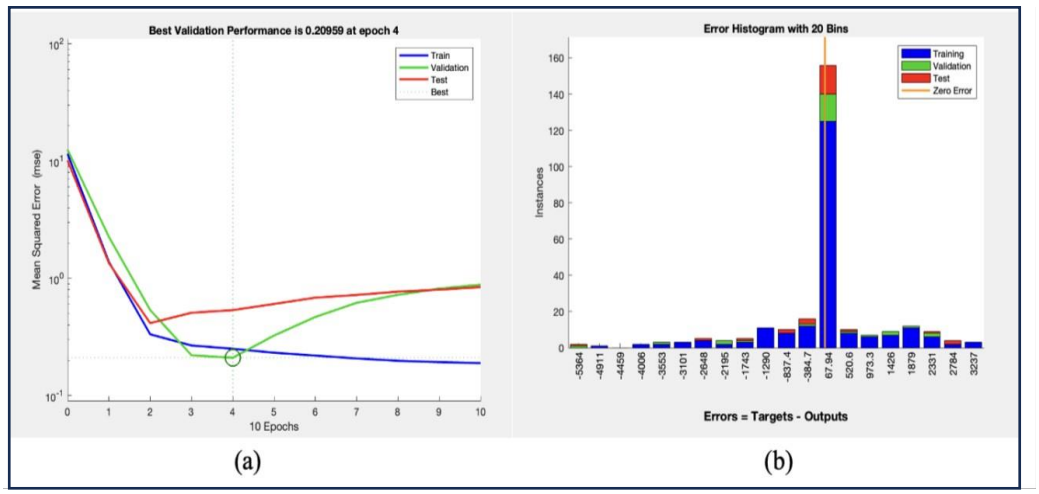

Figure 4.32: (a) Performance plot with MSE function; (b) error histogram plot with 20 Bins in ANNModel

ANN model has proven to show the lowest MSE and highest R^2 value as shown in the above section. Fromsix months operation data, a total of 135 sets of data are used to plot the graph of methane yield against biogas production rate. Based on Figure 4.34, the strong linearity correlation observed between methane yield and biogas production rate signifies direct proportionality.

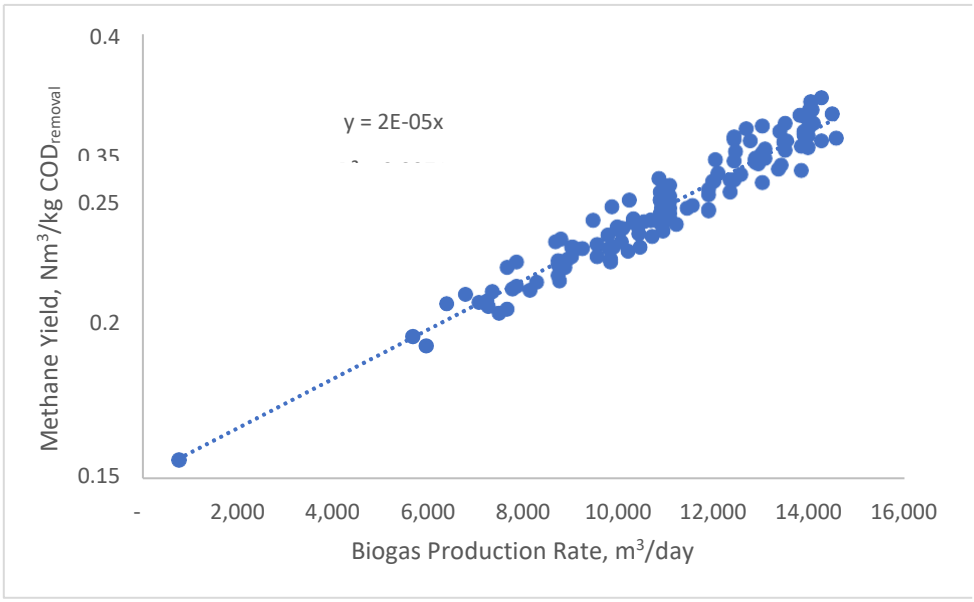

Figure 4.33: Plot of methane yield against biogas production rate

The optimization strategy increases simulated biogas production to 12,683 m^3/day, a 28% improvement over average levels. Similarly, methane yield rose to 0.31 Nm^3/kg CODremoved, up to 11% from baseline average (0.28 Nm^3/kg CODremoved) . This demonstrates the potential to considerably enhance digester performance and economics by shifting operating points to algorithmically derived optimum input values, implying optimization elevates overall production capacity beyond just increasing methane fraction itself. While further real-world validation is required,the strategy charts a feasible path to extract greater value from existing infrastructures through data-driven process alterations that could outpace returns from capital investments.

The optimization model also predicted an ideal temperature of 38.9 ˚C from cooling tower for mesophilic anaerobic digester operation, closely matching known optimal levels. This estimated parameter aligns with the findings from (Moestedt et al., 2017) who also reported 38 ˚C as the peak temperature for mesophilic digesters through previous experimental work. Overall, the independent optimization and derivation of nearly identical optimal temperatures by two separate approaches lends increased confidence regarding 38-39 ˚C being the truly optimal target given the underlying biological kinetics. Future industrial efforts can now use this temperature set point when designing and operating mesophilic digesters for POME without needing to re-verify assumptions.

A key technical challenge faced when training ANN models is the risk of overfitting, evident when a model fits training data very closely but cannot generalize well to unseen inputs. Overfitting creates fragility and

uncertainty issues when attempting to apply the model practically on varying real- world data. Careful generalization testing reduces deployment risks of unexpected behavior (Piotrowski & Napiorkowski, 2013).

4.4.5.2 Sensitivity analysis of cooling tower study

At optimized biogas modelling, biogas production yields to 12,683 m^3/day and methane quality yields to 0.31 Nm^3/kg $COD_{removal}$ at temperature 38.9 ˚C and POME feeding rate of 503 m^3/day with organic loading rate (OLR) of 1.12 (kg/m^3.day). A sensitivity analysis based on Figure 4.35(a) for biogas production rate when input parameters are increased 80% and 120% respectively. It was observed that biogas production rate is sensitive to both temperature and POME feeding rate. At lower optimized value (80%), biogas production rate is more sensitive to temperature. At high optimized value (120%),biogas production rate should show a linear increase when POME feed rate was also increased. However, it is not true in this case as increased POME feed rate caused accumulation of biogas in the covered anaerobic digester which are not collected as they are measured daily. Temperature affects biogas production rate as POME contains mesophilic microbial activity which performs best at optimum temperature.

Based on Figure 68(b) methane yield is highly sensitive to temperature changes. This is because mesophilic microbes in POME can impact biogas quality under or beyond optimal temperature. Fluctuations in temperature can affect microbial ecology and process parameters like pH and volatile fatty acids, leading to instability which reduces methane gas

yields. Temperature also directly controls the reaction rates of biomass hydrolysis, acidogenesis, and methanogenesis steps that generate biogas. This highlights the importance of the cooling tower in providing a foundation for stable and efficient biogas production in the palm oil industry. Methane yield is not as sensitive to POME feeding rate as microbial presence is linear to the amount of POME fed.

Hence, the ANN model proposed that the most optimal operating conditions would be the feeding POME at the rate of 503 m^3/day at 38.9 ˚C to promote the optimal biogas production rate and methane yield.

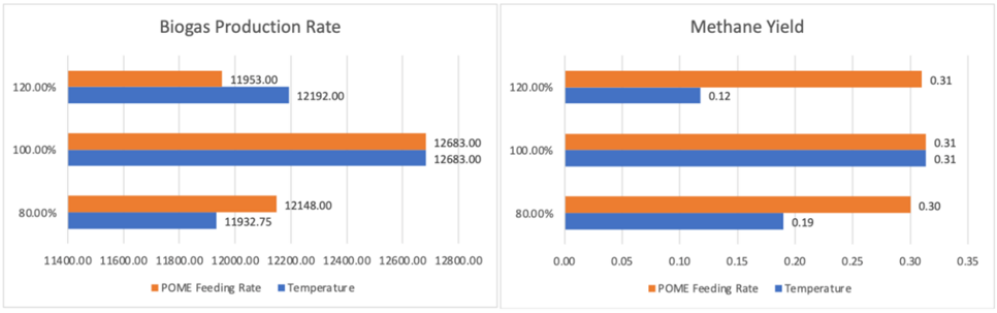

(a) (b)

Figure 4.34: Sensitivity analysis on input parameters to (a) biogas production rate (b) methaneyield

4.4.5.3 Parameter Comparison between Process Simulation and BGP A Data

Comparing between simulation results to real industrial values recorded in BGP A serves important purpose such as modelvalidation where this ensures the simulation accurately represents true physical systems before relying on predictions. This also builds credibility as correlation with plant data demonstrates model viability to end users for driving decisions. Hence, matching models to industrial data ensures actionable and responsible decision support (Mourtzis, 2020).

Figure 4.36 outlines the modified process flow diagram for biogas generation from POME as modeled in SuperPro Designer software. The updated arrangement incorporates consolidating the existing separate cooling pond and mixing tank units into a combined cooling tower system responsible for a more efficient heat removal duties. Visual mapping the interconnected equipment topology allows tracing mass, energy, and cost flows across the integrated biological, separation, and heat exchange steps. Comparing the redesigned flowsheet architecture versus traditional layout enables assessing infrastructure and operational changes and consider its cost-effective alternatives. Simulating the flowsheet with optimized variables and economics quantifies the system-wide impact beyond just individual unit efficiencies.

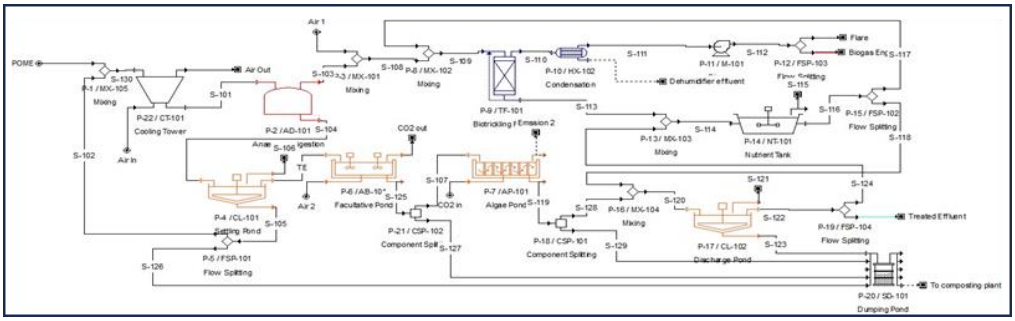

Figure 4.35: Simulation flowsheet for biogas production from pome with cooling tower

Based on Table 4.17, comparing simulation outputs to real industrial data indicates robust model performance and reliability. Across key system parameters, SuperPro predictions closely matched with historical data provided – meeting the performance target of less than 15% deviation. This low deviation demonstrates the simulated model suitability to accurately mirror real industrial size anaerobic digester and serve as a reliable virtual environment testing to guide better decisions.

Table 4.16: Summary of parameter performance between simulation and BGP A

Parameter	Units	Process Simulation	BGP A Data	Percentage Difference
POME Flowrate	m^3/day	500	449.3	10.1
CT Outlet Temperature	˚C	39.1	39.3	0.5
Biogas Flowrate	m^3/day	11,062.8	11,028.1	0.3
Methane Composition	%	61.3	64	4.2
COD Removal	%	97	87	10.3
Methane Yield	Nm^3/COD removed	0.28	0.3	6.7

4.4.6 Techno-Economic Analysis of Cooling Tower Application

Table 4.18 summarised the capital for equipment/process expenditure in Lepar Hilir for pretreatment of POME focusing on temperature control aspect. Transitioning from cooling pond and mixing tanks to an integrated cooling tower system reduced estimated capital expenditure on equipment 65%. Similarly, projected yearly maintenance overhead lowered by 67% with the upgraded configuration. The stark savings demonstrated substantial higher upfront affordability and lower sustaining cost offered through consolidation using cooling towers for waste heat removal and stable temperature control. Further validation of energy, water, andchemical costs would show a fuller picture of expense reduction opportunities. Hence, quantifying financial factors would thereby build a business case for proactively updating aging infrastructure with advanced heat exchanger equipment for enhanced profitability.

Table 4.17: Indicative CAPEX and OPEX for cooling Pond, mixing tank and cooling tower

Equipment	Estimated Equipment Price (RM)	Approximated Maintenance Price (RM)	Maintenance Justification
Cooling Pond	60k	100k/year	Desludging ponds everyyear
Mixing Tank	100k	15k/year	Mixer and coating in the tank
Cooling Tower	55k	20k/year	Cleaning works and mechanical or parts change

4.4.6.1 Capital and Operational Expenditure

Low CAPEX and OPEX of CT application offers a great economics return to the projects. Table 4.19 summarised the CAPEX and OPEX for CT application.

Table 4.18: CAPEX and OPEX of cooling tower application

No	Item	Unit Cost (RM/unit)	Amount	Cost (RM/year)
1	Capital Expenditure (CAPEX); Construction of CT facility			
	Industrial Cooling Tower	55,000	1	55,000
	Concrete tank and pump station	100,000	1	100,000
	Pumps (duty and standby unit)	12,000	2	24,000
	Supply and install of piping system	50,000	1	50,000
	Temperature indicator	500	2	1,000
	Mechanical and electrical	30,000	1	30,000
	TOTAL CAPEX			205,000
2	Operational Expenditure (OPEX)			
	CT cleaning (2 times a year)	15,000	1	15,000
	Scheduled Maintenance	5,000	1	5,000
	TOTAL OPEX			20,000

4.4.6.2 Potential Revenue with CT application

Based on simulation data, CT application is able to improve the biogas generation by 20% if the temperature control set at 38.9 ^{0}C with 503 m^3 of POME feeding on daily basis. This offers a great benefit to the FiT biogas plant developer to improve the economics of the project. Table 4.20 summarised the potential revenue of CT application.

Table 4.19: Potential revenue calculation with implementation of CT

No	Item	Unit	Value
1	Fresh fruit bunches (FFB) processed	ton/yr	200,000
2	Effluent generation factor (EGF)	m^3/TFFB	0.7
3	Total POME produced per year	m^3 POME/yr	140,000
4	POME COD	kg/m3	67
5	Total COD load	kgCOD/yr	9,380,000
6	COD removal (85%)	$kgCOD_{rem}$/yr	7,973,000
7	Methane yield	Nm^3 CH_4/ $kgCOD_{rem}$/yr	0.315
8	Total methane production- POME	Nm^3 CH_4/yr	2,511,495
9	Min methane concentration in biogas	%	60
10	Total biogas production per year	Nm^3 bg/yr	4,185,825
11	Additional biogas from CT application @ 20% extra biogas	Nm^3 bg/yr	837,165
12	Max 10% biogas use for internal consumption	Nm^3 bg/yr	83,717
13	Balance 90% biogas for power generation	Nm^3 bg/yr	753,449
14	Biogas electricity conversion	kW/Nm^3 bg	2.5
15	Total power production	kW/yr	1,883,621
16	Feed-in-Tariff (FiT) rate	RM/kW	0.4669
17	Revenue from CT application	RM/yr	879,463

4.4.6.3 Economic analysis indicator

Table 4.21 summarise all of the important indicators related to the optimization project using CT. The potential of this project is exceptionally good and outstanding based on the value recorded by the internal rate of return (IRR), return of investment (ROI) and project payback period. The economic analysis was conducted based on the remaining years of the Renewable Energy Power Purchase Agreement (REPPA), which is approximately 11 years. The period of this analysis is from 2024 to 2034. 2023 was reserved for the construction of the project.

Table 4.20: Economic analysis indicators for CT application

No	Item	Unit	Value
1	Capital expenditure (CAPEX)	RM	205,000
2	OPEX inflation rate	%	5
3	Revenue from CT application	RM/yr	879,463
4	Operation expenditure (OPEX)	RM/yr	20,000
5	Net profit from CT application	RM/yr	853,632
6	Project IRR	%	419%
7	ROI	%	4719%
8	Payback period	year	0.23

4.5 Six Months Operation Data Analysis of Decanter Cake Application

4.5.1 Analysis of Decanter Cake Characteristics

The palm oil mill process flow and technology, the kind or age of fruit, and the production process condition and climate heavily influence the quality of POME and DC. In this section, the characteristics of POME and DC are evaluated based on the effluent parameters, including pH, COD, TS, SS, and BOD, which are summarised in Table 4.22 and Table 4.23. The characteristics of DC are also compared to existing literature.

4.5.1.1 pH

One of the most critical feedstock characteristics for biogas production is the effluent pH. The average pH value obtained from POME was 4.80, while the average pH values for DC at different dilution factors were slightly more acidic. It was also discovered that the pH increases with increased DC dilution rates. DC diluted at a ratio of 1:20 has the highest pH of 4.34, whereas DC diluted at a ratio of 1:1 has the lowest pH of 4.07. Nonetheless, the pH values of DC at dilution ratios of 1:20, 1:10 and 1:5 are still within a range relative to the pH of POME, indicating that their addition as a feedstock to the anaerobic digester will not significantly alter

the operating pH. DC diluted at a ratio of 1:1, however, would be unsuitable for use as a co-substrate in the AD because of its very low pH, as it could potentially disrupt the anaerobic digestion process by inhibiting microbial growth. According to a literature study reported in Chapter 2, the reported pH in DC is around 5, which is higher than that of DC from Kilang Sawit Lepar Hilir. The optimum pH for AD is 6.8 to 7.2. Hence, the pH of the substrate must be increased and maintained during anaerobic digestion.

4.5.1.2 Chemical Oxygen Demand (COD)

COD is another critical parameter because it typically reflects the number of organics present in the effluent. COD has a huge potential for significantly enhancing methane gas production during anaerobic digestion. The COD of POME was found to be 66,900 mg/L. This value is similar to the average value of the past two years operation data. The average COD of diluted DC at ratios 1:20 and 1:10 were found to be 22,363 and 48,146 mg/L, respectively, which were much lower than POME. Meanwhile, the average COD of DC at dilution ratios 1:5 and 1:1 was found to be 86,385 and 132,428 mg/L, respectively, significantly higher than that of POME. Generally, a moderate COD content is found to be more favourable for the AD process as it contributes to the organic loading in the digester. All COD data obtained from these four dilution ratios were in a similar range to the literature study.

4.5.1.3 Total Solids (TS)

TS is a type of organic matter abundant in DC and usually contributes to an increase in BOD and COD content. In general, DC had much higher TS values compared to POME. The average TS present in POME was 25,580 mg/L, while the DC at dilution ratios 1:20, 1:10, 1:5, and 1:1 had average TS values of 18,223, 33,542, 48,319 and 60,474 mg/L, respectively. DC at a dilution ratio of 1:20 has the lowest TS due to the abundance of water added to the DC. In general, a higher TS would be more favourable for anaerobic digestion. However, high TS could also be contributed to the presence of indigestible content, which could inhibit the anaerobic digestion process. It is also important to note that a higher TS content in the effluent will require higher electricity usage for the pumps in the biogas plant to function effectively. The TS data from the dilution ratio of 1:20 and 1:10 is within a similar range to two years historical POME TS data recorded for Kilang Sawit Lepar Hilir.

4.5.1.4 Suspended Solids (SS)

SS is the amount of indigestible matter found in effluent. Out of all the dilution ratios, DC at a dilution ratio of 1:20 had the lowest SS of 8,474 mg/L, which was also much lower than the SS of 15,295 mg/L found in POME. The low SS found in 1:20 diluted DC was caused by the high amount of water used for dilution. DC with dilution ratios of 1:10, 1:5 and 1:1 had high SS values of 15,585, 29,108 and 45,088 mg/L respectively. Due to its indigestibility, the presence of SS in an effluent tends to reduce the efficacy of the AD process. It has the potential to produce scaling and clogging concerns in downstream equipment. It is much preferred that

the SS of the effluent is low, as it would improve the AD process and reduce wear and tear in biogas plant equipment. Regarding SS, ratio 1:20 and 1:10 is considered safe for AD operation.

4.5.1.5 Biological Oxygen Demand (BOD)

BOD is a measure of biodegradable organics in an effluent. It was found that the average values of BOD in DC were much lower than that of POME. The BOD of DC at dilution ratios 1:20, 1:10, 1:5 and 1:1 was measured at 8,417, 8,281, 8,421 and 8,006 mg/L respectively, whereas POME had a high BOD value of 27,264 mg/L. BOD levels can be detected when COD levels decrease throughout the anaerobic treatment process due to a slower decomposition rate by microbes. Hence, these parameters are considered not so important for this study. A high BOD content has a less significant effect on anaerobic digestion and biogas production.

Table 4.21: Characteristics of POME and diluted DC from Kilang Sawit Lepar Hilir

Characteristics	POME	DC A (1:20)	DC B (1:10)	DC C (1:5)	DC D (1:1)
pH	4.80	4.34	4.31	4.26	4.07
COD (mg/L)	66,900	22,363	48,146	86,385	132,428
TS (mg/L)	25,580	18,223	33,542	48,319	60,474
SS (mg/L)	15,295	8,474	15,585	29,108	45,088
BOD (mg/L)	27,264	8,417	8,281	8,421	8,006

Table 4.22: Characteristics of DC dilutions from Kilang Sawit Lepar Hilir

Characteristics	DC A (1:20)		DC B (1:10)		DC C (1:5)		DC D (1:1)	
	Diluted	Raw	Diluted	Raw	Diluted	Raw	Diluted	Raw
COD (mg/L)	22,363	447,267	48,146	481,458	86,385	431,923	127,800	127,800
TS (mg/L)	18,223	364,450	33,542	335,417	48,319	241,596	60,474	60,474
SS (mg/L)	8,474	169,483	15,585	155,854	29,108	145,539	45,088	45,088
VS (mg/L)	16,153	323,067	29,408	294,075	43,108	215,542	51,943	51,943
BOD (mg/L)	8,417	168,338	8,281	82,808	8,421	42,103	8,006	8,006

4.5.2 Analysis of Decanter Cake Dilutions

The diluted samples of DC, at ratios 1:20 (DC A), 1:10 (DC B), 1:5 (DC C), and 1:1 (DC D), were studied. It was found that the measurements of the raw characteristics for dilutions A, B and C are generally similar. Dilution D generated anomalous results as its raw characteristics had very different values despite being a dilution of the same raw DC, i.e., raw DC from the mill should have a COD value that ranges between 431,923 and 481,458 mg/L; however, DC D has a raw COD of 132,428 mg/L. The analysis can be concluded as an error due to a very thick dilution that might interrupt the

The 1:10 dilution ratio was applied to the biogas plant to study anaerobic digester performance and biogas quality. It can be seen that the dilution ratio of 1:10 is an ideal selection due to its moderate COD value and tolerable TS and pH value, which makes it applicable for the anaerobic digester. The overall reading obtained from this ratio is considered within a similar range of raw POME, which will possibly reduce the risk of anaerobic digester upset, process interruption and operation instability.

4.5.3 Performance of Anaerobic Co-digestion of POME with DC

A period of 6 months, from 1st July 2021 to 31st December 2021, was set to evaluate the AD's performance with an application of DC. Due to DC characteristics rich with solids and nutrients, the AD performance analysis focused on the biogas composition quality, AD bottom sludge condition, and biogas yield.

4.5.3.1 Bottom Sludge Quality

Fundamentally, DC has high COD and TS contents despite being diluted with treated effluent at a 1:10 ratio, as shown in Tables 4.22 and 4.23. There is a concern that adding DC for the co-digestion with POME may significantly increase the TS content in the digester, which may result in the accumulation of TS in the digester. Hence, the quality of the bottom sludge must be studied to provide information on the stability and condition of the anaerobic digester.

The TS content in the bottom sludge from co-digestion was found to be slightly higher than that of the bottom sludge from mono-digestion, as shown in Table 4.24. This is to be expected as DC is naturally rich in TS content. The slight increase in TS content in the bottom sludge may not be alarming, but it may cause TS accumulation if kept uncontrolled. Hence, it would be ideal for practicing frequent desludging in a controlled manner in the anaerobic digester to avoid sudden fluctuations in bottom sludge quality and maintain the effective digester volume.

Table 4.23: Bottom sludge quality from mono- and co-digestion

Bottom Sludge Quality	POME (2 years of historical data)	POME+DC	POME (3 months post DC and POME co-digestion
pH	7.15±0.09	7.11±0.04	7.10±0.02
COD (mg/L)	26,863±4,286	23,016±1,888	21,591±1,553
TS (mg/L)	23,616±5,328	24,292±1,729	22,256±1,636
SS (mg/L)	20,039±5,861	23,238±1,771	19,970±989

4.5.3.2 Biogas Composition

As seen from Table 4.25, it was found that mono-digestion generated a higher percentage of methane than co-digestion on average. However, this does not necessarily mean that mono-digestion produced a higher

methane yield. Additionally, the maximum methane percentage produced from mono-digestion was only 63.91% based on two years of historical data and 63.72% based on post-DC and POME co-digestion, whereas co-digestion generated 64.90%. It was also found that although the average H_2S generation rate in mono-digestion is lower, its maximum range is 1073 ppm, whereas the maximum range H_2S in co-digestion is 970 ppm. It is preferable that the percentage of H_2S in biogas is minimal as it is responsible for wear and tear in pipes caused by corrosion. Hence, the quality of biogas produced by co-digestion is arguably superior to that produced by mono-digestion.

Table 4.24: Biogas compositions from mono- and co-digestion

Biogas Component	POME (2 years of historical data)	POME+DC	POME (3 months post DC and POME co-digestion
CH_4 (%)	62.75±0.96	61.87±1.33	62.19±0.96
CO_2 (%)	33.32±1.48	32.02±1.40	32.23±1.03
O_2 (%)	0.41±0.08	0.44±0.11	0.46±0.09
H_2S (ppm)	654±280	785±84	749±87

4.5.3.3 Biogas Yield

During the month of July, co-digestion cumulatively yielded up to 377,517 m^3 of biogas, whereas mono-digestion would have theoretically yielded 314,247 m^3 of biogas, which is roughly a 20% increase. Almost similar trend was recorded in August, September and October 2021, which resulted of 25%, 23% and 16% increased respectively. During this period, decanter cake was fed almost consistently on daily basis at 10 m^3/day, with an average of 250 m^3/month. Then, in the subsequent months (November and December 2021) the decanter cake amount was reduced in the mill due to the maintenance and few occasions of machine

breakdown. Over the course of six months, from July to December as shown in Figure 4.37, the total cumulative biogas yield for co-digestion was 1,991,991 m^3, and theoretically 1,780,307 m^3 for mono-digestion, which is a 12% increase in biogas yield. Hence, it is clear that, under the different operational conditions and parameters, the co-digestion of DC with POME is capable of yielding more biogas in comparison to the mono-digestion of POME. Once the DC application was slowly reduced from November to December 2021 and completely stopped from January to March 2022, the potential biogas yield is reduced. As shown in Figure 4.38, the biogas production per m^3 of POME is reduced over a time from November to March 2022. This is also correlate with the amount of DC co-digested with POME. This shows that if more DC added into the AD, the potential biogas production is more, as shown in the month of July to October 2021. The data shows that without co-digestion of DC, the biogas yield is approximately 19 Nm^3 biogas/m^3 POME, which is within the similar range to the data recorded between June 2019 to July 2021.

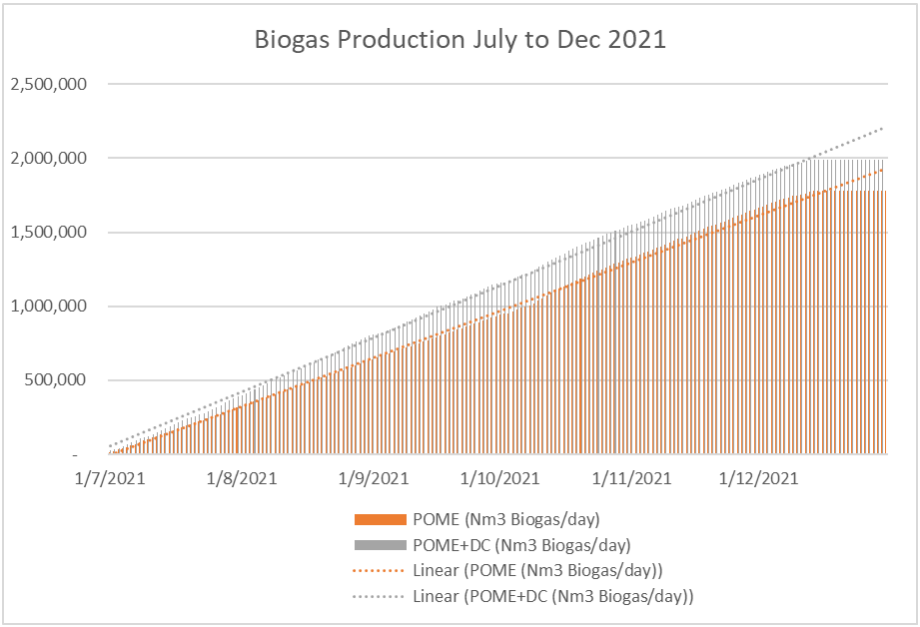

Figure 4.36: Chart of cumulative biogas yield over time

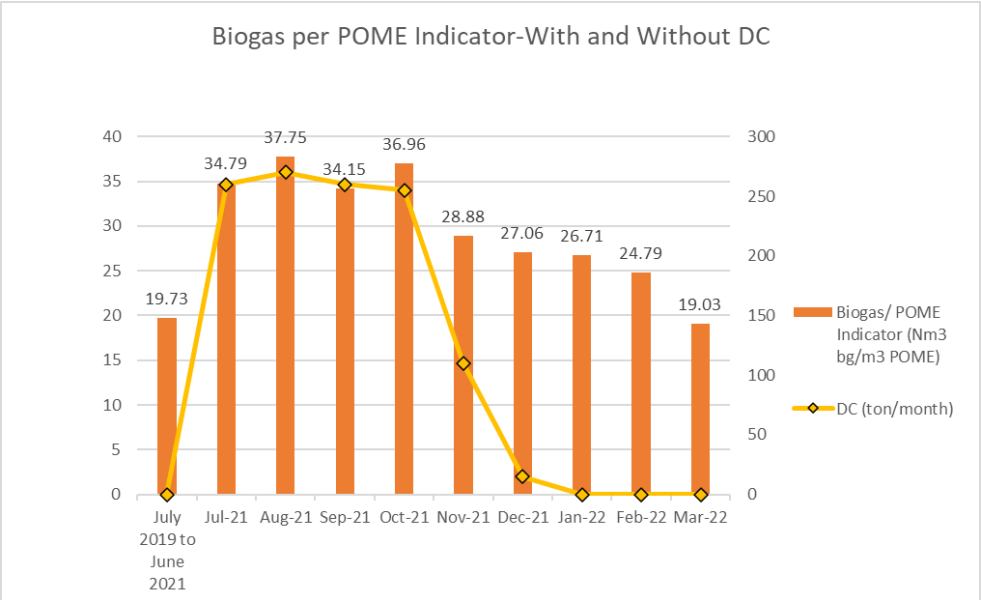

Figure 4.37: Biogas production indicator

4.5.4 Simulation Results

The simulation of anaerobic co-digestion of POME with DC is performed under continuous flow, steady-state conditions. The objective of running simulation is to investigate the viability and feasibility of DC as co-substrate in enhancing the biogas production while removing environmental contaminants and pollutants such as COD and BOD. The Monod kinetic model is used in the simulation, owing to its versatility in representing microbial growth kinetics and substrate utilization rates in complex biological systems. The empirical equation and rate of substrate utilization for Monod kinetic are shown in Table 4.26 respectively. In anaerobic co-digestion systems, microorganisms play a pivotal role in decomposing complex organic matter, therefore Monod model is applicable to describe substrate utilization by diverse microbial populations in POME and DC. It can effectively simulate how

microorganisms prioritize and utilize different substrates, aiding in understanding their interplay during anaerobic co-digestion.

Table 4.25: Equation for Monod kinetic and rate of substrate utilization

Equation	
Monod Equation	$\mu = \mu_{max} \frac{[S]}{K_s + [S]}$
Rate of Substrate Utilization	$r_s = \frac{\mu X}{Y}$

μ = Growth rate of a considered microorganisms
μ_{max} = Maximum growth rate of this microorganisms
$[S]$ = Concentration of the limiting substrate S for growth
K_s = Half velocity constant – the value of [S] when $\frac{\mu}{\mu_{max}} = 0.5$
X = Total biomass (since the specific growth rate, μ is normalized to the total biomass
Y = Yield Coefficient

The simulated based scenario yields a methane composition of 60.27%, which proved the accuracy of kinetic models, stoichiometry and coefficient, these aspects should be taken into consideration when comparing with the Lepar Hilir (BGP A) co-digestion data. The integrand simulation shows 14,474 m^3/day of biogas is produced, marked approximately 85% reduction in COD value with the methane yield of 0.348 Nm^3 CH_4/ kg COD_r. All these values are compared with the BGP A data, to prove the stability and feasibility of the anaerobic co-digestion process, a summary is provided in Table 4.27.

Table 4.26: Summary of ACoD performance in simulation scenario and industrial case

Parameter	**Simulation**	**BGP A Data**	**Percentage Differences (%)**
Flowrate of DC (m^3/day)	8.00	7.42	7.82
Flowrate of POME (m^3/day)	384.00	371.00	3.50
Flowrate of Biogas Produced (m^3/day)	14,474.12	11,874.98	21.88
Methane Composition (%)	60.27	62.19	1.92
COD Removal (%)	84.13	85[a]	0.87
Methane Yield (Nm^3 CH_4/ kg COD_r)	0.348	0.334	4.19
Bottom Sludge TS (mg/L)	10,699.60	23,889.03	55.19

a = Assumption made: COD removal of 85%.

The simulation-based scenario employed the dilution ratio of DC: Treated Effluent (TE) of 1:20 by considering the recycling ratio of TE, for instance 60% of TE is recycled to dilute DC. Conversely, the BGP A characteristics study of DC co-digestion has discovered the best dilution ratio is 1:10, to maximize the methane yield. Notably, only a small difference (4.19%) is spotted in methane yield, showing a positive result in long run. Percentage difference for each parameter is calculated and included Table 4.27, marked a huge difference in bottom sludge TS. While the COD removal has recorded 0.87% differences, as the BGP A co-digestion study has assumed 85% removal.

The bottom sludge TS for simulation case is 55.2% less than BGP A setting, owing to higher inoculum volume in the influent. As more sludge is recycled to dilute DC, high inoculum volume leads to enhanced microbial activity during ACoD process. Inoculum volume represents the initial microbial consortium introduced to the digester, which may significantly impact the microbial population establishment and activity, leading to different composition and characteristics for bottom sludge. A higher inoculum volume often leads to an increase in microbial activity, potentially accelerating the degradation of organic matter and subsequent conversion into biogas constituents (H. Zhang et al., 2023). This enhanced microbial activity might result in the production of bottom sludge with reduced TS content due to more efficient substrates utilization.

The divergence between the simulation and BGP A data might be due to the simplicity of the Monod kinetic model in SuperPro Designer v9.0. The

simulation potentially oversimplifies the intricate microbial interactions and substrate utilization dynamics inherent in co-digestion systems. Moreover, the critical factor of pH, pivotal in biogas production, remains unexamined and unfixed in the simulation. Optimal pH levels, typically between 6.8 to 7.2 for anaerobic co-digestion, are not determined in the simulation. In contrast, BGP A data analysis indicates a pH around 5 for both POME and diluted DC. Consequently, maintaining and elevating substrate pH during the process becomes crucial to prevent potential disruptions to anaerobic digestion by impeding microbial growth.

4.5.5 Optimisation of Anaerobic Co-digestion Process

Comparing the simulation-based scenario with BGP A data output at a 1:10 dilution ratio (as illustrated in Table 4.28), a higher biogas yield of 14,141.62 m^3/day is noted in the simulation, representing a 16% increase over BGP A production. However, the discrepancy could be attributed to the simplification of Monod kinetics in defining microbial activity and substrate utilization, as discussed in Section 0 above. Nonetheless, the simulation results demonstrate the potential for process optimization within industrial practices, in terms of enhancing microbial activities and substrates utilization while maintaining the optimal operating parameters for the ACoD process. Overall, the observed differences, all below 10%, affirm the stability and feasibility of the industrial process.

Table 4.27: Summary of ACoD performance with dilution ratio of DC: TE of 1:10

Parameter	Simulation	BGP A Data	Percentage Differences (%)
Flowrate of DC (m^3/day)	8.00	7.42	7.82
Flowrate of POME (m^3/day)	384.00	371.00	3.50
Flowrate of Biogas Produced (m^3/day)	14, 141.62	11, 874.98	16.03
Methane Composition (%)	60.72	62.19	1.47
COD Removal (%)	90.78	85[a]	5.78
Methane Yield (Nm^3 CH_4/ kg COD_r)	0.327	0.334	2.10
Bottom Sludge TS (mg/L)	21, 710. 33	23, 889.03	9.12

a = Assumption made: COD removal of 85%.

In the optimization stage, the chosen variable parameter revolves around the dilution ratio of DC: TE, specifically targeting the BGP A process's established ratio of 1:10 (DC:TE), in addition to POME flowrate as it has significant impact on OLR. OLR denotes the amount of organic matter fed into the digester within a specific volume or timeframe, thus POME as a substrate, different flowrates will fluctuate the OLR. SuperPro Designer v9.0 is utilized to investigate the effects of dilution ratio of DC: TE and POME flowrate on methane yield as well as the total solid content of bottom sludge. Whereas Design Expert Trial Version is employed to generate three-dimensional (3D) surface plots for better visualization of optimized results, using response surface methodology (RSM). Despite the compliance with environmental effluent discharge limits, the optimization phase also considers the trade-offs between capital costs, operations expenses and revenue.

Figure 4.39 illustrates the 3D response surface plot depicting methane yield concerning the TE/DC dilution ratio and the flow rate of POME. Higher methane yield aligns positively with variations in the TE/DC ratio

and POME flow rate, albeit this trend diminishes when the POME input flow rate rises, indicating a subsequent drop in ACoD performance. This decline is attributed to escalated volatile fatty acids (VFAs) levels in the digester, linked to increased Organic Loading Rate (OLR) due to higher substrate amounts. A response surface plot, as depicted in Figure 4.39, reinforces the significant interaction between OLR, TE/DC ratio, and methane yield, highlighting the highest methane yield (0.379 Nm^3 CH_4/ kg COD) at an OLR of 2.5 kg COD/m^3.day and a TE/DC ratio of 10. However, excessively high TE/DC ratios, while favouring microbial activity and efficient substrate utilization, may adversely impact ACoD process performance.

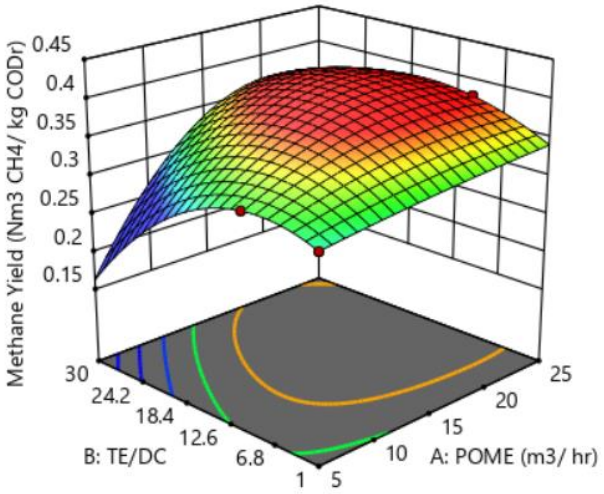

Figure 4.38: Response surface curve of methane yield with variable POME flowrate and TE/DC dilution ratios

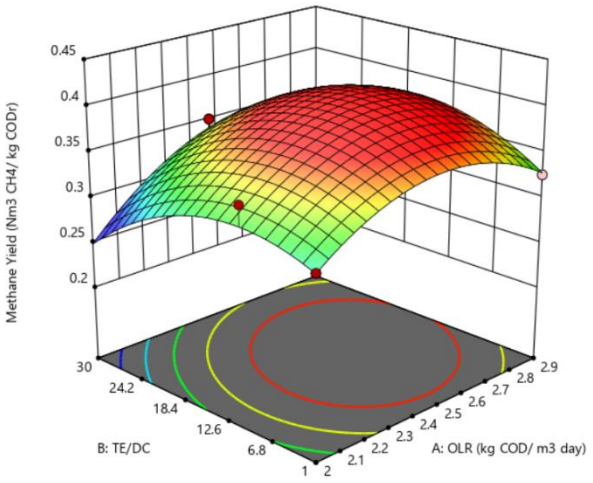

Figure 4.39: Response surface curve of methane yield with variable OLR and TE/DC dilution ratios

Additionally, Figure 4.40 and Figure 4.41 present surface and contour plots detailing the total solid content in bottom sludge, demonstrating a similar trend in both graphs. TE/DC ratios notably impact TS content, reaching the highest TS content (ranging between 15,000 to 19,000 mg/L) at a TE/DC ratio of 30. Excessive sludge might impede substrate utilization due to reduced availability of biodegradable organic matter, influencing the composition and characteristics of the bottom sludge. The lowest TS content (around 11,000 mg/L) is observed in Figure 4.41 at a TE/DC ratio of 20, while Figure 4.40 emphasizes that mono-digestion of POME exhibits the lowest TS content. Both the flow rate of POME and OLR have minimal influence on TS content.

Validation of the optimized data involves implementing the optimized conditions within the ACoD process at the biogas plant over six months to evaluate the efficacy of optimized parameters and the predicted performance accuracy. Assessment metrics such as percentage error

and standard deviation for each variable gauge the accuracy of the optimized model, deemed reliable if the deviation between predicted and experimental values remains below 10%.

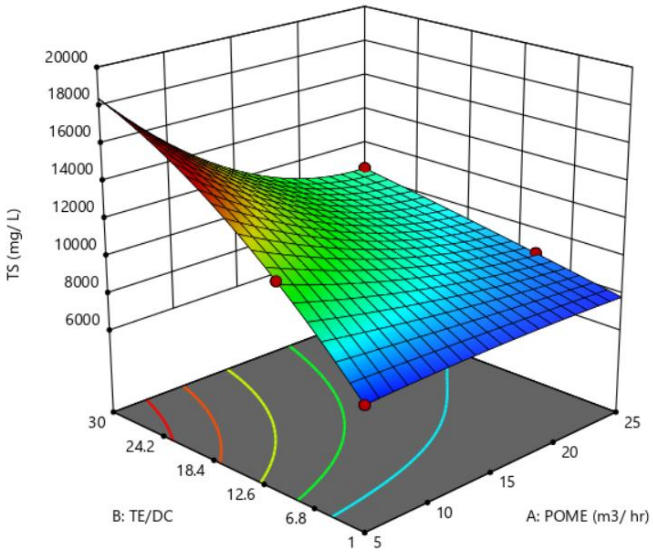

Figure 4.40: Response surface curve of TS content with variable POME flowrate and TE/DC dilution ratios

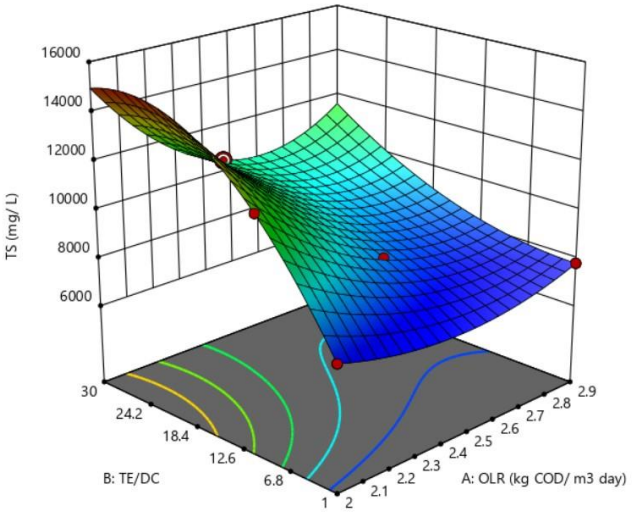

Figure 4.41: Response surface curve of TS content with variable OLR and TE/DC dilution ratios

4.5.6 Artificial Neural Network (ANN) of anaerobic co-digestion study

The ANN machine learning model finds extensive application in predicting biogas production from various substrates in anaerobic digestion (AD), as seen in previous studies involving cattle dung, bamboo dust, sugar-cane bagasse (Ghatak & Ghatak, 2018b), sawdust, and food waste samples (Gonçalves Neto et al., 2021). The regression model's representation in Figure 4.42 delineates distinct phases: training, testing, validation, and an overarching evaluation. These datasets undergo comprehensive assessment to derive two critical output parameters: methane yield and total solid content. The construction of the ANN model with dual output variables necessitates normalization of output values concerning the input variables. The input dataset comprises four crucial parameters: flowrate of DC, flowrate of POME, temperature, and organic loading rate (OLR).

Table 4.29 demonstrates the implementation of a feed-forward network utilizing the Levenberg-Marquardt algorithm to forecast the output variables. This network incorporates two hidden layers, each hosting 15 hidden neurons, alongside an output layer comprising two neurons representing the output variables. In the hidden layer, the '*tansig*' transfer function is applied using a sigmoid function, while the activation function is set as the linear function '*purelin*' (Chong et al., 2023). The four plotted figures in Figure 4.43 exhibit exceptional results with an R^2 value approximating 1, suggesting a robust linearity between the neural network model and the target values. Additionally, when utilizing

MATLAB for these predictions, the platform offers valuable tools and features within its neural network toolbox to optimize network architecture and performance for such predictive tasks.

Table 4.28: Summary of characteristics of neural network

Parameters	Description/ Value
Network Type	Feed-Forward Network (FFN)
Number of Input Layer Neurons	4
Number of Hidden Layer(s)	2
Number of Neurons per Hidden Layer	15
Number of Output Layer Neurons	2
Transfer Function	Tangent Sigmoid
Training Function	Training Levenberg-Marquardt
Performance Function	MSE
Learning Cycle (Epochs)	3

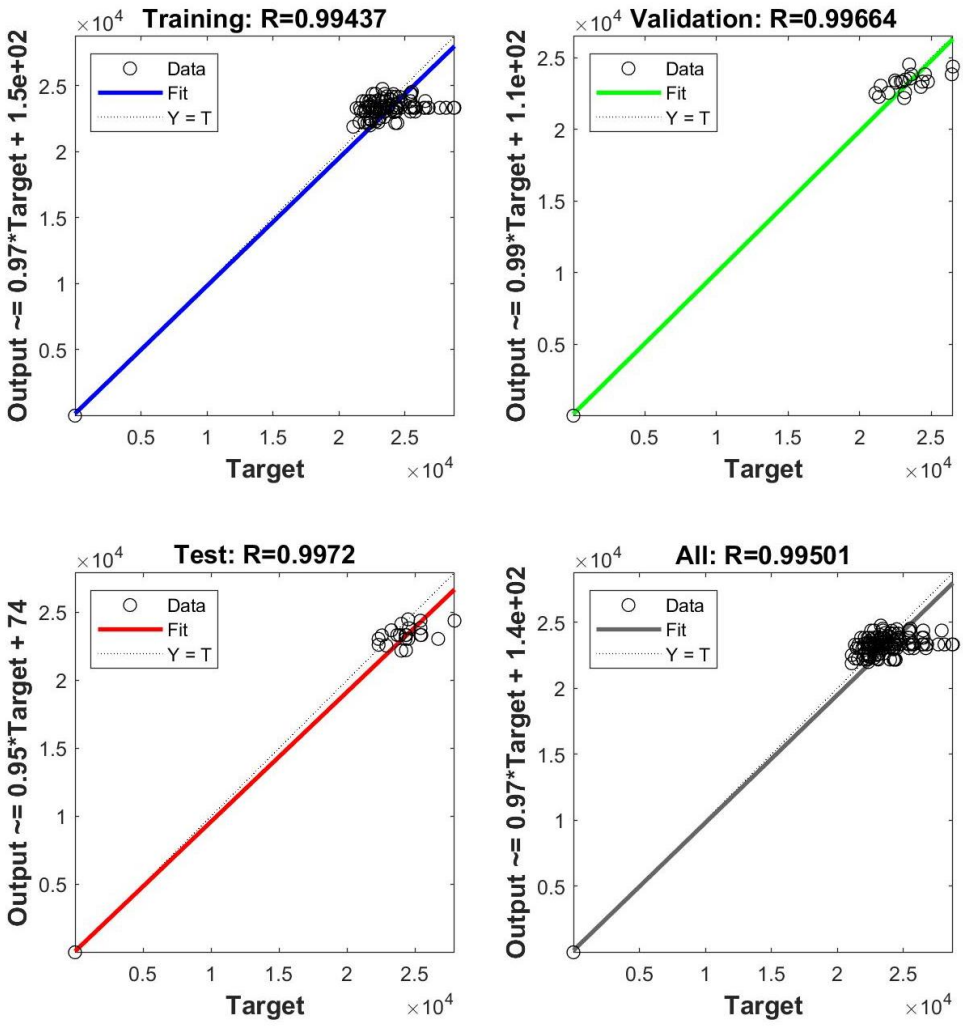

Figure 4.42: Regression analysis of neural network for distinct phases: training, validation, testing and overall phase

Figure 4.44 illustrates the error histogram of ANN model, utilizing 20 bins within the feed-forward neural network model. This visual representation outlines the quantitative differences between the expected values and the output values post-ANN construction. It's important to note that errors can be negative, indicating variations between predicted and actual values. Each bin in the histogram corresponds to a specific error value; for instance, a bin displaying an error value of 23.47 signifies that the training dataset requires around 100 to 120 instances to achieve a lower error. The zero-error line on the X-axis represents a zero-error value, positioned beneath the 23.47 bin in the histogram. Moreover, error histograms generated by neural networks in MATLAB offer insights into the distribution and magnitude of errors, aiding in understanding the model's performance and identifying areas for improvement.

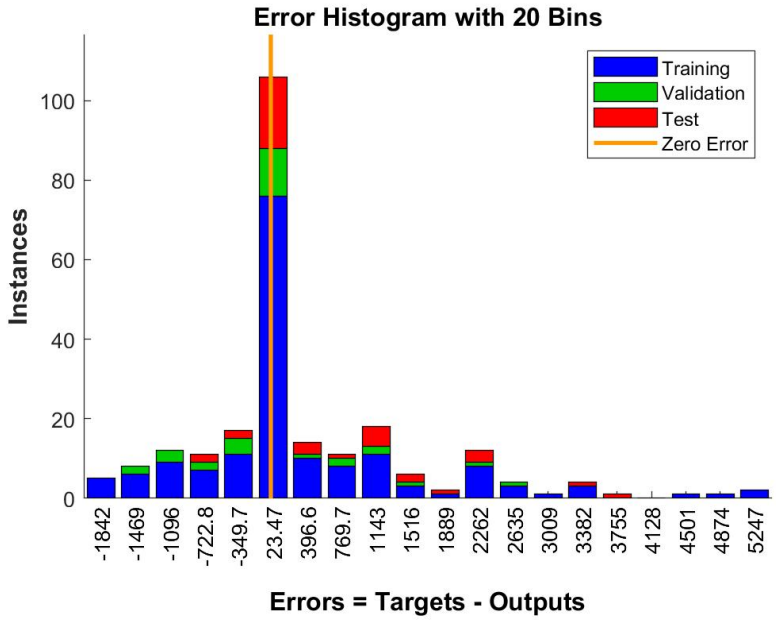

Figure 4.43: Error histogram of ANN model

In MATLAB 2020b, the Mean Squared Error (MSE) and the coefficient of determination (R^2) serve as essential metrics in assessing the accuracy and performance of neural networks model. MSE throughout the training, testing and validation stages of the ANN model is shown in Figure 4.45, in terms of epoch. MSE quantifies the average squared difference between predicted and actual output values. The model's optimization is guided by MSE, acting as an indicator alongside the coefficient of determination (R^2). In this context, the lowest MSE, seen at epoch 2 with a value of 856, 550.14 using the Levenberg-Marquardt algorithm during training, reflects better performance, signifying smaller errors in predictions. However, larger MSE values indicate substantial errors between calculated and actual outcomes. For instance, huge error might be occurring in this case, between the calculated and actual outcomes.

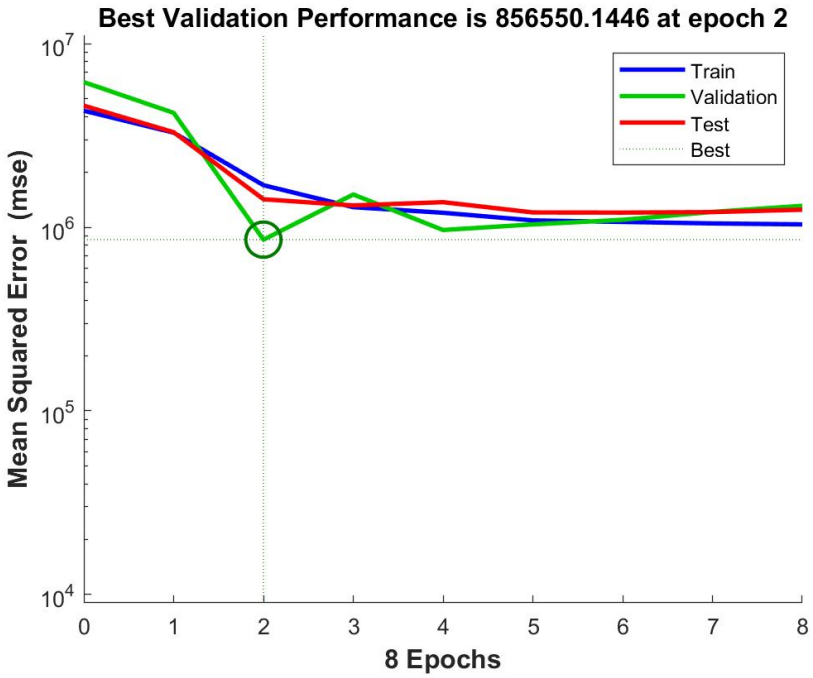

Figure 4.44: Performance graph of ANN model: MSE versus Epochs

The R^2 is elucidating the variance in observable parameters predicted from the independent variable (Chicco, J. Warrens, et al., 2021), typically, undergoes minimization during training via weight configurations in the ANN. Consequently, higher MSE in the testing and validation phases is observed in Figure 4.45. Despite this, the neural network model demonstrates strong predictive ability, reflected in high R^2 values across training, testing, and validation stages. Through 10 simulations, the model achieved optimal performance, showcasing lower MSE in the validation phase and high overall correlation (R^2), approximately equal to 1, indicating an accurate model and a close alignment between calculated and actual values.

4.5.7 Economic analysis of anaerobic co-digestion of DC with POME

The economic performance of anaerobic co-digestion with POME is evaluated to determine the project's financial and economic feasibility.

4.5.7.1 Capital and operational expenditure

The capital cost to build the DC dilution facility, including civil and structural works, purchase of equipment and instrumentation, and mechanical and electrical works, are obtained through a procurement exercise with the biogas plant owner, CGESB. The operational cost covered the salary of two operators, the cost of transporting DC from POM to the biogas plant, maintenance, and purchasing the DC from the mill. Table 4.20 summarises the capital expenditure (CAPEX) and operational expenditure (OPEX) of the anaerobic co-digestion project.

Table 4.29: CAPEX and OPEX of anaerobic co-digestion

No	Item	Unit Cost (RM/unit)	Amount	Cost (RM/year)
1	Capital Expenditure (CAPEX); Construction of DC dilution facility			
	Concrete tank and pump station	150,000	1	150,000
	Pumps (duty and standby unit)	12,000	2	24,000
	Mixer (duty and standby unit)	30,000	2	60,000
	Supply and install of piping system	50,000	1	50,000
	Effluent flowmeter	8,000	1	8,000
	Pressure gauge	500	2	1,000
	Temperature indicator	500	2	1,000
	Mechanical and Electrical	50,000	1	50,000
	TOTAL CAPEX			344,000
2	Operational Expenditure (OPEX)-based on 85% biogas plant uptime			
	Workers (26 days a month, 12 months)	200	312	62,400
	Transport (RM150/trip, 2 trips per day (5 tons lorry), 312 days a year)	300	312	93,600
	Maintenance	15,000	1	15,000
	Purchase of DC (RM20/ton, 10 tons/day)	200	312	62,400
	TOTAL OPEX			233,400

4.5.7.2 Potential Revenue from anaerobic co-digestion of DC with POME

The potential revenue was calculated based on the findings from the study conducted and summarised in Table 4.31 below. The DC co-digestion with POME potentially increases the biogas production with an average of 20% compared to mono digestion. Lepar Hilir Biogas Plant was constructed for power generation and electricity sales to Tenaga Nasional Berhad. The Feed-in-Tariff (FiT) approved based on the certificate signed by the Sustainable Energy Development Authority (SEDA) Malaysia is at RM0.4669/kWh. CGESB obtained this approval for 16 years, from 2019 to 2034. Based on the plant's biogas engine performance data, the biogas engine's electricity conversion rate is at 2.5 kW/Nm^3 biogas. Table 4.31 summarises all of the data to calculate the potential revenue. In one year, with the addition of 10 m^3 of DC for 310

days (85% plant uptime), the potential income that can be obtained is RM879,463.

Table 4.30: Potential revenue calculation with co-digestion of DC

No	Item	Unit	Value
1	Fresh fruit bunches (FFB) processed	ton/yr	200,000
2	Effluent generation factor (EGF)	m^3/TFFB	0.7
3	Total POME produced per year	m^3 POME/yr	140,000
4	POME COD	kg/m^3	67
5	Total COD load	kgCOD/yr	9,380,000
6	COD removal (85%)	$kgCOD_{rem}$/yr	7,973,000
7	Methane yield	Nm^3 CH_4/ $kgCOD_{rem}$/yr	0.315
8	Total methane production- POME	Nm^3 CH_4/yr	2,511,495
9	Min methane concentration in biogas	%	60
10	Total biogas production per year	Nm^3 bg/yr	4,185,825
11	Additional biogas from DC co-digestion @ 20% extra biogas	Nm^3 bg/yr	837,165
12	Max 10% biogas use for internal consumption	Nm^3 bg/yr	83,717
13	Balance 90% biogas for power generation	Nm^3 bg/yr	753,449
14	Biogas electricity conversion	kW/Nm^3 bg	2.5
15	Total power production	kW/yr	1,883,621
16	Feed-in-Tariff (FiT) rate	RM/kW	0.4669
17	Revenue from DC co-digestion	RM/yr	879,463

4.5.7.3 Economic Analysis Indicator

Table 4.32 summarise all of the important indicators related to the anaerobic co-digestion of DC with the POME project. The potential of this project is exceptionally good and outstanding based on the value recorded by the internal rate of return (IRR), return of investment (ROI) and project payback period. The economic analysis was conducted based on the remaining years of the Renewable Energy Power Purchase Agreement (REPPA), which is approximately 11 years. The period of this analysis is from 2024 to 2034. 2023 is reserved for the construction of the project.

Table 4.31: Potential revenue calculation

No	Item	Unit	Value
1	Capital expenditure (CAPEX)	RM	344,000
2	OPEX inflation rate	%	5
3	Revenue from DC co-digestion	RM/yr	879,462
4	Operation expenditure (OPEX)	RM/yr	233,400
5	Project IRR	%	186%
6	ROI	%	2812%
7	Payback period	year	0.4

CHAPTER FIVE

CONCLUSIONS AND RECOMMENDATIONS

5.1 Conclusions

In the present research, the palm oil mill profiling and two years in-ground lagoon anaerobic digester performance has been discussed in details. Critical parameters affected biogas generation and quality, and it is relationship to the POME characteristic derived from different processes philosophy in the palm oil mill has been investigated. All of these aspects contributed and affected the income generation for CGESB FIT biogas plants. Two major optimisation plans were introduced in Lepar Hilir Biogas Plant to investigate their effectiveness improving the economics aspect of the biogas plants, which subsequently can be replicated into CGESB existing and new biogas plants in near future. The findings from this research not only benefited CGESB, but to all FiT Biogas Plant Developers in Malaysia.

1. Optimizing the process flow of POMs is essential in enhancing POME characteristics as a valuable bio-energy source. Based on the collected data in this research, it was found that the highest polluting strength of POME is generated from the POM that adopted the conventional process and technology. To meet environmental, social, and governance (ESG) criteria, a more sustainable milling process can be developed by altering the existing process flow and utilizing the latest technologies.

However, this is not in favour to the FiT Biogas Plant Developer objective.

a) The methane yield for POM A, B, C, and D were found to be 0.221, 0.25, 0.246, and 0.237 Nm^3 CH_4/kg COD removed, respectively. The lower methane yield observed in Plant A is attributed to the usage of a three-phase decanter in the milling process, which results in a lower TS and COD content in the POME. This lower TS and COD content have limited the amount of substrate available for the methanogens, leading to a lower methane yield.
b) Steriliser condensate discharged directly to the sludge pit or cooling pond will produce higher COD content in POME than the condensate recycled through the clarification tank before discharging to the sludge pit or cooling pond.
c) POM equipped with combined sludge treatment facilities (using a three-phase decanter and sludge separator) after the palm fruit digester will significantly reduce the TS content of POME. This in turn led to a reduction in COD content in the POME, since the TS and COD are directly correlated.
d) EFB juice produced from the EFB plant will significantly increase the COD content of POME. Additionally, hydro cyclone effluent produced from fiber and nut cracking plants must be diverted from the POME line because it will dilute and reduce the COD content.
e) High water usage in the palm oil mill processes will greatly reduce the COD content in POME.

2. Two years in-ground lagoon anaerobic digester performances study give a valuable insight in understanding the factors affected its performances.

   a) BGP B plant has achieved the highest COD removal as well as the biogas production rate of 1.21 X 10^6 kg COD_{in}/month and 4.12 X 10^5 Nm^3/month with a corresponding methane yield of 0.28 Nm^3 CH_4/kg $COD_{removed}$ respectively. This is supported by the Box Plot analysis where BGP B demonstrated good stability in terms of biogas production as compared to BGP A, C and D.

   b) The highest average composition of methane (62.75%) in biogas is obtained in BGP A, which the inlet pH and temperature fluctuation into its AD is the lowest compared to other BGP's. Although BGP D has the highest HRT, it produced the lowest average amount of biogas during the analysis period (272,378.5 Nm^3/month) due to the unstable performance of the digester and fluctuating temperature and pH of raw POME.

   c) The low percentage of COD removals (69.9% – 84.8%) in BGP D is responsible for the low methane yield, which is reflected in the high COD levels in the effluent. Inefficient pretreatment processes contributed to this issue.

   d) All in-ground lagoon anaerobic digesters operated below its designed OLR value (2.1 kg COD_{in}/m^3 day). The fluctuation of OLR input to the digester because of the inconsistency of daily POME produced by each POMs resulted fluctuation of daily

biogas production volume, which in general affected income generation of the biogas plant.

e) Existing pretreatment facilities (combination of cooling pond and mixing tank with recirculation effluent) failed to provide the best solution and ecosystem to optimise AD performances. Both facilities were not able to control, stabilise and provide consistent temperature of POME entering the AD.

f) Two years data analysis concluded that three critical parameters affected the AD performances which are OLR, temperature and recirculation ratio. The performances of four different biogas plants are successfully optimised with a high methane yield of 0.655 $mLCH_4/gVS$. The optimised values of OLR, temperature and recirculation ratio for BGP A, B, C, and D are in the ranges of 1.49-1.64 kg COD_{in}/m^3.day, 37.7 – 40.0 ℃, and 1.0 – 2.08 respectively. This indicates that moderate OLR (<1.6), moderate T (<44°C), and moderate RR (<2.3) are required to achieve optimum COD removal and biogas production.

g) Sensitivity analysis reveals that BGP A, B, and C show a similar trend of sensitivity (OLR>Temperature>RR). Conversely, BGP D is more sensitive to the temperature which is mainly due to its smaller cooling pond size which results in lower cooling efficiency.

3. The implementation of a cooling tower for regulating the temperature of raw palm oil mill effluent (POME) has demonstrated remarkable efficiency. The improvement on biogas

quality and potential in producing more biogas will surely benefit biogas plant developer.

a) This temperature control strategy not only resulted in higher biogas production rates (12,683 m^3/day) but also enhanced methane yield (0.31 Nm^3/kg $COD_{removed}$) by 40%.
b) Employing Artificial Neural Networks (ANN) added a predictive dimension to this study, enabling the effective prediction of cooling tower's performance. This predictive modelling aimed at achieving an optimum outlet temperature at 38.9 ˚C conducive to maximizing both biogas production rates and methane yield was proven with a high R^2 value of 0.9732 and a low MSE value of 0.2096.
c) Simulated data consistently matched BGP A's values within an acceptable 15% margin of deviation between prediction and reality. Sensitivity analysis was also carried out which proved that temperature played a significant role in affecting methane yield.
d) An increase of biogas production through optimisation strategy by 20% offers additional revenue of approximately RM890,000 per year for BGP A. This optimisation project resulted a very promising economics return with a payback period of less than a year. Hence, to incorporate the cooling tower into the AD design will surely benefit the plant owner.
e) Cooling tower is the better option for pretreatment compared to conventional cooling pond, and combination of mixing tank and recirculation effluent method.

4. The investigation into anaerobic co-digestion (ACoD) of palm oil decanter cake and POME presents a promising pathway towards sustainable energy production and environmental stewardship. Leveraging the organic richness of these residues demonstrates a substantial potential to generate biogas efficiently.

a) From July to October 2021, DC was consistently fed at 10 m^3/day, resulting in an average of 250 m^3/month and yielding very promising results, with an average increase in biogas of 20% compared to mono digestion. However, during the final two months (November and December), the feeding of DC was interrupted, leading to a decline in overall performance. Over the course of a six-month trial period, there was an approximate 12% increase in the total biogas produced.

b) DC with dilution rates of 1:10 and 1:20 are viable options for feeding into the AD and for co-digestion purposes. According to data from BGP A plant, a dilution ratio of 1:10 was consistently applied to the AD throughout the entire six-month period. However, for simulation purposes, a dilution ratio of 1:20 was utilized and demonstrated results that were approximately similar, with a methane yield variance of only 4.19%. This signalling further process optimisation can be done.

c) Optimized parameters indicate that a TE/DC ratio of 10 and a POME flowrate of 25 m^3/hour result in the highest methane content. However, the total solid content in the bottom sludge is significantly affected by the TE/DC dilution ratio. The lowest total

solid content is approximately 11,000 mg/L, observed at a TE/DC ratio of 20. Total solids increase proportionally with the amount of DC fed into the AD. This represents one of the operational risks that must be carefully managed.

d) If based on 4 months data, where the DC was consistently fed into the AD, 20% more biogas can be produced. This will bring additional income to the biogas plant by RM 879,000 per year. The payback period is less than a year.

5.2 Recommendations

1. To maintain a sustainable and profitable biogas plant with minimal operational problems such as over-acidification, in-active sludge accumulation and low biogas production, POME should have the following characteristics as shown in Table 5.1.

Table 5.1: Desirable POME characteristics for maximum biogas generation

No	Parameters	Polluting Strength	Range	Ways to achieve
1	COD	Moderate	60,000-85,000 mg/L	a) Water: FFB ratio below 1.2 m^3/TFFB b) Use a single sludge treatment facility (either sludge separator or three-phase decanter). It is recommended to use sludge separators instead of the three-phase decanter to maintain high COD and BOD c) Reduce water usage for cleaning and flushing the equipment in the POM d) Maximize the operation of the EFB plant to produce as much as possible of EFB pressed juice
2	BOD	Moderate	30,000-42,000 mg/L	
3	TSS	Moderate	19,000 - 27,000 mg/L	a) All type of steriliser is suitable to be used. However, CS is the most recommended due to its performance b) It is recommended to use a sludge separator to maintain a moderate total solid amount

				c) To check the clarifier system's performance and the overflow and underflow quality more frequently. A sampling at least twice a month d) To ensure the sludge separator and/or three-phase decanter operates efficiently e) To train and monitor the operator's work quality over the time
4	Oil & Grease	Minimum	<3,500 mg/L	a) All type of steriliser is suitable to be used. However, CCS is the most recommended due to the lowest O&G result b) To check the clarifier system's performance and the overflow and underflow quality more frequently. A sampling at least twice a month c) To ensure the sludge separator and/or three-phase decanter operates efficiently

2. The two years performance study and analysis data can be further improved by using different machine learning activities and analyses methods. Larger sets of data are essential for predictive analysis and mathematical model development.

   a) Due to the dependency on the quality and flow rate of raw POME inlet affecting the anaerobic performance of palm oil mills, the incoming capacity of POME is often irregular due to the harvest season of the FFB. Therefore, there are uncertainties which affect the generation prediction model using the plants' historical data. In addition, since the performance monitoring is conducted monthly, any spike would not be captured in the data as it only reflects the mean operating conditions during the uptime of the mill. This would reduce the prediction range as the process parameters are only controlled in a certain desirable range.

b) The low R^2 values would also cause several complications when estimating the biogas and COD removal. Moreover, the design models implemented for the study are reduced quadratic models. This is because there is insufficient data to represent the prediction model to a higher order polynomial equation. In addition, the development of mathematical model from the given number of datasets are surreal (Ng et al., 2020). This is because most responses could not be defined using polynomial equations and the development of polynomial model without validation steps are generally unreliable.

c) Prediction models could be applied to accurately estimate the anaerobic performance of the biogas plant. Supervised machine learning models such as Support Vector Regression (SVR), Adaptive Neuro-Fuzzy Inference System (ANFIS), and Artificial Neural Network (ANN) can be employed in this scenario. SVR has the capability to minimise prediction errors by assuming the shortest distance between the actual and estimated output values (Martín et al., 2020). It is particularly suitable in this historical dataset as statistical evaluation witnesses a high MAE and RMSE for both reduced order quadratic output models.

d) ANN machine learning model has been extensively employed in the prediction of biogas using different types of substrates (Ghatak & Ghatak, 2018c). Furthermore, the application of ANN machine learning model in biogas prediction has been further improved by coupling optimisation algorithms such as Genetic Algorithm and

Particle Swarm Optimisation. This approach can troubleshoot various complex mathematical modelling that requires huge computational operations (W. Zhang et al., 2018) . ANN modelling could be implemented since the anaerobic digestion exhibit several complex reactions such as hydrolysis, acidogenesis, acetogenesis and methanogenesis. Similarly, ANFIS has been adopted in the palm oil mill industry to study the effect of pH, COD, TTS and methane composition (Tan et al., 2018b) . Literature findings support the usage of ANFIS as it had successfully maximised the biogas production from AD after optimising the input process parameters (Zareei & Khodaei, 2017b).

3. Cooling tower optimisation study can be improved by few approaches as below:

   a) A longer study period is required to assess how various weather conditions affect the cooling process of raw POME. Given that the proposed cooling tower is the cross flow induced draft type, the ambient temperature significantly influences its efficiency.
   b) More precise data is necessary to assess the effect of temperature control through cooling tower implementation on biogas production. Since the time gap between the study involving decanter cake and the cooling tower is less than a month, there's a possibility that the performance data from January 2022 may not accurately serve as a basis for evaluating the overall impact of the cooling tower application.

c) It is essential to test the AD using simulated data to ascertain its real impact on AD performance. Subsequently, a comparison between the simulation output and industrial AD data can be conducted.

4. The inclusion of DC and POME as feedstocks introduces varied compositions, leading to diverse qualities in the feedstock. Such dynamic characteristics, encompassing fluctuating nutrient content and potential contaminants, pose challenges to the stability and efficiency of the ACoD process by potentially hindering microbial activity and biogas production. Consequently, maintaining optimal process parameters becomes notably challenging due to these factors.

a) This study was exclusively designed to assess the suitability of DC for application in industrial-scale AD. Although the results are promising, further investigation is necessary, particularly through trials involving various DC organic loading rates (OLR) into the AD. Such studies would provide a comprehensive understanding of co-digestion across the entire spectrum.

b) Developing a feeding formulation for DC based on daily or weekly POME feeding rates is feasible. This method would maintain consistent operation of the AD at optimal OLR. Assessing the effects of this operational strategy on AD performance is essential for gaining deeper insights and optimizing its functionality.

c) Utilizing a simulation model using SuperPro Designer v9.0 to forecast biogas production and methane yield might be limited by

the Monod kinetic model's simplicity. This model assumes a simplistic growth rate response, solely based on substrate concentration, oversimplifies intricate interactions within microbial communities.

d) Artificial Neural Network (ANN) models, although powerful predictors, often operate as 'black-box' models, which complicates understanding the learned relationships between inputs and outputs. Reliance on data quality and quantity makes them susceptible to inaccuracies if industrial data inadequacies exist, potentially leading to overfitting or data extrapolation issues and requiring extensive datasets for accurate predictions. In this case, only 6 months data is available for the ANN model, thus larger datasets, in which 1 to 2 years industrial data are required for accurate predictions.

5. During this study, enhancing the efficiency of AD performance hinges on effectively managing the daily operations of the biogas plant. Consequently, a recommendation for both the developer and owner of the biogas plant is outlined in Appendix 5. This document elucidates crucial operational parameters and provides guidelines for process monitoring for the biogas plant operation team.

REFERENCES

Decanters | Alfa Laval. (n.d.). Retrieved May 10, 2022, from https://www.alfalaval.my/products/separation/centrifugal-separators/decanters/

Scale and Fouling Control in Cooling Tower Systems – Water Technology Report. (n.d.).

A Aziz, M. M., Kassim, K. A., ElSergany, M., Anuar, S., Jorat, M. E., Yaacob, H., Ahsan, A., Imteaz, M. A., & Arifuzzaman. (2020). Recent advances on palm oil mill effluent (POME) pretreatment and anaerobic reactor for sustainable biogas production. In *Renewable and Sustainable Energy Reviews* (Vol. 119). Elsevier Ltd. https://doi.org/10.1016/j.rser.2019.109603

A., B. J., E., B. C., & J., B. M. (1975). *SOME ASPECTS OF SEDIMENTATION POND DESIGN USDA-ARS, Western Region* (pp. 117–121).

Abdeen, F. R. H., Mel, M., Jami, M. S., Ihsan, S. I., Ismail, A. F., Abdeen, F. R. H., Mel, M., Jami, M. S., Ihsan, S. I., & Ismail, A. F. (2016). A review of chemical absorption of carbon dioxide for biogas upgrading. 中国化学工程学报, *24*(6), 693–702. https://doi.org/10.1016/J.CJCHE.2016.05.006

Abdulkareem, H. A., Tanimu, M. A., Muhammad, I. T., & Suleiman, S. M. (2015). Design of a Settling Basin for Small Scale Water Treatment Plant in Borno State, Nigeria. *American Journal of Engineering Research (AJER)*, *4*(9), 35–39. www.ajer.org

Abdullah, N., & Sulaiman, F. (2013). The Oil Palm Wastes in Malaysia. *Biomass Now - Sustainable Growth and Use*. https://doi.org/10.5772/55302

Abdulsalam, M., Man, H. C., Idris, A. I., Yunos, K. F., & Abidin, Z. Z. (2018). Treatment of Palm Oil Mill Effluent Using Membrane Bioreactor: Novel Processes and Their Major Drawbacks. *Water 2018, Vol. 10, Page 1165*, *10*(9), 1165. https://doi.org/10.3390/W10091165

Abdurahman, N. H., Rosli, Y. M., & Azhari, N. H. (2013). The Performance Evaluation of Anaerobic Methods for Palm Oil Mill Effluent (POME) Treatment: A Review. *International Perspectives on Water Quality Management and Pollutant Control*. https://doi.org/10.5772/54331

Abis, K. L., & Mara, D. D. (2005). Primary facultative ponds in the UK: The effect of operational parameters on performance and algal

populations. *Water Science and Technology*, *51*(12), 61–67. https://doi.org/10.2166/wst.2005.0427

Adela Bukhari, N., & Kheang Loh, S. (2013). Characteristics of palm oil mill effluent (Pome) in an anaerobic biogas digester PILOT SCALE BIOCHAR PRODUCTION FROM PALM KERNEL SHELL (PKS) IN A FIXED BED ALLOTHERMAL REACTOR View project bioethanol View project Muzzammil Ngatiman Malaysian Palm Oil Board Malaysian Palm Oil Board. In *Article in Asian Journal of Microbiology*. https://www.researchgate.net/publication/270763229

Adnan, A. I., Ong, M. Y., Nomanbhay, S., Chew, K. W., & Show, P. L. (2019). Technologies for Biogas Upgrading to Biomethane: A Review. *Bioengineering (Basel, Switzerland)*, *6*(4). https://doi.org/10.3390/BIOENGINEERING6040092

Ahmed, Y., Yaakob, Z., Akhtar, P., & Sopian, K. (2015). Production of biogas and performance evaluation of existing treatment processes in palm oil mill effluent (POME). In *Renewable and Sustainable Energy Reviews* (Vol. 42, pp. 1260–1278). Elsevier Ltd. https://doi.org/10.1016/j.rser.2014.10.073

Akhbari, A., Kutty, P. K., Chuen, O. C., & Ibrahim, S. (2020). A study of palm oil mill processing and environmental assessment of palm oil mill effluent treatment. *Environmental Engineering Research*, *25*(2), 212–221. https://doi.org/10.4491/EER.2018.452

Alepu, O. E., Li, Z., Odion Ikhumhen, H., Kalakodio, L., Wang, K., & Segun, G. A. (2016). *Effect of Hydraulic Retention Time on Anaerobic Digestion of Xiao Jiahe Municipal Sludge*. https://doi.org/10.4172/2252-5211.1000231

Alexiou, G. E., & Mara, D. D. (2003). Anaerobic waste stabilization ponds. *Applied Biochemistry and Biotechnology 2003 109:1*, *109*(1), 241–252. https://doi.org/10.1385/ABAB:109:1-3:241

Alhaji, M. H., Sanaullah, K., Lim, S. F., Khan, A., Hipolito, C. N., Abdullah, M. O., Bhawani, S. A., & Jamil, T. (2016). Photocatalytic treatment technology for palm oil mill effluent (POME) - A review. In *Process Safety and Environmental Protection* (Vol. 102, pp. 673–686). Institution of Chemical Engineers. https://doi.org/10.1016/j.psep.2016.05.020

Ali Shah, F., Mahmood, Q., Maroof Shah, M., Pervez, A., & Ahmad Asad, S. (2014). Microbial ecology of anaerobic digesters: The key players of anaerobiosis. *The Scientific World Journal*, *2014*. https://doi.org/10.1155/2014/183752

American Society of Heating, R. and A.-C. E., & American Society of Heating, R. and A.-C. E. (n.d.). *2020 ASHRAE handbook : heating, ventilating, and air-conditioning systems and equipment*.

Anderson, R. M., & Tullis, B. P. (2012). Comparison of Piano Key and Rectangular Labyrinth Weir Hydraulics. *Journal of Hydraulic Engineering*, *138*(4), 358–361. https://doi.org/10.1061/(asce)hy.1943-7900.0000509

Andrew, J., Sulaiman, A., Fairuz, K., & Busu, Z. (2017). Oil Loss in Palm Biomass Using Continuous Sterilizers, Conventional, and Compact Modular Concept: a Case Study for Felda Palm Oil Mills. *Solid State Science and Technology*, *25*(2), 118–127. http://myjms.moe.gov.my/index.php/masshp/article/view/3379

Anlauf, H. (2007). Recent developments in centrifuge technology. *Separation and Purification Technology*, *58*(2), 242–246. https://doi.org/https://doi.org/10.1016/j.seppur.2007.05.012

Appels, L., Baeyens, J., Degrève, J., & Dewil, R. (2008). Principles and potential of the anaerobic digestion of waste-activated sludge. *Progress in Energy and Combustion Science*, *34*(6), 755–781. https://doi.org/10.1016/J.PECS.2008.06.002

Ariunbaatar, J., Panico, A., Esposito, G., Pirozzi, F., & Lens, P. N. L. (2014). Pretreatment methods to enhance anaerobic digestion of organic solid waste. *Applied Energy*, *123*, 143–156. https://doi.org/10.1016/J.APENERGY.2014.02.035

Asgharzadeh, H., Firoozabadi, B., & Afshin, H. (2011). Experimental investigation of effects of baffle configurations on the performance of a secondary sedimentation tank. *Scientia Iranica*, *18*(4 B), 938–949. https://doi.org/10.1016/j.scient.2011.07.005

Awalludin, M. F., Sulaiman, O., Hashim, R., & Nadhari, W. N. A. W. (2015). An overview of the oil palm industry in Malaysia and its waste utilization through thermochemical conversion, specifically via liquefaction. *Renewable and Sustainable Energy Reviews*, *50*, 1469–1484. https://doi.org/10.1016/J.RSER.2015.05.085

Aznury, M., Amin, J. M., Hasan, A., -, al, Purnomo, A., Romli, M., Trisakti, B., Tomiuchi, Y., Harahap, U., & Daimon, H. (2017). Effect of Recycle Sludge on Anaerobic Digestion of Palm Oil Mill Effluent in A Thermophilic Continuous Digester. *IOP Conference Series: Materials Science and Engineering*, *206*(1), 012094. https://doi.org/10.1088/1757-899X/206/1/012094

Babaei, A., & Shayegan, J. (2020). *Effects of temperature and mixing modes on the performance of municipal solid waste anaerobic slurry digester*. https://doi.org/10.1007/s40201-019-00422-6

Bajón Fernández, Y., Green, K., Schuler, K., Soares, A., Vale, P., Alibardi, L., & Cartmell, E. (2015). Biological carbon dioxide utilisation in food waste anaerobic digesters. *Water Research*, *87*, 467–475. https://doi.org/10.1016/J.WATRES.2015.06.011

Bala, J. D., Lalung, J., & Ismail, N. (2015). Studies on the reduction of organic load from palm oil mill effluent (POME) by bacterial strains. *International Journal of Recycling of Organic Waste in Agriculture*, *4*(1), 1–10. https://doi.org/10.1007/S40093-014-0079-6/FIGURES/8

Bari, S. (1996). Effect of carbon dioxide on the performance of biogas/diesel duel-fuel engine. *Renewable Energy*, *9*(1–4), 1007–1010. https://doi.org/10.1016/0960-1481(96)88450-3

Beccari, M., Bonemazzi, F., Majone, M., & Riccardi, C. (1996). Interaction between acidogenesis and methanogenesis in the anaerobic treatment of olive oil mill effluents. *Water Research*, *30*(1), 183–189. https://doi.org/10.1016/0043-1354(95)00086-Z

Belyakov, N. (2019). Power island and balance of plant. *Sustainable Power Generation*, 201–243. https://doi.org/10.1016/B978-0-12-817012-0.00020-7

Bergland, W. H., Dinamarca, C., & Bakke, R. (2015). Temperature Effects in Anaerobic Digestion Modeling. *Proceedings of the 56th Conference on Simulation and Modelling (SIMS 56), October, 7-9, 2015, Linköping University, Sweden*, *119*, 261–269. https://doi.org/10.3384/ECP15119261

Bharathiraja, B., Sudharsana, T., Jayamuthunagai, J., Praveenkumar, R., Chozhavendhan, S., & Iyyappan, J. (2018). RETRACTED: Biogas production–A review on composition, fuel properties, feed stock and principles of anaerobic digestion. *Renewable and Sustainable Energy Reviews*, *90*, 570–582. https://doi.org/10.1016/J.RSER.2018.03.093

Bhattacharya, J., Dev, S., & Das, B. (2017). *Low cost wastewater bioremediation technology : innovative treatment of sulfate and metal-rich wastewater*.

Bhorkar, M., Bhole, A. G., & Nagarnaik, P. B. (2019). Application of Tube Settlers in Water Treatment Process—A Review. *Smart Technologies for Energy, Environment and Sustainable Development*.

Bilhan, O., Emiroglu, M. E., & Miller, C. J. (2016). Experimental Investigation of Discharge Capacity of Labyrinth Weirs with and without Nappe Breakers. *World Journal of Mechanics*, *06*(07), 207–221. https://doi.org/10.4236/wjm.2016.67017

Bird, R. B., Stewart, W. E., & Lightfoot, E. N. (2002). *Transport Phenomena Second Edition*.

Biswas, W. K. (1994). *USE OF BIOGAS AS DIESEL ENGINE FUEL*.

Boe, K. (2006). *Online monitoring and control of the biogas process*.

Botheju, D., Lie, B., & Bakke, R. (2010). Oxygen Effects in Anaerobic Digestion-II. *Identification and Control*, *31*(2), 55–65. https://doi.org/10.4173/mic.2010.2.2

Bouallagui, H., Haouari, O., Touhami, Y., Cheikh, R., Marouani, L., & Hamdi, M. (2004). Effect of temperature on the performance of an anaerobic tubular reactor treating fruit and vegetable waste. *Process Biochemistry*, *39*, 2143–2148. https://doi.org/10.1016/j.procbio.2003.11.022

Chia, W. Y., Chong, Y. Y., Chew, K. W., Vimali, E., Jayaram, M., Selvarajoo, A., Muthuvelu, K. S., Varalakshmi, P., Show, P. L., & Arumugasamy, S. K. (2020). Outlook on biorefinery potential of palm oil mill effluent for resource recovery. *Journal of Environmental Chemical Engineering*, *8*(6). https://doi.org/10.1016/J.JECE.2020.104519

Brethauer, S., Shahab, R. L., & Studer, M. H. (2020). Impacts of biofilms on the conversion of cellulose. *Applied Microbiology and Biotechnology*, *104*(12), 5201–5212. https://doi.org/10.1007/s00253-020-10595-y

Busetto, L., Wick, W., & Gumbinger, C. (2020). How to use and assess qualitative research methods. *Neurological Research and Practice*, *2*(1). https://doi.org/10.1186/s42466-020-00059-z

Butler, E., Hung, Y.-T., Suleiman Al Ahmad, M., Yeh, R. Y.-L., Liu, R. L.-H., & Fu, Y.-P. (2017). Oxidation pond for municipal wastewater treatment. *Applied Water Science*, *7*(1), 31–51. https://doi.org/10.1007/S13201-015-0285-Z/TABLES/7

Cadena, S., Cervantes, F. J., Falcón, L. I., & García-Maldonado, J. Q. (2019). The Role of Microorganisms in the Methane Cycle. *Frontiers for Young Minds*, *7*. https://doi.org/10.3389/FRYM.2019.00133

Carlsson, B. (1998). *An introduction to sedimentation theory in wastewater treatment*.

Carlsson, M., Lagerkvist, A., & Morgan-Sagastume, F. (2012). The effects of substrate pre-treatment on anaerobic digestion systems: A review. *Waste Management*, *32*(9), 1634–1650. https://doi.org/10.1016/J.WASMAN.2012.04.016

Chae, K. J., Jang, A., Yim, S. K., & Kim, I. S. (2008). The effects of digestion temperature and temperature shock on the biogas yields from the mesophilic anaerobic digestion of swine manure. *Bioresource Technology*, *99*(1), 1–6. https://doi.org/10.1016/J.BIORTECH.2006.11.063

Chai, S., Phang, F., Yeo, L., Ngu, L., & Shen, H. (2022). Future era of techno-economic analysis: Insights from review. *Frontiers in Sustainability*, *3*, 924047. https://doi.org/10.3389/frsus.2022.924047

Chaikitkaew, S., Kongjan, P., & O-Thong, S. (2015). Biogas production from biomass residues of palm oil mill by solid state anaerobic digestion. *Energy Procedia*, *79*, 838–844. https://doi.org/https://doi.org/10.1016/j.egypro.2015.11.575

Chaiprapat, S., & Laklam, T. (2011). Enhancing digestion efficiency of POME in anaerobic sequencing batch reactor with ozonation pretreatment and cycle time reduction. *Bioresource Technology*, *102*(5), 4061–4068. https://doi.org/10.1016/j.biortech.2010.12.033

Chan, Y. J., Lee, H. W., & Selvarajoo, A. (2021). Comparative study of the synergistic effect of decanter cake (DC) and empty fruit bunch (EFB) as the co-substrates in the anaerobic co-digestion (ACD) of palm oil mill effluent (POME). *Environmental Challenges*, *5*. https://doi.org/10.1016/J.ENVC.2021.100257

Chen, D., & Li, Y. (2020). A development on multimodal optimization technique and its application in structural damage detection. *Applied Soft Computing*, *91*, 106264. https://doi.org/https://doi.org/10.1016/j.asoc.2020.106264

Chen, Y., Cheng, J. J., & Creamer, K. S. (2007). Inhibition of anaerobic digestion process: a review. *Bioresource Technology*, *99*(10), 4044–4064. https://doi.org/10.1016/J.BIORTECH.2007.01.057

Chen, Y., Xiao, K., Jiang, X., Shen, N., Zeng, R. J., & Zhou, Y. (2018). Long solid retention time (SRT) has minor role in promoting methane production in a 65°C single-stage anaerobic sludge digester. *Bioresource Technology*, *247*, 724–729. https://doi.org/10.1016/J.BIORTECH.2017.09.153

Chew, C. L., Low, L. E., Chia, W. Y., Chew, K. W., Liew, Z. K., Chan, E. S., Chan, Y. J., Kong, P. S., & Show, P. L. (2021). Prospects of Palm Fruit Extraction Technology: Palm Oil Recovery Processes and Quality Enhancement. *Https://Doi.Org/10.1080/87559129.2021.1890117*. https://doi.org/10.1080/87559129.2021.1890117

Chew, C. L., Ng, C. Y., Hong, W. O., Wu, T. Y., Lee, Y.-Y., Low, L. E., Kong, P. S., & Chan, E. S. (2021). *Improving Sustainability of Palm*

Oil Production by Increasing Oil Extraction Rate: a Review. https://link.springer.com/article/10.1007/s11947-020-02555-1#citeas

Chia, Wen Yi & Chong, Yen Yee & Kit Wayne, Chew & Elamathi, Vimali & Jayaram, Moorthy & Selvarajoo, Anurita & Muthuvelu, Kirupa Sankar & Varalakshmi, Perumal & Show, Pau-Loke & Arumugasamy, S. K. (2020). Outlook on biorefinery potential of palm oil mill effluent for resource recovery. *Journal of Environmental Chemical Engineering*. https://doi.org/http://dx.doi.org/10.1016/j.jece.2020.104519

Chicco, D., Warrens, M. J., & Jurman, G. (2021). The coefficient of determination R-squared is more informative than SMAPE, MAE, MAPE, MSE and RMSE in regression analysis evaluation. *PeerJ Computer Science*, *7*, e623. https://link.gale.com/apps/doc/A667442646/AONE?u=anon~d3bac83b&sid=googleScholar&xid=3b1d82fb

Chin, M. J., Poh, P. E., Tey, B. T., Chan, E. S., & Chin, K. L. (2013). Biogas from palm oil mill effluent (POME): Opportunities and challenges from Malaysia's perspective. *Renewable and Sustainable Energy Reviews*, *26*, 717–726. https://doi.org/10.1016/J.RSER.2013.06.008

Choong, Y. Y., Chou, K. W., & Norli, I. (2018). Strategies for improving biogas production of palm oil mill effluent (POME) anaerobic digestion: A critical review. In *Renewable and Sustainable Energy Reviews* (Vol. 82, pp. 2993–3006). Elsevier Ltd. https://doi.org/10.1016/j.rser.2017.10.036

Choorit, W., & Wisarnwan, P. (2007). Effect of temperature on the anaerobic digestion of palm oil mill effluent. *Electronic Journal of Biotechnology*, *10*(3), 717–3458. https://doi.org/10.2225/vol10-issue3-fulltext-7

Choudhury, A., Shelford, T., Felton, G., Gooch, C., & Lansing, S. (2019). Evaluation of Hydrogen Sulfide Scrubbing Systems for Anaerobic Digesters on Two U.S. Dairy Farms. *Energies 2019, Vol. 12, Page 4605*, *12*(24), 4605. https://doi.org/10.3390/EN12244605

Cioabla, A. E., Ionel, I., Dumitrel, G. A., & Popescu, F. (2012). Comparative study on factors affecting anaerobic digestion of agricultural vegetal residues. *Biotechnology for Biofuels*, *5*(1), 1–9. https://doi.org/10.1186/1754-6834-5-39/FIGURES/9

Concha, F., & Bustos, M. C. (1991). Settling velocities of particulate systems, 6. Kynch sedimentation processes: batch settling. *International Journal of MIneral Processiong*, *32*, 193–212. https://doi.org/10.1007/978-3-319-02484-4_5

Crookston, B. M., & Tullis, B. P. (2013). *The Design and Analysis of Labyrinth Weirs Hydraulic Design and Analysis of Labyrinth Weirs. I: Discharge Relationships*. https://doi.org/10.1061/(ASCE)IR.1943-4774

Demirel, B., & Scherer, P. (2008). The roles of acetotrophic and hydrogenotrophic methanogens during anaerobic conversion of biomass to methane: A review. *Reviews in Environmental Science and Biotechnology*, *7*(2), 173–190. https://doi.org/10.1007/S11157-008-9131-1

Denys, F. J. M., & Basson, G. R. (2018). Transient hydrodynamics of piano key weirs. *7th IAHR International Symposium on Hydraulic Structures, ISHS 2018*, 518–527. https://doi.org/10.15142/T30M0J

Denys, F. J. M., & Basson, G. R. (2018). Transient hydrodynamics of piano key weirs. *7th IAHR International Symposium on Hydraulic Structures, ISHS 2018*, 518–527. https://doi.org/10.15142/T30M0J

Dermeche, S., Nadour, M., Larroche, C., Moulti-Mati, F., & Michaud, P. (2013). Olive mill wastes: Biochemical characterizations and valorization strategies. *Process Biochemistry*, *48*(10), 1532–1552. https://doi.org/10.1016/J.PROCBIO.2013.07.010

Deublein, D., & Steinhauser, A. (2008). Biogas from Waste and Renewable Resources. *Biogas from Waste and Renewable Resources*. https://doi.org/10.1002/9783527621705

Divya, D., Gopinath, L. R., & Merlin Christy, P. (2015). A review on current aspects and diverse prospects for enhancing biogas production in sustainable means. *Renewable and Sustainable Energy Reviews*, *42*, 690–699. https://doi.org/10.1016/J.RSER.2014.10.055

Dobre, P., Nicolae, F., & Matei, F. (2014). Main factors affecting biogas production-an overview. *Romanian Biotechnological Letters*, *19*(3).

Dohdoh, A. M., & Aboulfotoh, A. M. (2017). Start-up performance of a mesophilic anaerobic digester without external inoculums. *Environment Protection Engineering*, *43*(4), 29–39. https://doi.org/10.5277/epe170403

Ehsan, S., Mazlan, H. &, Wahid, A., Hosseini, S. E., & Wahid, M. A. (2015). Pollutant in palm oil production process. *Http://Dx.Doi.Org/10.1080/10962247.2013.873092*, *65*(7), 773–781. https://doi.org/10.1080/10962247.2013.873092

Ekama, G. A., Barnard, J. L., & Günthert, F. W. (1997). *Secondary settling tanks : theory, modelling, design and operation*.

El Shahawy, A., Ahmed, I. A., Nasr, M., Ragab, A. H., Al-Mhyawi, S. R., & Elamin, K. M. A. (2021). Organic pollutants removal from olive mill wastewater using electrocoagulation process via central composite design (Ccd). *Water (Switzerland)*, *13*(24). https://doi.org/10.3390/w13243522

El-mashad, H. (2004). Effect of temperature and temperature fluctuation on thermophilic anaerobic digestion of cattle manure. *Bioresource Technology*, *95*(2), 191–201. https://www.academia.edu/34777845/Effect_of_temperature_and_temperature_fluctuation_on_thermophilic_anaerobic_digestion_of_cattle_manure

Elvitriana, E., Munir, E., Delvian, D., & Wahyuningsih, H. (2021). Organic Substances Reduction in Palm Oil Mill Effluent (POME) After Cultivation with Locally Isolated Microalgae. *Journal of Advanced Research in Fluid Mechanics and Thermal Sciences*, *80*(2), 98–105. https://doi.org/10.37934/arfmts.80.2.98105

Embas, D. U. (2009). *Environmental Quality (Industrial Effluent) Regulations 2009*. Ministry of Natural Resources and the Environment.

Engin, Ö. G. (2017). Comparison of thermophilic and mesophilic anaerobic treatments for potato processing wastewater using a contact reactor. *Global NEST Journal*, *19*(2), 318–326.

Environmental Protection Division. (2015). *Technical Guidance 7 Environmental Management Act*.

Eslami, H., Hashemi, H., Fallahzadeh, R. A., Khosravi, R., Fard, R. F., & Ebrahimi, A. A. (2018). Effect of organic loading rates on biogas production and anaerobic biodegradation of composting leachate in the anaerobic series bioreactors. *Ecological Engineering*, *110*, 165–171. https://doi.org/10.1016/J.ECOLENG.2017.11.007

Fang, H. H. P., & Yu, H. Q. (2000). Effect of HRT on Mesophilic Acidogenesis of Dairy Wastewater. *Journal of Environmental Engineering*, *126*(12), 1145–1148. https://doi.org/10.1061/(ASCE)0733-9372(2000)126:12(1145)

Fang, H. H. P., & Chui, H. K. (1994). Comparison of startup performance of four anaerobic reactors for the treatment of high-strength wastewater. *Resources Conservation and Recycling*, *11*(1–4), 123–138. https://doi.org/10.1016/0921-3449(94)90084-1

Fang, X., Zech, W. C., & Logan, C. P. (2015). Stormwater field evaluation and its challenges of a sediment basin with skimmer and baffles at a highway construction site. *Water (Switzerland)*, *7*(7), 3407–3430. https://doi.org/10.3390/w7073407

Fikri Hamzah, M. A., Md Jahim, J., & Mohamed Abdul, P. (2019). Comparative start-up between mesophilic and thermophilic for acidified palm oil mill effluent treatment. *IOP Conference Series: Earth and Environmental Science*, *268*(1). https://doi.org/10.1088/1755-1315/268/1/012028

Foong, S. Z. Y., Lam, Y. L., Andiappan, V., Foo, D. C. Y., & Ng, D. K. S. (2018). A Systematic Approach for the Synthesis and Optimization of Palm Oil Milling Processes. *Industrial and Engineering Chemistry Research*, *57*(8), 2945–2955. https://doi.org/10.1021/acs.iecr.7b04788

García-Cubero, M. T., Coca, M., Bolado, S., & González-Benito, G. (2010). Chemical oxidation with ozone as pre-treatment of lignocellulosic materials for bioethanol production. *Chemical Engineering Transactions*, *21*, 1273–1278. https://doi.org/10.3303/CET1021213

GEA. (2021). *Crude Palm Oil Processing Separators, Decanters and Process Lines*.

Genderen, G. F. (1995). *The Performance of Full-Scale Waste Stabiliation Ponds Treating Saline Wastewater With Particular Reference to Bateriophage as a Hydraulic Tracer.* University of Surrey. https://openresearch.surrey.ac.uk/esploro/outputs/doctoral/The-Performance-of-Full-Scale-Waste-Stabiliation-Ponds-Treating-Saline-Wastewater-With-Particular-Reference-to-Bateriophage-as-a-Hydraulic-Tracer/99513267302346

Georgiadis, A. G., Charisiou, N. D., & Goula, M. A. (2020). Removal of Hydrogen Sulfide From Various Industrial Gases: A Review of The Most Promising Adsorbing Materials. *Catalysts 2020, Vol. 10, Page 521*, *10*(5), 521. https://doi.org/10.3390/CATAL10050521

Ghatak, M. Das, & Ghatak, A. (2018). Artificial neural network model to predict behavior of biogas production curve from mixed lignocellulosic co-substrates. *Fuel*, *232*, 178–189. https://doi.org/https://doi.org/10.1016/j.fuel.2018.05.051

Gillberg, L., Hansen, B., & Karlsson, I. (2003). *About water treatment*. Kemira Kemwater. www.kemira.com/aboutwatertreatment

Google Developers. (2023). *Normalization | Machine Learning | Google for Developers*. Google Developers.

Gozan, M., Aulawy, N., Rahman, S. F., & Budiarto, R. (2018). Techno-Economic Analysis of Biogas Power Plant from POME (Palm Oil Mill Effluent). *International Journal of Applied Engineering Research*, *13*(8), 6151–6157. http://www.ripublication.com

Grangeiro, L. C., Almeida, S. G. C. de, Mello, B. S. de, Fuess, L. T., Sarti, A., & Dussán, K. J. (2019). New trends in biogas production and utilization. *Scopus*, 199–223. https://doi.org/10.1016/B978-0-12-817654-2.00007-1

Haman, D. Z., & Zazueta, F. S. (2021). *Settling Basins for Trickle Irrigation in Florida* (pp. 3–4). http://edis.ifas.ufl.edu.

Hamdi, M., & Garcia, J. L. (1991). Comparison Between Anaerobic Filter and Anaerobic Contact Process for Fermented Olive Mill Wastewaters. In *Bioresource Technology* (Vol. 38, pp. 23–29).

Hamzah, M. A. F., Abdul, P. M., Mahmod, S. S., Azahar, A. M., & Jahim, J. M. (2020). Performance of Anaerobic Digestion of Acidified Palm Oil Mill Effluent under Various Organic Loading Rates and Temperatures. *Water 2020, Vol. 12, Page 2432*, *12*(9), 2432. https://doi.org/10.3390/W12092432

Hansen, S. P., & Culp, G. L. (1967). Applying Shallow Depth Sedimentation Theory. *Journal (American Water Works Association)*, *59*(9), 1134–1148. http://www.jstor.org/stable/41265168

Harris, P. W., & McCabe, B. K. (2020). Process optimisation of anaerobic digestion treating high-strength wastewater in the australian red meat processing industry. In *Applied Sciences (Switzerland)* (Vol. 10, Issue 21, pp. 1–17). MDPI AG. https://doi.org/10.3390/app10217947

Harsono, S. S., Grundmann, P., & Soebronto, S. (2014). Anaerobic treatment of palm oil mill effluents: potential contribution to net energy yield and reduction of greenhouse gas emissions from biodiesel production. *Journal of Cleaner Production*, *64*, 619–627. https://doi.org/10.1016/J.JCLEPRO.2013.07.056

Hashim, A. B., Giwa, saidat O., Ibrahim, M., & Giwa, A. (2015). (PDF) FINDING THE OPTIMUM PARAMETERS FOR OIL EXTRACTION FROM SESAME SEED USING RESPONSE SURFACE METHODOLOGY. *International Journal of Scientific Research & Management Studies*, *2(1)*, 1–13. https://www.researchgate.net/publication/275353567_FINDING_THE_OPTIMUM_PARAMETERS_FOR_OIL_EXTRACTION_FROM_SESAME_SEED_USING_RESPONSE_SURFACE_METHODOLOGY

Hill, G. B. (Gerald B., Pring, E. J., Osborn, P. D. (Peter D., & Stanford, W. (William). (1990). *Cooling towers : principles and practice*. 191.

Hoang, A. T., Nižetić, S., Ong, H. C., Mofijur, M., Ahmed, S. F., Ashok, B., Bui, V. T. V., & Chau, M. Q. (2021). Insight into the recent

advances of microwave pretreatment technologies for the conversion of lignocellulosic biomass into sustainable biofuel. *Chemosphere*, *281*, 1–22. https://doi.org/https://doi.org/10.1016/j.chemosphere.2021.130878

Hobson, P. N., Bousfield, S., & Summers, R. (1981). Methane Production from Agricultural and Domestic Wastes. *Methane Production from Agricultural and Domestic Wastes*. https://doi.org/10.1007/978-94-009-8102-7

Holland, P. G. (1998). Weir: weirsflow measurementFlow measurement. In *Encyclopedia of Hydrology and Lakes* (pp. 785–787). Springer Netherlands. https://doi.org/10.1007/1-4020-4497-6_259

Hu, Y., Kobayashi, T., Zhen, G., Shi, C., & Xu, K. Q. (2018). Effects of lipid concentration on thermophilic anaerobic co-digestion of food waste and grease waste in a siphon-driven self-agitated anaerobic reactor. *Biotechnology Reports*, *19*. https://doi.org/10.1016/j.btre.2018.e00269

Huertas, J. K., Quipuzco, L., Hassanein, A., & Lansing, S. (2020). Comparing Hydrogen Sulfide Removal Efficiency in a Field-Scale Digester Using Microaeration and Iron Filters. *Energies 2020, Vol. 13, Page 4793*, *13*(18), 4793. https://doi.org/10.3390/EN13184793

Hwang, M. H., Jang, N. J., Hyun, S. H., & Kim, I. S. (2004). Anaerobic bio-hydrogen production from ethanol fermentation: the role of pH. *Journal of Biotechnology*, *111*(3), 297–309. https://doi.org/10.1016/J.JBIOTEC.2004.04.024

Ibrahim, A., Yeah, B. G., Cheah, S. C., Ma, A. N., Ahmad, S., Chew, T. Y., Raj, R., & Wahid, M. J. A. (1984). THERMOPHILIC ANAEROBIC CONTACT DIGESTION OF PALM OIL MILL EFFLUENT. In *Wat. Sci. Tech* (Vol. 17, pp. 155–166). https://iwaponline.com/wst/article-pdf/17/2-3/155/96848/155.pdf

Igwe, J. C., & Onyegbado, C. (2007). *A Review of Palm Oil Mill Effluent (Pome) Water Treatment*.

Index Mundi. (2021). *Country Facts*. https://www.indexmundi.com/

Iskandar, M. J., Baharum, A., Anuar, F. H., & Othaman, R. (2018). Palm oil industry in South East Asia and the effluent treatment technology—A review. *Environmental Technology & Innovation*, *9*, 169–185. https://doi.org/10.1016/J.ETI.2017.11.003

Izzah, N., Aziz, H. A., & Hanafiah, M. M. (2017). THE POTENTIAL OF PALM OIL MILL EFFLUENT (POME) AS A RENEWABLE ENERGY SOURCE. *Acta Scientifica Malaysia*, *2*(2), 09–11. https://doi.org/10.26480/ASM.02.2017.09.11

Jaromír Klemeš, J., Yen Liew, P., Shin Ho, W., Shiun Lim, J., Hadi Abdullah, A., Mat, R., Shah Abd Aziz, A., & Roslan, F. (2017). Use of Kaolin as Adsorbent for Removal of Hydrogen Sulphide from Biogas. *Chemical Engineering Transactions*, *56*, 763–768. https://doi.org/10.3303/CET1756128

Jeong, J. Y., Son, S. M., Pyon, J. H., & Park, J. Y. (2014). Performance comparison between mesophilic and thermophilic anaerobic reactors for treatment of palm oil mill effluent. *Bioresource Technology*, *165*(C), 122–128. https://doi.org/10.1016/J.BIORTECH.2014.04.007

Johnson, P., & Schielzeth, H. (2017). The coefficient of determination R2 and intra-class correlation coefficient from generalized linear mixed-effects models revisited and expanded. *Journal of The Royal Society Interface*, *14*, 20170213. https://doi.org/10.1098/rsif.2017.0213

Jun, D., Yong-sheng, Z., Mei, H., & Wei-hong, Z. (2009). Influence of alkalinity on the stabilization of municipal solid waste in anaerobic simulated bioreactor. *Journal of Hazardous Materials*, *163*(2–3), 717–722. https://doi.org/10.1016/J.JHAZMAT.2008.07.066

Junaidah, M. J., Norizzah, A. R., Zaliha, O., & Mohamad, S. (2015). Optimisation of sterilisation process for oil palm fresh fruit bunch at different ripeness. *International Food Research Journal*, *22*(1), 275–282.

Kainthola, J., Podder, A., Fechner, M., & Goel, R. (2021). An overview of fungal pretreatment processes for anaerobic digestion: Applications, bottlenecks and future needs. *Bioresource Technology*, *321*, 1–11. https://doi.org/https://doi.org/10.1016/j.biortech.2020.124397

Kamyab, H., Chelliapan, S., Fadhil, M., Din, M., Rezania, S., Khademi, T., & Kumar, A. (2018). Palm Oil Mill Effluent as an Environmental Pollutant. *Palm Oil*. https://doi.org/10.5772/INTECHOPEN.75811

Kanchanasuta, S., & Pisutpaisal, N. (2016). Waste utilization of palm oil decanter cake on biogas fermentation. *International Journal of Hydrogen Energy*, *41*(35), 15661–15666. https://doi.org/https://doi.org/10.1016/j.ijhydene.2016.04.129

Kandiah, S., Basiron, Y., Suki, A., Ramli, ;, Taha, M., Tan, + ;, ++ Y. H., & Sulong, M. (2006). Continuous Sterilization: the New Paradigm for Modernizing Palm Oil Milling. *Journal of Oil Palm Research*, 144–152.

Kandiah, S., & Batumalai, R. (2013). *PALM OIL CLARIFICATION USING EVAPORATION*. Journal of Oil Palm Research. http://jopr.mpob.gov.my/palm-oil-clarification-using-evaporation/

Kanimozhi, R., & Vasudevan, N. (2010). An overview of wastewater treatment in distillery industry. *International Journal of Environmental Engineering*, *2*(1/2/3), 159. https://doi.org/10.1504/IJEE.2010.029826

Kaosol, T., & Rungarunanotai, W. (2016). Effect of microwave pre-treatment on BMP of decanter cake from palm oil mill factory. *American Journal of Applied Sciences*, *13*(5), 609–617.

Kaosol, T., & Sohgrathok, N. (2014). INCREASING ANAEROBIC DIGESTION PERFORMANCE OF WASTEWATER WITH CO-DIGESTION USING DECANTER CAKE. *American Journal of Environmental Sciences*, *10*(5), 469–479. https://doi.org/10.3844/AJESSP.2014.469.479

Karthikeyan, O. P., & Visvanathan, C. (2013). Bio-energy recovery from high-solid organic substrates by dry anaerobic bio-conversion processes: a review. *Reviews in Environmental Science and Bio/Technology*, *12*(3), 257–284. https://doi.org/10.1007/s11157-012-9304-9

Kayombo, S., Mbwette, T. S. A., Katima, J. H. Y., Ladegaard, N., & Jørgensen, S. E. (n.d.). *WASTE STABILIZATION PONDS AND CONSTRUCTED WETLANDS DESIGN MANUAL*.

Kelleher, B. P., Leahy, J. J., Henihan, A. M., O'Dwyer, T. F., Sutton, D., & Leahy, M. J. (2002). Advances in poultry litter disposal technology--a review. *Bioresource Technology*, *83*(1), 27–36. https://doi.org/10.1016/S0960-8524(01)00133-X

Kenton, W. (2023). *Sensitivity Analysis Definition*. Investopedia . https://www.investopedia.com/terms/s/sensitivityanalysis.asp

Khadaroo, S. N. B. A., Poh, P. E., Gouwanda, D., & Grassia, P. (2019). Applicability of various pretreatment techniques to enhance the anaerobic digestion of Palm oil Mill effluent (POME): A review. *Journal of Environmental Chemical Engineering*, *7*(5), 103310. https://doi.org/10.1016/J.JECE.2019.103310

Khairul Anuar, N., Che Man, H., Idrus, S., & Nik Daud, N. N. (2018). Biochemical methane potential (BMP) from anaerobic co-digestion of sewage sludge and decanter cake. *IOP Conference Series: Materials Science and Engineering*, *368*(1), 012027. https://doi.org/10.1088/1757-899X/368/1/012027

Kiener, A., & Leisinger, T. (1983). Oxygen Sensitivity of Methanogenic Bacteria. *Systematic and Applied Microbiology*, *4*(3), 305–312. https://doi.org/10.1016/S0723-2020(83)80017-4

Kim, J. K., Oh, B. R., Chun, Y. N., & Kim, S. W. (2006). Effects of temperature and hydraulic retention time on anaerobic digestion of food waste. *Journal of Bioscience and Bioengineering*, *102*(4), 328–332. https://doi.org/10.1263/JBB.102.328

Kim, J., Oh, B., Chun, Y., & Kim, S. (2006). Effects of temperature and hydraulic retention time on anaerobic digestion of food waste. *Journal of Bioscience and Bioengineering*, *102*, 328–332. https://doi.org/10.1263/jbb.102.328

Konkol, I., Cebula, J., & Cenian, A. (2021). Oxidization of hydrogen sulfide in biogas by manganese (IV) oxide particles. *Environmental Engineering Research*, *26*(2). https://doi.org/10.4491/EER.2019.343

Kumar Mamindlapelli, N., Arelli, V., Jukanti, A., Maddala, R., & Anupoju, G. R. (2022). Anaerobic Co-digestion of Biogenic Wastes Available at Palm Oil Extraction Factory: Assessment of Methane Yield, Estimation of Kinetic Parameters and Understanding the Microbial Diversity. *Bioenergy Research*. https://doi.org/10.1007/S12155-022-10472-8

Kumaraswamy, B. (2021). *Neural networks for data classification* (pp. 109–131). https://doi.org/10.1016/B978-0-12-820601-0.00011-2

Kynch, G. J. (1952). A theory of sedimentation. *Transactions of the Faraday Society*, *48*, 166–176. https://doi.org/10.1039/tf9524800166

L Chen, & H Neiibling. (2014). *Benefits of Anaerobic Digestion*. www.engr.colostate.edu

Lam, M. K., & Lee, K. T. (2011). Renewable and sustainable bioenergies production from palm oil mill effluent (POME): win-win strategies toward better environmental protection. *Biotechnology Advances*, *29*(1), 124–141. https://doi.org/10.1016/J.BIOTECHADV.2010.10.001

Lang, L. Y. (2007). *TREATABILITY OF PALM OIL MILL EFFLUENT (POME) USING BLACK LIQUOR IN AN ANAEROBIC TREATMENT PROCESS*.

Laurance, W. F., Koh, L. P., Butler, R., Sodhi, N. S., A Bradshaw, C. J., David Neidel, J., Consunji, H., & Mateo Vega, J. (2010). *Improving the Performance of the Roundtable on Sustainable Palm Oil for Nature Conservation*. https://doi.org/10.1111/j.1523-1739.2010.01448.x

Lee, Z. S., Chin, S. Y., Lim, J. W., Witoon, T., & Cheng, C. K. (2019). Treatment technologies of palm oil mill effluent (POME) and olive mill wastewater (OMW): A brief review. In *Environmental*

Technology and Innovation (Vol. 15). Elsevier B.V. https://doi.org/10.1016/j.eti.2019.100377

Lee, Z. S., Chin, S. Y., Lim, J. W., Witoon, T., & Cheng, C. K. (2019). Treatment technologies of palm oil mill effluent (POME)and olive mill wastewater (OMW): A brief review. *Environmental Technology and Innovation*, *15*. https://doi.org/10.1016/J.ETI.2019.100377

Leela, D., Nur, S. M., Yandri, E., & Ariati, R. (2018). Performance of Palm Oil Mill Effluent (POME) as Biodiesel Source Based on Different Ponds. *E3S Web of Conferences*, *67*. https://doi.org/10.1051/e3sconf/20186702038

Leone, A., Romaniello, R., Zagaria, R., & Tamborrino, A. (2015). Mathematical modelling of the performance parameters of a new decanter centrifuge generation. *Journal of Food Engineering*, *166*, 10–20. https://doi.org/https://doi.org/10.1016/j.jfoodeng.2015.05.011

Liew, W. L., Kassim, M. A., Muda, K., Loh, S. K., & Affam, A. C. (2015). Conventional methods and emerging wastewater polishing technologies for palm oil mill effluent treatment: a review. *Journal of Environmental Management*, *149*, 222–235. https://doi.org/10.1016/J.JENVMAN.2014.10.016

Lim, S., & Teong, L. K. (2010). Recent trends, opportunities and challenges of biodiesel in Malaysia: An overview. *Renewable and Sustainable Energy Reviews*, *14*(3), 938–954. https://doi.org/10.1016/J.RSER.2009.10.027

Lim, Y. F., Chan, Y. J., Hue, F. S., Ng, S. C., & Hashma, H. (2021). Anaerobic co-digestion of palm oil mill effluent (POME) with decanter cake (DC): Effect of mixing ratio and kinetic study. *Bioresource Technology Reports*, *15*, 1–13. https://doi.org/https://doi.org/10.1016/j.biteb.2021.100736

Lin, J., Zuo, J., Gan, L., Li, P., Liu, F., Wang, K., Chen, L., & Gan, H. (2011). Effects of mixture ratio on anaerobic co-digestion with fruit and vegetable waste and food waste of China. *Journal of Environmental Sciences*, *23*(8), 1403–1408. https://doi.org/10.1016/S1001-0742(10)60572-4

Loh, S. K., Nasrin, A. B., Mohamad Azri, S., Nurul Adela, B., Muzzammil, N., Daryl Jay, T., Stasha Eleanor, R. A., Lim, W. S., Choo, Y. M., & Kaltschmitt, M. (2017). First Report on Malaysias experiences and development in biogas capture and utilization from palm oil mill effluent under the Economic Transformation Programme: Current and future perspectives. *Renewable and Sustainable Energy Reviews*, *74*, 1257–1274. https://doi.org/10.1016/J.RSER.2017.02.066

Lok, X., Chan, Y. J., & Foo, D. C. Y. (2020). Simulation and optimisation of full-scale palm oil mill effluent (POME) treatment plant with biogas production. *Journal of Water Process Engineering*, *38*. https://doi.org/10.1016/J.JWPE.2020.101558

Lokman, N. A., Ithnin, A. M., Yahya, W. J., & Yuzir, M. A. (2021). A brief review on biochemical oxygen demand (BOD) treatment methods for palm oil mill effluents (POME). *Environmental Technology and Innovation*, *21*. https://doi.org/10.1016/J.ETI.2020.101258

Madaki, Y. S., & Seng, L. (2013). Palm oil mill effluent (POME) from Malaysia palm oil mills: Waste or resource. *International Journal of Science, Environment and Technology*, *2*, 1138–1155.

Mamat, R., Astimar, ;, Aziz, A., & Halim, R. M. (2016). Feature Article Waste Minimisation for Palm Oil Mills: A Case Study. *Palm Oil Engineering Bulletin*.

Mamimin, C., Kongjan, P., O-Thong, S., & Prasertsan, P. (2019). Enhancement of biohythane production from solid waste by co-digestion with palm oil mill effluent in two-stage thermophilic fermentation. *International Journal of Hydrogen Energy*, *44*(32), 17224–17237. https://doi.org/https://doi.org/10.1016/j.ijhydene.2019.03.275

Maniruzzaman Aziz Khairul Anuar Kassim Moetaz ElSergany, M. A., Syed Anuar Ehsan Jorat H Yaacob Amimul Ahsan Monzur A Imteaz Arifuzzaman, M. M., Maniruzzaman Aziz, M. A., Anuar Kassim, K., ElSergany, M., Anuar, S., Ehsan Jorat, M., Yaacob, H., Ahsan, A., & Imteaz, M. A. (2019). *Recent advances on palm oil mill effluent (POME) pretreatment and anaerobic reactor for sustainable biogas production*. https://doi.org/10.1016/j.rser.2019.109603

Mara, D. D. (David D., Pearson, H., European Investment Bank., & Mediterranean Environmental Technical Assistance Program. (1998). *Design manual for waste stabilization ponds in Mediterranean countries*. Lagoon Technology International.

Margaret, A. H., Abhinav Choudhury, Gary Felton, & Stephanie A. Lansing. (2018). *Hydrogen Sulfide (H2S) Removal at a Northeastern Dairy Farm Digester using Iron Oxide: Case Study*.

Martín, C., Villuendas-Rey, Y., Azzeh, M., Nassif, A., & Banitaan, S. (2020). Transformed k-nearest neighborhood output distance minimization for predicting the Defect Density of Software Projects. *Journal of Systems and Software*, *167*, 110592. https://doi.org/10.1016/j.jss.2020.110592

MathWorks. (2023). *What is the error histogram in neural network MATLAB? - MATLAB Answers - MATLAB Central*. MathWorks.

https://www.mathworks.com/matlabcentral/answers/495218-what-is-the-error-histogram-in-neural-network-matlab

Mayer-Laigle, C., Blanc, N., Rajaonarivony, R. K., & Rouau, X. (2018). Comminution of dry lignocellulosic biomass, a review: Part I. from fundamental mechanisms to milling behaviour. *Bioengineering*, *5*(2), 1–14. https://doi.org/10.3390/bioengineering5020041

McLaughlin, R. A. (2005). *Using Baffles to Improve Sediment Basins Solid baffles*.

Mechichi, T., & Sayadi, S. (2005). Evaluating process imbalance of anaerobic digestion of olive mill wastewaters. *Process Biochemistry*, *40*(1), 139–145. https://doi.org/10.1016/J.PROCBIO.2003.11.050

Meegoda, J. N., Li, B., Patel, K., & Wang, L. B. (2018). A Review of the Processes, Parameters, and Optimization of Anaerobic Digestion. *International Journal of Environmental Research and Public Health 2018, Vol. 15, Page 2224*, *15*(10), 2224. https://doi.org/10.3390/IJERPH15102224

Mehariya S, Patel AK, Obulisamy PK, Punniyakotti E, W. J. (2018). *Co-digestion of food waste and sewage sludge for methane production: Current status and perspective. Bioresour Technol.* https://doi.org/10.1016/j.biortech.2018.04.030. Epub 2018 Apr 10. PMID: 29861300.

Mei, R., Narihiro, T., Nobu, M. K., & Liu, W. T. (2016). Effects of heat shocks on microbial community structure and microbial activity of a methanogenic enrichment degrading benzoate. *Letters in Applied Microbiology*, *63*(5), 356–362. https://doi.org/10.1111/LAM.12629

Mirahmadi, K., Kabir, M. M., Jeihanipour, A., Karimi, K., & Taherzadeh, M. J. (2010). Alkaline pretreatment of spruce and birch to improve bioethanol and biogas production. *BioResources*, *5*(2), 928–938.

Mirmohamadsadeghi, S., Karimi, K., Tabatabaei, M., & Aghbashlo, M. (2019). Biogas production from food wastes: A review on recent developments and future perspectives. *Bioresource Technology Reports*, *7*, 100202. https://doi.org/10.1016/j.biteb.2019.100202

MODIPALM ENGINEERING SDN BHD. (n.d.). *CONTINUOUS STERILIZATION SYSTEM*.

Moestedt, J., Rönnberg, J., & Nordell, E. (2017). *The effect of different mesophilic temperatures during anaerobic digestion of sludge on the overall performance of a WWTP in Sweden*. https://doi.org/10.2166/wst.2017.367

Mohamad Anuar Kamaruddin, Norli Ismail, Tan Hwee Kuen, & Rasyidah Alrozi. (2021). *Sustainable Treatment of Palm Oil Mill Effluent (POME) by using Pectin and Chitosan in Jar Test Protocol – Sequential Comparison | International Journal of Integrated Engineering*. https://publisher.uthm.edu.my/ojs/index.php/ijie/article/view/2422

Mohammad, S., Baidurah, S., Kobayashi, T., Ismail, N., & Leh, C. P. (2021). Palm oil mill effluent treatment processes—A review. In *Processes* (Vol. 9, Issue 5). MDPI AG. https://doi.org/10.3390/pr9050739

Mohammad, S., Baidurah, S., Kobayashi, T., Ismail, N., Peng Leh, C., & Wang, W. (2021). *processes Palm Oil Mill Effluent Treatment Processes-A Review*. https://doi.org/10.3390/pr9050739

Monnet, F. (2003). *An Introduction to Anaerobic Digestion of Organic Wastes Final Report*.

Motte, J.-C., Trably, E., Escudié, R., Hamelin, J., Steyer, J.-P., Bernet, N., Delgenes, J.-P., & Dumas, C. (2013). Total solids content: a key parameter of metabolic pathways in dry anaerobic digestion. *Biotechnology for Biofuels*, *6*(1), 1–9. https://doi.org/10.1186/1754-6834-6-164

Mourtzis, D. (2020). Simulation in the design and operation of manufacturing systems: state of the art and new trends. *International Journal of Production Research*, *58*(7), 1927–1949. https://doi.org/10.1080/00207543.2019.1636321

MPOB. (2021). *MPOB portal*. https://www.mpob.gov.my/

Mrosso, R., Machunda, R., & Pogrebnaya, T. (2020). Removal of Hydrogen Sulfide from Biogas Using a Red Rock. *Journal of Energy*, *2020*, 1–10. https://doi.org/10.1155/2020/2309378

Musa, M. A., Idrus, S., Hasfalina, C. M., & Daud, N. N. N. (2018). Effect of Organic Loading Rate on Anaerobic Digestion Performance of Mesophilic (UASB) Reactor Using Cattle Slaughterhouse Wastewater as Substrate. *International Journal of Environmental Research and Public Health 2018, Vol. 15, Page 2220*, *15*(10), 2220. https://doi.org/10.3390/IJERPH15102220

Mustafa, A. M., Poulsen, T. G., Xia, Y., & Sheng, K. (2017). Combinations of fungal and milling pretreatments for enhancing rice straw biogas production during solid-state anaerobic digestion. *Bioresource Technology*, *224*, 174–182. https://doi.org/https://doi.org/10.1016/j.biortech.2016.11.028

Najib, N., Sethu, V., Arumugasamy, S. K., & Selvarajoo, A. (2020). Artificial Neural Network (ANN) Modelling of Palm Oil Mill Effluent (POME) Treatment with Natural Bio-coagulants. *Environmental Processes*, *7*, 1–27. https://doi.org/10.1007/s40710-020-00431-w

Ng, F. Y., Yew, F. K., Basiron, Y., & Sundram, K. (2011). A renewable future driven with Malaysian palm oil-based green technology. *Journal of Oil Palm, Environment and Health*, *2*, 1–7. https://doi.org/10.5366/jope.2011.01

Ng, W. J., Goh, A. C. C., & Tay, J. H. (n.d.). Palm oil mill effluent (POME) treatment-An assessment of coagulants used to aid liquid-solid separation. *Scopus*.

Norhan, M. 'Aqilah, Abdullah, S. R. S., Hasan, H. A., & Ismail, N. 'Izzati. (2021). A constructed wetland system for bio-polishing palm oil mill effluent and its future research opportunities. *Journal of Water Process Engineering*, *41*, 102043. https://doi.org/10.1016/J.JWPE.2021.102043

Parry, R. J. (1999). Biosynthesis of Sulfur-containing Natural Products. *Comprehensive Natural Products Chemistry*, 825–863. https://doi.org/10.1016/B978-0-08-091283-7.00031-X

Piotrowski, A. P., & Napiorkowski, J. J. (2013). A comparison of methods to avoid overfitting in neural networks training in the case of catchment runoff modelling. *Journal of Hydrology*, *476*, 97–111. https://doi.org/10.1016/j.jhydrol.2012.10.019

Poh, P. E., & Chong, M. F. (2009). Development of anaerobic digestion methods for palm oil mill effluent (POME) treatment. In *Bioresource Technology* (Vol. 100, Issue 1, pp. 1–9). Elsevier Ltd. https://doi.org/10.1016/j.biortech.2008.06.022

Pratap Singh, R., Hakimi Ibrahim, M., Fatemeh Rupani, P., & Esa, N. (2010). Review of Current Palm Oil Mill Effluent (POME) Treatment Methods: Vermicomposting as a Sustainable Practice. *World Applied Sciences Journal*, *10*(10), 1190–1201. https://www.researchgate.net/publication/213965918

Purnomo, A., . S., Romli, M., & Hasanudin, U. (2018). Comparison of Biogas Production from Oil Palm Empty Fruit Bunches of Post-Mushroom Cultivation Media (EFBMM) from Semi Wet and Dry Fermentation. *Journal of Environment and Earth Science*, *8*(6), 88–96. https://www.iiste.org/Journals/index.php/JEES/article/view/42830

Ramanathan, A., Begum, K. M., Pereira, A., & Cohen, C. (2022). *Energy recovery from biomass through gasification technology* (pp. 107–132). https://doi.org/10.1016/B978-0-12-824357-2.00007-3

Ramos, L. P. (2003). The chemistry involved in the steam treatment of lignocellulosic materials. *Química Nova*, *26*(6), 863–871. https://doi.org/10.1590/s0100-40422003000600015

Rima, J., Rahme, K., & Assaker, K. (2014). Advanced Oxidation of Olive Mill Wastewater OMW by an Oxidative Free- Radical Process Induced With Zero Valent Iron. *Journal of Food Research*, *3*(6), 70. https://doi.org/10.5539/jfr.v3n6p70

Rongwang, C., Polprasert, S., & Kanchanasuta, S. (2017). Effect of partial ozonation and thermal pretreatment on biogas production from palm oil decanter cake. *Chemical Engineering Transactions*, *57*, 1987–1992. https://doi.org/10.3303/CET1757332

Roussel, J., Bartlett, N., Mary, C., Severn, C.-M., Water, T., Roussel, J., Bartlett, N., & Carliell-Marquet, C. (2014). *Proceedings Venice*. https://www.researchgate.net/publication/282849626

Ruffino, B., Campo, G., Genon, G., Lorenzi, E., Novarino, D., Scibilia, G., & Zanetti, M. (2015). Improvement of anaerobic digestion of sewage sludge in a wastewater treatment plant by means of mechanical and thermal pre-treatments: Performance, energy and economical assessment. *Bioresource Technology*, *175*, 298–308. https://doi.org/10.1016/J.BIORTECH.2014.10.071

S. Kayombo, T.S.A. Mbwette, J. H. . K. (n.d.). *WASTE STABILIZATION PONDS AND CONSTRUCTED WETLANDS DESIGN MANUAL*.

Saad, M. S., Wirzal, M. D. H., & Putra, Z. A. (2021). Review on current approach for treatment of palm oil mill effluent: Integrated system. *Journal of Environmental Management*, *286*, 112209. https://doi.org/10.1016/J.JENVMAN.2021.112209

Saady, N. (2011). EXPERIMENTAL VERIFICATION OF INCLINED PLATE SETTLING MODELS. *Journal of Applied Sciences in Environmental Sanitation*, *6*, 309–315.

Said, M., Ba-Abbad, M., Rozaimah Sheik Abdullah, S., -, al, Rasit, N., Chee Kuan -, O., Rajani, A., Santosa, A., Saepudin, A., Gobikrishnan, S., & Andriani, D. (2019). Review on biogas from palm oil mill effluent (POME): Challenges and opportunities in Indonesia. *IOP Conference Series: Earth and Environmental Science*, *293*(1), 012004. https://doi.org/10.1088/1755-1315/293/1/012004

Samsu Baharuddin, A., Aini, N. ', Rahman, A., Kalsom, U., Shah, M., Hassan, M. A., Wakisaka, M., & Shirai, Y. (2013). Evaluation of pressed shredded empty fruit bunch (EFB)-palm oil mill effluent (POME) anaerobic sludge based compost using Fourier transform infrared (FTIR) and nuclear magnetic resonance (NMR) analysis.

African Journal of Biotechnology, *10*(41), 8082–8289. https://doi.org/10.4314/ajb.v10i41.

Saraf, A., Kasulla, S., & Malik, S. J. (2020). Biogas Production from Decanter Cake of Palm Oil Mill from South India. *International Journal of Trend in Scientific Research and Development*, *Volume-5*(Issue-1). www.ijtsrd.com

Schmidt, T., McCabe, B., & Harris, P. (2018). Process Monitoring and Control for an Anaerobic Covered Lagoon Treating Abattoir Wastewater. *Chemical Engineering and Technology*, *41*(4), 755–760. https://doi.org/10.1002/ceat.201700391

SEDA Malaysia. (2022). *SEDA Malaysia 2022 Annual Report*. https://www.seda.gov.my/wp-content/uploads/2024/04/Laporan-Tahunan-SEDA-Malaysia-2022_071123_opt_opt.pdf

Seekao, N., Sangsri, S., Rakmak, N., Dechapanya, W., & Siripatana, C. (2021). Co-digestion of palm oil mill effluent with chicken manure and crude glycerol: biochemical methane potential by monod kinetics. *Heliyon*, *7*(2), e06204. https://doi.org/10.1016/J.HELIYON.2021.E06204

Seng Fook, L. (2007). *Pre-cleaner System-Operation and Performance in the Palm Oil Mill*.

Sethupathi, S. (2004). *Removal Of Residue Oil From Palm Oil Mill Effluent (Pome) Using Chitosan [TD899.I27 S955 2004 f rb] [Microfiche 7577].*

Shakib, N., & Rashid, M. (2019). Biogas Production Optimization from POME by Using Anaerobic Digestion Process. *Journal of Applied Science & Process Engineering*, *6*(2), 369–377. https://doi.org/10.33736/JASPE.1711.2019

Sharvini, S. R., Noor, Z. Z., Chong, C. S., Stringer, L. C., & Glew, D. (2020). Energy generation from palm oil mill effluent: A life cycle assessment of two biogas technologies. *Energy*, *191*. https://doi.org/10.1016/J.ENERGY.2019.116513

Singh, B., Szamosi, Z., & Siménfalvi, Z. (2020). Impact of mixing intensity and duration on biogas production in an anaerobic digester: a review. *Https://Doi.Org/10.1080/07388551.2020.1731413*, *40*(4), 508–521. https://doi.org/10.1080/07388551.2020.1731413

Singh, L., Wahid, Z. A., Siddiqui, M. F., Ahmad, A., Rahim, M. H. A., & Sakinah, M. (2013). Biohydrogen production from palm oil mill effluent using immobilized Clostridium butyricum EB6 in polyethylene glycol. *Process Biochemistry*, *48*(2), 294–298. https://doi.org/10.1016/j.procbio.2012.12.007

Sivasothy, K., Halim, R., & Basiron, Y. (2005). A NEW SYSTEM FOR CONTINUOUS STERILIZATION OF OIL PALM FRESH FRUIT BUNCHES. *Undefined*.

Sodri, A., & Septriana, F. E. (2022). Biogas Power Generation from Palm Oil Mill Effluent (POME): Techno-Economic and Environmental Impact Evaluation. *Energies*, *15*(19). https://doi.org/10.3390/en15197265

Solarte-Toro, J. C., Romero-García, J. M., Martínez-Patiño, J. C., Ruiz-Ramos, E., Castro-Galiano, E., & Cardona-Alzate, C. A. (2019). Acid pretreatment of lignocellulosic biomass for energy vectors production: A review focused on operational conditions and techno-economic assessment for bioethanol production. *Renewable and Sustainable Energy Reviews*, *107*, 587–601. https://doi.org/https://doi.org/10.1016/j.rser.2019.02.024

Sperling, M. Von. (2007). Waste Stabilisation Ponds. *Water Intelligence Online*, *6*(0), 9781780402109–9781780402109. https://doi.org/10.2166/9781780402109

Sri, A., Karsiwulan, R. D., Yuwono, H., Trisnawati, I., Mulyasari, S., Rahardjo, S., Hokermin, S., Paramita, V., Castermans, B., & Hardison, R. (2015). *POME to Biogas*.

Stangierski, J., Weiss, D., & Kaczmarek, A. (2019). Multiple regression models and Artificial Neural Network (ANN) as prediction tools of changes in overall quality during the storage of spreadable processed Gouda cheese. *European Food Research and Technology*, *245*. https://doi.org/10.1007/s00217-019-03369-y

Stams, A. J. M., De Bok, F. A. M., Plugge, C. M., Van Eekert, M. H. A., Dolfing, J., & Schraa, G. (2006). Exocellular electron transfer in anaerobic microbial communities. *Environmental Microbiology*, *8*(3), 371–382. https://doi.org/10.1111/J.1462-2920.2006.00989.X

Subramaniam, V., Muhamad, H., Hashim, Z., & Yuen May, C. (2014). WATER FOOTPRinT: PART 3-THE PRODUCTiOn OF CRUDE PALM OiL in MALAYSiAn PALM OiL MiLLS. In *Journal of oil Palm research* (Vol. 26, Issue 4).

Suksong, W., Kongjan, P., & O-Thong, S. (2015). Biohythane production from co-digestion of palm oil mill effluent with solid residues by two-stage solid state anaerobic digestion process. *Energy Procedia*, *79*, 943–949. https://doi.org/https://doi.org/10.1016/j.egypro.2015.11.591

Surahmad, R. C., Inung, A. A., Adnyano, A., & Purnomo, H. (2021). *Rancangan Teknis Sistem Penyaliran Pada Kolam Pengendapan (Settling Pond) di Pit Durian PT J Resources Bolaang Mongondow*

Site Bakan, Sulawesi Utara. 226–237. http://journal.itny.ac.id/index.php/ReTII

Sustainable Energy Development Agency. (2020). *2020 Annual Report*. https://www.seda.gov.my/wp-content/uploads/2022/01/SEDA-KWSM-Annual-Report-2020_2.pdf

Taghi Sattari, M., Yurekli, K., & Pal, M. (2012). Performance evaluation of artificial neural network approaches in forecasting reservoir inflow. *Applied Mathematical Modelling*, *36*(6), 2649–2657. https://doi.org/https://doi.org/10.1016/j.apm.2011.09.048

Tamborrino, A., Leone, A., Romaniello, R., Catalano, P., & Bianchi, B. (2015). Comparative experiments to assess the performance of an innovative horizontal centrifuge working in a continuous olive oil plant. *Biosystems Engineering*, *129*, 160–168. https://doi.org/https://doi.org/10.1016/j.biosystemseng.2014.10.005

Tan, H. M., Gouwanda, D., & Poh, P. E. (2018). Adaptive neural-fuzzy inference system vs. anaerobic digestion model No.1 for performance prediction of thermophilic anaerobic digestion of palm oil mill effluent. *Process Safety and Environmental Protection*, *117*. https://doi.org/10.1016/j.psep.2018.04.013

Tepsour, M., Usmanbaha, N., Rattanaya, T., Jariyaboon, R., O-Thong, S., Prasertsan, P., & Kongjan, P. (2019). Biogas Production from Oil Palm Empty Fruit Bunches and Palm Oil Decanter Cake using Solid-State Anaerobic co-Digestion. *Energies 2019, Vol. 12, Page 4368*, *12*(22), 4368. https://doi.org/10.3390/EN12224368

Texier, P. (2008). EFFECT OF ACIDIFICATION ON SLUDGE DEWATERING PROPERTIES. *Undefined*.

The Department of Industrial Works Thailand. (1997). *Environmental Management Guideline for the Palm Oil Industry*.

Tjahjono, E. wahju, Arfiana, A., Finalis, E. R., & Nurdin, A. (2020). DESIGN OF BIOGAS COOLING PROCESSING FROM POME FOR (CSTR) CONTINUOUS STIRRED TANK REACTOR SYSTEM. *Majalah Ilmiah Pengkajian Industri*, *14*(2), 137–144. https://doi.org/10.29122/MIPI.V14I2.3856

Toerien, D. F., & Hattingh, W. H. J. (1969). Anaerobic digestion I. The microbiology of anaerobic digestion. *Water Research*, *3*(6), 385–416. https://doi.org/10.1016/0043-1354(69)90002-5

Toprak, H. (1995). Temperature and organic loading dependency of methane and carbon dioxide emission rates of a full-scale anaerobic waste stabilization pond. *Water Research (Oxford) (United Kingdom)*. https://doi.org/10.3/JQUERY-UI.JS

Treve, M., Patra, I., Prabu, P., Rama Sree, S., Keerthi Kumar, N., Methkal Abd Algani, Y., Kiran Bala, B., & Balaji, S. (2022). Performance evaluation of artificial neural networks in sustainable modelling biodiesel synthesis. *Sustainable Energy Technologies and Assessments*, *52*, 102098. https://doi.org/https://doi.org/10.1016/j.seta.2022.102098

Turovskiĭ, I. S., & Mathai, P. K. (2006). *Wastewater sludge processing*. 354. https://www.wiley.com/en-us/Wastewater+Sludge+Processing-p-9780471700548

Udoka, O. (2016). USING LEVENBERG-MARQUARDT STANDARD BACK-PROPAGATION ALGORITHM IN SPEED EXTRAPOLATION FOR DC MOTORS. In *Int. J. Elec&Electr.Eng&Telecoms*. www.ijeetc.com

USDA. (2024). *World Palm Oil Production*. https://fas.usda.gov/data/production/commodity/4243000

USDA. (2021). *Oilseeds: World Markets and Trade*. 1–40. https://apps.fas.usda.gov/psdonline/app/index.html#/app/home.

Vasco-Correa, J., & Shah, A. (2019). Techno-economic bottlenecks of the fungal pretreatment of Lignocellulosic biomass. In *Fermentation* (Vol. 5, Issue 2, pp. 1–23). https://doi.org/10.3390/fermentation5020030

Wahab, A. G. (2020). Biofuels annual. *United States Department of Agricultural, Foreign Agricultural Service*.

Walczak, S., & Cerpa, N. (2003). Artificial Neural Networks. In *Encyclopedia of Physical Science and Technology* (pp. 631–645). https://doi.org/10.1016/B0-12-227410-5/00837-1

Wallach, D., & Goffinet, B. (1989). Mean squared error of prediction as a criterion for evaluating and comparing system models. *Ecological Modelling*, *44*(3), 299–306. https://doi.org/https://doi.org/10.1016/0304-3800(89)90035-5

Wang, J., Mahmood, Q., Qiu, J. P., Li, Y. S., Chang, Y. S., & Li, X. D. (2015). Anaerobic Treatment of Palm Oil Mill Effluent in Pilot-Scale Anaerobic EGSB Reactor. *BioMed Research International*, *2015*. https://doi.org/10.1155/2015/398028

Wang, J., Qiu, J., Li, Y.-S., Jiao, S., Mahmood, Q., Qiu, J.-P., Chang, Y.-S., Li, X.-D., & Khawar, K. M. (2015). Anaerobic Treatment of Palm Oil Mill Effluent in Pilot-Scale Anaerobic EGSB Reactor. In *Article in Journal of Biomedicine and Biotechnology*. https://www.researchgate.net/publication/273989630

Wang, S., Ma, F., Ma, W., Wang, P., Zhao, G., & Lu, X. (2019). Influence of Temperature on Biogas Production Efficiency and Microbial Community in a Two-Phase Anaerobic Digestion System. *Water 2019, Vol. 11, Page 133*, *11*(1), 133. https://doi.org/10.3390/W11010133

Watcharajinda, W., Asanakham, A., Deethayat, T., & Kiatsiriroat, T. (2021). Performance study of open pond as heat sink of water-cooled air conditioner. *Case Studies in Thermal Engineering*, *25*. https://doi.org/10.1016/J.CSITE.2021.100988

Weiland, P. (2009). Biogas production: current state and perspectives. *Applied Microbiology and Biotechnology 2009 85:4*, *85*(4), 849–860. https://doi.org/10.1007/S00253-009-2246-7

Wett, B. (2002). A straight interpretation of the solids flux theory for a three-layer sedimentation model. In *Water Research* (Vol. 36, pp. 2949–2958).

Whiting, D. A. M. (1980). *The Treatment of Liquid Wastes from Oil Palm Fruit Processing Factories*. Market Development of Palm Oil Products, International Trade Centre.

WHO. (2016). *WHO | World Health Organization*. https://www.who.int/

Wong, Y.-S., Tow Teng, T., Ong, S.-A., Norhashimah, M., Rafatullah, M., & Lee, H.-C. (2013). Anaerobic acidogenesis biodegradation of palm oil mill effluent using Suspended Closed Anaerobic Bioreactor (SCABR) at mesophilic temperature. *Procedia Environmental Sciences*, *18*, 433–441. https://doi.org/10.1016/j.proenv.2013.04.058

Won-Kee Hong. (2023). *Artificial Neural Network-based Optimized Design of Reinforced Concrete Structures* (1st ed.). CRC Press.

Wu, T. Y., Mohammad, A. W., Jahim, J. M., & Anuar, N. (2010). Pollution control technologies for the treatment of palm oil mill effluent (POME) through end-of-pipe processes. *Journal of Environmental Management*, *91*(7), 1467–1490. https://doi.org/10.1016/J.JENVMAN.2010.02.008

Wu, Y., & Feng, J. (2018). Development and Application of Artificial Neural Network. *Wireless Personal Communications*, *102*. https://doi.org/10.1007/s11277-017-5224-x

Yacob, S., Ali Hassan, M., Shirai, Y., Wakisaka, M., & Subash, S. (2006). Baseline study of methane emission from anaerobic ponds of palm oil mill effluent treatment. *Science of The Total Environment*, *366*(1), 187–196. https://doi.org/10.1016/J.SCITOTENV.2005.07.003

Yacob, S., Shirai, Y., Hung, Y.-T., & Ali Hassan, M. (2004). Treatment of Palm Oil Wastewaters. *Handbook of Industrial and Hazardous Wastes Treatment*, 719–735. https://doi.org/10.1201/9780203026519.CH16

Yap, A., Chung, K., Zaman, N. Q., Yah, F., Manaf, A., Halim, R. M., Rusnani, &, & Majid, A. (2021). Palm Oil Mills Odour Emission Survey based on Different POME Treatment System. *Jurnal Kejuruteraan*, *33*(1), 113–131. https://doi.org/10.17576/jkukm-2020-33(1)-12

Yap, C. C., Chan, Y. J., Loh, S. K., Supramaniam, C. V., Soh, A. C., Chong, M. F., Chew, C. L., & Lim, L. K. (2020). Comparison of different industrial scale palm oil mill effluent anaerobic systems in degradation of organic contaminants and kinetic performance. *Journal of Cleaner Production*, *262*, 121361. https://doi.org/https://doi.org/10.1016/j.jclepro.2020.121361

Yap, C. C., Chan, Y. J., Loh, S. K., Supramaniam, C. V., Soh, A. C., Chong, M. F., & Lim, L. K. (2021). Pilot-scale investigation of the integrated anaerobic−aerobic bioreactor (IAAB) treating palm oil mill effluent (POME): Startup and performance evaluation. *Industrial and Engineering Chemistry Research*, *60*(10), 3839–3859. https://doi.org/10.1021/ACS.IECR.0C05878/SUPPL_FILE/IE0C05878_SI_001.PDF

Yap, L. J. (2005). *Evaluation of wet scrubber systems*.

Yi, J., Dong, B., Jin, J., & Dai, X. (2014). Effect of increasing total solids contents on anaerobic digestion of food waste under mesophilic conditions: Performance and microbial characteristics analysis. *PLOS ONE*, *9*(7). https://doi.org/10.1371/journal.pone.0102548

Yong, G. T. X., Chan, Y. J., Lau, P. L., Ethiraj, B., Ghfar, A. A., Mohammed, A. A. A., Shahid, M. K., & Lim, J. W. (2023). Optimization of the Performances of Palm Oil Mill Effluent (POME)-Based Biogas Plants Using Comparative Analysis and Response Surface Methodology. *Processes*, *11*(6). https://doi.org/10.3390/pr11061603

Yoochatchaval, W., Kumakura, S., Tanikawa, D., Yamaguchi, T., Yunus, M. F. M., Chen, S. S., Kubota, K., Harada, H., & Syutsubo, K. (2011). Anaerobic degradation of palm oil mill effluent (POME). *Water Science and Technology*, *64*(10), 2001–2008. https://doi.org/10.2166/wst.2011.782

Young, michelle N., Krajmalnik-Brown, R., Liu, W., Doyle, M. L., & Rittmann, B. (2012). The role of anaerobic sludge recycle in improving anaerobic digester performance. *Bioresource Technology*, *128*. https://doi.org/10.1016/j.biortech.2012.11.079

Yule, C. M. (2008). Loss of biodiversity and ecosystem functioning in Indo-Malayan peat swamp forests. *Biodiversity and Conservation 2008 19:2*, *19*(2), 393–409. https://doi.org/10.1007/S10531-008-9510-5

Yunos, N. S. H. M., Baharuddin, A. S., Yunos, K. F. M., Naim, M. N., & Nishida, H. (2012). Physicochemical property changes of oil palm mesocarp fibers treated with high-pressure steam. *BioResources*, *7*(4), 5983–5994. https://doi.org/10.15376/biores.7.4.5983-5994

Yusof, M. A. B. M., Chan, Y. J., Chong, D. J. S., & Chong, C. H. (2024). In-ground lagoon anaerobic digester in the treatment of palm oil mill effluent (POME): Effects of process parameters and optimisation analysis. *Fuel*, *357*(PB), 129916. https://doi.org/10.1016/j.fuel.2023.129916

Yusof, M. A. B. M., Chan, Y. J., Chong, D. J. S., & Chong, C. H. (2024). In-ground lagoon anaerobic digester in the treatment of palm oil mill effluent (POME): Effects of process parameters and optimisation analysis. *Fuel*, *357*(March 2023). https://doi.org/10.1016/j.fuel.2023.129916

Zainal, N. H., Jalani, N. F., Mamat, R., & Astimar, A. A. (2017). A review on the development of palm oil mill effluent (POME) final discharge polishing treatments. *Journal of Oil Palm Research*, *29*(4), 528–540. https://doi.org/10.21894/JOPR.2017.00012

Zareei, S., & Khodaei, J. (2017). Modeling and optimization of biogas production from cow manure and maize straw using an adaptive neuro-fuzzy inference system. *Elsevier*, *114*.

Zebra BI. (2023). *How to Conduct Sensitivity Analysis in Excel - Zebra BI*. Zebra BI . https://zebrabi.com/guide/how-to-conduct-sensitivity-analysis-in-excel/

Zhai, N., Zhang, T., Yin, D., Yang, G., Wang, X., Ren, G., & Feng, Y. (2015). Effect of initial pH on anaerobic co-digestion of kitchen waste and cow manure. *Waste Management*, *38*(1), 126–131. https://doi.org/10.1016/J.WASMAN.2014.12.027

Zhang, M., & Zang, L. (2019). *IOP Conference Series: Earth and Environmental Science A review of interspecies electron transfer in anaerobic digestion*. https://doi.org/10.1088/1755-1315/310/4/042026

Zhang, R., El-Mashad, H. M., Hartman, K., Wang, F., Liu, G., Choate, C., & Gamble, P. (2007). Characterization of food waste as feedstock for anaerobic digestion. *Bioresource Technology*, *98*(4), 929–935. https://doi.org/10.1016/J.BIORTECH.2006.02.039

Zhang, W., Xing, W., & Li, R. (2018). Real-time recovery strategies for volatile fatty acid-inhibited anaerobic digestion of food waste for methane production. *Bioresource Technology*, *265*, 8292.

Zhang, W., Lang, Q., Pan, Z., Jiang, Y., Liebetrau, J., Nelles, M., Dong, H., & Dong, R. (2017). Performance evaluation of a novel anaerobic digestion operation process for treating high-solids content chicken manure: Effect of reduction of the hydraulic retention time at a constant organic loading rate. *Waste Management*, *64*, 340–347. https://doi.org/10.1016/J.WASMAN.2017.03.034

Zhou, J., Yan, B. H., Wang, Y., Yong, X. Y., Yang, Z. H., Jia, H. H., Jiang, M., & Wei, P. (2016). Effect of steam explosion pretreatment on the anaerobic digestion of rice straw. *RSC Advances*, *6*(91), 88417–88425. https://doi.org/doi.org/10.1039/C6RA15330E

Zicari, S. M. (2003). *REMOVAL OF HYDROGEN SULFIDE FROM BIOGAS USING COW-MANURE COMPOST*.

Zinatizadeh, A. A. L., Mohamed, A. R., Najafpour, G. D., Hasnain Isa, M., & Nasrollahzadeh, H. (2006). Kinetic evaluation of palm oil mill effluent digestion in a high rate up-flow anaerobic sludge fixed film bioreactor. *Process Biochemistry*, *41*(5), 1038–1046. https://doi.org/10.1016/J.PROCBIO.2005.11.011

Zuberer, D. A., & Zibilske, L. M. (2021). Composting: the microbiological processing of organic wastes. *Principles and Applications of Soil Microbiology*, 655–679. https://doi.org/10.1016/B978-0-12-820202-9.00024-1

Ministry of Economy. (2023). National Energy Transition Roadmap (NETR). In *Ministry of Economy Malaysia*. https://www.ekonomi.gov.my/sites/default/files/2023-09/National Energy Transition Roadmap_0.pdf

Anukam, A., Mohammadi, A., Naqvi, M., & Granström, K. (2019). A Review of the Chemistry of Anaerobic Digestion: Methods of Accelerating and Optimizing Process Efficiency. *Processes 2019, Vol. 7, Page 504*, *7*(8), 504. https://doi.org/10.3390/PR7080504

Chow, W. L., Chong, S., Lim, J. W., Chan, Y. J., Chong, M. F., Tiong, T. J., Chin, J. K., & Pan, G. T. (2020). Anaerobic Co-Digestion of Wastewater Sludge: A Review of Potential Co-Substrates and Operating Factors for Improved Methane Yield. *Processes 2020, Vol. 8, Page 39*, *8*(1), 39. https://doi.org/10.3390/PR8010039

Subramaniam, V., Muhamad, H., Hashim, Z., & Yuen May, C. (2014). WATER FOOTPRinT: PART 3-THE PRODUCTiOn OF CRUDE PALM OiL in MALAYSiAn PALM OiL MiLLS. *Journal of Oil Palm Research*, *26*(4), 292–299.

APPENDICES

Appendix 1: Questionnaire for POM Profiling Study

MILL BACKGROUND			REMARKS
Mill Name			
Address			
Coordinate			
Name of mill manager and contact number			
What is the capacity of the mill?	tons/hr		
QUESTIONNAIRE			
1) What is the front line system used in the POM? Please choose and explain the size and capacity			
Conventional cages system (CCS)			
Indexing system (IS)			
Continuous steriliser system (CS)			
Vertical steriliser system (VS)			
Other than the above (please specify the details)			
Number of screw press	unit		
2) What is the steam and power generation system used in the POM?			
Boiler capacity	tons/hr		
Number of boilers	unit		
Steam turbine	kW		
Other than the above (please specify the details)			
3) What is the clarifier system used in the POM? Please select and answer the respective questions			
Decanter	unit		Please specify 2 phases or 3 phases
Decanter capacity	tons/hr		
Sludge separator	unit		
Sludge separator capacity	tons/hr		
Sludge pit	unit		
Pre cleaner	unit		
How is the bottom sludge handled in the clarifier system?			To check operator's competency and what are the common problems found? How to make sure there are no oil losses?
How is the handling of the light phase and heavy phase from the decanter?			
How is the handling of steriliser condensate?			
How is the handling of waste from pre-cleaner?			

4) Empty fruit bunches (EFB) plant			
Number of EFB shredded	unit		
Number of EFB press machine	unit		
Where is the discharge point of EFB juice?			
5) Kernel recovery plant			
Number of hydro cyclones	unit		
Where is the discharge point of wastewater from a hydro cyclone?			
6) Conventional effluent treatment pond			
Number and capacity of cooling pond	unit/ m3		To check what are the common issues and problems handling the open ponding system. Desludging activities? Cost every year?
Number and capacity of mixing pond	unit/ m3		
Number and capacity of anaerobic pond	unit/ m3		
Number and capacity of facultative pond	unit/ m3		
Number and capacity of algae pond	unit/ m3		
Is there any polishing plant used? If yes, please explain			

Appendix 2: Biogas Plant and AD Profiling Study Form

PLANT NAME		**XX**
ADDRESS		
Net Export Capacity	kW/hr	
Installed Capacity	kW/hr	
Commissioning Year		
AD Capacity	m^3	
Type of AD		
Type of Feedstock		
Organic Loading Rate (OLR)	kgCOD/ m^3.d	
Hydraulic Retention Time (HRT)	days	
Mode of AD Operation		
POME Pretreatment Information		
Post AD Treatment Information		
Mixing Mechanism in AD		
Sludge Handling		
Process issues encounter since commissioning of the plant		
How to optimise profitability of the plant? Any method used previously?		
How is the performance of feedstock supply since operation? Shortage of POME supply? Frequent mill breakdown? Equipment failure? FFB diversion due to pricing? Flood and weather issue?		

Appendix 3: Biogas Plant and AD Logsheet and Checklist

Appendix 3(a): Shift Logsheet

Company Logo

Morning shift: _____

Afternoon shift: _____

Date: _____

Area	Item	Units	Time:		Time:		Time:		Comments
1. Raw effluent									
Mill	FFB processed fruit	Ton/d							
	Hours of processing	h/d							
	POME Totalizer to Biodigester	m^3							
Cooling towers	Temperature inlet	°C							
	Temperature outlet	°C							
	pH								
Mixing Tank	Temperature with recirculation	°C							
	pH								
2. Biodigester									
Bottom Sludge	pH								
	Purged sludge	m^3							
	Hours of purged	h							
	Decantation - Imhoff cone	ml/L							
Biodigester (Reactor) outlet	pH								
	Temperature	°C							
	Decantation - Imhoff cone	ml/L							
Biodigester (Reactor) outlet	pH								
	Temperature	°C							
	Decantation - Imhoff cone	ml/L							
Biodigester (Reactor)	Height of the covers (Point A)	VH/H/L/VL							
	Height of the covers (Point B)	VH/H/L/VL							
External Recirculation to reactor	Instantaneous flowrate	m^3/h							
	Hours	h							
	Daily flow	m^3/day							
	Temperature	°C							
Sedimentation pond/tank	pH at External								
	Decantation - Imhoff cone	ml/L							
	COD								
	pH at Sedimentation outlet								
	Sedimentation - Imhoff cone	ml/L							
	Temperature	°C							
	COD	mg/L							
Ambient	Temperature	°C							
Portable Analyzer	Sample point		Engine	Flare	Engine	Flare	Engine	Flare	
	CH4	%							
	CO_2	%							
	O_2	%							
	H_2S	ppm							
General comments									

Operator incharged : _____

Verified by : _____

Company Logo	**Morning shift:** _____ **Afternoon shift:** _____				**Date:** _____	
Area	**Item**	**Units**	**Time:**	**Time:**	**Time:**	**Comments**
3. Operation of biogas system						
Suction	Pressure Biogas Engine	mbar				
	Pressure Biogas Flare	mbar				
Filters	Pressure Before Wet Filter	mbar				
	Pressure After Wet Filter	mbar				
	Pressure Before Dry Filter	mbar				
	Pressure After Dry Filter	mbar				
Intercooler	Temperature Before	°C				
	Temperature After	°C				
Biogas Discharge	Pressure Engine	mbar				
	Pressure Flare	mbar				
4. Equipments						
Cooling towers	Totalizer hours fan 1	h				
	Totalizer hours fan 2	h				
Air compressors	Totalizer hrs air compressor no.1	h				
	Totalizer hrs air compressor no.2	h				
	Totalizer hrs air compressor no.3	h				
Agitation pumps	Totalizer hours pump no.1	h				
	Totalizer hours pump no.2	h				
External recirculation pumps	Totalizer hours pump no.1	h				
	Totalizer hours pump no.2	h				
Treated effluent pumps	Totalizer hours pump no.1	h				
	Totalizer hours pump no.2	h				
WF/S treated effluent pumps	Totalizer hours pump no.1	h				
	Totalizer hours pump no.2	h				
Chiller	Totalizer hours Chiller	h				
5. Equipments						
Gas Blowers	B1 totalizer hours	h				
	B2 totalizer hours	h				
Flare	Flare Totalizer	m^3				
	Instantaneous flow	m^3/h				
	Temperature	°C				
Engine	Engine Totalizer	m^3				
	Instantaneous flow	m^3/h				
	Temperature	°C				
Auto-Consumption (Mill)	Active energy	kWh		Total hour		
Self Consumption (Biogas)	Active energy	kWh		Total hour		
General comments						
Operator incharged : _____			Verified by : _____			

Appendix 3(b): Operation and Process Monthly Logsheet

Company Logo	Monthly Operation Data Sheet 1 - Effluent																			PROJECT/CLIENT LOGO
Project														Made by						
Country														Consecutive						
Date	Milling								Procesed POME					Effluent Temperature						
	Mill A			Mill B			Total		Mill A											
(DD/MM/YY)	Ton/d	h/d	Ton/h	Ton/d	h/d	Ton/h	Ton/d	Ton/h	Total Volume (m3)	m³/d	EFG (m³/TFF)	T (°C)	pH (units)	Inlet RA Mill A (°C)	Inlet RA Mill B (°C)	Outlet (°C)	≠ I - O	≠ T between 2 days	Optional CT	FAN MODE
Operation Range	XXX	0 - 24	XX	XXX	0 - 24	XXX	XXX	XXX		XXX	0,7<x<1,2	<85	>3.4	<85	<85	<42		<2	CT1/CT2	ON/OFF
1/01/25																				
2/01/25																				
3/01/25																				
4/01/25																				
5/01/25																				
6/01/25																				
7/01/25																				
8/01/25																				
9/01/25																				
10/01/25																				
Average																				
Total	0	0			0	0	0			0										

Company Logo	Monthly Operation Data Sheet 2 - Biodigester Operation																			
																PROJECT/CLIENT LOGO				
Project																				
Country																				
Date	Mixing Tank			External Recirculation				Internal Recirculation			AD Overflow			Sedimentation Pond/Tank Overflow			Purging System			
								AD 1			AD 1						Reactor 1			
(DD/MM/YY)	Inlet Raw Effluent (m^3/d)	pH	T (ºC)	Total volume (m3)	Flow (m^3/d)	Recirc./ POME (%)	pH	Total volume (m3)	Flow (m^3/d)	Recirc./ POME (%)	pH	T (ºC)	Settleable Solids (mL/L/h)	pH	T (ºC)	Settleable Solids (mL/L/h)	Purged Sludge (m3)	Settleable solids (mL/L/h)	pH	%TS
Operation Range	XXX	>6.8	<40		#VALUE!	>150%	7		0	0%	7	37	<600	7	37	<100		>900	7	3.0%
1/01/25																				
2/01/25																				
3/01/25																				
4/01/25																				
5/01/25																				
6/01/25																				
7/01/25																				
8/01/25																				
9/01/25																				
10/01/25																				
Average																				
Total	0				0				0								0			

Company Logo	Monthly Operation Data Sheet 3B - Biogas Quality	PROJECT/CLIENT LOGO

Project		Made by	
Country		Consecutive	

Date	Time	Biogas Quality										
		Before Filter/Scrubber				After Blowers						
(DD/MM/YY)	AM/PM	CH_4 (%)	CO_2 (%)	O_2 (%)	H_2S (ppm)	CH_4 (%)	CO_2 (%)	O_2 (%)	H_2S (ppm)	T Bulb (°C)	Temp Dry (°C)	% HR
Operation Range		>50%	<40%	<1.5%	<2500	>50%	<40%	<1.5%	<100			
1/01/25												#REF!
2/01/25												#REF!
3/01/25												#REF!
4/01/25												#REF!
5/01/25												#REF!
6/01/25												#REF!
7/01/25												#REF!
8/01/25												#REF!
9/01/25												#REF!
10/01/25												#REF!
Average												
Total												

Company Logo	Monthly Operation Data Sheet 4 - Lab Tests																								
																	FC0-R01				PROJECT/CLIENT LOGO				
Project																									
Country																									
Date	POME								Raw Effluent Measured (Mixing Pit: POME + Recirculation)						Bottom Sludge					AD Overflow				
	Pumping Station 1				Recirculation										Pumping Station X					AD 1				
(DD/MM/YY)	COD (mg/L)	TS (%)	VS (%)	VS/TS	COD (mg/L)	TS (%)	VS (%)	VS/TS	COD (mg/L)	TS (%)	pH	Temp	VS (%)	VS/TS	COD (mg/L)	TS (%)	pH	VS (%)	VS/TS	COD (mg/L)	TS (%)	VS (%)	VS/TS		
Operation Range	+/-60000	5.0%	4.0%	85%	+/-60000	5.0%	4.0%	85%	+/-60000	5.0%	>7	<42 °C	4.0%	85%		3.0%	>7		65.0%	<15000	<1.0%				
1/01/25																									
2/01/25																									
3/01/25																									
4/01/25																									
5/01/25																									
6/01/25																									
7/01/25																									
8/01/25																									
9/01/25																									
10/01/25																									
Average	#DIV/0!	#DIV/0!	#DIV/0!	#DIV/0!	#DIV/0!	#DIV/0!	#DIV/0!	#DIV/0!	#DIV/0!	#DIV/0!			#DIV/0!	#DIV/0!	#DIV/0!	#DIV/0!		#DIV/0!	#DIV/0!	#DIV/0!	#DIV/0!	#DIV/0!	#DIV/0!		
Total																									

Company Logo	Monthly Operation Data Sheet 3A - Biogas Users Consumption													FC0-R01		PROJECT/CLIENT LOGO		
Project														Made by				
Country														Consecutive				
Date	Biogas consumption						Power Generation							Biogas Plant Electrical self-consumption		Milling Plant Electrical Consumption		
	Genset 1 TYPE			Flare		Total biogas consumption	Genset 1 TYPE					Total Electrical generation				Mill A		Total Electrical Consumption (kW/d)
(DD/MM/YY)	Total Volume (Nm3)	Daily Flow (Nm³/d)	Flow (Nm³/h)	Total Volume (Nm3)	Daily Flow (Nm³/d)	Nm³/d	Total (kWh)	kWh/day	h tot	h/d	Average Power capacity (kW)	kWh/day	Power capacity (kW)	Total (kWh)	kWh/d	Total (kWh)	kWh/d	
Operation Range		XXX	XXX		XXX	XXX		XXX		XXX	XXX	XXX	XXX					
1/01/25						#REF!						#REF!	#REF!					#REF!
2/01/25						#REF!						#REF!	#REF!					#REF!
3/01/25						#REF!						#REF!	#REF!					#REF!
4/01/25						#REF!						#REF!	#REF!					#REF!
5/01/25						#REF!						#REF!	#REF!					#REF!
6/01/25						#REF!						#REF!	#REF!					#REF!
7/01/25						#REF!						#REF!	#REF!					#REF!
8/01/25						#REF!						#REF!	#REF!					#REF!
9/01/25						#REF!						#REF!	#REF!					#REF!
10/01/25		#REF!	#REF!		#REF!	#REF!		#REF!			#REF!	#REF!	#REF!					#REF!
Average																		
Total		#REF!			#REF!	#REF!		#REF!		0		#REF!	#REF!		0		0	#REF!

Appendix 4: Biogas Plant 2 Years Processes and Operational Datasheets

Appendix 4(a): POME Quality

Month/ Year	POME QUALITY-LEPAR HILIR (POM A)					POME QUALITY-ADELA (POM B)					POME QUALITY-KERATONG 2 (POM C)					POME QUALITY-LOK HENG (POM D)				
	COD (mg/L)	pH	TS (mg/L)	SS (mg/L)	BOD (mg/L)	COD (mg/L)	pH	TS (mg/L)	SS (mg/L)	BOD (mg/L)	COD (mg/L)	pH	TS (mg/L)	SS (mg/L)	BOD (mg/L)	COD (mg/L)	pH	TS (mg/L)	SS (mg/L)	BOD (mg/L)
Jul-19	65,012	4.45	24,500	12,300	28,858	78,230	4.52	38,690	20,620	32,100	64,025	4.59	27,760	21,340	34,476	89,800	4.65	56,420	45,240	44,320
Aug-19	59,002	5.23	21,033	17,065	23,261	77,230	4.61	42,386	25,580	37,000	61,300	4.61	32,390	24,300	35,110	78,645	4.77	54,283	39,850	40,800
Sep-19	55,957	5.20	25,276	12,683	23,700	79,820	4.43	45,114	28,600	33,560	60,233	5.00	27,385	16,783	25,389	92,844	4.68	49,378	37,144	45,780
Oct-19	72,442	5.10	27,543	13,635	29,573	76,230	4.38	49,900	24,829	36,700	60,546	5.14	25,460	12,987	28,683	81,788	4.73	45,000	38,442	40,700
Nov-19	63,473	4.90	25870	13,655	30,233	81,713	4.45	42300	28,313	40,600	53,654	4.76	27620	15,760	22,900	77,340	4.49	43000	29,943	36,500
Dec-19	63,195	4.65	28,000	14,500	23,027	75,340	4.29	46,500	20,984	33,240	56,330	4.84	21,450	17,210	23,587	78,400	4.50	53,214	38,871	40,380
Jan-20	64,300	4.67	24,540	18,600	22,650	82,950	4.37	51,100	25,875	41,200	56,179	4.63	29,100	16,926	25,430	83,400	4.70	44,300	56,450	39,800
Feb-20	69,800	4.84	23,670	14,434	26,900	85,500	4.34	49,100	23,450	39,730	55,900	4.75	32,520	18,900	24,800	87,200	4.50	48,000	57,650	41,290
Mar-20	69,200	4.74	28,500	16,500	22,500	86,300	4.20	46,780	29,300	44,890	68,354	4.87	34,110	19,856	29,800	82,300	4.50	55,505	34,600	40,540
Apr-20	68,900	4.38	32,520	15,430	23,829	90,550	4.40	45,600	35,460	43,080	60,000	4.73	34,800	23,900	29,650	84,000	4.55	41,474	26,900	44,100
May-20	67,300	4.60	21,610	16,980	25,400	79,600	4.59	40,500	26,500	40,100	65,603	4.74	33,500	23,450	26,780	88,700	4.79	42,738	22,250	46,700
Jun-20	68,000	4.73	23,470	15,670	28,900	78,100	4.57	49,700	24,000	43,200	61,200	5.02	31,820	19,000	27,100	85,600	4.96	48,625	29,458	45,600
Jul-20	67,500	4.90	27,500	16,510	33,576	81,900	4.61	47,830	29,030	39,000	59,340	4.78	32,171	25,600	36,504	84,200	4.73	41,105	29,175	44,440
Aug-20	68,819	5.00	20,148	15,700	34,476	88,600	4.42	42,800	26,303	45,780	62,300	4.76	21,300	18,700	36,700	88,300	4.76	48,635	27,900	40,800
Sep-20	72,838	4.90	30,630	20,420	27,378	85,000	4.59	48,900	22,340	44,760	55,700	4.82	27,152	17,174	28,900	88,700	4.76	53,170	32,733	43,560
Oct-20	67,700	5.00	28,420	17,600	30,400	83,600	4.51	44,560	29,700	35,700	59,900	4.72	29,913	19,000	27,650	86,300	4.48	51,700	30,145	38,790
Nov-20	69,583	4.80	31100	18,954	32,900	81,900	4.53	48000	33,260	39,020	55,300	4.81	30139	21,000	29,000	85,400	4.71	49,300	25,623	39,760

Dec-20	71,000	4.80	22,750	16,700	29,800	80,100	4.57	53,700	29,430	44,780	56,900	4.75	25,413	21,000	27,430	79,300	4.70	46,740	36,012	41,450
Jan-21	65,012	4.45	25,670	19,640	28,858	80,150	4.43	41,906	25,400	33,450	58,300	4.51	24,320	18,902	27,885	72,648	4.70	50,333	28,963	38,760
Feb-21	70,790	4.60	24,100	17,065	23,261	81,140	4.43	44,780	27,820	39,600	59,000	4.65	28,563	20,100	33,462	75,205	4.67	44,125	28,073	42,310
Mar-21	69,800	4.80	25,276	12,683	23,700	80,560	4.46	51,340	28,500	42,300	64,375	4.63	33,017	21,450	28,760	92,400	4.94	37,700	24,978	47,520
Apr-21	72,442	5.10	27,543	13,635	29,573	89,820	4.71	46,200	28,760	44,320	53,450	4.60	30,607	16,540	27,885	91,113	4.81	44,517	30,027	41,290
May-21	65,400	4.90	25,870	13,655	30,233	82,430	4.65	44,320	28,040	37,640	57,890	4.55	28,600	18,650	25,857	78,667	4.69	38,105	26,519	44,670
Jun-21	69,230	4.65	25,480	13,670	23,027	80,920	4.58	41,200	26,450	41,890	61,300	4.61	29,780	23,450	28,710	90,800	4.78	49,800	30,600	43,290
AVG 2019	63,177	4.98	24,844	13,868	27,125	78,645	4.48	43,678	25,588	35,992	59,952	4.82	28,123	18,234	29,312	84,083	4.66	49,616	38,124	41,620
AVG 2020	68,745	4.78	26,238	16,958	28,226	83,675	4.47	47,381	27,887	41,770	59,723	4.78	30,162	20,376	29,145	85,283	4.68	47,608	34,075	42,236
AVG 2021	68,779	4.75	25,657	15,058	26,442	82,503	4.54	44,958	27,495	39,867	59,053	4.59	29,148	19,849	28,760	83,472	4.77	44,097	28,193	42,973

Appendix 4(b): Pretreatment Process

Month/ Year	PRETREATMENT INFORMATION-LEPAR HILIR									PRETREATMENT INFORMATION-ADELA								
	POME from Cooling Pond (EFM 01)	Temperature and pH Inlet Mixing Tank (ETT 01)		Temperature and pH Outlet Mixing Tank (ETT 02)		BS Recirculation to Mixing Tank	TE Recirculation to Mixing Tank	Total Recirculation to Mixing Tank	Ratio of Recirculation to POME in the Mixing Tank	POME from Cooling Pond (EFM 01)	Temperature and pH Inlet Mixing Tank (ETT 01)		Temperature and pH Outlet Mixing Tank (ETT 02)		BS Recirculation to Mixing Tank	TE Recirculation to Mixing Tank	Total Recirculation to Mixing Tank	Ratio of Recirculation to POME in the Mixing Tank
	Total Feeding to AD (m^3/month)	Temp Inlet (°C)	pH Inlet	Temp Outlet (°C)	pH Outlet	BS Rec. (m^3/month)	TE Rec. (m^3/month)	Total Rec. (m3/month_	Ratio of Total Rec. To POME (%)	Total Feeding to AD (m^3/month)	Temp Inlet (°C)	pH Inlet	Temp Outlet (°C)	pH Outlet	BS Rec. (m^3/month)	TE Rec. (m^3/month)	Total Rec. (m3/month_	Ratio of Total Rec. To POME (%)
Jul-19	14,748	56.0	4.45	41.8	7.40	16,740	16,812	33,552	228%	16,640	48.6	4.52	37.6	7.00	13,775	6,908	20,683	124%
Aug-19	17,239	53.7	5.23	42.3	7.30	17,499	14,861	32,360	188%	18,115	53.4	4.61	41.4	7.08	17,992	12,735	30,727	170%
Sep-19	22,977	54.0	5.20	42.8	7.10	9,868	12,084	21,952	96%	15,256	52.7	4.43	42.5	6.90	15,738	27,167	42,905	281%
Oct-19	19,316	55.2	5.10	42.7	7.10	7,674	16,152	23,826	123%	16,438	54.7	4.38	43.2	7.00	19,010	32,180	51,190	311%
Nov-19	19,833	54.0	4.90	41.5	7.20	9,431	11,005	20,436	103%	14,042	55.2	4.45	41.4	6.90	16,816	25,796	42,612	303%
Dec-19	16,761	53.0	4.65	40.0	7.10	12,739	14,105	26,844	160%	13,957	46.8	4.29	37.9	6.90	16,787	22,533	39,320	282%
Jan-20	10,508	54.2	4.67	39.0	7.01	8,811	4,817	13,628	130%	11,170	55.3	4.37	39.2	6.90	17,176	20,158	37,334	334%
Feb-20	12,789	56.5	4.84	38.6	7.06	3,553	3,845	7,398	58%	13,330	55.0	4.34	39.5	6.84	15,839	24,796	40,635	305%
Mar-20	16,072	54.0	4.74	41.3	7.05	10,678	11,440	22,118	138%	5,323	55.8	4.20	39.1	6.90	11,672	11,871	23,543	442%
Apr-20	19,416	56.0	4.38	43.6	7.00	10,532	2,400	12,932	67%	13,991	54.4	4.40	41.0	7.00	15,631	21,470	37,101	265%
May-20	18,864	55.0	4.60	44.7	7.03	3,366		3,366	18%	12,660	56.0	4.59	41.4	7.10	16,088	14,253	30,341	240%

Jun-20	13,103	53.7	4.73	43.8	6.99	7,178		7,178	55%	16,019	54.0	4.57	41.0	7.00	17,562	21,314	38,876	243%
Jul-20	14,298	56.5	4.90	44.1	7.01	8,043		8,043	56%	16,741	55.1	4.61	40.1	7.10	17,912	26,799	44,711	267%
Aug-20	14,734	57.3	5.00	43.6	7.05	11,991		11,991	81%	15,331	55.8	4.42	40.1	6.97	16,397	27,542	43,939	287%
Sep-20	12,827	58.0	4.90	43.2	7.10	10,055		10,055	78%	17,763	55.8	4.59	40.8	6.99	18,043	18,043	36,086	203%
Oct-20	13,174	56.7	5.00	46.2	7.01	12,647		12,647	96%	15,479	55.8	4.51	42.3	6.85	17,230	17,230	34,460	223%
Nov-20	9,983	56.4	4.80	44.4	7.08	9,520		9,520	95%	17,324	55.9	4.53	42.1	6.90	16,088	16,088	32,176	186%
Dec-20	9,556	52.2	4.80	43.0	7.10	12,628		12,628	132%	13,969	54.7	4.57	41.1	6.80	16,031	16,031	32,062	230%
Jan-21	12,145	55.4	4.45	39.0	6.91	13,697		13,697	113%	11,225	50.9	4.43	38.6	6.92	14,263	8,018	22,281	198%
Feb-21	5,525	56.2	4.60	35.9	6.98	2,712		2,712	49%	12,670	54.5	4.43	39.5	6.98	8,731	9,050	17,781	140%
Mar-21	13,016	52.9	4.80	38.7	6.99	9,359		9,359	72%	12,041	54.8	4.46	40.7	6.92	8,431	8,601	17,032	141%
Apr-21	14,015	55.5	5.10	40.6	7.03	10,267		10,267	73%	10,759	53.6	4.71	40.2	7.06	10,419	7,685	18,104	168%
May-21	15,492	54.0	4.90	41.2	7.01	12,341		12,341	80%	12,558	55.5	4.65	40.3	7.03	17,125	8,970	26,095	208%
Jun-21	14,500	55.0	4.65	40.8	7.00	12,300		12,300	85%	15,641	53.8	4.58	40.2	7.01	18,600	9,100	27,700	177%
AVG 2019	18,479	54.3	4.98	41.9	7.20	12,325	14,170	26,495	150%	15,741	51.9	4.48	40.7	6.96	16,686	21,220	37,906	245%
AVG 2020	13,777	55.5	4.78	43.0	7.04	9,084	5,626	10,959	84%	14,092	55.3	4.47	40.6	6.95	16,306	19,633	35,939	269%
AVG 2021	12,449	54.8	4.75	39.4	6.99	10,113		10,113	79%	12,482	53.8	4.54	39.9	6.99	12,928	8,571	21,499	172%

Month/ Year	PRETREATMENT INFORMATION-KERATONG 2									PRETREATMENT INFORMATION-LOK HENG									
	POME from Cooling Pond (EFM 01)	Temperature and pH Inlet Mixing Tank (ETT 01)		Temperature and pH Outlet Mixing Tank (ETT 02)		BS Recirculation to Mixing Tank	TE Recirculation to Mixing Tank	Total Recirculation to Mixing Tank	Ratio of Recirculation to POME in the Mixing Tank	POME from Cooling Pond (EFM 01)	Temperature and pH Inlet Mixing Tank (ETT 01)		Temperature and pH Outlet Mixing Tank (ETT 02)		BS Recirculation to Mixing Tank	TE Recirculation to Mixing Tank	Total Recirculation to Mixing Tank	Ratio of Recirculation to POME in the Mixing Tank	
	Total Feeding to AD (m^3/month)	Temp Inlet (°C)	pH Inlet	Temp Outlet (°C)	pH Outlet	BS Rec. (m^3/month)	TE Rec. (m^3/month)	Total Rec. (m3/month_	Ratio of Total Rec. To POME (%)	Total Feeding to AD (m^3/month)	Temp Inlet (°C)	pH Inlet	Temp Outlet (°C)	pH Outlet	BS Rec. (m^3/month)	TE Rec. (m^3/month)	Total Rec. (m3/month_	Ratio of Total Rec. To POME (%)	
Jul-19	17,016	62.4	4.59	44.0	6.92	28,392	23,642	52,034	306%	14,805	57.0	4.65	44.4	6.78		9,109	9,109	62%	
Aug-19	19,863	60.6	4.61	44.1	6.90	30,195	18,845	49,040	247%	12,831	54.7	4.77	46.1	6.80		7,165	7,165	56%	
Sep-19	22,507	62.0	5.00	44.1	6.90	28,441		28,441	126%	11,035	52.9	4.68	48.6	6.90		7,094	7,094	64%	
Oct-19	24,236	59.9	5.14	44.2	6.86	25,557		25,557	105%	14,644	55.5	4.73	48.7	6.80		8,250	8,250	56%	
Nov-19	13,076	56.1	4.76	40.6	6.92	20,022	301	20,323	155%	13,473	59.8	4.49	46.0	6.75		7,808	7,808	58%	
Dec-19	12,536	53.8	4.84	38.4	6.90	29,444	1,064	30,508	243%	14,858	60.1	4.50	46.1	6.90		8,238	8,238	55%	
Jan-20	9,390	55.2	4.63	37.9	6.82	21,478	2,670	24,148	257%	9,859	58.4	4.70	41.0	6.98	16,283	7,432	23,715	241%	
Feb-20	16,069	58.1	4.75	39.9	6.88	19,302		19,302	120%	8,746	58.0	4.50	41.6	6.97	15,475	6,568	22,043	252%	
Mar-20	13,258	55.3	4.87	42.4	6.89	20,012		20,012	151%	10,817	60.1	4.50	43.8	6.96	5,820	7,721	13,541	125%	
Apr-20	16,867	56.3	4.73	43.8	6.90	15,830		15,830	94%	7,264	57.6	4.55	43.5	6.96	6,002	4,691	10,693	147%	
May-20	15,375	57.7	4.74	44.2	6.98	12,031		12,031	78%	7,036	58.3	4.79	44.4	6.94	6,004	1,509	7,513	107%	
Jun-20	18,326	58.9	5.02	44.0	6.95	14,570		14,570	80%	6,709	57.5	4.96	43.4	6.94	5,020	6,027	11,047	165%	
Jul-20	15,894	57.5	4.78	42.0	6.88	17,117		17,117	108%	6,497	59.3	4.73	44.0	6.94	4,711	6,115	10,826	167%	
Aug-20	15,711	56.3	4.76	42.4	6.84	18,116		18,116	115%	3,577	58.0	4.76	41.5	7.02	9,074		9,074	254%	

Sep-20	18,779	58.5	4.82	43.9	6.85	19,524		19,524	104%	4,060	59.3	4.76	39.7	7.05	12,456		12,456	307%
Oct-20	19,988	55.4	4.72	44.0	6.85	21,491		21,491	108%	4,776	58.0	4.48	44.2	6.99	9,178	2,658	11,836	248%
Nov-20	17,994	56.0	4.81	42.9	6.93	18,881		18,881	105%	9,190	57.9	4.71	45.6	6.93	5,725	5,446	11,171	122%
Dec-20	20,457	57.2	4.75	44.1	6.95	18,232		18,232	89%	10,462	59.2	4.70	44.1	6.95	7,181	8,697	15,878	152%
Jan-21	21,349	47.8	4.51	38.4	6.90	19,700		19,700	92%	10,096	57.5	4.70	37.8	6.91	6,180	10,478	16,658	165%
Feb-21	8,927	50.8	4.65	38.2	6.90	9,004		9,004	101%	9,350	57.9	4.67	39.5	6.88	3,287	5,935	9,222	99%
Mar-21	16,760	50.4	4.63	39.8	6.80	12,670		12,670	76%	10,568	55.9	4.94	40.1	6.78	905	6,898	7,803	74%
Apr-21	20,785	53.7	4.60	39.2	6.80	18,700		18,700	90%	11,552	56.7	4.81	39.8	6.86	5,117	9,533	14,650	127%
May-21	20,010	47.8	4.55	42.0	6.85	20,010		20,010	100%	10,328	56.1	4.69	39.8	6.86	6,749	4,207	10,956	106%
Jun-21	21,001	51.3	4.61	42.1	6.78	24,300		24,300	116%	10,800	55.8	4.78	40.0	6.90	9,720	4,300	14,020	130%
AVG 2019	18,206	59.1	4.82	42.6	6.90	27,009	10,963	34,317	197%	13,608	56.7	4.66	46.7	6.82		7,944	7,944	59%
AVG 2020	16,509	56.9	4.78	42.6	6.89	18,049	2,670	18,271	117%	7,416	58.5	4.68	43.1	6.97	8,577	5,686	13,316	190%
AVG 2021	18,139	50.3	4.59	40.0	6.84	17,397	#DIV/0!	17,397	96%	10,449	56.7	4.77	39.5	6.87	5,326	6,892	12,218	117%

Appendix 4(c): Treated Effluent Quality

Month/ Year	TREATED EFFLUENT QUALITY-LEPAR HILIR						TREATED EFFLUENT QUALITY-ADELA						TREATED EFFLUENT QUALITY-KERATONG 2						TREATED EFFLUENT QUALITY-LOK HENG					
	pH	**Temp (°C)**	**COD (mg/L)**	**TS mg/l**	**SS (mg/L)**	**BOD (mg/L)**	**pH**	**Temp (°C)**	**COD (mg/L)**	**TS mg/l**	**SS (mg/L)**	**BOD (mg/L)**	**pH**	**Temp (°C)**	**COD (mg/L)**	**TS mg/l**	**SS (mg/L)**	**BOD (mg/L)**	**pH**	**Temp (°C)**	**COD (mg/L)**	**TS mg/l**	**SS (mg/L)**	**BOD (mg/L)**
Jul-19	7.20	37.8	20,800	15,400	16,540	3,650	7.40	38.0	18,540	16,780	12,450	5,530	7.16	41.8	18,300	14,650	10,710	5,780	7.28	40.8	15,300	13,000	10,800	3,650
Aug-19	7.10	39.1	17,500	11,200	16,660	3,230	7.34	37.0	15,400	12,900	9,990	4,980	7.18	42.3	17,100	15,400	1,220	4,230	7.55	44.3	18,700	15,400	11,900	2,970
Sep-19	7.21	40.3	18,600	13,450	11,111	4,050	7.40	37.0	19,340	16,700	9,790	5,670	7.21	41.7	16,700	15,400	386	4,440	7.42	44.5	15,400	11,300	10,670	4,100

Oct-19	7.15	40.1	15,320	10,900	10,230	3,860	7.65	37.5	18,650	20,900	11,778	3,999	7.12	41.7	15,230	12,600	415	3,980	7.39	44.1	21,300	12,141	9,991	2,970
Nov-19	7.10	39.6	12,780	10,800	8,769	3,570	7.68	40.0	16,790	14,300	10,162	4,120	7.11	40.0	15,230	19,000	618	4,627	7.50	43.5	15,400	12,000	10,234	3,360
Dec-19	7.20	40.4	18,650	16,540	14,322	3,990	7.57	39.0	16,390	14,300	12,340	4,530	7.10	36.5	16,500	12,450	561	4,100	7.44	41.3	18,400	15,400	15,340	3,590
Jan-20	7.18	41.7	11,528	11,822	10,714	4,230	7.39	38.0	17,800	12,755	10,605	4,560	7.08	36.0	9,200	8,570	5,130	3,250	7.23	39.8	14,400	19,100	12,300	3,340
Feb-20	7.31	42.3	11,300	11,997	11,064	4,440	7.47	38.0	16,500	11,150	8,460	5,640	7.11	36.5	14,300	13,200	10,600	3,448	7.45	38.8	13,900	11,300	9,535	2,990
Mar-20	7.28	42.1	12,700	12,951	12,428	3,450	7.35	39.0	16,800	12,340	16,300	3,450	7.02	40.5	12,600	10,800	9,395	2,383	7.15	39.7	13,600	10,100	8,700	3,200
Apr-20	7.10	42.4	10,330	12,958	12,324	2,990	7.46	37.0	17,300	13,000	10,600	4,320	7.12	40.5	10,300	9,005	11,010	1,990	7.22	38.9	14,500	15,400	12,980	3,560
May-20	7.20	42.5	14,020	8,600	12,789	2,356	7.46	36.7	15,400	15,430	11,960	3,980	7.00	42.3	11,900	9,995	5,690	2,687	7.27	37.4	13,500	15,800	10,800	2,890
Jun-20	7.41	40.9	13,443	7,505	12,916	4,100	7.45	39.6	14,500	15,220	19,900	3,860	7.14	42.3	13,600	11,180	8,980	3,006	7.40	37.5	17,800	18,300	14,641	3,800
Jul-20	7.20	40.8	12,000	9,700	12,031	4,348	7.40	39.1	15,800	16,230	12,000	4,400	7.10	42.5	10,299	9,820	8,805	2,789	7.24	37.6	17,000	22,475	16,200	3,750
Aug-20	7.10	40.9	13,730	10,800	15,367	3,900	7.40	39.0	17,800	19,340	14,635	4,510	7.14	42.4	10,496	11,200	8,809	3,040	7.20	36.7	13,900	16,800	12,600	2,680
Sep-20	7.10	40.9	11,800	14,648	13,916	3,456	7.41	38.6	16,900	16,530	11,940	3,990	7.10	41.5	12,100	10,800	9,842	3,130	7.32	37.2	13,450	12,000	10,800	2,990
Oct-20	7.20	40.9	12,606	15,495	14,720	2,694	7.43	40.5	18,300	17,770	12,270	4,190	7.13	40.8	10,900	9,920	10,618	2,560	7.28	35.3	18,300	19,602	15,400	4,250
Nov-20	7.20	41.1	13,820	15,833	13,782	3,120	7.38	41.0	18,800	17,320	13,725	4,590	7.04	41.5	11,400	8,910	10,192	3,090	7.35	36.4	18,470	21,320	18,326	4,050
Dec-20	7.20	41.0	14,515	14,452	13,908	3,370	7.34	40.6	19,200	21,480	17,090	4,800	7.08	41.0	11,718	10,230	10,172	3,350	7.28	35.6	20,766	25,652	16,200	4,560
Jan-21	7.20	38.8	14,670	11,822	10,714	3,460	7.33	38.7	17,230	18,600	12,340	4,440	7.06	35.8	10,595	9,700	8,830	2,789	7.21	37.6	21,300	20,800	21,300	3,350
Feb-21	7.20	38.9	16,320	11,997	11,064	3,870	7.38	39.1	18,180	15,900	12,900	3,980	7.08	35.9	12,262	11,900	6,706	3,100	7.25	38.0	18,200	20,140	18,650	3,100
Mar-21	7.10	39.0	11,230	12,951	12,428	2,970	7.64	40.4	17,770	14,640	11,400	4,620	7.09	38.1	12,220	12,300	10,841	3,190	7.30	37.5	19,980	17,540	14,980	3,750
Apr-21	7.20	38.9	15,670	12,958	12,324	3,330	7.55	39.5	19,210	17,650	15,400	4,780	7.12	38.4	11,719	10,920	11,659	2,738	7.25	37.8	22,670	20,650	18,240	4,090
May-21	7.20	39.5	13,870	13,429	12,789	2,910	7.50	37.0	18,230	14,280	10,900	4,310	7.14	40.2	11,817	10,230	9,722	2,930	7.41	39.0	23,670	20,900	16,200	2,850
Jun-21	7.15	39.1	15,340	12,670	11,008	3,390	7.51	38.3	17,540	15,550	12,900	5,020	7.10	40.1	12,560	10,500	10,105	3,080	7.35	39.3	22,440	21,450	17,230	2,900
AVG 2019	7.16	39.6	17,275	13,048	12,939	3,725	7.51	38.1	17,518	15,980	11,085	4,805	7.15	40.7	16,510	14,917	2,318	4,526	7.43	43.1	17,417	13,207	11,489	3,440
AVG 2020	7.21	41.5	12,649	12,230	12,997	3,538	7.41	38.9	17,092	15,714	13,290	4,358	7.09	40.6	11,568	10,303	9,104	2,894	7.28	37.6	15,799	17,321	13,207	3,505
AVG 2021	7.18	39.0	14,517	12,638	11,721	3,474	7.49	38.8	18,027	16,103	12,640	4,525	7.10	38.1	11,862	10,925	9,644	2,971	7.30	38.2	21,377	20,247	17,767	3,340

Appendix 4(d): Bottom Sludge Quality

Month/ Year	BOTTOM SLUDGE QUALITY-LEPAR HILIR					BOTTOM SLUDGE QUALITY-ADELA					BOTTOM SLUDGE QUALITY-KERATONG 2					BOTTOM SLUDGE QUALITY-LOK HENG				
	pH	Temp (°C)	COD (mg/L)	TS mg/l	SS (mg/L)	pH	Temp (°C)	COD (mg/L)	TS mg/l	SS (mg/L)	pH	Temp (°C)	COD (mg/L)	TS mg/l	SS (mg/L)	pH	Temp (°C)	COD (mg/L)	TS mg/l	SS (mg/L)
Jul-19	7.29	39.4	30,711	30,700	27,737	7.02	32.3	30,900	36,790	31,633	7.05	41.7	28,900	26,275	21,940	7.28	42.0	36,300	34,500	46,700
Aug-19	7.25	40.1	30,140	30,910	25,557	7.15	36.4	30,660	35,696	37,440	7.05	42.0	28,678	26,068	18,088	7.33	44.0	22,070	36,033	30,943
Sep-19	7.25	41.0	28,591	26,177	16,189	7.01	39.4	39,340	33,498	29,100	7.05	41.7	25,670	25,630	18,870	7.38	44.0	33,174	39,678	24,218
Oct-19	7.09	40.1	34,902	27,543	13,635	7.08	41.4	34,233	37,800	38,933	7.06	41.7	26,500	25,600	20,800	7.38	43.7	32,175	31,300	25,755
Nov-19	7.16	39.9	29,255	22,213	23,210	7.16	40.6	38,100	33,200	34,225	7.00	40.0	25,400	27,450	18,880	7.41	43.4	36,667	33,560	24,433
Dec-19	7.02	38.8	30,287	22,723	18,050	7.09	37.5	27,875	38,850	32,175	7.01	36.8	21,400	22,486	20,300	7.48	41.5	22,125	28,350	20,875
Jan-20	7.05	36.0	33,069	20,718	16,058	7.13	37.6	35,800	42,550	29,870	7.03	35.6	27,799	25,090	18,900	7.19	39.7	33,500	31,290	30,980
Feb-20	7.00	37.0	33,384	20,860	16,840	7.10	37.9	31,200	35,500	28,300	7.00	36.0	20,981	21,390	23,450	7.31	39.9	40,200	36,500	29,870
Mar-20	7.02	38.0	25,600	28,600	19,040	7.21	38.6	31,570	33,800	24,400	6.94	39.5	26,112	21,780	16,595	7.08	39.9	33,000	33,450	32,650
Apr-20	7.00	40.0	15,920	11,550	9,356	7.13	40.4	30,200	35,400	34,150	6.96	40.5	29,801	24,560	17,680	7.20	40.2	39,700	38,900	29,450
May-20	7.01	41.0	27,710	8,460	7,060	7.30	41.8	31,000	33,450	18,100	7.00	41.5	25,700	25,670	21,390	7.25	39.7	34,000	33,670	31,450
Jun-20	7.22	39.0	25,670	15,670	8,765	7.27	39.8	33,400	36,540	29,300	7.07	41.8	30,200	23,526	22,780	7.27	38.6	33,450	39,800	34,807
Jul-20	7.10	40.0	25,216	19,122	11,934	7.32	39.1	32,400	37,000	29,400	7.16	41.8	33,900	22,600	23,000	7.28	39.9	40,075	41,350	38,169
Aug-20	7.10	40.0	28,540	24,670	25,400	7.26	38.9	33,330	36,700	33,270	7.11	41.2	24,500	24,392	21,570	7.34	36.8	41,000	43,250	41,300
Sep-20	7.10	41.0	27,650	24,900	21,450	7.26	38.4	30,800	32,900	28,900	7.02	40.7	28,500	23,387	22,780	7.34	37.1	39,870	45,690	40,200
Oct-20	7.20	42.0	26,500	25,670	22,700	7.31	40.5	31,800	37,650	34,500	7.05	40.6	29,400	27,306	26,900	7.35	34.0	32,070	44,670	39,800
Nov-20	7.20	43.0	25,900	25,400	18,700	7.27	41.0	42,355	38,600	32,500	7.01	38.0	22,800	28,846	25,300	7.28	35.6	37,215	45,465	42,133
Dec-20	7.20	42.0	26,700	23,231	21,890	7.23	40.6	36,516	37,500	31,900	7.06	36.9	22,680	26,464	26,700	7.32	35.7	45,232	49,070	41,090
Jan-21	7.16	37.0	23,210	21,450	25,655	7.23	38.7	36,590	39,672	39,700	7.05	35.2	28,340	26,426	21,300	7.34	35.6	37,222	44,200	41,375

Feb-21	7.20	35.6	21,985	23,400	24,816	7.23	39.1	33,200	40,400	41,881	7.01	35.3	22,820	26,589	19,700	7.38	36.1	35,455	42,300	42,063
Mar-21	7.20	37.3	23,165	22,450	22,016	7.31	40.3	35,670	38,710	38,000	7.04	37.3	24,000	27,297	26,575	7.30	36.3	31,580	39,921	37,068
Apr-21	7.11	38.0	26,503	25,600	24,714	7.29	40.2	38,875	38,400	35,400	7.12	37.9	22,900	26,157	25,282	7.44	38.2	27,600	34,678	30,100
May-21	7.18	39.1	22,398	26,700	23,118	7.31	40.2	35,600	40,110	37,490	7.09	39.7	26,200	26,350	23,090	7.40	38.3	36,133	33,241	30,230
Jun-21	7.13	39.5	21,460	20,800	16,400	7.28	40.5	34,449	38,600	35,100	7.05	39.8	27,500	29,100	25,430	7.41	39.0	33,500	31,200	28,700
AVG 2019	7.18	39.9	30,648	26,711	20,730	7.08	37.9	33,518	35,972	33,918	7.04	40.7	26,091	25,585	19,813	7.38	43.1	30,419	33,904	28,821
AVG 2020	7.10	39.9	26,822	20,738	16,599	7.23	39.6	33,364	36,466	29,549	7.03	39.5	26,864	24,584	22,254	7.27	38.1	37,443	40,259	35,992
AVG 2021	7.16	37.8	23,120	23,400	22,787	7.28	39.8	35,731	39,315	37,928	7.06	37.5	25,293	26,986	23,563	7.38	37.2	33,582	37,590	34,923

Appendix 4(e): Biogas Production and Quality

Month/ Year	BIOGAS QUANTITY AND QUALITY-LEPAR HILIR						BIOGAS QUANTITY AND QUALITY-ADELA						BIOGAS QUANTITY AND QUALITY-KERATONG 2						BIOGAS QUANTITY AND QUALITY-LOK HENG					
	Total Biogas (Nm^3/month)	% CH_4	% CO_2	% O_2	H_2S Raw Biogas (ppm)	H_2S Biogas to Engine (ppm)	Total Biogas (Nm^3/month)	% CH_4	% CO_2	% O_2	H_2S Raw Biogas (ppm)	H_2S Biogas to Engine (ppm)	Total Biogas (Nm^3/month)	% CH_4	% CO_2	% O_2	H_2S Raw Biogas (ppm)	H_2S Biogas to Engine (ppm)	Total Biogas (Nm^3/month)	% CH_4	% CO_2	% O_2	H_2S Raw Biogas (ppm)	H_2S Biogas to Engine (ppm)
Jul-19	219,655	63.48 %	32.95 %	0.46 %	773	4	333,352	60.80 %	36.86 %	0.19 %	1,132	19	261,546	57.82 %	33.82 %	0.02 %	1,480	9	339,925	57.90 %	38.20 %	0.59 %	777	62
Aug-19	264,108	63.43 %	34.05 %	0.58 %	835	21	443,300	59.70 %	38.26 %	0.28 %	1,310	10	349,714	59.04 %	33.96 %	0.05 %	1,310	16	366,223	61.60 %	33.59 %	0.47 %	913	54
Sep-19	312,693	62.48 %	32.90 %	0.52 %	1,007	12	425,146	55.74 %	43.57 %	0.21 %	1,448	8	289,653	64.02 %	33.35 %	0.11 %	1,604	25	373,238	62.53 %	32.92 %	0.34 %	658	17

Oct-19	334,646	63.61 %	34.06 %	0.43 %	610	1	457,064	56.98 %	38.84 %	0.32 %	1,346	41	355,464	62.38 %	33.80 %	0.16 %	1,680	21	396,169	59.92 %	35.33 %	0.50 %	963	51
Nov-19	312,703	63.66 %	33.95 %	0.43 %	386	0	411,041	57.97 %	33.44 %	0.01 %	905	5	239,492	61.23 %	33.91 %	0.23 %	943	10	361,256	61.96 %	33.60 %	0.54 %	840	39
Dec-19	248,195	63.21 %	32.93 %	0.40 %	261	0	341,079	59.46 %	34.43 %	0.60 %	1,178	4	227,830	63.10 %	31.94 %	0.20 %	793	1	314,103	60.26 %	34.30 %	0.46 %	958	185
Jan-20	161,655	61.00 %	32.25 %	0.40 %	246	1	367,177	58.96 %	35.90 %	0.44 %	805	7	204,275	60.73 %	35.20 %	0.20 %	535	6	357,034	60.20 %	33.68 %	0.61 %	923	32
Feb-20	197,186	63.42 %	34.37 %	0.40 %	220	0	387,919	58.75 %	35.36 %	0.58 %	939	12	287,514	60.99 %	34.01 %	0.22 %	902	5	294,628	60.38 %	34.43 %	0.67 %	1,025	31
Mar-20	299,175	62.74 %	35.14 %	0.37 %	604	0	223,490	59.63 %	33.92 %	0.71 %	1,172	18	286,485	60.10 %	34.80 %	0.13 %	1,130	7	374,309	59.94 %	34.50 %	0.63 %	978	59
Apr-20	371,367	62.62 %	34.48 %	0.38 %	1,046	0	459,193	58.88 %	35.51 %	0.71 %	1,150	21	358,272	61.81 %	35.46 %	0.16 %	1,280	11	216,891	60.96 %	36.09 %	0.70 %	991	50
May-20	339,122	62.22 %	34.50 %	0.42 %	1,073	1	398,659	57.68 %	34.56 %	0.95 %	1,261	16	372,075	60.40 %	34.89 %	0.21 %	1,195	23	161,894	59.97 %	34.87 %	0.75 %	822	30
Jun-20	216,612	62.12 %	34.68 %	0.47 %	776	1	459,086	58.45 %	33.82 %	1.00 %	1,461	101	391,762	60.71 %	35.80 %	0.22 %	1,256	29	179,462	60.10 %	34.78 %	0.74 %	1,143	90
Jul-20	340,934	61.43 %	35.35 %	0.48 %	752	1	454,332	58.38 %	33.75 %	1.02 %	1,386	45	367,611	60.64 %	35.12 %	0.20 %	1,181	18	202,151	59.80 %	34.67 %	0.61 %	1,163	35
Aug-20	483,126	61.16 %	36.42 %	0.43 %	896	2	391,150	58.95 %	33.65 %	0.90 %	1,112	13	313,986	59.96 %	35.72 %	0.36 %	1,020	25	67,710	61.92 %	35.47 %	0.55 %	913	23
Sep-20	407,753	61.87 %	36.20 %	0.41 %	1,023	1	400,098	59.20 %	33.57 %	0.85 %	1,138	11	339,102	61.65 %	35.00 %	0.40 %	1,316	17	18,320	61.90 %	35.93 %	0.58 %	246	7
Oct-20	322,014	62.00 %	32.53 %	0.43 %	993	1	468,521	58.72 %	34.41 %	0.85 %	1,515	19	424,648	60.29 %	35.16 %	0.45 %	1,289	13	83,575	61.00 %	34.90 %	0.55 %	1,019	14
Nov-20	304,594	60.90 %	33.27 %	0.46 %	1,020	1	414,815	58.53 %	34.27 %	0.83 %	1,352	36	279,551	62.04 %	34.90 %	0.49 %	744	9	247,918	59.79 %	34.55 %	0.46 %	645	4
Dec-20	226,238	60.80 %	31.81 %	0.59 %	540	2	416,654	58.71 %	34.02 %	0.85 %	1,275	10	360,609	60.76 %	35.10 %	0.42 %	1,100	11	313,765	59.74 %	35.90 %	0.47 %	782	5

Jan-21	172,838	63.91 %	29.95 %	0.42 %	325	4	261,353	59.37 %	32.88 %	1.04 %	1,047	60	285,264	61.76 %	33.24 %	0.46 %	1,153	8	253,847	60.21 %	33.16 %	0.61 %	797	14
Feb-21	64,731	62.89 %	32.45 %	0.38 %	339	9	312,689	57.42 %	35.10 %	0.93 %	1,463	13	173,153	60.76 %	33.07 %	0.55 %	739	9	221,848	59.98 %	34.77 %	0.54 %	1,002	17
Mar-21	267,341	63.00 %	33.38 %	0.28 %	513	5	437,945	57.83 %	34.74 %	0.88 %	1,432	12	382,123	61.24 %	33.53 %	0.55 %	959	3	258,505	60.62 %	35.02 %	0.44 %	1,059	12
Apr-21	309,341	63.58 %	32.38 %	0.26 %	641	2	255,721	56.60 %	37.30 %	0.73 %	1,887	46	379,887	60.66 %	34.55 %	0.49 %	1,352	6	257,771	60.10 %	35.00 %	0.35 %	1,102	5
May-21	289,150	63.05 %	32.04 %	0.35 %	667	3	324,186	58.56 %	34.13 %	0.86 %	1,548	174	423,162	60.80 %	34.34 %	0.52 %	1,322	7	198,572	60.89 %	34.29 %	0.42 %	1,125	15
Jun-21	354,936	62.13 %	33.29 %	0.32 %	819	6	396,322	62.38 %	35.16 %	0.91 %	1,264	1	414,620	61.84 %	33.39 %	0.15 %	1,203	21	302,527	59.70 %	35.75 %	0.58 %	1,797	35
AVG 2019	282,000	63.31 %	33.47 %	0.47 %	645	6	401,830	58.44 %	37.57 %	0.27 %	1,220	14	287,283	61.27 %	33.46 %	0.13 %	1,302	13	358,486	60.70 %	34.66 %	0.48 %	852	68
AVG 2020	305,815	61.86 %	34.25 %	0.44 %	766	1	403,425	58.74 %	34.39 %	0.81 %	1,214	26	332,158	60.84 %	35.10 %	0.29 %	1,079	15	209,805	60.48 %	34.98 %	0.61 %	888	32
AVG 2021	243,056	63.09 %	32.25 %	0.34 %	551	5	331,369	58.69 %	34.88 %	0.89 %	1,440	51	343,035	61.18 %	33.69 %	0.45 %	1,121	9	248,845	60.25 %	34.67 %	0.49 %	1,147	16

Appendix 5: Biogas Plant Process Monitoring Guideline

No	Process/ Operation	Description	Monitoring Parameters	Unit	Operation Range	Operation Spec	Data Source	Corrective Action/Remarks		Alert Level
DIGESTER and DECANTER AREA										
1	POME Inlet / Cooling Tower	Cooling tower function as a cooling equipment for the inffluent (POME) before entering to the digester.	$Temp_{POME,IN}$	deg. C	60 to 85	60 to 85	measured		Inlet temperature of POME is variable and not within Biogas In-charge and Admin (BIA) scope of control. However, feedback can be given to the mill if POME temperature exceeded operation range value.	Mill Manager
			$Temp_{POME,OUT}$	deg. C	37 to 42	< 40	measured	> 40 (for 3 consecutive days)	1. Reduce flow into the CT 2. Online cleaning (spray system) and reduce the CT fin 3. Conduct major maintenance (if all 2 above actions failed)	COP
			COD_{POME}	kg/m3	40 to 95	40 to 95	Lab analysis		Sample must be analyzed once a week by accredited external lab. In a month, minimum 2 data	COP
			BOD_{POME}	kg/m3	20 to 60	20 to 60	Lab analysis		Sample must be analyzed once a week by accredited external lab. In a month, minimum 2 data	COP
			TS_{POME}	mg/L	35000 to 75000	40000 to 60000	Lab analysis		Sample must be analyzed once a week by accredited external lab. In a month, minimum 2 data	COP
			$SO_4^{2-}{}_{POME}$	mg/L	variable	variable	Lab analysis		Sample must be analyzed once a week by accredited external lab. In a month, minimum 2 data	COP

			pH_{POME}	NA	3.8 to 5	3.8 to 5	measured	<3.8 (for 3 consecutive days)	Information must be shared with Mill Manager in order to find the root cause. pH of POME become critical as it affects the pH of mix effluent in DGB. As long as pH in DGB is within the accepatable range, POME feeding can be continued as usual. Frequency of the reading collection is at least 2-3 times per day.	FM
			Q_{POME}	m3/day	varies	varies	measured		If daily flow > maximum flow design, open by-pass and close entrance to reactor.	COP
2	Mixing tank	There are 3 main functions of mixing tank: 1. To mix POME with recirculation effluent (internal or external) for improving pH feeding and for reducing POME temperature. 2. To distribute the mix effluent into the digester. 3. Gauging instrument of the effluent	$Temp_{DGB}$	deg. C	36 to 40	37 < T < 40	measured	> 40 (for 3 consecutive days)	1. Increase amount of recirculation. 2.Check cooling tower condition and performance (same as outlet T corrective maintenance). 3. Reduce POME feeding and increase external and internal recirculation.	COP
			pH_{DGB}	NA	6.5 to 7.0	> 6.8	measured	< 6.8 (for 3 consecutive days)	Increase sludge recirculation (max 80% to POME entering) or decrease amount of POME per hour entering to the cooling tower (max. 50%). Frequency of the reading collection is at least 3 time per day (during POME feeding)	FE
3	Anaerobic Reactor	3 major functions of AR are: 1. To produce biogas through anaerobic condition 2. To capture biogas produced 3. To treat the effluent	Organic Loading Rate (OLR)	kg COD/m3/d	up to 2.5	up to 2.5	calculated		OLR must be calculated if real COD and flow entering to reactor are too different from design considerations. Verifiy OLR when overload is suspected. In a case OLR is too low, decanter cake cam be introduced to AD	FE
			$COD_{AR,\ Overflow}$	kg/m3	6 to 20	< 15	Lab analysis		Sample must be analyzed once a week by accredited external lab. In a month, minimum 2 data	COP

			$TS_{AR,\ Overflow}$	mg/L	9000 to 30000	< 10000	Lab analysis		Sample must be analyzed once a week by accredited external lab. In a month, minimum 2 data. If TS too high, consider increasing sludge purging and reducing agitation time.	COP
			$SO_4^{2-}{}_{Overflow}$	mg/L	variable	variable	Lab analysis		Sample must be analyzed once a week by accredited external lab. In a month, minimum 2 data	COP
			Sedimentable Solids	mL/L/h	400 - 800	< 600	measured		If Sed Solids too high, consider increasing sludge purging and reducing agitation time.	
			$pH_{AR,\ Overflow}$	NA	6.8 - 7.5	6.9 - 7.5	measured		If below than 6.8, POME feeding must be reduced immediately and find out the reason for pH drop. Then, inform to BIA Facility Engineer. Frequency of the reading collection is at least 1 time per day. In the condition of pH drop, the frequency of the reading collection must be done 3 times per day.	FE
4	Agitation Pit(s)	Agitation function as a mixer inside digester. Purging is to remove excess solid inside the anaerobic reactor	Agitation hours	h/day	4 to 10	< 10	pre-determinded		Must be perform during POME feeding. Minimum agitation hours are function of overflow pH, organic load and drums presence in agitation system and SSED for overflow	COP
			Purging amount	m3/day	variable	variable	calculated		Purging must be conducted if bottom sludge more than 5%. Purging amount must be calculated to ensure the solid content of the digester remain between 2.5 and 3%.	COP

			TS_{AP}	mg/L	20,000 to 50,000	25,000 to 30,000	Lab analysis	< 25,000 or > 30,000 (average per month)	If less than 25,000 mg/L, purging amount must be stopped. If more than 30,000 mg/L, purging amount must be increased. Sample must be analyzed once a week by accredited external lab. In a month there will be 4 data.	FE
			VS_{AP}	% of TS	55 - 70	60 - 65	Lab analysis		Sample must be analyzed once a week by accredited external lab. In a month minimum 2 data	COP
			Sedimentable Solids	mL/L/h	850 - 1000	> 900	measured		If Sed solids too low, reduce or stop purging activities.	
			pH_{AP}	NA	6.9 to 7.3	7 to 7.3	measured		If pH below than 6.9, POME feeding must be reduced immediately. If pH more than 7.5, increase purging amount. Information must be shared with BIA Facility Engineer. Frequency of the reading collection is at least 1 time per day. In the condition of pH out of range, the frequency of the reading collection must be done 3 times per day.	FE
5	Sedimentation Pond/Tank Overflow	Sedimentation pond/tank will help to sediment sludge carried out by digester overflow. Decanter overflow is the effluent top layer from the decanter. This effluent normally represent the performance of biogas plant in terms of effluent treatment capacity	$COD_{DECANTER, Overflow}$	mg/L	4000 - 8000	< 6500	Lab analysis		COD sedimentation pond/tank overflow could be higher than 8 kg/m3. However,	COP
			$BOD_{DECANTER, Overflow}$	mg/L	1000 to 2500	1000 to 2500	Lab analysis		Sample must be analyzed once a week by accredited external lab. In a month minimum 2 data	COP
			$TS_{DECANTER, Overflow}$	mg/L	3000 to 9000	< 7000	Lab analysis		Sample must be analyzed once a week by accredited external lab. In a month minimum 2 data	COP
			$pH_{DECANTER, Overflow}$	NA	7 to 7.5	7 to 7.5	measured		Inform BIA Facility Engineer immediately	FE
			Sedimentable Solids	mL/L/h	50 - 400	< 100	measured		If Sed solids too high, reduce reactor agitation time and increase purging amount.	

6	External Recirculation	External recirculation use as one of the POME pretreatment method before entering to the digester. The source of this effluent is comes from decanter bottom sludge. Its help to stabilize the pH and temperature of effluent at DGB.	ER : POME ratio	%	50 - 80	50-80	pre-determinded			FE
			pH_{ER}	NA	7.0-7.5	7.0-7.5	measured		Amount of ER must be reduce immediately (max 50%). This will affect the pH of mix effluent at DGB. If pH at DGB drop below than the standard, external recirculation must be stop immediately. Internal recirculation can be use to replace ER for temporary period only.	FE
7	Air Injection	Function as a H2S gas neutralized agent inside digester. The amount of air injection every week is depend on the total gas production for previous 5 days data.	Air volume	%	3.0-6.0	3%	pre-determinded		Air injection amount is flexible depending on the gas quality produced by the digester. High amount of air injection will dilute the H_2S concentration as well as CH_4 inside the digester. So, continuous monitoring system of gas quality must be observed especially for oxygen level inside the biogas. Oxygen level must be maintained below 2%. If O_2 level exceeded 2%, amount of air injection must be reduced immediately.	FE
BIOGAS MANAGEMENT AREA										
8	Biogas under cover	The data collection must be done twice a day. H2S measurements before and after each filter.	$CH4_{BG, AR}$	%	50 to 65	> 50	measured	< 50 (for 3 consecutive days)	1. Verify process variables: pH reactor outlet. 2. If proceed, reduce air injection percentage inside the digester. 3. Increase agitation hours and external recirculation, if necessary 4. Inform BIA Facilty Engineer	FE/FM

			$CO2_{BG, AR}$	%	30 to 40	< 40	measured	> 40 (for 3 consecutive days)	1. Check CH4 and O2 trend 2. Increase external recirculation amount. 3. Inform BIA Facility Engineer	FE/FM
			$O2_{BG, AR}$	%	0.1 to 1.5	< 1.5	measured	> 1.2 (for 3 consecutive days)	1. Check CH4 and O2 trend. 2. Reduce air injection percentage inside the digester 3. Inform BIA Facility Engineer	FE/FM
			$H2S_{BG, AR}$	ppm	< 1500	< 1000	measured	> 1500 (for 3 consecutive days)	1. Increase air injection (max 6%) 2. Reduce the amount of POME and feed as consistent as possible in longer hour	FE/FM
9	Wet Filters/biological scrubber efficiency	The data collection must be done twice a day. H2S measurements before and after each filter.	$Q_{BG, filters}$	Nm3/h			measured			FE/FM
			$H2S_{BG, filters\ outlet}$	ppm	< 200	< 100	measured	> 100 (2 consecutive days)	1. Verify filters performance. 2. If proceed, schedule filters maintenance.	FE/FM
11	Engine line	The data collection must be done twice a day	$Q_{BG, engine}$	Nm3	variable	variable	measured		Depend on the engine size and requirement.	FE/FM
			$Temp_{BG, engine}$	°C	35 to 50	< 50	measured	> 50 (3 consecutive days)	1. Check intercooler and chiller performance. 2. Inform BIA Facility Engineer immediately.	FE/FM

			$CH4_{BG, engine}$	%	50 to 65	> 50	measured	< 50 (3 consecutive days)	1. Reduce air injection percentage inside the digester. 2. Increase agitation hours in digester if necessary. 3. Check and compare biogas composition in engine line and biogas under cover. If too much different it indicates a leakage issue between the line. 4. Verifiy analyzer's calibration if any doubt about instruments accuracy. 5. Inform BIA Facilty Engineer immediately.	FE/FM
			$CO2_{BG, engine}$	%	30 to 40	< 40	measured	> 40 (3 consecutive days)	1. Compare with biogas under cover data. If too much different, there is a possibility of leakage within the engine pipeline and digester. Inspection of the line must be carried out immediately 2. Inform BIA Facility Engineer immediately	FE/FM
			$O2_{BG, engine}$	%	0.1 to 1.5	< 1.5	measured	> 1.5 (3 consecutive days)	1. Compare with biogas under cover data. If too much different, there is a possibility of leakage within the engine pipeline and digester. Inspection of the line must be carried out immediately 2. Inform BIA Facility Engineer immediately	FE/FM
			$H2S_{BG, engine}$	ppm	< 200	< 100	measured	> 100 (2 consecutive days)	Check dry filter/wet filter performance. If there is no problem found, inform BIA Facility Engineer immediately	FE/FM
			$Pres_{BG, engine}$	bar	variable	variable	measured		Depend on the engine size and requirement	FE/FM